NICKEL CATALYZED CYCLOADDITION REACTIONS: ALKYNE CYCLOTRIMERIZATIONS AND REDUCTIVE VINYLIDENE TRANSFER REACTIONS

by

Sudipta Pal

A Dissertation

Submitted to the Faculty of Purdue University

In Partial Fulfillment of the Requirements for the degree of

Doctor of Philosophy

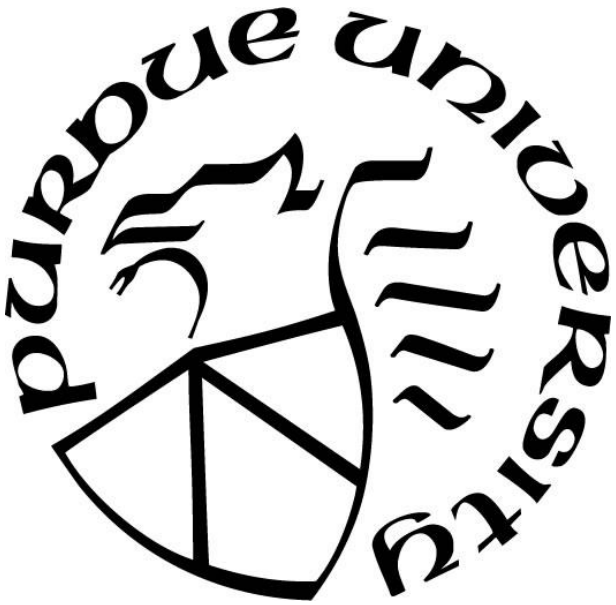

Department of Chemistry

West Lafayette, Indiana

December 2018

THE PURDUE UNIVERSITY GRADUATE SCHOOL
STATEMENT OF COMMITTEE APPROVAL

Dr. Christopher Uyeda, Chair
Department of Chemistry
Dr. Chengde Mao
Department of Chemistry
Dr. Suzanne Bart
Department of Chemistry
Dr. Mingji Dai
Department of Chemistry

Approved by:
Dr. Christine Hrycyna
Head of the Graduate Program

This thesis work is dedicated to my parents Sujata and Dilip Pal who inspired me to work hard for the things I aspire to achieve for. This work is also dedicated to my best friend Mayank, who continuously supported me throughout my graduate life in my difficult times.

ACKNOWLEDGMENTS

I would like to express my deep regards for my advisor Prof. Christopher Uyeda, and thank him for his tremendous support and help throughout my graduate studies. Without his encouragement and guidance, my PhD thesis would not have materialized.

I would like to thank Phil Fanwick, Dr. Matt Zeller and Dr. Ian Powers for their help in X-Ray Crystallography. I am also grateful to my friend Ravi Kiran Yerabolu for helping me in HRMS data collection.

Above all, I am really thankful to my parents for always being with me as a source of my strength and inspiration.

I would like to acknowledge my friends Mayank, Colby, Yen, Dexter, Kwaku, Sidhu, Sourish, Seulah, Ankita, Susmita, Satrajit, Mike, Dr. You-Yun and Kuam for their constant support and help throughout my graduate life.

TABLE OF CONTENTS

LIST OF TABLES

LIST OF FIGURES

LIST OF SCHEMES

ABSTRACT

Author: Pal, Sudipta,. PhD
Institution: Purdue University
Degree Received: December 2018
Title: Nickel Catalyzed Cycloaddition Reactions: Alkyne Cyclotrimerizations and Reductive Vinylidene Transfer Reactions
Committee Chair: Christopher Uyeda

The advent of transition metal catalysis has greatly expanded the scope of viable cycloaddition reactions, allowing for the direct synthesis of highly functionalized and complex biologically active compounds. By manipulating various aspects of catalyst structure, including the supporting ligands and the central metal, the function of a catalyst can be modified. In this context, the catalytic properties of dinuclear complexes have not been greatly explored in cycloaddition reactions. Our research has focused on studying the catalytic properties of dinuclear complexes in cycloaddition reactions. Comparative studies between dinuclear and mononuclear Ni-complexes led us to discover and develop an efficient route to synthesize 1,2,4-trisubstituted benzene derivatives from terminal alkynes. The key organometallic intermediates in this process were isolated, and computational studies were performed to unravel a novel bimetallic mechanism for alkyne cyclotrimerizations. As an extension of this study, we have found that the dinuclear catalyst is capable of catalyzing the methylenecyclopropanation of olefins. The reaction uses 1,1-dichloroalkene as a vinylidene precursor along with Zn as a stoichiometric reductant. A wide range of monosubstituted terminal alkenes and relatively unhindered internal alkenes are viable substrates. Furthermore, to understand the mechanism of vinylidene transfer, various stoichiometric and stereochemical experiments were performed. Furthermore, we discovered that mononuclear and dinuclear Ni-complexes are highly efficient in achieving vinylidene insertions into Si–H bonds to synthesize Si-containing heterocyclic molecules. Ongoing efforts are directed toward optimizing the reaction conditions and elucidating the substrate scope of the reaction.

CHAPTER 1. EVALUATING THE EFFECT OF CATALYST NUCLEARITY IN NI-CATALYZED ALKYNE CYCLOTRIMERIZATIONS

1.1 Abstract

An evaluation of catalyst nuclearity effects in Ni-catalyzed alkyne oligomerization reactions is presented. A dinuclear complex, featuring a Ni–Ni bond supported by a naphthyridine–diimine (NDI) ligand, promotes rapid and selective cyclotrimerization to form 1,2,4-substituted arene products. Mononickel congeners bearing related N-donor chelates (2-iminopyridines, 2,2'-bipyridines, or 1,4,-diazadienes) are significantly less active and yield complex product mixtures. Stoichiometric reactions of the dinickel catalyst with hindered silyl acetylenes enable characterization of the alkyne complex and the metallacycle that are implicated as catalytic intermediates. Based on these experiments and supporting DFT calculations, the role of the dinuclear active site in promoting regioselective alkyne coupling is discussed. Together, these results demonstrate the utility of exploring nuclearity as a parameter for catalyst optimization.

1.2 Introduction

Transition metal catalysts containing polynuclear active sites are underdeveloped alternatives to mononuclear catalysts for organic transformations.[1] Polynuclear complexes have the potential to exhibit unique catalytic properties by binding substrates and delocalizing redox activity across multiple metals. Platforms featuring direct metal–metal bonds are particularly well-suited to capitalize on these cooperative processes due to the enforced proximity of the metals and the strong electronic coupling between them. Consequently, ligands that support reactive metal–metal bonds have emerged as synthetic targets. The resulting complexes have been demonstrated to engage organic and small inorganic molecules in well-defined stoichiometric reactions.[2] Despite these advances, the cooperativity effects attributed to metal–metal bonds have rarely been evaluated in a catalytic process.[3] Such studies would complement those characterizing dinuclear effects

in catalyst systems where direct metal–metal interactions are either not relevant[4] or are formed transiently.[5]

Dinuclear complexes of naphthyridine–diimine (NDI) ligands are versatile platforms to study stoichiometric and catalytic redox processes at discrete metal–metal bonds.[6] The [$^{i\text{-Pr}}$NDI]Ni$_2$(C_6H_6) complex (**1**) is an analog of known mononickel complexes bearing N-donor chelates (eg. 2-iminopyridines, 2,2'-bipyridines, and 1,4-diazadienes), providing an opportunity to probe nuclearity effects within a family of related catalysts (Scheme 1). Here, we report a comparative study of mono- and dinickel catalysts in the oligomerization of terminal alkynes. Whereas mononuclear [N,N]Ni catalysts **2**–**4** uniformly yield complex product mixtures, the dinuclear catalyst **1** promotes rapid and selective cyclotrimerizations to form 1,2,4-trisubstituted arenes (Figure 1). Stoichiometric reactivity studies, combined with DFT calculations, provide insight into this pronounced nuclearity effect.

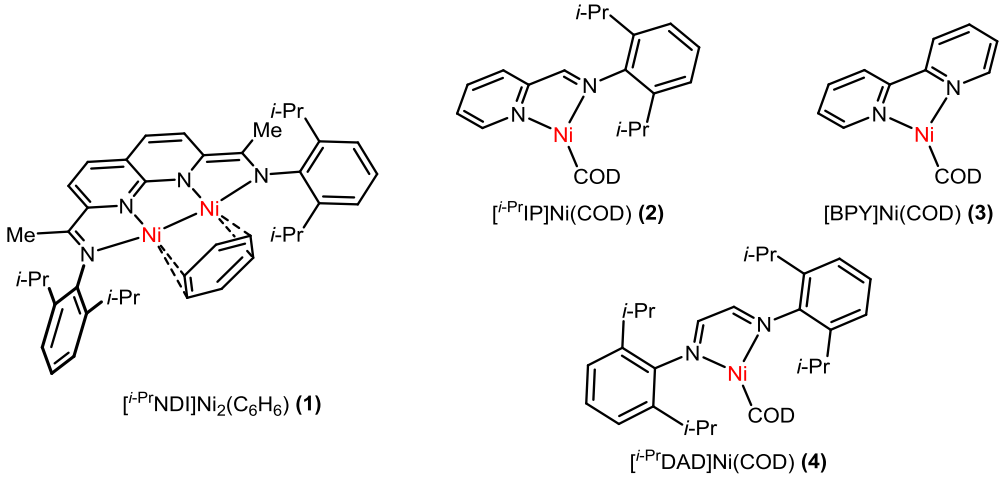

Scheme 1.1. Mononuclear and dinuclear Ni complexes of chelating N-donor ligands

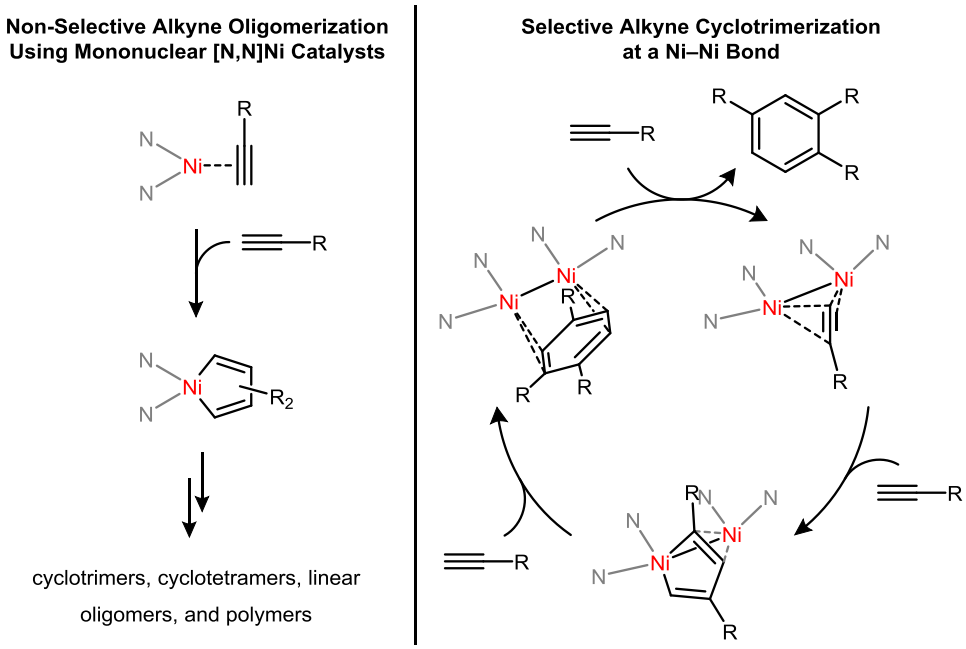

Figure 1.1. Mononuclear and dinuclear pathways for alkyne oligomerizations using Ni catalysts.

1.3 Catalyst Comparison Studies

Transition metal-catalyzed cycloadditions are direct and efficient routes to cyclic organic molecules;[7] however, complex selectivity considerations must be addressed in order to obtain high yields of a single product. Among the catalysts that have been surveyed in alkyne oligomerization reactions, the low-valent Ni catalysts initially reported by Reppe are unusual in the breadth of accessible products.[8] Simple Ni(0) sources such as $Ni(COD)_2$[9], activated Ni metal[10], and combinations of divalent Ni halide salts and reductants[11] convert terminal alkynes to mixtures of cyclic (arene and cyclooctatetraene regioisomers) and acyclic (oligomers and polymers) products. Supporting ligands have been effectively utilized to improve the selectivity of these reactions.[12] For example, phosphine-ligated complexes generally yield benzene derivatives[12a-g] whereas 1,4-diazadiene complexes favor cyclooctatetraenes.[12h-j]

In order to assess the viability of using catalyst nuclearity to control selectivity in these reactions, terminal alkyne substrates with diverse electronic properties were selected for comparison studies (Figure 2). For ethyl propiolate, all examined mononuclear and dinuclear catalysts (Scheme 1) were active, with **1** affording the highest conversion of

substrate under a standardized set of conditions. Consistent with previous reports,[12j] [*i*-^{Pr}IP]Ni(COD) (**2**), [BPY]Ni(COD) (**3**), [*i*-^{Pr}DAD]Ni(COD) (**4**), and Ni(COD)$_2$ (**5**) yielded significant amounts of both cyclotrimerized and cyclotetramerized products. Among these four mononickel catalysts, no greater than 14% combined yield of aromatic products was observed, with cyclooctatetraenes being formed in 11–71% yield. By comparison, **1** was selective for cyclotrimerization, affording a 90% combined yield of the 1,2,4- and 1,3,5-regioisomer. No cyclooctatetraene products were detected using **1**.

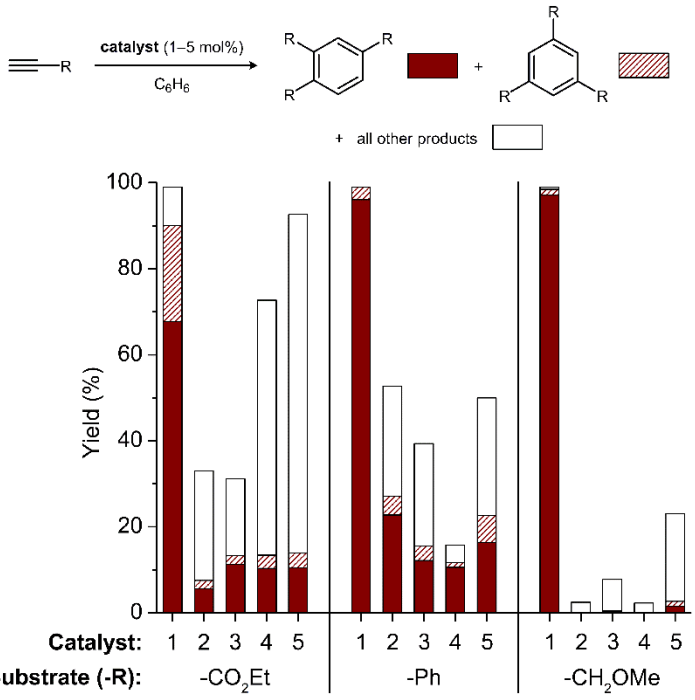

Figure 1.2. A comparison of catalytic activity for the cyclotrimerization of ethyl propiolate, phenylacetylene, and methyl propargyl ether. Data for catalysts **1**, **2**, **3**, **4**, and Ni(COD)$_2$ (**5**) are shown. Reaction conditions for ethyl propiolate and methyl propargyl ether: 22 °C, 11 min, 1 mol % catalyst. Reaction conditions for phenylacetylene: 60 °C, 40 min, 5 mol % catalyst. Yields and conversions are averaged over two runs and determined by GC-FID analysis. The total heights of the bars are the total conversion of starting material. The product fraction corresponding to the 1,2,4-isomer (solid red), 1,3,5-isomer (dashed red), and all other products (white) are plotted.

Similar effects were observed using more electron-rich alkyl- and aryl-substituted terminal alkynes. Phenylacetylene and methyl propargyl ether were poorly reactive using catalysts **2**–**5** and produced a mixture of coupled products. Catalyst **1** effected rapid cyclotrimerization, with nearly exclusive formation of the 1,2,4-regioisomer. Methyl propargyl ether is converted to 1,2,4-tris(methoxymethyl)benzene in 98% GC yield using 1 mol % of **1** in less than 15 min at room temperature. This rate and selectivity is noteworthy among those observed using the most efficient cyclotrimerization catalysts, including catalysts containing precious metals.[13] For example, the reaction of methyl propargyl ether with an optimized (diphosphine)Rh(I) complex, [Rh(DTBM-SEGPHOS)]BF_4, requires longer reaction times at 5 mol % loading and forms a 6:1 mixture of 1,2,4- to 1,3,5-substituted products.[13a]

1.4 Substrate Scope for Alkyne Cyclotrimerizations

The high selectivity for cyclotrimerization using **1** is general across a range of terminal alkynes (Figure 3). In all cases, the 1,2,4-regioisomer is highly favored, and no competing formation of cyclooctatetraenes is observed. Alkylacetylenes reach full conversion within 1 h at room temperature using 1 mol % of **1**. A higher catalyst loading of 5 mol % was used for arylacetylenes. To probe electronic effects, a series of para-substituted phenylacetylenes was studied. Substrates bearing electron-withdrawing substituents reacted at a faster rate than substrates bearing electron-donating substituents. Using cyclopropylacetylene, cyclotrimerization occurred without cyclopropane rearrangement through either a radical or organometallic mechanism. Finally, 1,6-heptadiyne and propargyl ether reacted to form the corresponding tethered diarene products. This selectivity is complementary to that under the conditions reported by Wender (20 mol % (DME)$NiBr_2$ and 40 mol % Zn powder), which generate the dimeric cyclooctatetraene product from 1,6-heptadiyne in 89% yield.[14]

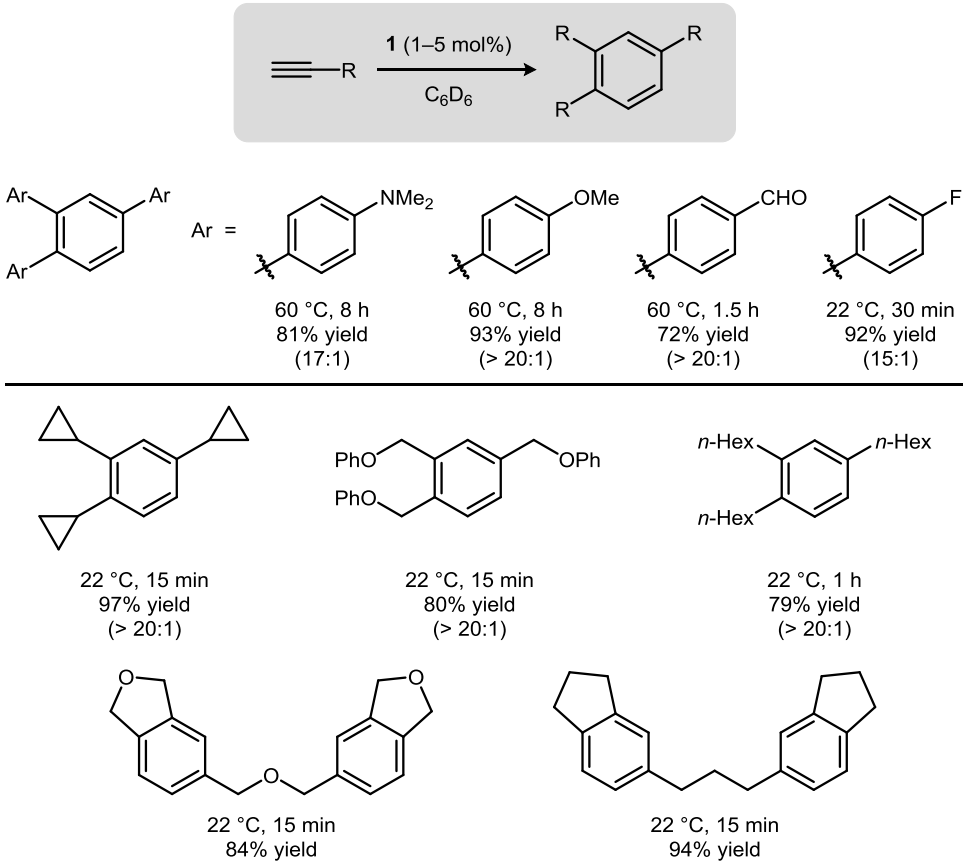

Figure 1.3. Substrate scope for alkyne cyclotrimerizations catalyzed by **1**. Conditions: 5 mol % catalyst loading for arylacetylenes and 1 mol % for all other substrates. Yields are of isolated products and are averaged over two runs. The ratio of the 1,2,4- to 1,3,5-regioisomer is shown in parentheses.

1.5 Stoichiometric Alkyne Coupling Reactions

We investigated the origin of the observed dinuclear effect by pursuing the characterization of plausible intermediates. Terminal alkynes bearing bulky silyl substituents, such as –$SiMe_3$ and –$SiMe_2Ph$, react with **1** but do not generate the cyclized product (Scheme 2). The reaction between **1** and dimethylphenylsilylacetylene (2.0 equiv or greater) in C_6D_6 is complete in 3 h at room temperature, producing the head-to-tail coupled product **6**. In the ^1H NMR spectrum, two signals are observed at 6.20 and 4.79 ppm (doublets with J = 4.5 Hz due to long-range coupling), corresponding to the two non-

equivalent *C*-H groups of the bound butadienyl fragment. No other isomeric complexes arising from head-to-head or tail-to-tail dimerization are detected under these conditions. The solid state structure (Figure 4a) reveals that the metallacycle incorporates one Ni into a five-membered ring. The second Ni provides secondary stabilization through an η^2-interaction with a double bond of the diene system. The formation of a directly analogous complex is observed with phenylacetylene under catalytic conditions (^{1}H NMR: 6.70 and 4.52 ppm, J = 4.3 Hz), supporting the catalytic relevance of the structurally characterized complex **6**.

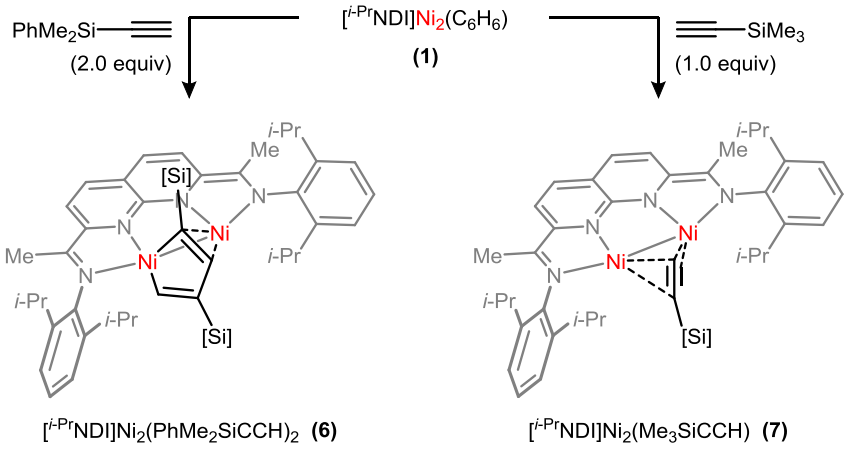

Scheme 1.2. Stoichiometric reactions of 1 with trialkylsilylacetylenes.

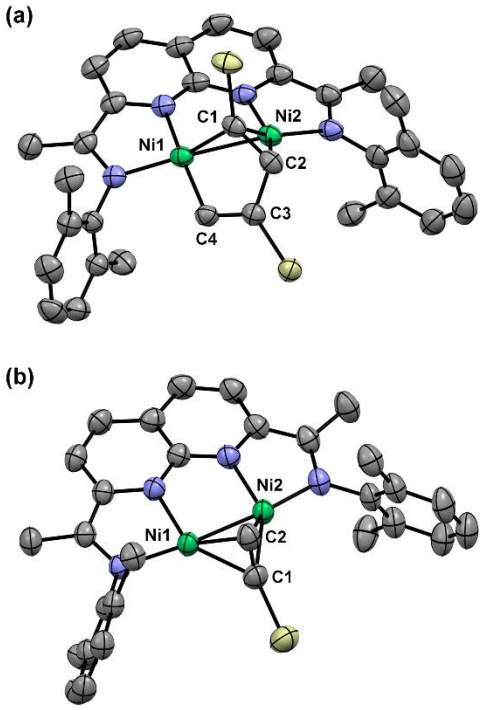

Figure 1.4. Solid state structures of (a) **6** and (b) **7** (ellipsoids at 50% probability). *i*-Pr groups on the NDI ligand and substituents on silicon are truncated for clarity. Selected bond distances for **6** (Å): Ni1–Ni2, 2.4814(6); Ni1–C1, 1.942(2); Ni1–C4, 1.868(2); Ni2–C1, 1.875(2); Ni2–C2, 2.042(2); C1–C2, 1.416(4); C2–C3, 1.482(3); C3–C4, 1.350(3). Selected bond distances for **7** (Å): Ni1–Ni2, 2.3140(6); Ni1–C1, 2.023(3); Ni1–C2, 1.911(3); Ni2–C1, 2.015(2); Ni2–C2, 1.904(2); C1–C2, 1.301(4).

The reversibility of the C–C coupling was examined to determine whether the regioisomer **6** is formed under thermodynamic or kinetic control. When **6** is exposed to trimethylsilylacetylene (10 equiv), no exchange of $–SiMe_2Ph$ for $–SiMe_3$ in the metallacycle is observed even after heating at 70 °C for 48 h. The formation of **6** is therefore sufficiently thermodynamically favorable to preclude the reverse reaction from occurring at catalytically relevant temperatures. A plausible explanation for the high head-to-tail selectivity is the steric hindrance imposed by the flanking 2,6-diisopropylphenyl substituents of the catalyst. The solid state structure of **6** suggests that substituents at C2 or C4 would be highly disfavored by interactions with a catalyst *i*-Pr group or arene respectively (Figure 4a).

The metallacycle **6** does not react with additional equivalents of dimethylphenylsilylacetylene; however, when a less hindered alkyne, methyl propargyl

ether, is introduced, cyclotrimerization proceeds to form the heterocoupled product **8** (Scheme 3). This reaction is accompanied by catalytic homocyclotrimerization of methyl propargyl ether. The regioselectivity in this stoichiometric process is consistent with that observed under standard catalytic conditions. Collectively, these experiments support the competence of metallacycles analogous to **6** as intermediates in the formation of 1,2,4-substituted arene products.

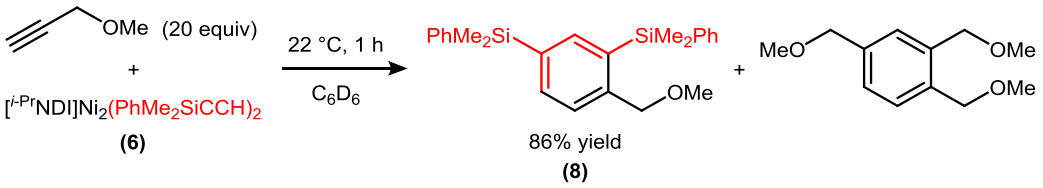

Scheme 1.3. Stoichiometric conversion of 6 to the heterocoupled product 8.

The presumed monoalkyne complex (**7**), en route to the metallacycle **6**, was characterized from reactions of **1** with one equivalent of trimethylsilylacetylene. In the solid state, the alkyne exhibits μ-η^2:η^2 coordination and is perpendicular to the Ni–Ni bond vector (Figure 4b). The C–C distance is significantly elongated from approximately 1.20 Å for free trimethylsilylacetylene[15] to 1.301(4) Å in the complex. The alkyne complex **7** is sufficiently stable to permit structural characterization; however, over the course of 24 h at room temperature in C_6D_6, it disproportionates to form a mixture of the corresponding metallacycle and the benzene complex **1**.

1.6 Origin of the Dinuclear Effect

The observed ratio of 1,2,4- to 1,3,5-substituted products in the alkyne cyclotrimerization arises from regioselectivity considerations in two sequential steps: the dimerization to form the metallacyclic intermediate and the subsequent incorporation of the third alkyne to yield the arene product. The stoichiometric reactivity studies described above provide insight into the selectivity of the first C–C coupling; however, less information is readily apparent regarding the product formation step.

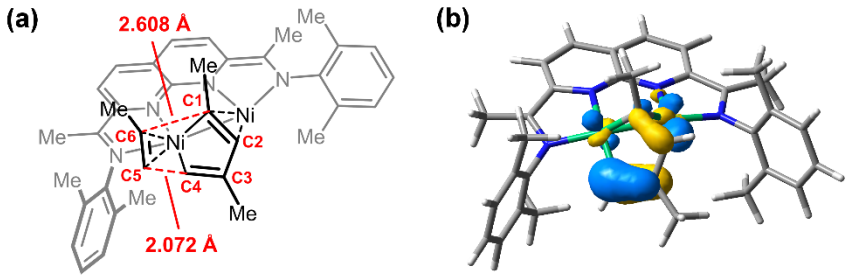

Figure 1.5. DFT calculations (M06/6-31g(d,p) level of theory) addressing the selectivity of alkyne addition to the bound butadienyl ligand. Propyne was used as a model substrate and *i*-Pr substituents on the catalyst were truncated to Me substituents. (a) The lowest-energy transition structure corresponding to the [4+2]-cycloaddition of the bound alkyne and butadienyl ligands. Distances for the two forming C–C bonds are shown in red. (b) The HOMO–1 for the metallacycle intermediate.

DFT calculations (M06/6-31G(d,p) level of theory) were performed on a model catalyst system (*i*-Pr groups on the aryl substituent were truncated to Me groups) to assess potential pathways for the conversion of this intermediate into the final product. Using propyne as a substrate, a concerted transition state was optimized, corresponding to a [4+2]-cycloaddition of a Ni-coordinated alkyne to the butadienyl system (Figure 5a). Stationary points associated with alternative stepwise pathways could not be located. Consistent with the fast rates observed experimentally for cyclotrimerizations with alkylacetylenes, the activation energy for this step was calculated to be only 9.3 kcal/mol. The competing transition state leading to the minor 1,3,5-substituted product was 2.0 kcal/mol higher in energy.

The calculated cycloaddition transition state (Figure 5a) is highly asynchronous with bond formation between C4 and C5 (2.07 Å) being significantly more advanced than that between C1 and C6 (2.61 Å). This asymmetry arises from stabilization of one of the double bonds through η^2 coordination to the second Ni center. The calculated HOMO–1, which primarily corresponds to the delocalized π-orbital of the diene system, shows significantly greater density at the uncoordinated double bond (Figure 5b). This electronic structure is manifested in the solid-state geometry of **6** as an elongated C1–C2 (1.416(4) Å) distance relative to the C3–C4 distance (1.350(3) Å). A hypothesis that emerges from

these calculations is that this electronic asymmetry, induced by the presence of the second Ni center in the catalyst, results in a steric preference for the substituent of the approaching alkyne to be positioned at the carbon where the forming C–C distance is longer in the transition state.

In summary, the dinuclear [NDI]Ni_2 platform provides access to an efficient cyclotrimerization pathway that is not available to its mononuclear counterparts. The catalyst nuclearity effect is particularly significant for alkyl-substituted alkynes: reactions are complete within 1 h at room temperature using 1 mol % loading of **1** with nearly exclusive formation of 1,2,4-substituted arene products. Stoichiometric reactivity studies provide structural insight into the metallacyclopentadiene intermediate that is implicated in the catalytic mechanism. Combined with DFT calculations, these experiments suggest several distinct features of the bimetallic system. First, binding across two metals constrains the geometry of the metallacycle, disfavoring the formation of other possible regioisomers. Second, the [4+2]-cycloaddition of the butadienyl ligand and the approaching alkyne is facilitated by metal coordination to both partners. Third, the selectivity of the cycloaddition is controlled by an electronic bias in the diene π-system, caused by a secondary η^2 interaction. Exploring the implications of these dinuclear effects for other catalytic cycloadditions is ongoing in our laboratory.

1.7 References

(1) (a) Doyle, M. P. J. Org. Chem 2006, 71, 9253-9260; (b) Davies, H. M. L.; Morton, D. Chem. Soc. Rev. 2011, 40, 1857-1869; (c) Cooper, B. G.; Napoline, J. W.; Thomas, C. M. Catal. Rev. 2012, 54, 1-40; (d) Kornecki, K. P.; Berry, J. F.; Powers, D. C.; Ritter, T. In Progress in Inorganic Chemistry; Karlin, K. D., Ed.; John Wiley & Sons, Inc.: Hoboken, New Jersey, 2014; Vol. 58, p 225-302.

(2) (a) Velian, A.; Lin, S.; Miller, A. J. M.; Day, M. W.; Agapie, T. J. Am. Chem. Soc. 2010, 132, 6296-6297; (b) Krogman, J. P.; Foxman, B. M.; Thomas, C. M. J. Am. Chem. Soc. 2011, 133, 14582-14585; (c) Powers, T. M.; Fout, A. R.; Zheng, S.-L.; Betley, T. A. J. Am. Chem. Soc. 2011, 133, 3336-3338; (d) Powers, T. M.; Betley, T. A. J. Am. Chem. Soc. 2013, 135, 12289-12296.

(3) (a) Magnus, P.; Principe, L. M. Tetrahedron Lett. 1985, 26, 4851- 4854; (b) Yamanaka, M.; Nakamura, E. J. Am. Chem. Soc. 2001, 123, 1703-1708; (c) Giordano, R.; Sappa, E.; Predieri, G. Inorg. Chim. Acta 1995, 228, 139-146; (d) Hostetler, M. J.; Bergman, R. G. J. Am. Chem. Soc. 1990, 112, 8621-8623; (e) Zhou, W.; Marquard, S. L.; Bezpalko, M. W.; Foxman, B. M.; Thomas, C. M. Organometallics 2013, 32, 1766- 1772; (f) Kornecki, K. P.; Briones, J. F.; Boyarskikh, V.; Fullilove, F.; Autschbach, J.; Schrote, K. E.; Lancaster, K. M.; Davies, H. M. L.; Berry, J. F. Science 2013, 342, 351-354; (g) Siedschlag, R. B.; Bernales, V.; Vogiatzis, K. D.; Planas, N.; Clouston, L. J.; Bill, E.; Gagliardi, L.; Lu, C. C. J. Am. Chem. Soc. 2015, 137, 4638-4641.

(4) (a) Shibasaki, M.; Sasai, H.; Arai, T. Angew. Chem., Int. Ed. 1997, 36, 1236-1256; (b) van den Beuken, E. K.; Feringa, B. L. Tetrahedron 1998, 54, 12985-13011; (c) Li, H.; Marks, T. J. Proc. Natl. Acad. Sci. U.S.A. 2006, 103, 15295-15302; (d) Park, J.; Hong, S. Chem. Soc. Rev. 2012, 41, 6931-6943.

(5) (a) Tsutsumi, H.; Sunada, Y.; Shiota, Y.; Yoshizawa, K.; Nagashima, H. Organometallics 2009, 28, 1988-1991; (b) Walker, W. K.; Kay, B. M.; Michaelis, S. A.; Anderson, D. L.; Smith, S. J.; Ess, D. H.; Michaelis, D. J. J. Am. Chem. Soc. 2015; (c) Powers, D. C.; Ritter, T. Acc. Chem. Res. 2011, 45, 840-850; (d) Mazzacano, T. J.; Mankad, N. P. J. Am. Chem. Soc. 2013, 135, 17258-17261.

(6) (a) Zhou, Y.-Y.; Hartline, D. R.; Steiman, T. J.; Fanwick, P. E.; Uyeda, C. Inorg. Chem. 2014, 53, 11770-11777; (b) Steiman, T. J.; Uyeda, C. J. Am. Chem. Soc. 2015, 137, 6104-6110.

(7) (a) Saito, S.; Yamamoto, Y. Chem. Rev. 2000, 100, 2901-2916; (b) Kotha, S.; Brahmachary, E.; Lahiri, K. Eur. J. Org. Chem. 2005, 2005, 4741-4767; (c) Chopade, P. R.; Louie, J. Adv. Synth. Catal. 2006, 348, 2307-2327; (d) Broere, D. L. J.; Ruijter, E. Synthesis 2012, 44, 2639-2672; (e) Kumar, P.; Louie, J. In Transition-Metal-Mediated Aromatic Ring Construction; Tanaka, K., Ed.; John Wiley & Sons, Inc.: Hoboken, New Jersey, 2013, p 37-70; (f) Amatore, M.; Aubert, C. Eur. J. Org. Chem. 2015, 2015, 265-286.

(8) Reppe, W.; Schlichting, O.; Klager, K.; Toepel, T. Justus Liebigs Ann. Chem. 1948, 560, 1-92.

(9) Čermák, J.; Blechta, V.; Chvalovský, V. Collect. Czech. Chem. Commun. 1988, 53, 1274-1286.

(10) Simons, L. H.; Lagowski, J. J. J. Org. Chem 1978, 43, 3247-3248.

(11) (a) Alphonse, P.; Moyen, F.; Mazerolles, P. J. Organomet. Chem. 1988, 345, 209-216; (b) Lawrie, C. J.; Gable, K. P.; Carpenter, B. K. Organometallics 1989, 8, 2274-2276; (c) Chini, P.; Palladino, N.; Santambrogio, A. J. Chem. Soc. C 1967, 836-840.

(12) (a) Reppe, W.; Schweckendiek, W. J. Justus Liebigs Ann. Chem. 1948, 560, 104-116; (b) Chini, P.; Santambrogio, A.; Palladino, N. J. Chem. Soc. C 1967, 830-835; (c) Sato, Y.; Nishimata, T.; Mori, M. J. Org. Chem 1994, 59, 6133-6135; (d) Mori, N.; Ikeda, S.-i.; Odashima, K. Chem. Commun. 2001, 181-182; (e) Müller, C.; Lachicotte, R. J.; Jones, W. D. Organometallics 2002, 21, 1975-1981; (f) Teske, J. A.; Deiters, A. J. Org. Chem 2008, 73, 342-345; (g) Rodrigo, S. K.; Powell, I. V.; Coleman, M. G.; Krause, J. A.; Guan, H. Org. Biomol. Chem. 2013, 11, 7653-7657; (h) Diercks, R.; Stamp, L.; Kopf, J.; tom Dieck, H. Angew. Chem., Int. Ed. 1984, 23, 893-894; (i) Diercks, R.; Stamp, L.; Dieck, H. T. Chem. Ber. 1984, 117, 1913-1919; (j) Diercks, R.; Dieck tom, H. Chem. Ber. 1985, 118, 428-435; (k) Xi, C.; Sun, Z.; Liu, Y. Dalton Trans. 2013, 42, 13327-13330.

(13) (a) Tanaka, K.; Toyoda, K.; Wada, A.; Shirasaka, K.; Hirano, M. Chem.–Eur. J. 2005, 11, 1145-1156; (b) Perekalin, D. S.; Karslyan, E. E.; Trifonova, E. A.; Konovalov, A. I.; Loskutova, N. L.; Nelyubina, Y. V.; Kudinov, A. R. Eur. J. Inorg. Chem. 2013, 2013, 481-493.

(14) For examples of cyclotrimerizations selective for the 1,2,4- regioisomer, see ref. 7 and: (a) Ozerov, O. V.; Ladipo, F. T.; Patrick, B. O. J. Am. Chem. Soc. 1999, 121, 7941-7942; (b) Ozerov, O. V.; Patrick, B. O.; Ladipo, F. T. J. Am. Chem. Soc. 2000, 122, 6423-6431.

(15) Wender, P. A.; Christy, J. P. J. Am. Chem. Soc. 2007, 129, 13402- 13403.

(16) (a) Bennett, M. A.; Donaldson, P. B. Inorg. Chem. 1978, 17, 1995- 2000; (b) Baxter, R. J.; Knox, G. R.; Pauson, P. L.; Spicer, M. D. Organometallics 1999, 18, 197-205.

(17) Bond, A. D.; Davies, J. E. Acta Crystallogr., Sect. E 2002, 58, o777-o778.

CHAPTER 2. CATALYTIC REDUCTIVE VINYLIDENE TRANSFER REACTIONS

2.1 Abstract

Methylenecyclopropanes are important synthetic intermediates that possess strain energies exceeding those of saturated cyclopropanes by >10 kcal/mol. This report describes a catalytic reductive methylenecyclopropanation reaction of simple olefins, utilizing 1,1-dichloroalkenes as vinylidene precursors. The reaction is promoted by a dinuclear Ni catalyst, which is proposed to access Ni_2(vinylidenoid) intermediates via C–Cl oxidative addition.

2.2 Introduction

Vinylidenes (methylidene carbenes) are reactive intermediates comprising a divalent carbon atom incorporated into a C=C double bond.[1] Like their saturated carbene counterparts, vinylidenes undergo reactions that allow the valence-deficient carbon to increase its coordination number—for example, through cheletropic reactions with π-systems or insertions into C–H bonds.[2] Free vinylidenes are accessible from the decomposition of transiently generated diazoalkenes.[3] Alternatively, $(R_2C{=}C)(M)(X)$ species (vinylidenoids) serve as $R_2C{=}C$: surrogates, eliminating metal halides as stoichiometric byproducts.[1d] A key challenge associated with developing efficient transfer reactions of vinylidenes is their susceptibility to competing Fritsch–Buttenberg–Wiechell (FBW) rearrangements that form alkynes (Figure 1).[4] The rate of the 1,2-shift varies as a function of the migrating group, but when one of the alkene substituents is an H atom, the rearrangement becomes nearly barrierless.[5] This process underlies the well-known Corey–Fuchs and Seyferth–Gilbert alkyne syntheses.[6]

Transition metal catalysis may provide an avenue to address the instability of vinylidenes, allowing group transfer reactions to be favored over competing FBW rearrangement. Nevertheless, current carbene transfer catalysts are largely unsuitable for vinylidene transfer due to their reliance on diazoalkane decomposition as an activation strategy.[7] Diazoalkenes, the equivalent vinylidene precursors, are not known to be isolable

and undergo N_2 elimination spontaneously at room temperature.[1d,3a] Transition metal-bound vinylidenes are accessible by an alternative route involving a metal-induced isomerization of an alkyne.[8] Buono described a Pd-catalyzed methylenecyclopropanation reaction that operates by this pathway and is effective for a range of norbornene-derived substrates.[9,10] Other classes of alkenes are not currently viable in catalytic vinylidene [2 + 1]-cycloadditions.

Our group is interested in developing new modes of carbene generation based on the reductive dehalogenation of readily available and indefinitely stable 1,1-dihaloalkanes. In this context, we recently described a dinuclear Ni catalyst that promotes the cyclopropanation of alkenes using CH_2Cl_2 as a carbene source and Zn as a terminal reductant.[11] Here, we report the reductive transfer of vinylidenes from 1,1-dichloroalkenes (Figure 1). This method provides direct access to methylenecyclopropanes, a class of synt synthetic intermediates valued for their ability to engage in strain-induced ring-opening reactions.[2d,2e,12]

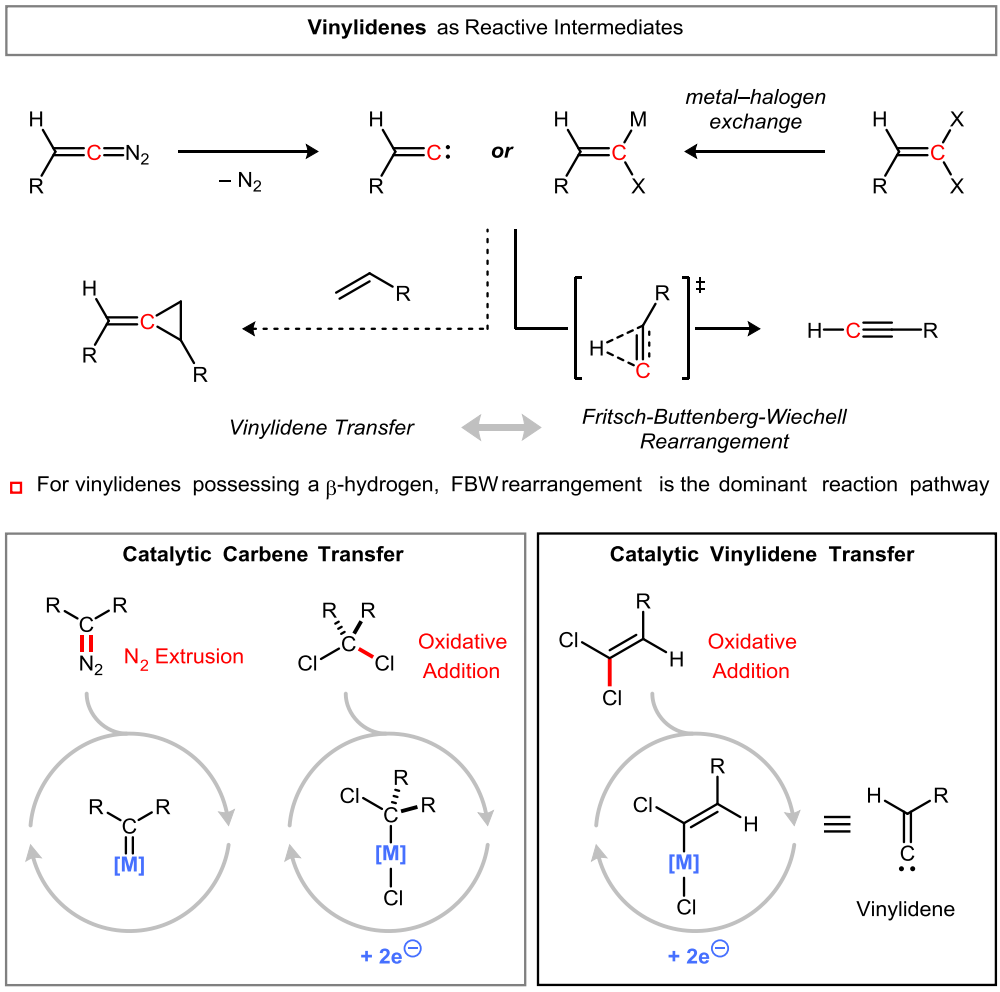

Figure 2.1. Vinylidenes as reactive intermediates and design principles for a catalytic reductive vinylidene transfer reaction.

2.3 Reaction Optimizations

In our initial studies, we arrived at an optimal set of conditions for a model methylenecyclopropanation reaction based on our previously reported CH_2 transfer method.[11] The Ni_2 catalyst **1**[13] promotes the addition of **2** to styrene in 94% yield using Zn as a reductant (Table 1, entry 1). Of note, none of the 1,1-dichloroalkene is lost to polymerization, reductive dehalogenation, or FBW rearrangement, allowing the reaction to be conducted with near-equimolar quantities of the two reaction partners. The [$^{i\text{-Pr}}$NDI]Ni_2Cl_2 complex **4** is also a high-yielding catalyst, demonstrating efficient entry into the catalytic cycle from multiple oxidation states of the Ni_2 complex (entry 2). The reaction is amenable to *in situ* catalyst generation using the free $^{i\text{-Pr}}$NDI ligand (**5**, 5 mol%) and

$Ni(DME)Cl_2$ (10 mol%) in the place of preformed **1** (entry 3). Decreasing the steric profile of the imine aryl substituents leads to rapidly diminishing yields (entries 4–5). Finally, the importance of the dinuclear catalyst structure was assessed using a series of mononickel complexes bearing structurally related N-donor ligands. In these cases, there is significant consumption of the 1,1-dichloroalkene (**2**) but no productive vinylidene transfer to form **3** (entries 6–9).

Table 2.1 . Catalyst Structure–Activity Relationships[a]

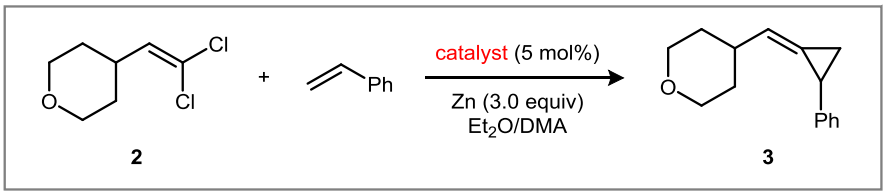

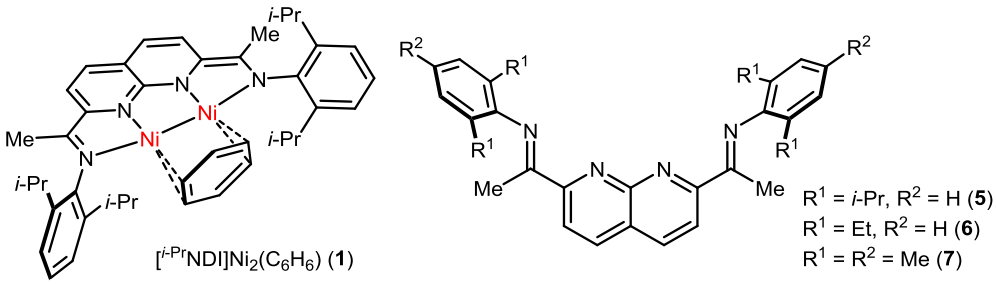

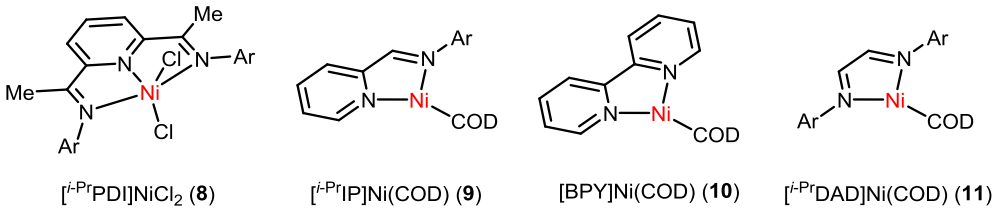

entry	catalyst	yield	*E*/*Z* ratio
1	[$^{i\text{-Pr}}$NDI]$Ni_2(C_6H_6)$ (**1**)	94%	1:5
2	[$^{i\text{-Pr}}$NDI]Ni_2Cl_2 (**4**)	87%	1:5
3[b]	$^{i\text{-Pr}}$NDI (**5**) + $Ni(DME)Cl_2$	92%	1:5
4[b]	^{Et}NDI (**6**) + $Ni(DME)Cl_2$	50%	1:1
5[b]	^{Me}NDI (**7**) + $Ni(DME)Cl_2$	<2%	–
6	[$^{i\text{-Pr}}$PDI]$NiCl_2$ (**8**)	<2%	–
7	[$^{i\text{-Pr}}$IP]Ni(COD) (**9**)	<2%	–
8	[BPY]Ni(COD) (**10**)	<2%	–
9	[$^{i\text{-Pr}}$DAD]Ni(COD) (**11**)	<2%	–

[a]Yields and E/Z ratios were determined by ^{1}H NMR integration. Reaction conditions: **2** (0.21 mmol), styrene (0.2 mmol), catalyst (5 mol%), 24 h, 22 °C. bReactions were conducted with 5 mol% of the NDI ligand and 10 mol% of $Ni(DME)Cl_2$.

2.4 Substrate Scope

The substrate scope of the catalytic methylenecyclopropanation is summarized in Table 2. 1,1-Dichloroalkenes bearing alkyl, aryl, or heteroaryl substituents afford high yields in their reactions with styrene (**12**–**18**). With regard to the alkene partner, monosubstituted terminal alkenes are effective substrates (**19**–**32**), and a variety of common functional groups are tolerated, including esters, ethers, nitriles, boronate esters, aryl chlorides, sulfonyl protecting groups, acetals, primary amides, and ketones. The observed *E*/*Z* ratios vary over a range of values and are dependent on the identity of the alkene substituent: alkyl groups with α-branching favor the *E*-isomer, linear alkyl groups afford low stereoselectivity, and aryl groups favor the *Z*-isomer.

Relatively unhindered internal alkenes, such as cyclopentene, 2,5-dihydrofuran, and norbornene, also react to form cyclopropanated products (**33**–**37**). More hindered alkenes than those shown in Table 2 are a current limitation and generally result in low yields. In accordance with these observations, the selectivity properties of the reaction are highly sensitive to steric effects. For example, norbornene and norbornadiene are selectively cyclopropanated on the exo face (**37**–**38**), and polyalkene substrates are monocyclopropanated at the less substituted alkene (**39**–**40**).

Table 2.2 . Substrate Scope for the Catalytic Methylenecyclopropanation Reaction[a]
[a]Isolated yields were determined following purification and are averaged over two runs. See Supporting Information for experimental details. [b]The alkene partner was used in excess (4–10 equiv).

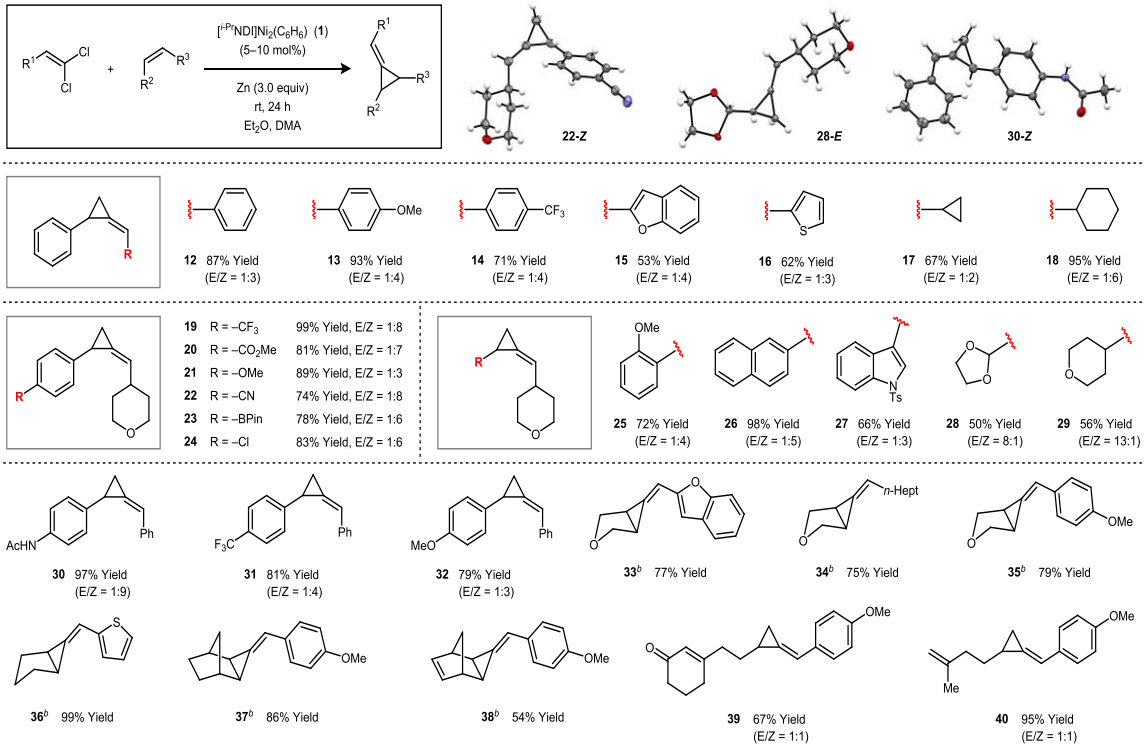

Unexpectedly, attempts to carry out the methylenecyclopropanation of ethylene (1 atm) yielded 1,3-diene products (**41**–**43**), a reaction that constitutes a formal vinylidene insertion into a C(sp^2)–H bond (Figure 2). We reasoned that these products may be forming in a catalyst-promoted ring-opening of a transient methylenecyclopropane intermediate.[14] At partial conversions, the reaction to form **42** contains significant amounts of the corresponding corresponding methylenecyclopropane, the concentration of which decreases as the reaction approaches completion.

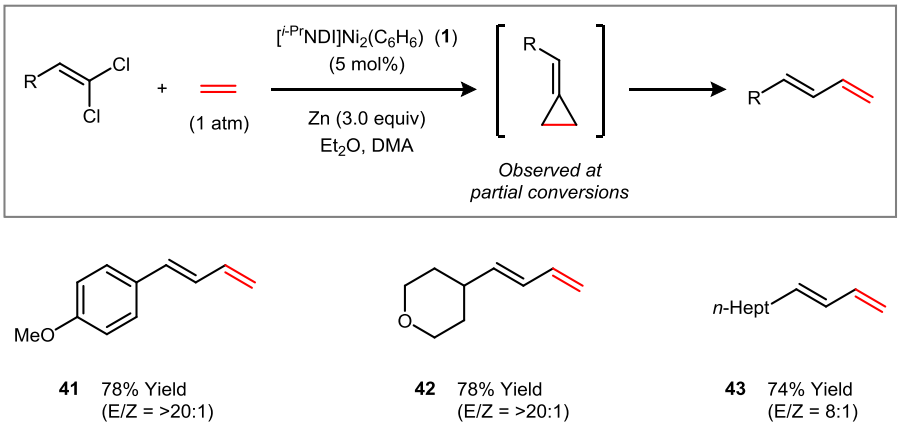

Figure 2.2 . Tandem methylenecyclopropanation–isomerization reactions.

2.5 Mechanistic Studies

Experiments pertaining to the mechanism of the catalytic methylenecyclopropanation are summarized in Figure 3a. By cyclic voltammetry, the Ni_2Cl_2 complex **4** exhibits two reversible reduction events at –1.15 and –1.72 V relative to the F_c/F_c^+ couple.[11] Zn is capable of accessing only the first of these two reductions, suggesting that the Ni_2Cl complex **44** is the most reduced state of the catalyst that is accessible. Next, we questioned whether the role of Zn is restricted to catalyst reduction[15] or whether it might be more intimately involved in the cyclopropane-forming steps of the mechanism—for example, through the generation of Zn vinylidenoid species.[16] This latter possibility was ruled out by conducting a cyclopropanation in the absence of Zn, where the Ni_2Cl complex **44** was used stoichiometrically as the only source of reducing equivalents. Accordingly, the reaction between β,β-dichlorostyrene (1.0 equiv), *p*-methoxystyrene (1.0 equiv), and **44** (2.0 equiv) provided **32** in 67% yield (1:2 *E*/*Z* ratio).

Finally, there is substantial evidence to support a stepwise mechanism for the cyclopropanation. The *E*- and *Z*-stereoisomers of β-deuterated *p*-methoxystyrene react with incomplete retention of the alkene stereochemistry, yielding product **32-*d*$_1$** as a mixture of cis and trans diastereomers. In principle, this loss of stereochemical fidelity may be due to an off-path, catalyst-promoted *E*/*Z* isomerization of the *p*-methoxystyrene starting material. This possibility was tested by running these reactions to partial conversion and examining the stereochemistry of the recovered alkene. At a reaction time of 20 min, the recovered

alkene is diastereomerically pure, suggesting that stereochemical scrambling is intrinsic to the mechanism of cyclopropane formation.

A proposed catalytic cycle based on these data is outlined in Figure 3b. Two-electron oxidative addition of the 1,1-dichloroalkene using the Ni_2Cl complex **44** would require an additional reducing equivalent provided by either a second molecule of **44** or by Zn. The resulting Ni_2(1-chloroalkenyl)Cl intermediate **45** could then engage the alkene partner and form the corresponding methylenecyclopropane product. An alternative possibility is that **45** first isomerizes by α-chloride migration to produce the Ni_2(vinylidene)Cl_2 species **46**.[17] According to DFT models (BP86/6-311G(d,p)), this isomerization is moderately endothermic but potentially accessible under the reaction conditions (ΔG = 10.5 kcal/mol, 298 K). In both scenarios, the Ni_2Cl_2 complex **4** is generated following vinylidene transfer, and a one-electron reduction closes the catalytic cycle.

Attempts to obtain characterization data on the postulated vinylidenoid intermediate **45/46** proved unsuccessful due to its instability. In order to access a more stable structural surrogate, the Ni_2(μ-styrenyl)Br complex **47** was prepared from an oxidative addition reaction between **1** and β-bromostyrene. This complex lacks the additional halogen at the β-position and is thus incapable of engaging in vinylidene transfer. A notable feature of the solid-state structure is the η^2-coordination of the alkenyl π-system to the second Ni. This interaction constrains the orientation of the β-hydrogen substituent and may contribute to the absence of FBW rearrangement side products in these reactions.

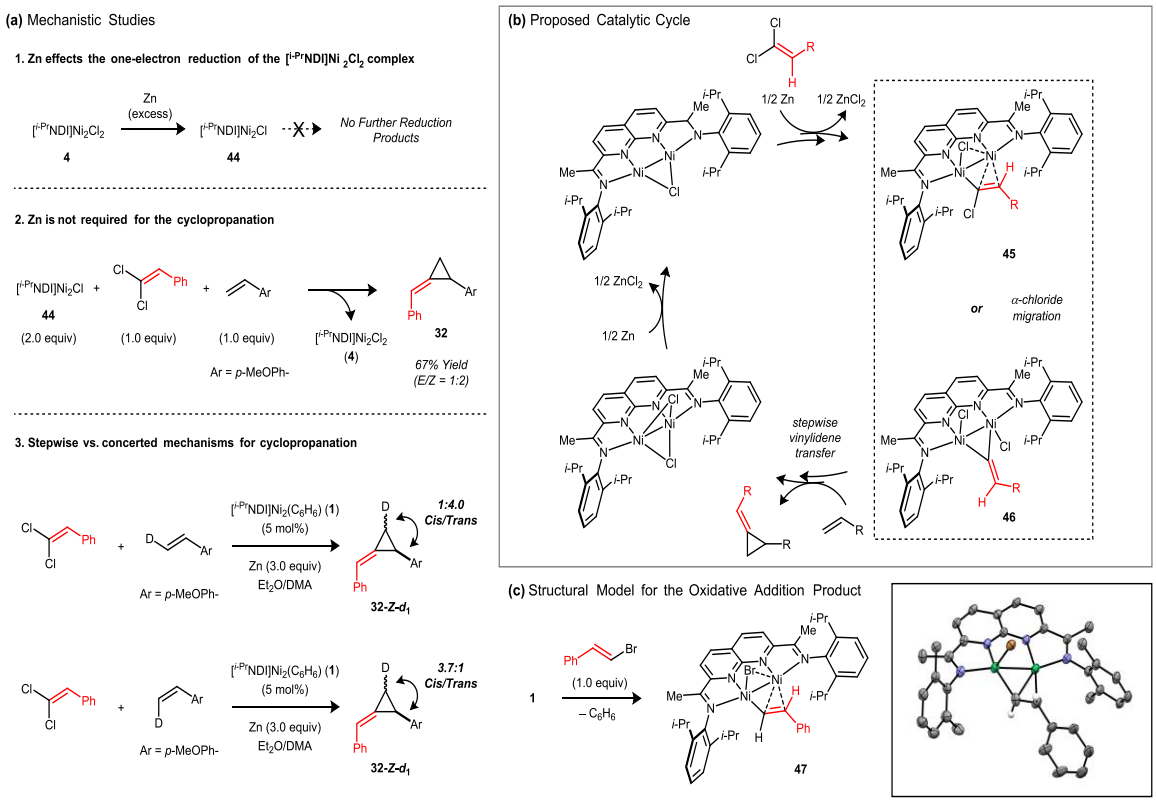

Figure 2.3 . (a) Mechanistic studies probing the relevant catalyst oxidation states, the role of Zn, and the concertedness of the cyclopropanation. (b) A proposed catalytic mechanism. (c) A structurally characterized model (47) for the proposed Ni_2 vinylidenoid intermediate (45).

In summary, the Ni_2 catalyst **1** has proven to be uniquely effective relative to analogous mononickel complexes in promoting reductive methylenecyclopropanation reactions using 1,1-dichloroalkenes. Of particular significance, vinylidene transfer predominates over competing rearrangement to the alkyne despite the presence of a β-hydrogen. Our current efforts are directed at generalizing this catalytic vinylidene transfer strategy to other classes of cycloadditions.

2.6 References

(1) (a) Stang, P. J. *Chem. Rev.* **1978**, *78*, 383-405; (b) Stang, P. J. *Acc. Chem. Res.* **1982**, *15*, 348-354; (c) Kirmse, W. *Angew. Chem., Int. Ed.* **1997**, *36*, 1164-1170; (d) Knorr, R. *Chem. Rev.* **2004**, *104*, 3795-3850; (e) Grainger, R. S.; Munro, K. R. *Tetrahedron* **2015**, *71*, 7795-7835.

(2) (a) Brandi, A.; Goti, A. *Chem. Rev.* **1998**, *98*, 589-636; (b) Audran, G.; Pellissier, H. *Adv. Synth. Catal.* **2010**, *352*, 575-608; (c) Yamaguchi, J.; Yamaguchi, A. D.; Itami, K. *Angew. Chem., Int. Ed.* **2012**, *51*, 8960-9009; (d) Brandi, A.; Cicchi, S.; Cordero, F. M.; Goti, A. *Chem. Rev.* **2014**, *114*, 7317-7420; (e) Pellissier, H. *Tetrahedron* **2014**, *70*, 4991-5031.

(3) (a) Gilbert, J. C.; Weerasooriya, U. *J. Org. Chem.* **1982**, *47*, 1837-1845; (b) Ohira, S.; Okai, K.; Moritani, T. *J. Chem. Soc., Chem. Commun.* **1992**, 721-722; (c) Gilbert, J. C.; Giamalva, D. H. *J. Org. Chem.* **1992**, *57*, 4185-4188.

(4) (a) Fritsch, P. *Justus Liebigs Ann. Chem.* **1894**, *279*, 319-323; (b) Buttenberg, W. P. *Justus Liebigs Ann. Chem.* **1894**, *279*, 324-337; (c) Wiechell, H. *Justus Liebigs Ann. Chem.* **1894**, *279*, 337-344; (d) Jahnke, E.; Tykwinski, R. R. *Chem. Commun.* **2010**, *46*, 3235-3249.

(5) (a) Ervin, K. M.; Ho, J.; Lineberger, W. C. *J. Chem. Phys.* **1989**, *91*, 5974-5992; (b) Chang, N.-Y.; Shen, M.-Y.; Yu, C.-H. *J. Chem. Phys.* **1997**, *106*, 3237-3242.

(6) (a) Corey, E. J.; Fuchs, P. L. *Tetrahedron Lett.* **1972**, *13*, 3769-3772; (b) Colvin, E. W.; Hamill, B. J. *J. Chem. Soc., Perkins Trans. 2* **1977**, 869-874; (c) Gilbert, J. C.; Weerasooriya, U. *J. Org. Chem.* **1979**, *44*, 4997-4998; (d) Habrant, D.; Rauhala, V.; Koskinen, A. M. P. *Chem. Soc. Rev.* **2010**, *39*, 2007-2017.

(7) (a) Doyle, M. P.; McKervey, M. A.; Ye, T. *Modern catalytic methods for organic synthesis with diazo compounds*; Wiley: New York, 1998; (b) Davies, H. M. L.; Manning, J. R. *Nature* **2008**, *451*, 417-424; (c) Ford, A.; Miel, H.; Ring, A.; Slattery, C. N.; Maguire, A. R.; McKervey, M. A. *Chem. Rev.* **2015**, *115*, 9981-10080.

(8) (a) Bruce, M. I. *Chem. Rev.* **1991**, *91*, 197-257; (b) Bruneau, C.; Dixneuf, P. H. *Acc. Chem. Res.* **1999**, *32*, 311-323; (c) Varela, J. A.; Saá, C. *Chem.–Eur. J.* **2006**, *12*, 6450-6456; (d) Bruneau, C.; Dixneuf, P. H. *Angew. Chem., Int. Ed.* **2006**, *45*, 2176-2203; (e) Bruneau, C.; Dixneuf, P., Eds. *Metal vinylidenes and allenylidenes in catalysis: from reactivity to applications in synthesis*; Wiley-VCH: Wenheim, Germany, 2008; (f) Lynam, J. M. *Chem.–Eur. J.* **2010**, *16*, 8238-8247.

(9) (a) Bigeault, J.; Giordano, L.; Buono, G. *Angew. Chem., Int. Ed.* **2005**, *44*, 4753-4757; (b) Clavier, H.; Lepronier, A.; Bengobesse-Mintsa, N.; Gatineau, D.; Pellissier, H.; Giordano, L.; Tenaglia, A.; Buono, G. *Adv. Synth. Catal.* **2013**, *355*, 403-408.

(10) Mao, J.; Bao, W. *Org. Lett.* **2014**, *16*, 2646-2649.

(11) Zhou, Y.-Y.; Uyeda, C. *Angew. Chem., Int. Ed.* **2016**, *55*, 3171-3175.

(12) (a) Trost, B. M. *Angew. Chem., Int. Ed.* **1986**, *25*, 1-20; (b) Nakamura, I.; Yamamoto, Y. *Adv. Synth. Catal.* **2002**, *344*, 111-129; (c) Yamago, S.; Nakamura, E. *Org. React.* **2002**, *61*, 1-217.

(13) (a) Zhou, Y.-Y.; Hartline, D. R.; Steiman, T. J.; Fanwick, P. E.; Uyeda, C. *Inorg. Chem.* **2014**, *53*, 11770-11777; (b) Steiman, T. J.; Uyeda, C. *J. Am. Chem. Soc.* **2015**, *137*, 6104-6110.

(14) (a) Englert, M.; Jolly, P. W.; Wilke, G. *Angew. Chem., Int. Ed.* **1971**, *10*, 77-77; (b) Binger, P.; Brinkmann, A.; Wedemann, P. *Chem. Ber.* **1983**, *116*, 2920-2930.

(15) For studies of Ni-catalyzed reductive cross-coupling reactions using Zn or Mn: (a) Everson, D. A.; Shrestha, R.; Weix, D. J. *J. Am. Chem. Soc.* **2010**, *132*, 920-921; (b) Weix, D. J. *Acc. Chem. Res.* **2015**, *48*, 1767-1775.

(16) Rezaei, H.; Yamanoi, S.; Chemla, F.; Normant, J. F. *Org. Lett.* **2000**, *2*, 419-421.

(17) (a) Fontaine, X. L. R.; Higgins, S. J.; Shaw, B. L.; Thornton-Pett, M.; Yichang, W. *J. Chem. Soc., Dalton Trans.* **1987**, 1501-1507; (b) Heise, J. D.; Nash, J. J.; Fanwick, P. E.; Kubiak, C. P. *Organometallics* **1996**, *15*, 1690-1696.

APPENDIX A. CHAPTER 1

A.1 General Information

General considerations. All manipulations were carried out using standard Schlenk or glovebox techniques under an atmosphere of N_2. Solvents were dried and degassed by passing through a column of activated alumina and sparging with Ar gas. Deuterated solvents were purchased from Cambridge Isotope Laboratories, Inc., degassed, and stored over activated 3 Å molecular sieves prior to use. All other reagents and starting materials were purchased from commercial vendors and used without further purification unless otherwise noted. Liquid reagents were degassed and stored over activated 3 Å molecular sieves prior to use. Elemental analyses were performed by Midwest Microlab (Indianapolis, IN). The [$^{i\text{-Pr}}$NDI]Ni$_2$(C_6H_6) complex **1** was prepared according to previously reported procedures.[1]

Physical methods. ^{1}H and ^{13}C{^{1}H} NMR spectra were collected at room temperature on a Varian INOVA 300 MHz, Bruker 400 MHz, or Bruker 500 MHz spectrometer. ^{1}H and ^{13}C{^{1}H} NMR spectra are reported in parts per million relative to tetramethylsilane, using the residual solvent resonances as an internal standard. GC/MS data was collected on a Shimadzu GCMS-QP2010 spectrometer containing a mini-bore capillary GC column and single quad EI detector. ATR-IR data were collected on a Thermo Scientific Nicolet Nexus spectrometer containing a MCT* detector and KBr beam splitter with a range of 350–7400 cm^{-1}. UV-vis measurements were acquired on a Cary 100 UV/vis spectrophotometer or Perkin Elmer Lambda 950 UV-VIS-NIR spectrophotometer using a 1-cm two-window quartz cuvette. High-resolution mass data were obtained using a Thermo Scientific LTQ Orbitrap XL mass spectrometer.

[1] Zhou, Y.-Y.; Hartline, D. R.; Steiman, T. J.; Fanwick, P. E.; Uyeda, C. *Inorg. Chem.* **2014**, *53*, 11770–11777.

X-ray crystallography. Single-crystal X-ray diffraction studies were carried out at the Purdue X-ray crystallography facility on either a Nonius KappaCCD or Rigaku Rapid II diffractometer. Data were collected at 150 or 200 K using Mo Kα (λ=0.71073 Å) or Cu Kα (λ=1.54178 Å) radiation. Structures were solved using direct methods using SHELXT and refined against F2 on all data by full-matrix least-squares.

A.2 Catalyst Comparison Data

Substrate	**Catalyst**	**Conversion**		**Combined Yield of Trimers**		**1,2,4- : 1,3,5- Ratio**	
		Run 1	**Run 2**	**Run 1**	**Run 2**	**Run 1**	**Run 2**
Ethyl propiolate	[$^{i\text{-Pr}}$NDI]Ni$_2$(C_6H_6) (**1**)	>99%	>99%	90%	90%	3.1:1	3.0:1
	[$^{i\text{-Pr}}$IP]Ni(COD) (**2**)	33%	33%	7.5%	7.5%	2.8:1	2.8:1
	[BPY]Ni(COD) (**3**)	29%	34%	12%	15%	5.6:1	5.6:1
	[$^{i\text{-Pr}}$DAD]Ni(COD) (**4**)	72%	74%	15%	11%	3.1:1	3.6:1
	Ni(COD)$_2$ (**5**)	93%	93%	14%	14%	3.0:1	3.0:1
Phenylacetylene	[$^{i\text{-Pr}}$NDI]Ni$_2$(C_6H_6) (**1**)	>99%	>99%	>99%	>99%	32:1	33:1
	[$^{i\text{-Pr}}$IP]Ni(COD) (**2**)	53%	52%	28%	27%	5.5:1	4.8:1
	[BPY]Ni(COD) (**3**)	35%	44%	14%	17%	3.5:1	3.7:1
	[$^{i\text{-Pr}}$DAD]Ni(COD) (**4**)	13%	18%	9%	15%	8.5:1	9.2:1
	Ni(COD)$_2$ (**5**)	52%	48%	23%	22%	2.9:1	2.3:1
Methyl propargyl ether	[$^{i\text{-Pr}}$NDI]Ni$_2$(C_6H_6) (**1**)	>99%	>99%	>99%	98%	70:1	66:1
	[$^{i\text{-Pr}}$IP]Ni(COD) (**2**)	2.3%	2.6%	<1%	<1%	1.0:1	1:1.2
	[BPY]Ni(COD) (**3**)	8.6%	6.9%	1%	<1%	1.2:1	1.2:1
	[$^{i\text{-Pr}}$DAD]Ni(COD) (**4**)	1.7%	2.8%	<1%	<1%	2.8:1	1.8:1
	Ni(COD)$_2$ (**5**)	23%	23%	2.4%	2.9%	1.2:1	1.2:1

Figure A.1.Catalyst (**1–5**) comparison data for the cyclotrimerization of ethyl propiolate,phenylacetylene, and methylpropargyl ether

General Procedure, Figure 2, Ethyl Propiolate. Under an atmosphere of N_2, a tube was charged with the catalyst (1 mol %). A stock solution of ethyl propiolate (0.4 mmol) and mesitylene (0.4 mmol) in C_6H_6 (1.0 ml) was added. After stirring for 11 min at rt in a sealed tube, the reaction mixture was quenched by exposing to air and diluting with C_6H_6. Conversion of substrate, combined yield of trimers, and the ratio of regioisomers were determined by GC-FID analysis.

General procedure, Figure 2, phenylacetylene. Under an atmosphere of N_2, a tube was charged with the catalyst (5 mol %). A stock solution of phenylacetylene (0.4 mmol) and mesitylene (0.4 mmol) in C_6H_6 (0.5 ml) was added. After stirring for 40 min at 60 °C in a sealed tube, the reaction mixture was quenched by exposing to air and diluting with C_6H_6. Conversion of substrate, combined yield of trimers, and the ratio of regioisomers were determined by GC-FID analysis.

General procedure, Figure 2, methyl propargyl ether. Under an atmosphere of N_2, a tube was charged with the catalyst (1 mol %). A stock solution of methyl propargyl ether (0.4 mmol) and mesitylene (0.4 mmol) in C_6H_6 (1.0 ml) was added. After stirring for 11 min at rt in a sealed tube, the reaction mixture was quenched by exposing to air and diluting with C_6H_6. Conversion of substrate, combined yield of trimers, and the ratio of regioisomers were determined by GC-FID analysis.

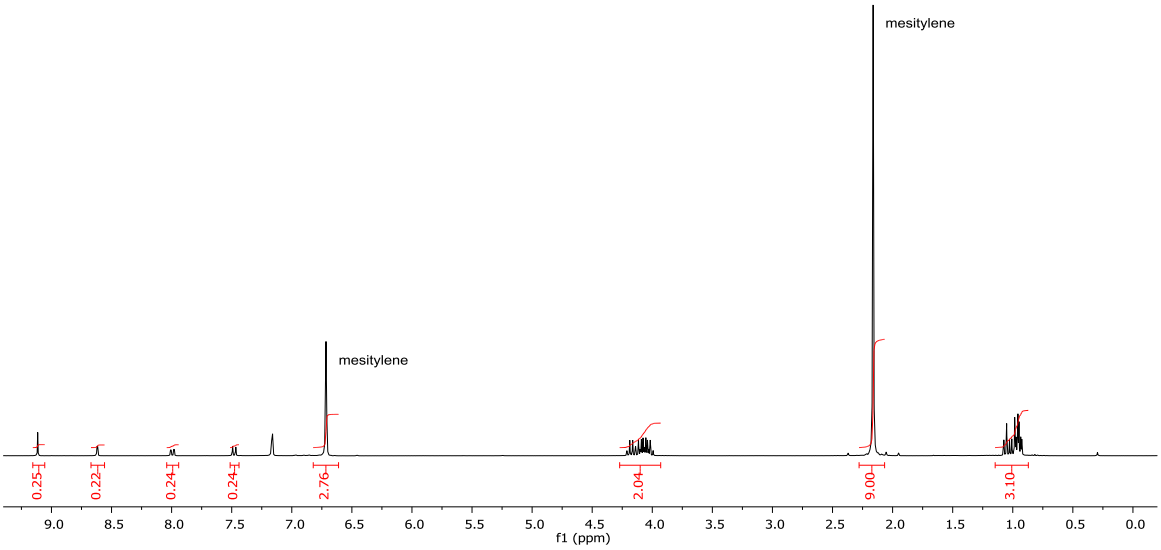

Figure A.2. ^{1}H NMR spectrum for the cyclotrimerization of ethyl propiolate catalyzed by **1** (crude reaction mixture containing catalyst and mesitylene).

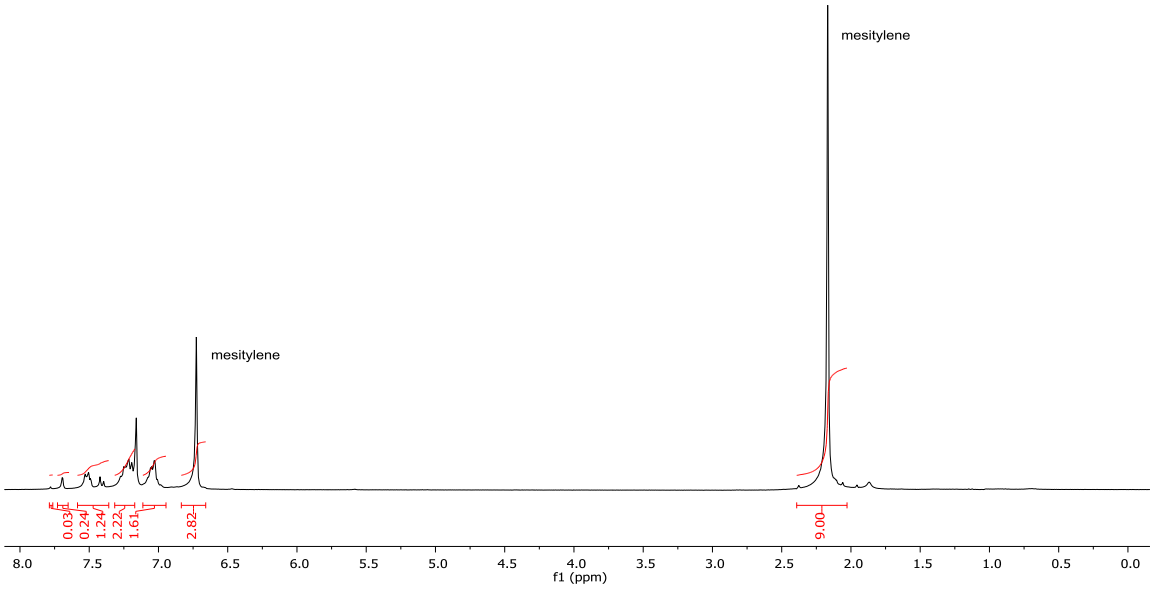

Figure A.3. ^{1}H NMR spectrum for the cyclotrimerization of phenylacetylene catalyzed by **1** (crude reaction mixture containing catalyst and mesitylene).

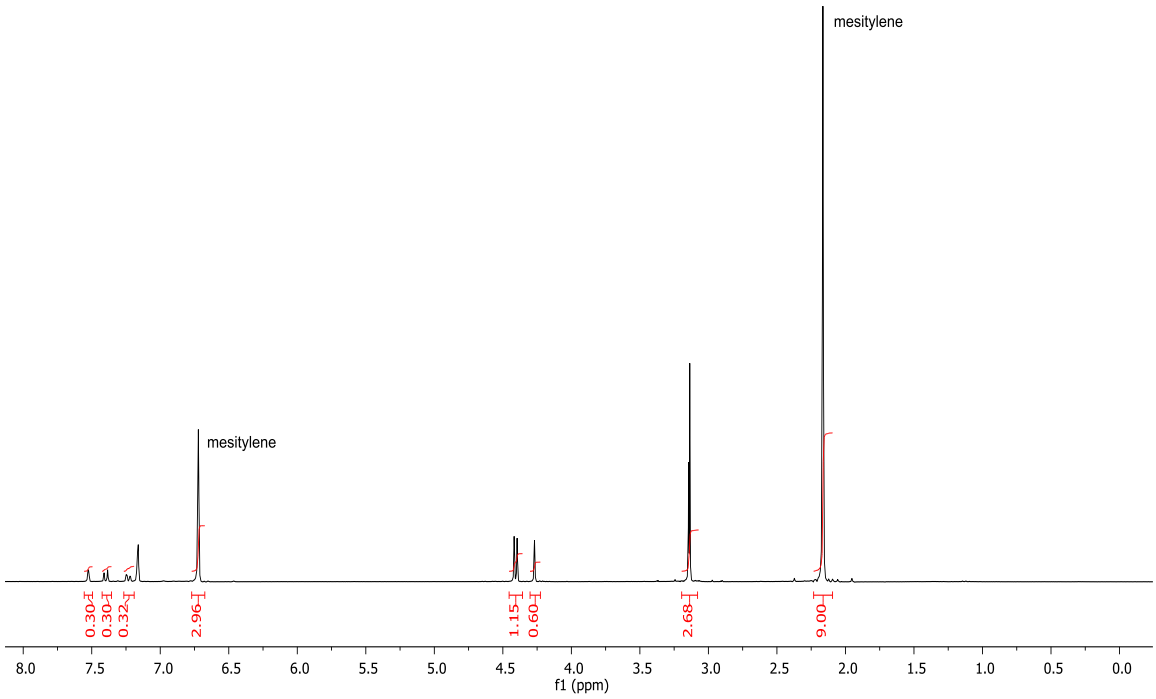

Figure A.4. ^{1}H NMR spectrum for the cyclotrimerization of methyl propargyl ether catalyzed by **1** (crude reaction mixture containing catalyst and mesitylene).

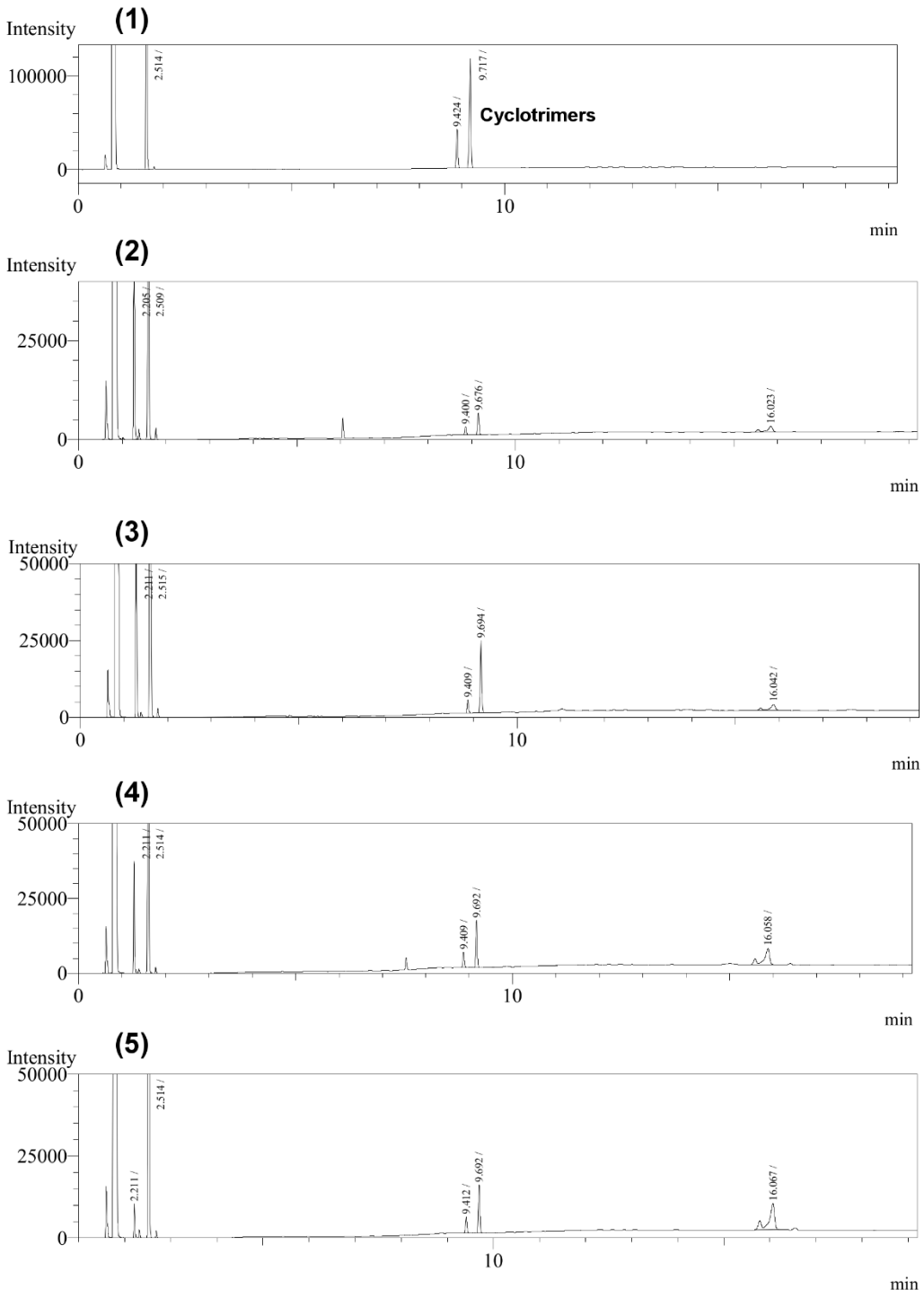

Figure A.5. GC-FID data for cyclotrimerizations of ethyl propiolate with catalysts 1–5.

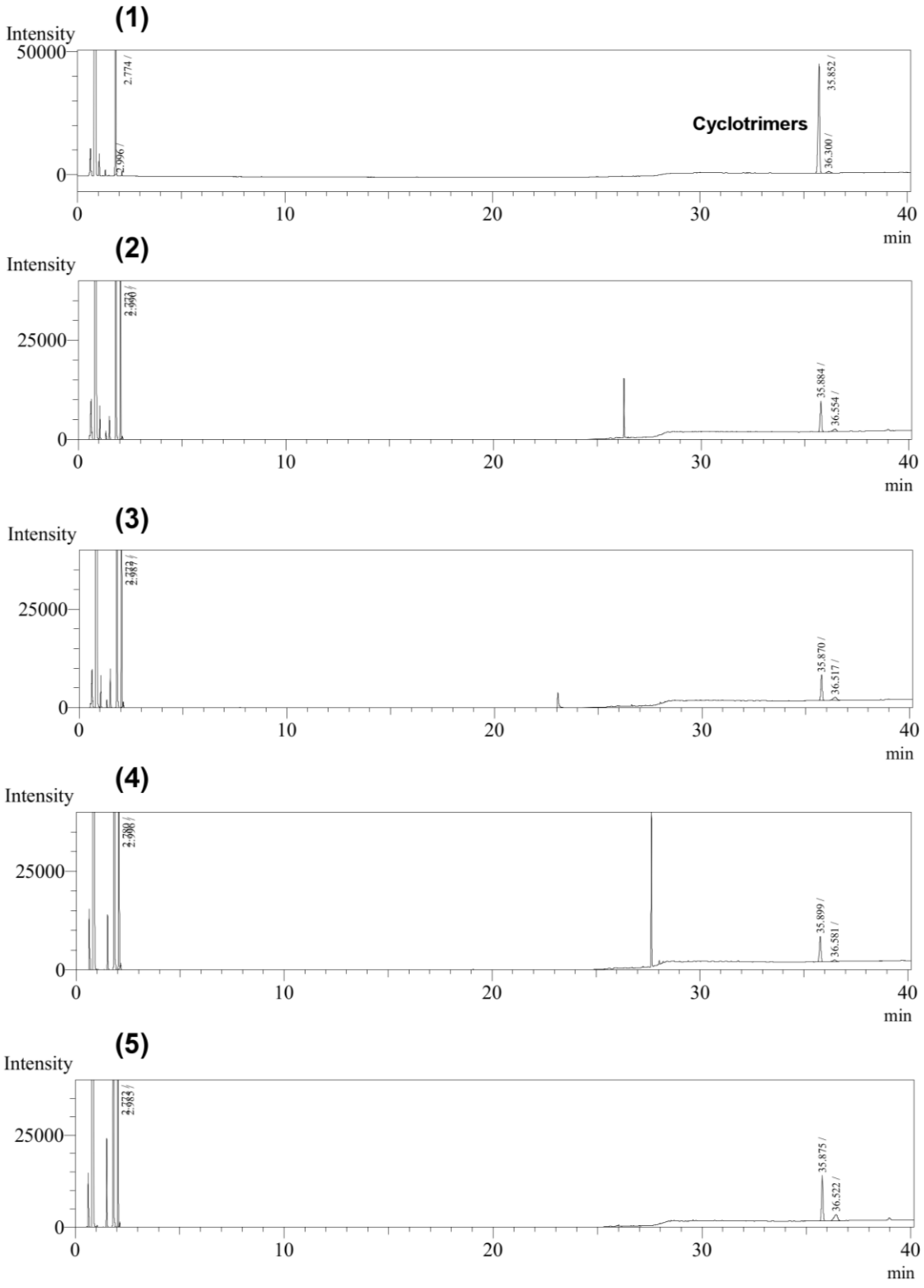

Figure A.6. GC-FID data for cyclotrimerizations of phenylacetylene with catalysts **1–5**.

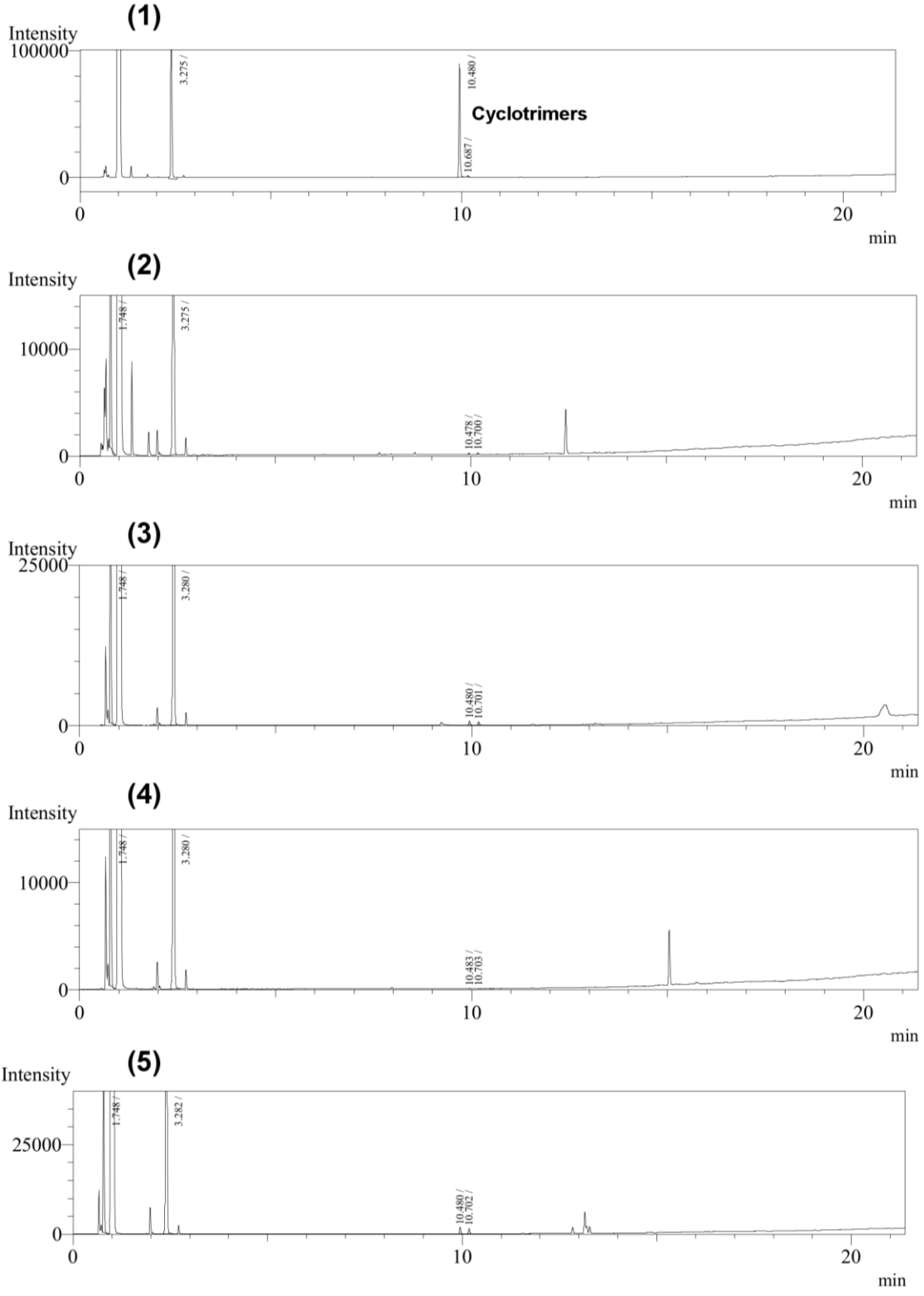

Figure A.7. GC-FID data for cyclotrimerizations of methyl propargyl ether with catalysts **1–5**.

A.3 Substrate Scope for Cyclotrimerizations Catalyzed by 1.

General procedure. Under an atmosphere of N_2, [$^{i\text{-Pr}}$NDI]Ni$_2$(C_6H_6) (**1**) was dissolved in C_6D_6 (1.0 mL) in a 20-mL scintillation vial (for reactions at room temperature) or a 2-mL crimp top vial (for reactions at 60 °C). The alkyne (0.50 mmol, 1.0 equiv) was added to the catalyst solution, and the vial was sealed. The reaction was allowed to stir at the indicated temperature, monitoring by ^{1}H NMR. After full conversion of the starting material, the crude mixture was exposed to air and loaded directly onto a column of SiO_2. Following purification by column chromatography, the yield of the isolated product was determined. The ratio of 1,2,4- to 1,3,5-regioisomers was determined by ^{1}H NMR and GC analysis.

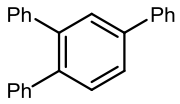

1,2,4-Triphenylbenzene [1165-53-3]. Phenylacetylene (51 mg, 0.50 mmol) was allowed to react in the presence of **1** (18.1 mg, 0.025 mmol, 5.0 mol %) in C_6D_6 (1 mL) for 1 h at 60 °C. Triphenylbenzene was obtained as a 32:1 mixture of 1,2,4- to 1,3,5-regioisomers. Run 1: 95% yield. Run 2: 96% yield. ^{1}H NMR (300 MHz, C_6D_6) δ 7.69 (d, *J* = 2.0 Hz, 1 H), 7.56–7.48 (m, 3 H), 7.41 (d, *J* = 6 Hz, 1 H), 7.28–7.17 (m, 7 H), 7.09–6.97 (m, 6 H); ^{13}C{^{1}H} NMR (101 MHz, C_6H_6) δ 142.2, 141.8, 141.5, 141.1, 140.9, 140.0, 131.6, 130.3, 130.3, 129.9, 129.1, 127.6, 127.5, 126.9, 126.5.

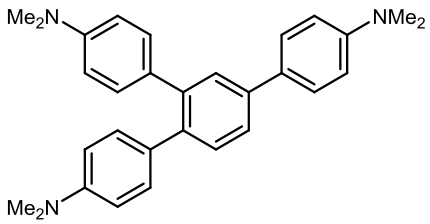

1,2,4-Tris(4-dimethylaminophenyl)benzene (6a) [189315-83-1]. 4-Dimethylaminophenylacetylene (72 mg, 0.50 mmol) was allowed to react in the presence of **1** (18.1 mg, 0.025 mmol, 5.0 mol %) in C_6D_6 (1 mL) for 8 h at 60 °C. Tris(4-dimethylphenyl)benzene was obtained as a 17:1 mixture of 1,2,4- to 1,3,5-regioisomers. Run 1: 81% yield. Run 2: 81% yield. ^{1}H NMR (400 MHz, C_6D_6) δ 7.99 (d, *J* = 1.9 Hz, 1

H), 7.76–7.62 (m, 4 H), 7.42–7.38 (m, 4 H), 6.73–6.66 (m, 2 H), 6.58–6.46 (m, 4 H), 2.56 (s, 6 H), 2.47 (s, 6 H), 2.46 (s, 6 H); $^{13}C\{^{1}H\}$ NMR (101 MHz, C_6H_6) δ 150.3, 149.4, 149.4, 141.6, 140.3, 139.1, 131.6, 131.1, 131.1, 130.0, 129.3, 125.1, 113.4, 112.7, 40.3, 40.2.

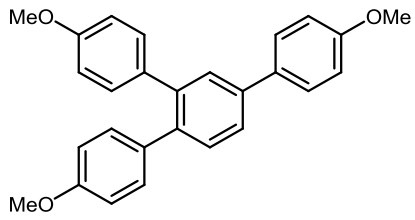

1,2,4-Tris(4-methoxyphenyl)benzene (6b) [136612-96-9]. 4-Methoxyphenylacetylene (66 mg, 0.50 mmol) was allowed to react in the presence of **1** (18.1 mg, 0.025 mmol, 5.0 mol %) in C_6D_6 (1 mL) for 8 h at 60 °C. Tris(4-methoxyphenyl)benzene was obtained as a 37:1 mixture of 1,2,4- to 1,3,5-regioisomers. Run 1: 94% yield. Run 2: 91% yield. ^{1}H NMR (300 MHz, C_6D_6) δ 7.77 (d, *J* = 1.9 Hz, 1 H), 7.58–7.46 (m, 4 H), 7.26–7.18 (m, 4 H), 6.93–6.86 (m, 2 H), 6.76–6.68 (m, 4 H), 3.37 (s, 3 H), 3.26 (s, 3 H), 3.25 (s, 3 H); $^{13}C\{^{1}H\}$ NMR (101 MHz, C_6H_6) δ 159.8, 158.9, 158.9, 141.1, 140.2, 139.1, 134.8, 134.4, 133.8, 131.6, 131.4, 129.6, 128.5, 125.9, 114.8, 114.1, 114.0, 55.0, 54.9.

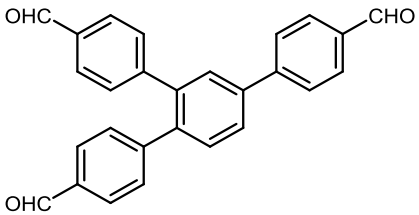

1,2,4-Tris(4-formylphenyl)benzene (6c) [1433220-07-5]. 4-Ethynylbenzaldehyde (65 mg, 0.50 mmol) was allowed to react in the presence of **1** (18.1 mg, 0.025 mmol, 5.0 mol %) in C_6D_6 (1 mL) for 1.5 h at 60 °C. Tris(4-formylphenyl)benzene was obtained as a >20:1 mixture of 1,2,4- to 1,3,5-regioisomers. Run 1: 74% yield. Run 2: 70% yield. ^{1}H NMR (300 MHz, C_6D_6) δ 9.79 (s, 1 H), 9.63 (s, 2 H), 7.68 (d, *J* = 8.0 Hz, 2 H), 7.47–7.33 (m, 7 H), 7.23–7.20 (m, 1 H), 6.98 (t, *J* = 7.4 Hz, 5 H). $^{13}C\{^{1}H\}$ NMR (101 MHz, C_6D_6) δ 190.8, 190.7, 146.8, 146.4, 145.6, 140.5, 140.3, 139.6, 136.4, 135.7, 131.5, 130.6, 130.6, 130.4, 129.8, 129.6, 129.0, 127.4, 109.0.

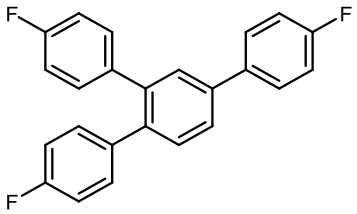

1,2,4-Tris(4-fluorophenyl)benzene (6d) [896102-02-6]. 4-fluorophenylacetylene (60 mg, 0.50 mmol) was allowed to react in the presence of **1** (18.1 mg, 0.025 mmol, 5.0 mol %) in C_6D_6 (1 mL) for 30 min at 22 °C. Tris(4-fluorophenyl)benzene was obtained as a 15:1 mixture of 1,2,4- to 1,3,5-regioisomers. Run 1: 91% yield. Run 2: 93% yield. ^{1}H NMR (400 MHz, C_6D_6) 7.41 (s, 1 H), 7.36–7.20 (m, 4 H), 6.95–6.86 (m, 6 H), 6.70 (t, *J* = 8.6 Hz, 4 H); ^{13}C{^{1}H} NMR (101 MHz, C_6H_6) δ 164.4, 163.6, 161.9, 161.1, 140.4, 140.0, 138.8, 137.6, 137.3, 136.9, 131.8, 131.7, 131.4, 129.6, 129.1, 129.0, 126.5, 116.5, 115.9, 115.4, 115.2.

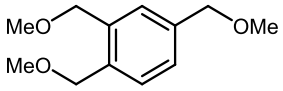

1,2,4-Tris(methoxymethyl)benzene [84941-00-4]. Methyl propargyl ether (35 mg, 0.50 mmol) was allowed to react in the presence of **1** (3.6 mg, 0.0050 mmol, 1.0 mol %) in C_6D_6 (1 mL) for 15 min at 22 °C. Tris(methoxymethyl)benzene was obtained as a 70:1 mixture of 1,2,4- to 1,3,5-regioisomers. Run 1: 94% yield. Run 2: 94% yield. ^{1}H NMR (300 MHz, C_6D_6) δ 7.52 (s, 1 H), 7.39 (d, *J* = 7.7 Hz, 1 H), 7.25–7.20 (m, 1 H), 4.42 (s, 2 H), 4.40 (s, 2 H), 4.27 (s, 2 H), 3.15 (s, 3 H), 3.14 (s, 6 H); ^{13}C{^{1}H} NMR (75 MHz, C_6H_6) δ 138.4, 137.0, 136.0, 128.8, 127.9, 126.8, 74.7, 72.5, 72.4, 58.2, 58.1

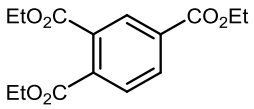

Triethyl benzene-1,2,4-tricarboxylate [14230-18-3]. Ethyl propiolate (49 mg, 0.50 mmol) was allowed to react in the presence of **1** (3.6 mg, 0.0050 mmol, 1.0 mol %) in C_6D_6 (1 mL) for 15 min at 22 °C. Triethyl benzene-1,2,4-tricarboxylate was obtained as

a 3:1 mixture of 1,2,4- to 1,3,5-regioisomers. Run 1: 88% yield. Run 2: 88% yield. ^{1}H NMR (300 MHz, C_6D_6) δ 8.61 (dd, *J* = 1.7, 0.5 Hz, 1 H), 7.99 (dd, *J* = 8.0, 1.7 Hz, 1 H), 7.48 (dd, *J* = 8.0, 0.5 Hz, 1 H), 4.30–3.90 (m, 6 H), 1.13–0.85 (m, 9 H); ^{13}C{^{1}H} NMR (101 MHz, C_6H_6) δ 167.0, 166.4, 164.7, 137.2, 133.1, 132.9, 132.1, 130.4, 129.2, 61.8, 61.7, 61.4, 14.1, 14.0.

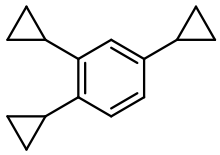

1,2,4-Tricyclopropylbenzene (7) [41009-68-1]. Cyclopropylacetylene (33 mg, 0.50 mmol) was allowed to react in the presence of **1** (3.6 mg, 0.0050 mmol, 1.0 mol %) in C_6D_6 (1 mL) for 15 min at 22 °C. 1,2,4-Tricyclopropylbenzene was obtained as a 74:1 mixture of 1,2,4- to 1,3,5 regioisomers. Run 1: 98% yield. Run 2: 96% yield. ^{1}H NMR (300 MHz, C_6D_6) δ 6.87 (d, *J* = 7.9 Hz, 1 H), 6.83 (d, *J* = 1.9 Hz, 1 H), 6.78 (dd, *J* = 7.8, 2.0 Hz, 1 H), 2.13–2.02 (m, 2 H), 1.77–1.68 (m, 1 H), 0.85–0.69 (m, 6 H), 0.69–0.55 (m, 6 H); ^{13}C{^{1}H} NMR (101 MHz, C_6H_6) δ 142.4, 141.4, 139.9, 125.7, 123.6, 123.2, 15.7, 13.7, 13.3, 9.0, 7.4.

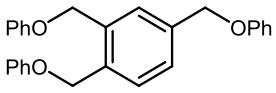

1,2,4-Tris(phenoxymethyl)benzene (8) [120819-22-9]. Phenyl propargyl ether (66 mg, 0.50 mmol) was allowed to react in the presence of **1** (3.6 mg, 0.0050 mmol, 1.0 mol %) in C_6D_6 (1 mL) for 15 min at 22 °C. 1,2,4-Tris(phenoxymethyl)benzene was obtained as a >20:1 mixture of 1,2,4- to 1,3,5-regioisomers. Run 1: 80% yield. Run 2: 79% yield. ^{1}H NMR (300 MHz, C_6D_6) δ 7.47 (d, *J* = 1.7 Hz, 1 H), 7.36 (d, *J* = 7.8 Hz, 1 H), 7.23–7.18 (m, 1 H), 7.15–7.06 (m, 6 H), 6.93–6.80 (m, 9 H), 4.87 (d, *J* = 3.7 Hz, 4 H), 4.66 (s, 2 H); ^{13}C{^{1}H} NMR (101 MHz, C_6H_6) δ 159.3, 137.8, 135.9, 135.2, 129.9, 129.8, 129.2, 128.2, 127.4, 121.4, 121.2, 115.2, 69.5, 67.9, 67.8.

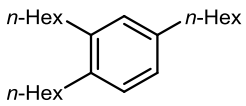

1,2,4-Trihexylbenzene (9) [10069-28-0]. 1-Octyne (55 mg, 0.50 mmol) was allowed to react in the presence of **1** (3.6 mg, 0.0050 mmol, 1.0 mol %) in C_6D_6 (1 mL) for 1 h at 22 °C. 1,2,4-Trihexylbenzene was obtained as a 47:1 mixture of 1,2,4- to 1,3,5-regioisomers. Run 1: 78% yield. Run 2: 79% yield. ^{1}H NMR (400 MHz, C_6D_6) δ 7.13 (s, 1 H), 7.07 (d, *J* = 2.0 Hz, 1 H), 7.03 (d, *J* = 7.7 Hz, 1 H), 2.70–2.52 (m, 6 H), 1.69–1.55 (m, 6 H), 1.44–1.32 (m, 6 H), 1.29–1.22 (m, 12 H), 0.94–0.84 (m, 9 H); ^{13}C{^{1}H} NMR (101 MHz, C_6H_6) δ 140.5, 140.5, 137.9, 129.8, 129.6, 128.5, 126.4, 36.2, 33.3, 32.9, 32.2, 32.2, 32.1, 32.0, 29.9, 29.9, 29.5, 23.1, 14.4.

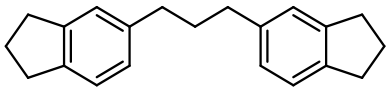

1,3-Bis(2,3-dihydro-1H-inden-5-yl)propane (10) [1785-55-3]. 1,6-Heptadiyne (46 mg, 0.50 mmol) was allowed to react in the presence of **1** (3.6 mg, 0.0050 mmol, 1.0 mol %) in C_6D_6 (1 mL) for 15 min at 22 °C. 1,3-Bis(2,3-dihydro-1H-inden-5-yl)propane was obtained as a single regioisomer. Run 1: 94% yield. Run 2: 93% yield. ^{1}H NMR (400 MHz, C_6D_6) δ 7.11 (d, *J* = 7.5 Hz, 2 H), 7.00 (s, 2 H), 6.98–6.93 (m, 2 H), 2.73 (t, *J* = 7.5 Hz, 8 H), 2.60 (t, *J* = 7.7 Hz, 4 H), 2.01–1.90 (m, 2 H), 1.88-1.79 (m, 4 H); ^{13}C{^{1}H} NMR (101 MHz, C_6H_6) δ 144.4, 141.6, 140.6, 126.8, 124.9, 124.5, 35.9, 34.4, 33.2, 32.8, 26.0.

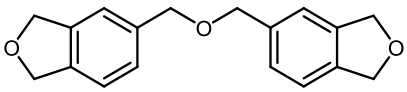

5,5'-(Oxybis(methylene))bis(1,3-dihydroisobenzofuran) (11) [288094-61-1]. Propargyl ether (47 mg, 0.50 mmol) was allowed to react in the presence of **1** (3.6 mg, 0.0050 mmol, 1.0 mol %) in C_6D_6 (1 mL) for 15 min at 22 °C. 5,5'-(Oxybis(methylene))bis(1,3-dihydroisobenzofuran) was obtained as a single regioisomer. Run 1: 85% yield. Run 2: 83% yield. ^{1}H NMR (300 MHz, C_6D_6) δ 7.15 (d, *J* = 3.9 Hz, 2

H), 6.98 (s, 2 H), 6.84 (d, J = 7.7 Hz, 2 H), 4.92 (s, 8 H), 4.39 (s, 4 H); $^{13}C\{^{1}H\}$ NMR (101 MHz, C_6H_6) δ 140.2, 139.2, 138.2, 126.9, 121.0, 120.6, 73.5, 73.4, 72.2.

A.4 Synthesis and Characterization Data for Ni_2 Complexes

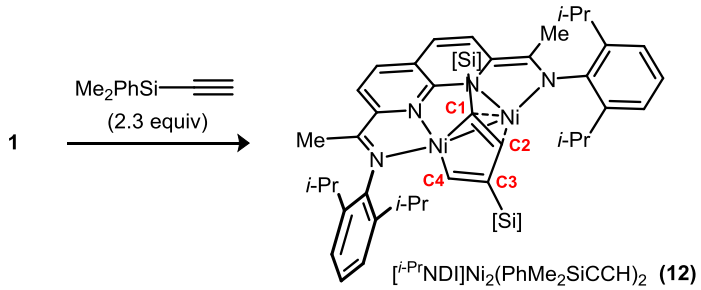

[$^{i\text{-Pr}}$NDI]Ni_2(PhMe$_2$SiCCH)$_2$ (12). Under an atmosphere of N_2, [$^{i\text{-Pr}}$NDI]Ni_2(C_6H_6) (1) (30 mg, 0.041 mmol, 1.0 equiv) was dissolved in C_6H_6 (2.0 mL) in a 20-mL vial. Dimethylphenylsilylacetylene (17 µL, 0.095 mmol, 2.3 equiv) was added, and the reaction was stirred at room temperature for 3 h to afford a dark purple homogeneous solution. The solvent was removed under vacuum. The residue was washed with three portions of cold pentane (–30 °C) and dried under reduced pressure to obtain [$^{i\text{-Pr}}$NDI]Ni_2(PhMe$_2$SiCCH)$_2$ (12) (35 mg, 87% yield). Single crystals suitable for XRD were obtained by slow evaporation of a saturated solution in C_6H_6. ^{1}H NMR (500 MHz, C_6D_6) δ 7.71–7.67 (m, 2 H), 7.56–7.52 (m, 2 H), 7.35–7.31 (m, 2 H), 7.29–7.18 (m, 5 H), 7.11–6.96 (m, 9 H), 6.19 (d, J = 4.5 Hz, 1 H, butadienyl C4-*H*), 4.79 (d, J = 4.5 Hz, 1 H, butadienyl C2-*H*), 3.56 (sept., J = 6.8 Hz, 1 H, C*H*(CH$_3$)$_3$), 2.54 (sept., J = 6.8 Hz, 1 H, C*H*(CH$_3$)$_3$), 2.34 (sept., J = 6.8 Hz, 1 H, C*H*(CH$_3$)$_3$), 1.98 (sept., J = 6.8 Hz, 1 H, C*H*(CH$_3$)$_3$), 1.61 (d, J = 6.8 Hz, 3 H, CH(C*H*$_3$)$_3$), 1.59 (s, 3 H, N=CCH$_3$), 1.55 (s, 3 H, N=CCH$_3$), 1.44 (d, J = 6.6 Hz, 3 H, CH(C*H*$_3$)$_3$), 1.21 (d, J = 6.9 Hz, 3 H, CH(C*H*$_3$)$_3$), 1.16 (d, J = 7.0 Hz, 3 H, CH(C*H*$_3$)$_3$), 1.01 (d, J = 6.7 Hz, 3 H, CH(C*H*$_3$)$_3$), 0.86 (d, J = 6.8 Hz, 3 H, CH(C*H*$_3$)$_3$), 0.82 (d, J = 6.8 Hz, 3 H, CH(C*H*$_3$)$_3$), 0.80 (d, J = 7.0 Hz, 3 H, CH(C*H*$_3$)$_3$), 0.36 (s, 3 H, Si(C*H*$_3$)$_2$Ph), 0.26 (s, 3 H, Si(C*H*$_3$)$_2$Ph), 0.06 (s, 3 H, Si(C*H*$_3$)$_2$Ph), 0.03 (s, 3 H, Si(C*H*$_3$)$_2$Ph). $^{13}C\{^{1}H\}$ NMR (101 MHz, C_6H_6) δ 193.4 (butadienyl C1), 177.3 (butadienyl C3), 169.6 (butadienyl C4), 162.6, 162.5, 159.7, 148.6, 147.2, 142.2, 141.9, 141.1, 140.3, 140.2, 136.7, 135.6, 135.5, 134.4, 134.2, 131.2, 129.7, 127.3, 126.6, 126.1, 123.8, 123.7, 123.4, 122.9, 115.1, 110.0, 75.6

(butadienyl C2), 28.9, 28.7, 28.1, 27.9, 25.9, 25.0, 24.6, 24.0, 23.9, 23.5, 23.2, 22.5, 16.9, 15.9, 1.1, 0.74, –2.11, –2.81. UV–vis: (C_6H_6): λ (nm) {ε, cm^{-1} M^{-1}} 996 {8100}, 772 {6200}, 548 {6700}, 476 {8100}. Anal. Calcd for 12 ([$^{i\text{-Pr}}$NDI]Ni_2($PhMe_2SiCCH$)$_2$): C, 69.36; H, 6.96; N, 5.78. Found: C, 69.26; H, 7.00; N, 5.61.

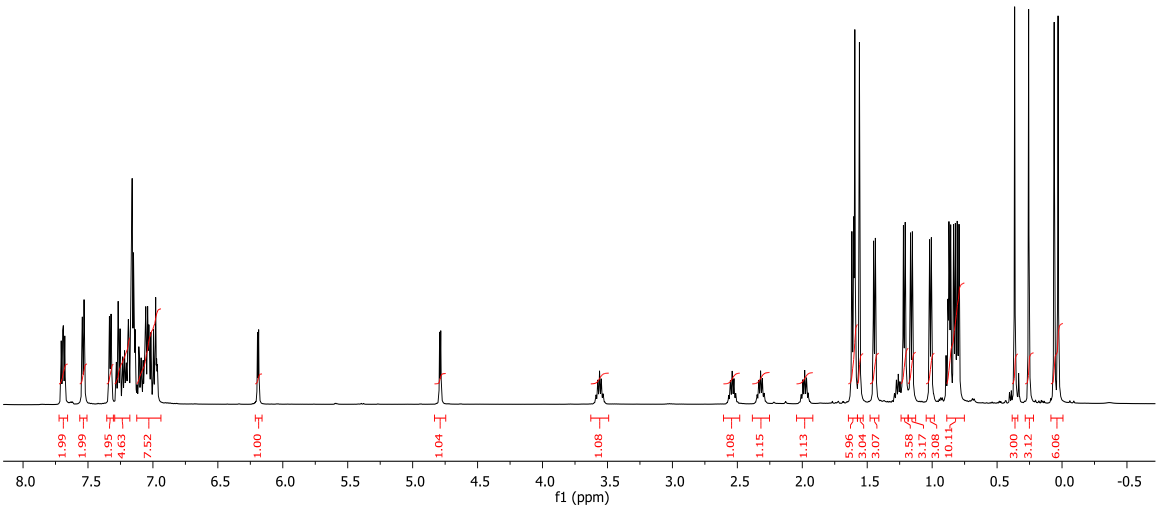

Figure A.8. ^{1}H NMR spectrum for **12** (C_6D_6, room temperature).

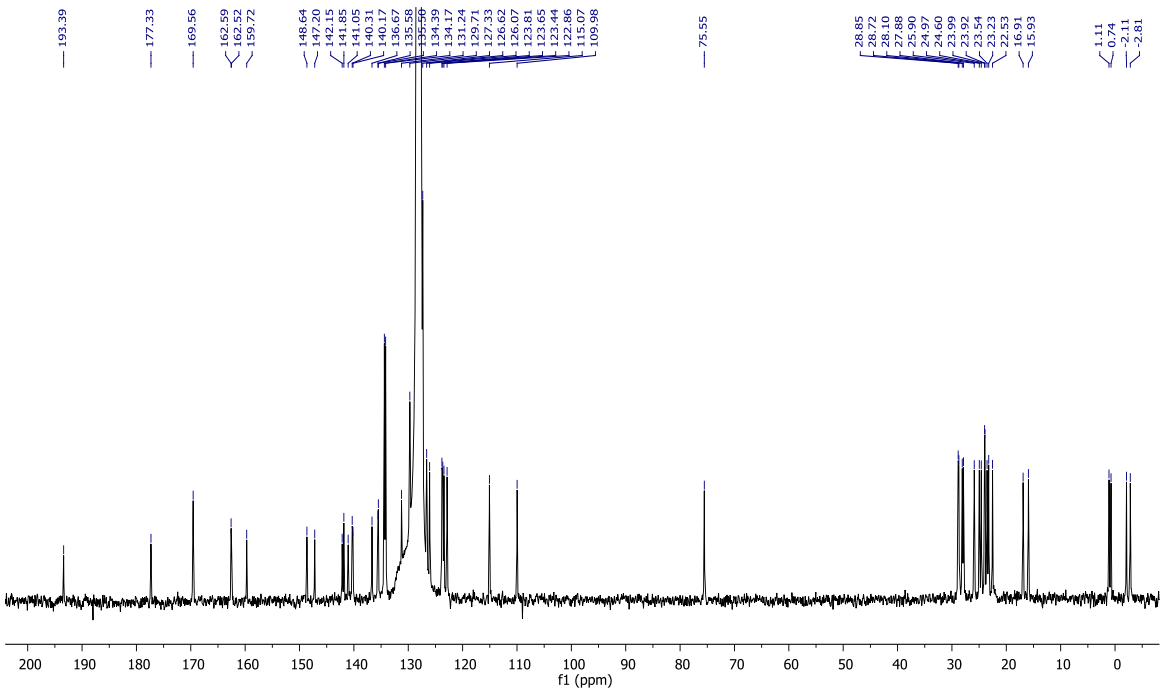

Figure A.9. $^{13}C\{^{1}H\}$ NMR spectrum for **12** (C_6D_6, room temperature).

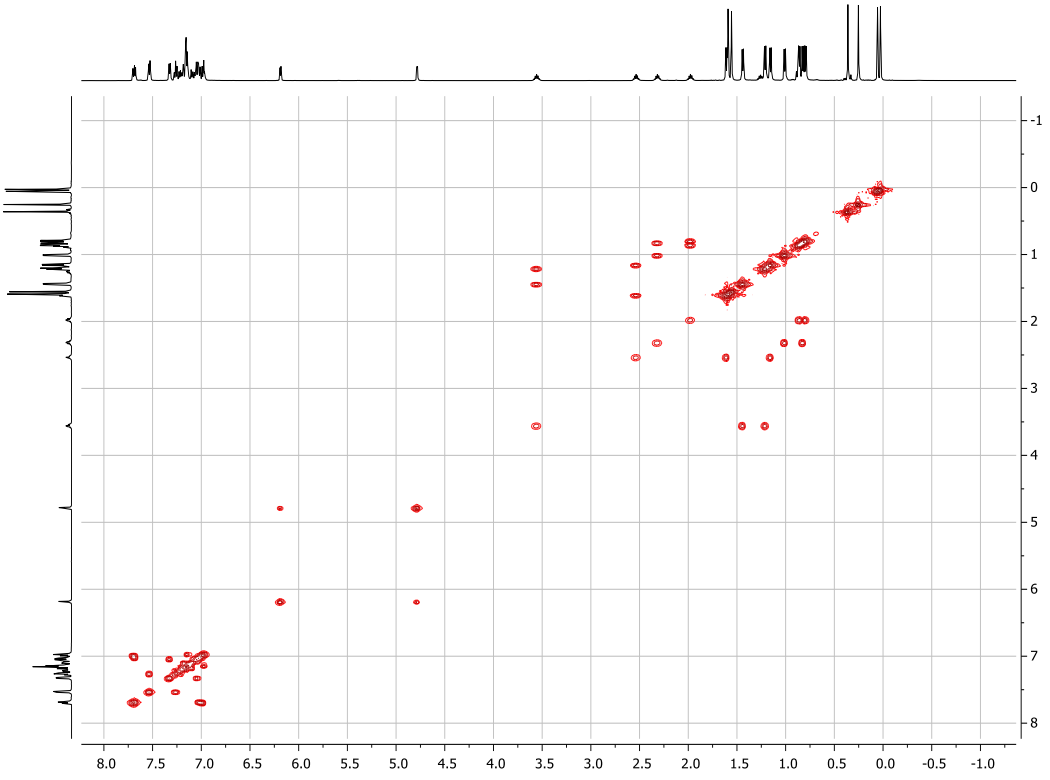

Figure A.10. ^{1}H–^{1}H COSY spectrum for **12** (C_6D_6, room temperature).

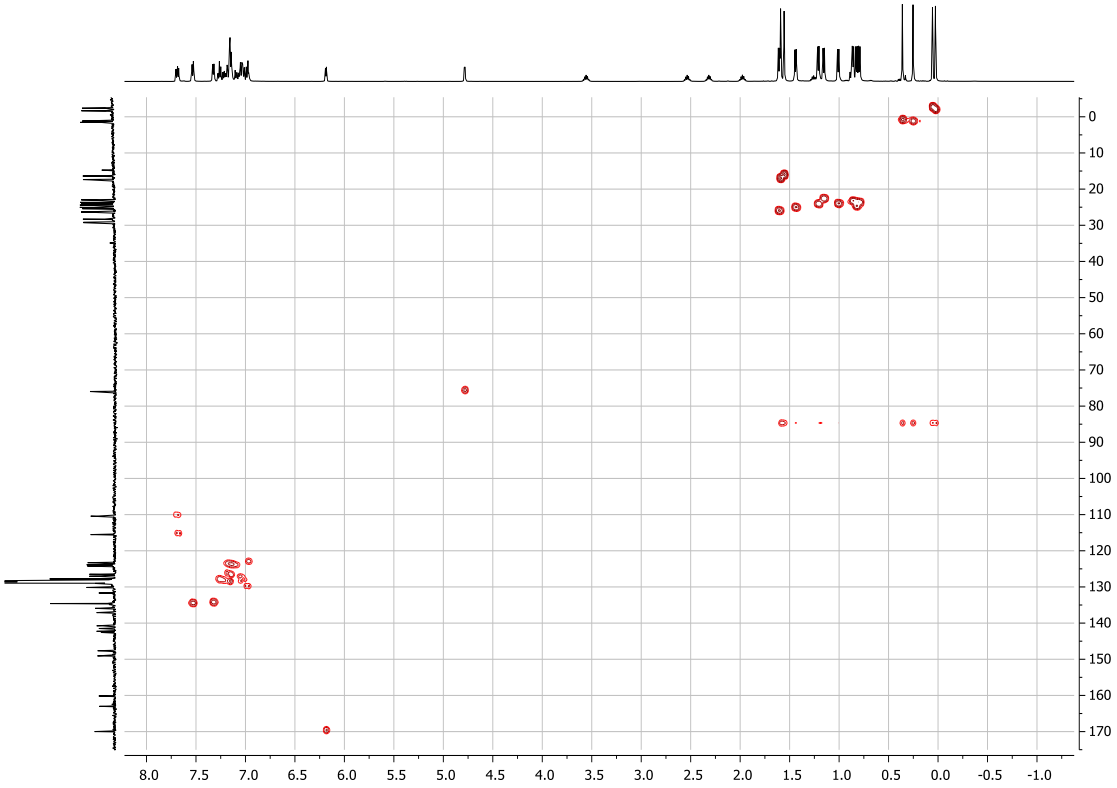

Figure S11. ^{1}H–^{13}C HMQC spectrum for **12** (C_6D_6, room temperature).

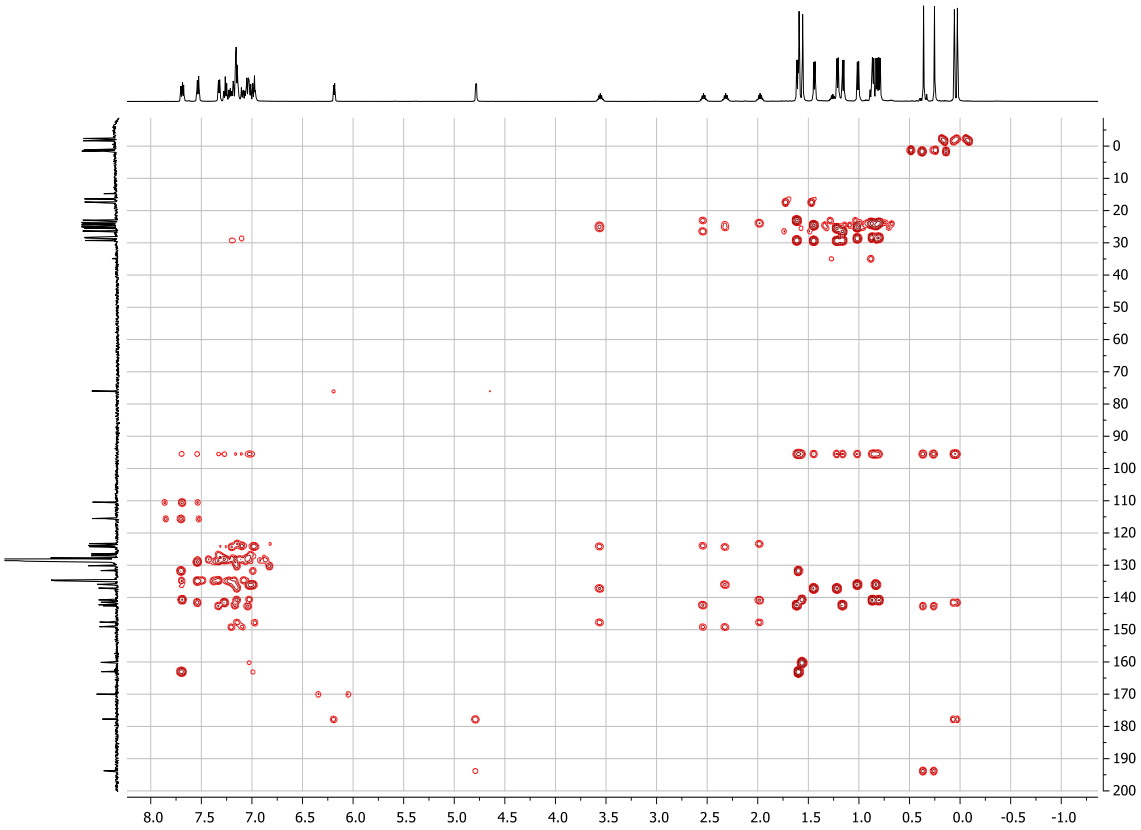

Figure A.12. $^{1}H–^{13}C$ HMBC spectrum for **12** (C_6D_6, room temperature).

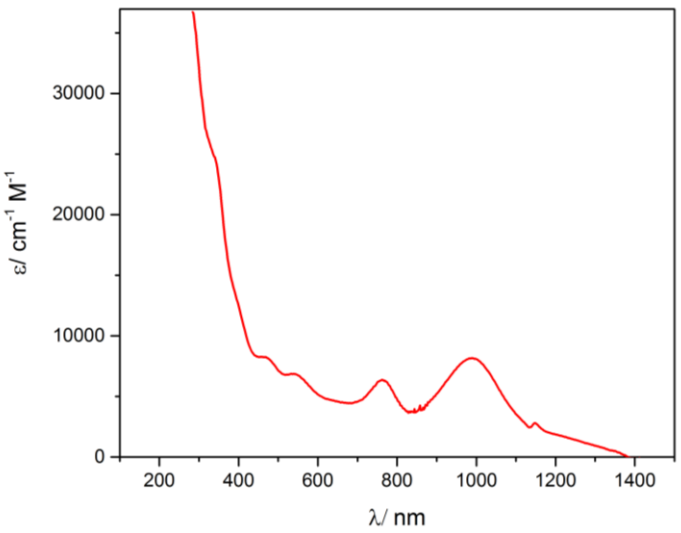

Figure A.13. UV–Vis spectrum for [$^{i\text{-Pr}}$NDI]Ni$_2$(PhMe$_2$SiCCH)$_2$ (**12**) in C_6H_6 (0.031 mM) at room temperature.

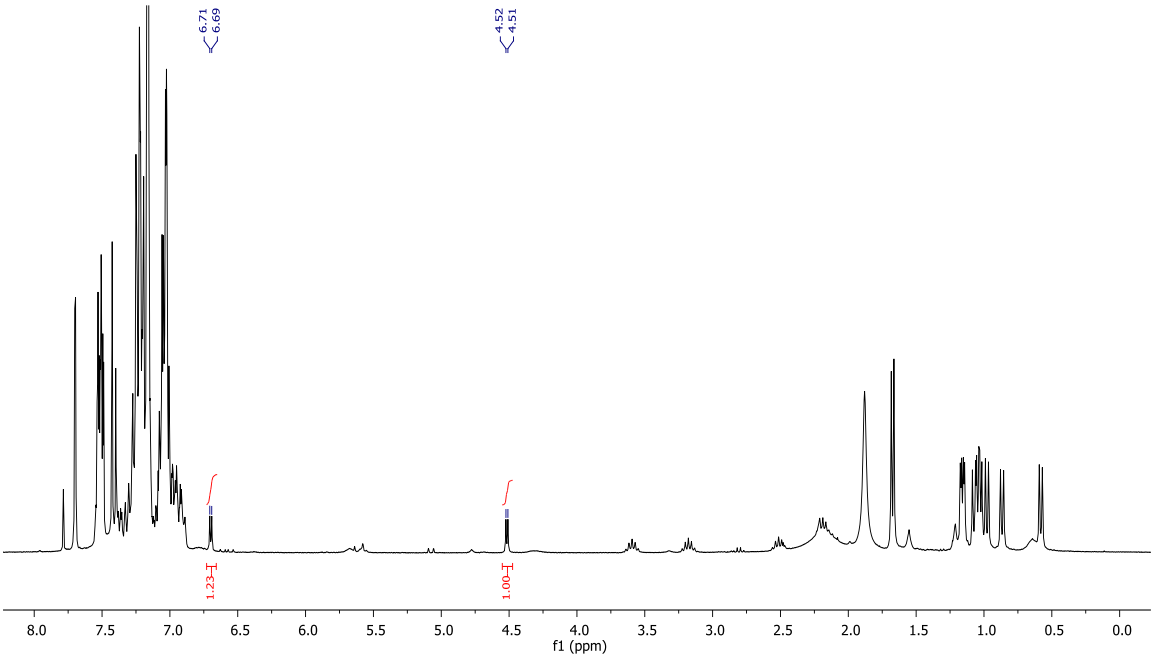

Figure A.14. ^{1}H NMR spectrum (C_6D_6, room temperature) for the crude reaction mixture between **1** and phenylacetylene (10 equiv after a 5 min reaction time at room temperature). The key doublets assigned to the *C*-H groups of a bound butadienyl fragment are highlighted.

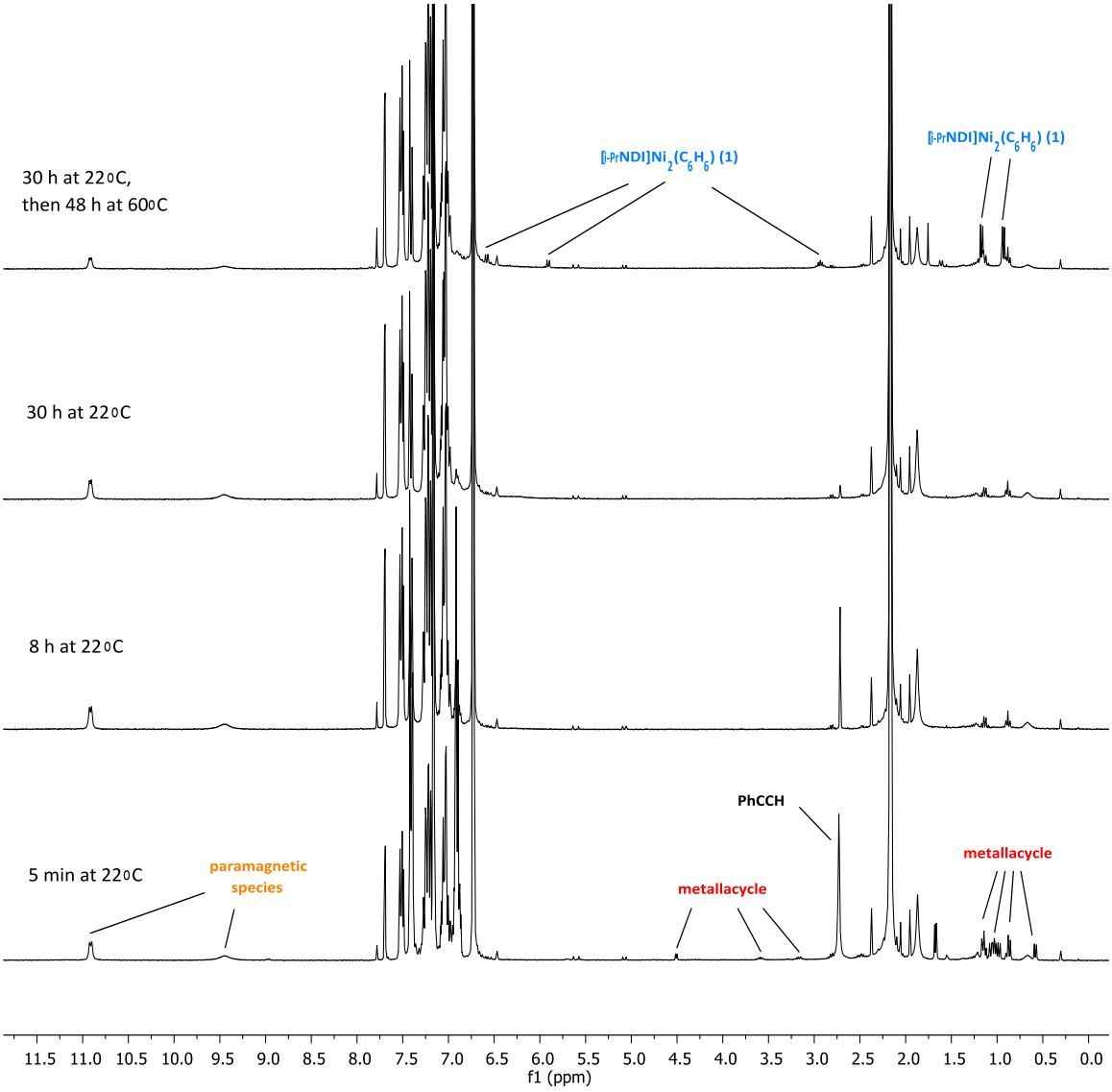

Figure A.15. ^{1}H NMR spectrum (C_6D_6, room temperature) for the cyclotrimerization of phenylacetylene catalyzed by **1** (5 mol%) highlighting the speciation of the catalyst. The reaction was run at room temperature for 30 h. At this time, full conversion of phenylacetylene was observed. The mixture was then heated at 60 °C for an additional 48 h. Three primary catalyst species are observed: a metallacycle with a structure analogous to complex **12**, an unknown paramagnetic species, and the [$^{i\text{-Pr}}$NDI]Ni$_2$(C_6H_6) (**1**).

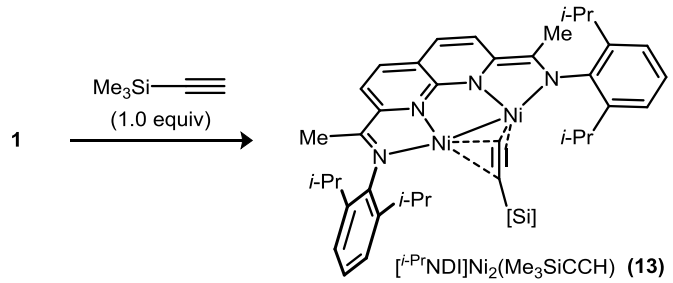

[$^{i\text{-Pr}}$NDI]Ni$_2$(Me$_3$SiCCH) (13). Under an atmosphere of N_2, [$^{i\text{-Pr}}$NDI]Ni$_2$(C_6H_6) (1) (20 mg, 0.027 mmol) was dissolved in C_6H_6 (2.0 mL) in a 20-mL vial. Trimethylsilylacetylene (3.9 μL, 0.027 mmol, 1.0 equiv.) was added, and the reaction was allowed to stir at room temperature for 5 min to produce a green homogeneous solution. The solvent was removed under reduced pressure to obtain [$^{i\text{-Pr}}$NDI]Ni$_2$(Me$_3$SiCCH) (13) (20.5 mg, 99% yield). Single crystals suitable for X-ray diffraction were obtained by slow evaporation of a saturated solution in Et_2O. ^{1}H NMR (300 MHz, C_6D_6) δ 7.07–6.99 (m, 6 H, Ar H), 6.07 (d, J = 8.1 Hz, 2 H, naphthyr H), 5.70 (d, J = 8.1 Hz, 2 H, naphthyr H), 3.40 (sept., J = 6.9 Hz, 4 H, C*H*(CH$_3$)$_2$), 2.44 (s, 1 H, TMSCC*H*), 1.49 (d, J = 6.8 Hz, 12 H, CH(C*H*$_3$)$_2$), 1.19 (s, 6 H, N=CCH$_3$), 1.03 (d, J = 6.8 Hz, 12 H, CH(C*H*$_3$)$_2$), –0.25 (s, 9 H, Si(CH$_3$)$_3$). ^{13}C{^{1}H} NMR (101 MHz, C_6D_6) δ 162.4, 160.8, 140.6, 139.6, 138.8, 128.6, 125.7, 124.5, 123.4, 113.5, 109.0, 79.0 (TMSC*C*H), 78.1 (TMS*C*CH), 28.5, 24.4, 23.9, 14.4, –0.33. UV–vis: (C_6H_6): λ (nm) {ε, cm^{-1} M^{-1}} 521 {1400}, 467 {2000}, 364 {4600}. Anal. Calcd for 13 ([$^{i\text{-Pr}}$NDI]Ni$_2$(Me$_3$SiCCH)): C, 65.80; H, 7.27; N, 7.49. Found: C, 65.74; H, 7.47; N, 7.51.

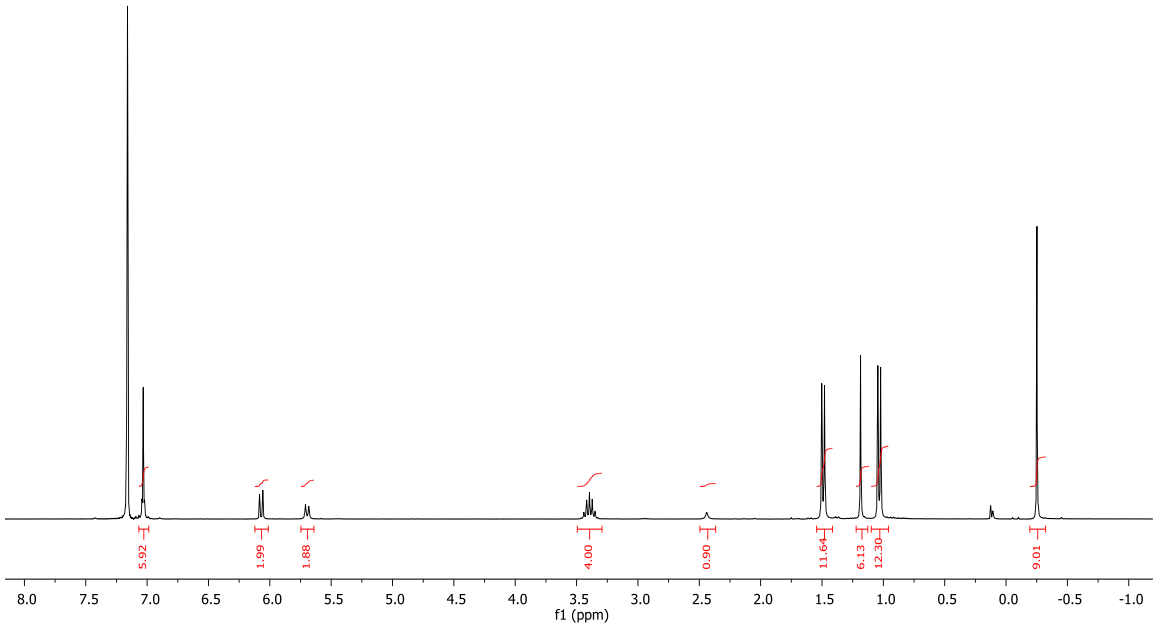

Figure A.16. ^{1}H NMR spectrum for **13** (C_6D_6, room temperature).

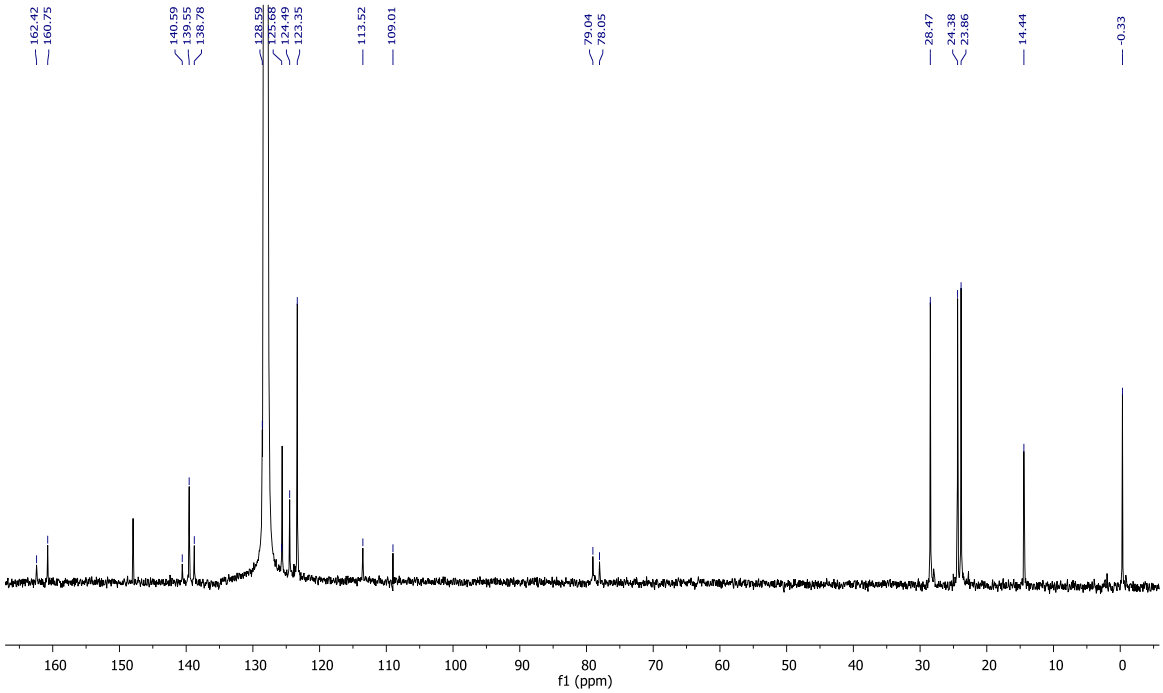

Figure A.17. $^{13}C\{^{1}H\}$ NMR spectrum for **13** (C_6D_6, room temperature).

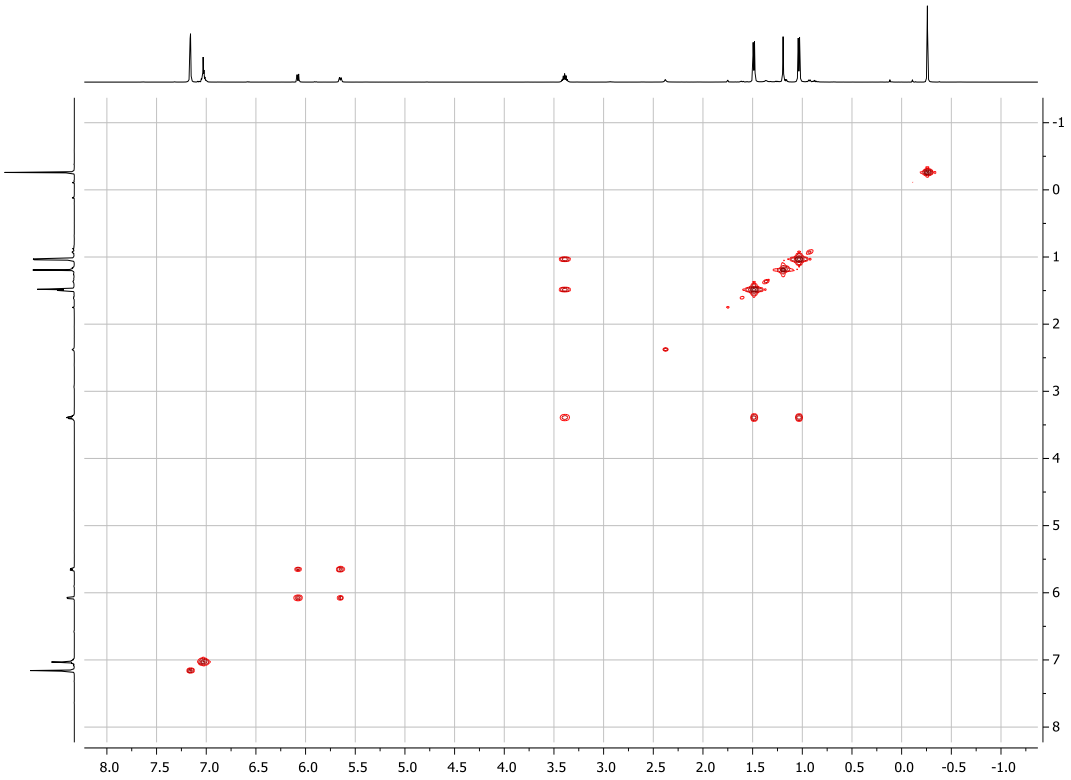

Figure A.18. ^{1}H–^{1}H COSY spectrum for **13** (C_6D_6, room temperature).

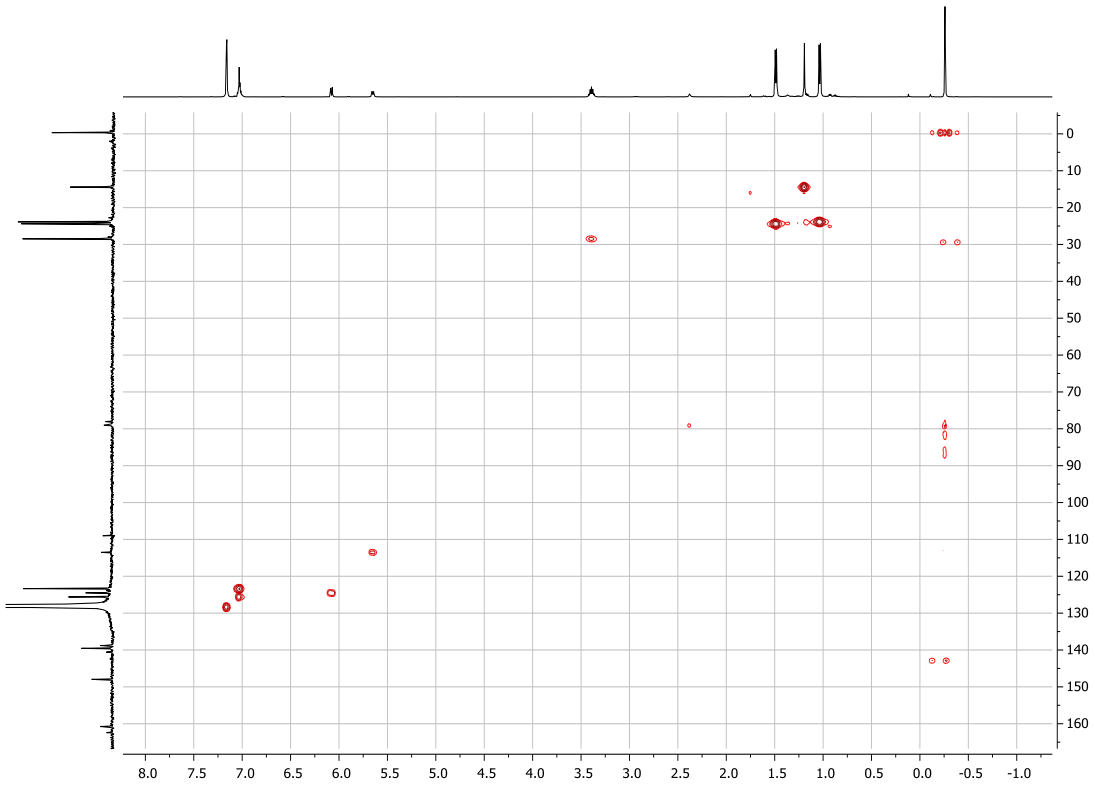

Figure A.19. ^{1}H–^{13}C HMQC spectrum for **13** (C_6D_6, room temperature).

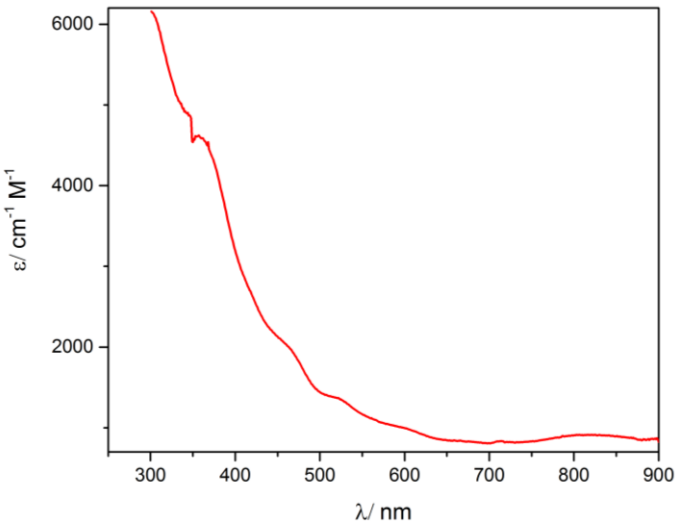

Figure A.20. UV–Vis spectrum for [$^{i\text{-Pr}}$NDI]Ni$_2$(Me$_3$SiCCH) (**13**) in C_6H_6 (0.098 mM) at room temperature.

A.5 . Stoichiometric Reactions of 12 and 13

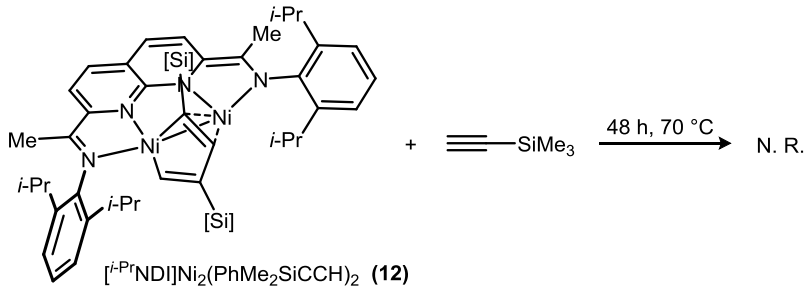

Reversibility of metallacycle formation. Under an atmosphere of N_2, complex **12** (22 mg, 0.023 mmol, 1 equiv.) was dissolved in C_6D_6 (1.5 mL) in a 20-mL vial. Trimethylsilylacetylene (32.2 µL, 10 equiv.) was added to the solution and was allowed to stir for 30 min at room temperature. The resulting reaction mixture was transferred to a J-Young tube and started heating at 70 °C for 48 h. The progress of the reaction was monitored by ^{1}H NMR. No exchange of –$SiMe_2Ph$ for –Me_3Si was observed.

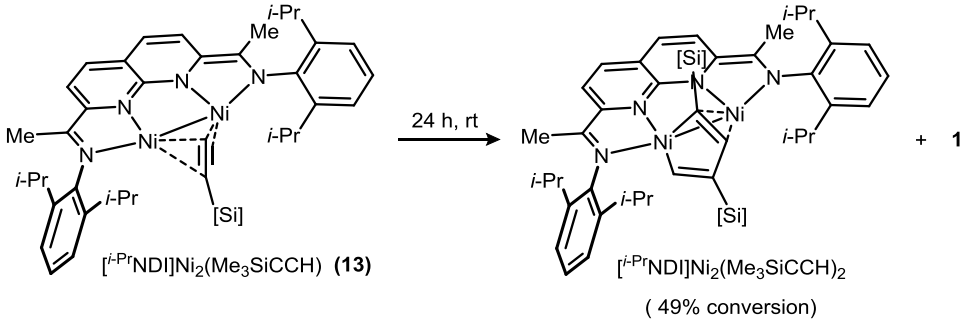

Disproportionation of 13. Under an atmosphere of N_2, freshly prepared complex **13** (15 mg, .020 mmol) was dissolved in C_6D_6 (1 mL) in a 20-mL vial. The green color solution was transferred to a J-Young tube and the disproportionation of complex **13** was monitored by ^{1}H NMR. After 24 h at room temperature, 49% conversion of **13** to form a mixture of the metallacycle and **1**.

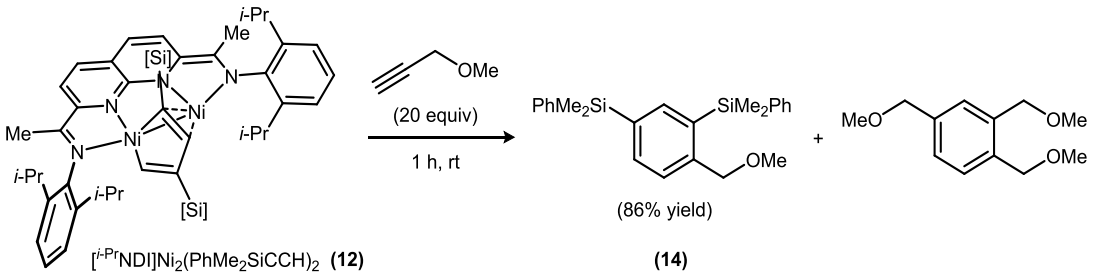

Reaction of 6 with methyl propargyl ether. Under an atmosphere of N_2, complex **12** (17 mg, 0.011 mmol, 1 equiv) was dissolved in C_6D_6 (1.0 mL) in a 20-mL vial. Methyl propargyl ether (30 µL, 0.35 mmol, 20 equiv) and mesitylene (2.4 µL, 0.011 mmol, 1 equiv) were added to the solution, and the reaction mixture was allowed to stir for 1 h at room temperature. Compound **14** was formed in 86% yield (98% relative to recovered **12**) by ^{1}H NMR integration against mesitylene. ^{1}H NMR (300 MHz, C_6D_6) δ 7.98 (d, J = 1.3 Hz, 1 H), 7.59 (dd, J = 7.5, 1.4 Hz, 1 H), 7.55–7.44 (m, 5 H), 7.24–7.16 (m, 5 H), 7.15–7.12 (m, 1 H), 4.31 (s, 2 H), 2.96 (s, 3 H), 0.57 (s, 6 H), 0.51 (s, 6 H); ^{13}C{^{1}H} NMR (101 MHz, C_6D_6) δ 146.0, 142.0, 139.5, 138.4, 136.7, 135.9, 135.7, 134.6, 134.4, 129.4, 129.2, 128.2, 75.0, 57.6, –0.9, –2.2. HRMS (*m*/*z*): $[M + H]^+$ calcd for $C_{24}H_{31}OSi_2$, 391.191; found, 391.190.

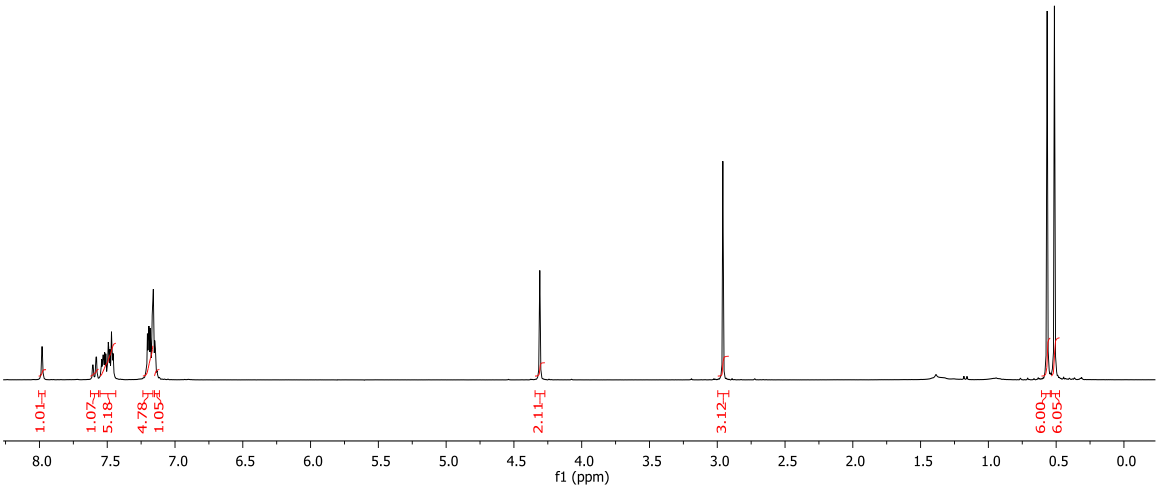

Figure A.21. ^{1}H NMR spectrum for **14** (C_6D_6, room temperature).

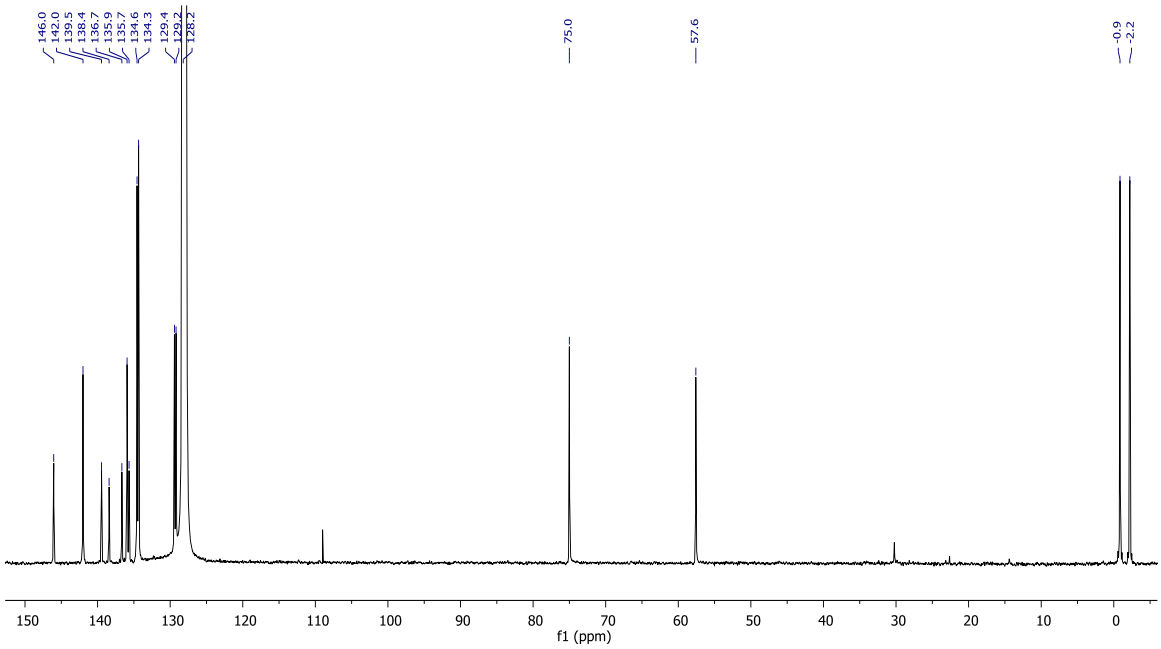

Figure A.22. $^{13}C\{^{1}H\}$ NMR spectrum for **14** (C_6D_6, room temperature).

A.6 XRD Data

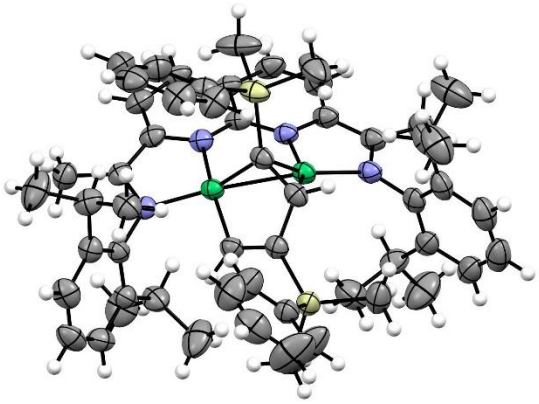

[$^{i\text{-Pr}}$NDI]$Ni_2(Me_2PhSiC_2H)_2$ (**12**): $C_{56}H_{68}N_4Ni_2Si_2$

formula	$C_{56}H_{68}N_4Ni_2Si_2$
formula weight	970.79
space group	P 1 21/n 1 (No. 14)
a, Å	10.4510(2)
b, Å	22.6010(4)
c, Å	22.0156(5)
b, deg	94.4090(10)
V, Å^3	5184.76(18)
Z	4
d_{calc}, g cm^{-3}	1.244
crystal dimensions, mm	0.50x 0.43x 0.28
temperature, K	200.
radiation (wavelength, Å)	Mo K_a (0.71073)
monochromator	graphite
linear abs coef, mm^{-1}	0.812
absorption correction applied	empirical[a]
transmission factors: min, max	0.56, 0.80
diffractometer	Nonius KappaCCD
h, k, l range	0 to 13 0 to 27 -29 to 29
2q range, deg	1.80-56.66
mosaicity, deg	4.63
programs used	SHELXTL
F_{000}	2064.0
data collected	34083
unique data	9125
R_{int}	0.038
data used in refinement	9125

cutoff used in R-factor calculations	$F_o^2>2.0s(F_o^2)$
data with I>2.0s(I)	6401
number of variables	591
largest shift/esd in final cycle	0.00
$R(F_o)$	0.036
$R_w(F_o^2)$	0.087
goodness of fit	1.024

_____

[a] Otwinowski Z. & Minor, W. Methods Enzymol. **1996**,276307.

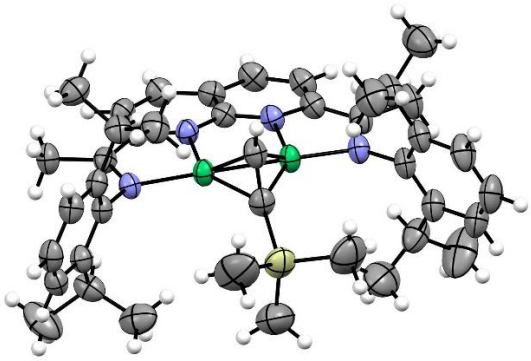

[$^{i\text{-Pr}}$NDI]Ni$_2$(Me$_3$SiC$_2$H) (**13**): $C_{41}H_{54}N_4Ni_2Si$

formula	$C_{41}H_{54}N_4Ni_2Si$
formula weight	748.42
space group	P -1 (No. 2)
a, Å	8.2242(3)
b, Å	14.3806(7)
c, Å	17.7803(6)
a, deg	107.132(4)
b, deg	93.402(3)
g, deg	102.319(3)
V, Å^3	1946.39(14)
Z	2
d_{calc}, g cm^{-3}	1.277
crystal dimensions, mm	0.20x 0.20x 0.18
temperature, K	298.
radiation (wavelength, Å)	Cu K_a (1.54184)
monochromator	graphite
linear abs coef, mm^{-1}	1.737
absorption correction applied	empirical[a]
transmission factors: min, max	0.56, 0.73
diffractometer	Nonius KappaCCD
h, k, l range	0 to 9 -17 to 16 -21 to 21
2q range, deg	5.25-135.83
mosaicity, deg	0.36
programs used	SHELXTL
F_{000}	796.0
data collected	46579
unique data	6835
R_{int}	0.044
data used in refinement	6835
cutoff used in R-factor calculations	$F_o^2>2.0s(F_o^2)$

data with I>2.0s(I)	6369
number of variables	446
largest shift/esd in final cycle	0.00
$R(F_o)$	0.049
$R_w(F_o^2)$	0.138
goodness of fit	1.059

[a] Otwinowski Z. & Minor, W. Methods Enzymol. **1996**,276307.

A.7 DFT Calculations and Optimized Structures

Computational Methods. Geometry optimizations were performed using the Gaussian09 package.[2] All geometries were fully optimized at the M06/6-31G(d,p) level of DFT.[3,4] Stationary points were verified by frequency analysis.

[2] Gaussian 09, Revision **D.01**, Frisch, M. J.; Trucks, G. W.; Schlegel, H. B.; Scuseria, G. E.; Robb, M. A.; Cheeseman, J. R.; Scalmani, G.; Barone, V.; Mennucci, B.; Petersson, G. A.; Nakatsuji, H.; Caricato, M.; Li, X.; Hratchian, H. P.; Izmaylov, A. F.; Bloino, J.; Zheng, G.; Sonnenberg, J. L.; Hada, M.; Ehara, M.; Toyota, K.; Fukuda, R.; Hasegawa, J.; Ishida, M.; Nakajima, T.; Honda, Y.; Kitao, O.; Nakai, H.; Vreven, T.; Montgomery, J. A., Jr.; Peralta, J. E.; Ogliaro, F.; Bearpark, M.; Heyd, J. J.; Brothers, E.; Kudin, K. N.; Staroverov, V. N.; Kobayashi, R.; Normand, J.; Raghavachari, K.; Rendell, A.; Burant, J. C.; Iyengar, S. S.; Tomasi, J.; Cossi, M.; Rega, N.; Millam, N. J.; Klene, M.; Knox, J. E.; Cross, J. B.; Bakken, V.; Adamo, C.; Jaramillo, J.; Gomperts, R.; Stratmann, R. E.; Yazyev, O.; Austin, A. J.; Cammi, R.; Pomelli, C.; Ochterski, J. W.; Martin, R. L.; Morokuma, K.; Zakrzewski, V. G.; Voth, G. A.; Salvador, P.; Dannenberg, J. J.; Dapprich, S.; Daniels, A. D.; Farkas, Ö.; Foresman, J. B.; Ortiz, J. V.; Cioslowski, J.; Fox, D. J. Gaussian, Inc., Wallingford CT, 2009.

[3] Zhao, Y.; Truhlar, D. G. *Theor. Chem. Acc.* **2008**, *120*, 215–241.

[4] (a) Ditchfield, R.; Hehre, W. J.; Pople, J. A. *J. Chem. Phys.* **1971**, *54*, 724. (b) Hehre, W. J.; Ditchfield, R.; Pople, J. A. *J. Chem. Phys.* **1972**, *56*, 2257. (c) Harihan, P. C.; Pople, J. A. *Theor. Chem. Acc.* **1973**, *27*, 213–222.

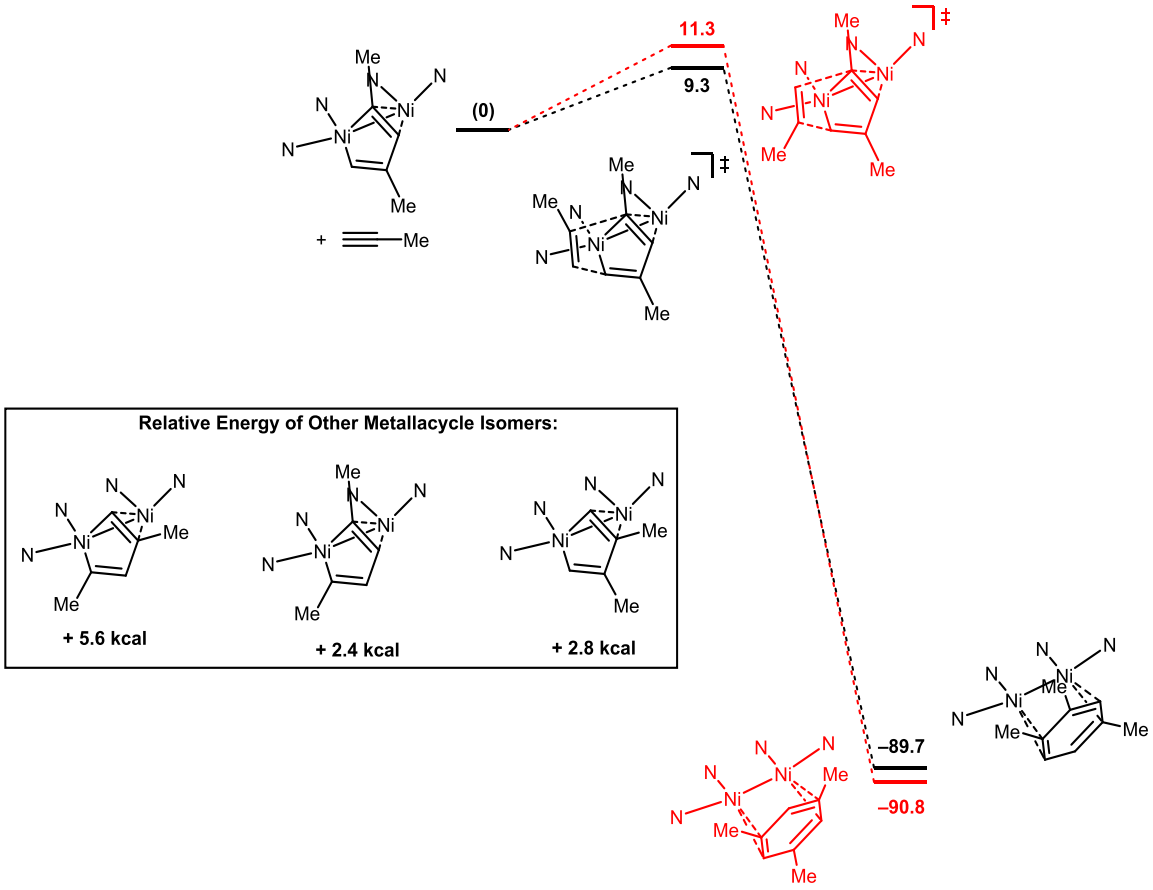

Figure A.23. Relative energies of the metallacycle intermediate, cycloaddition transition state, and arene product for the two pathways forming the 1,2,4- (black) and 1,3,5-regioisomers (red). Relative energies for the other three metallacycle regioisomers are shown.

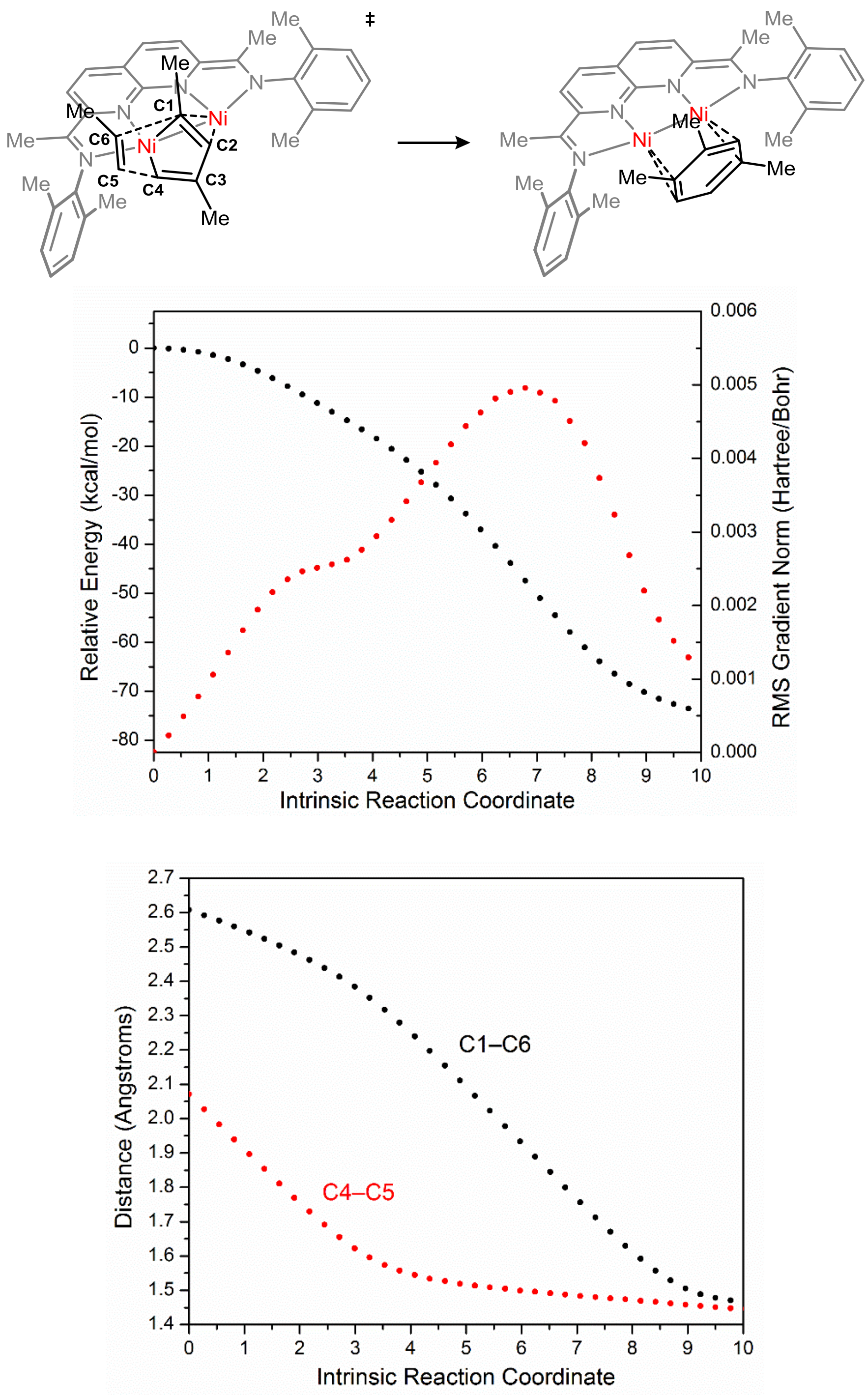

Figure A.24. Intrinsic reaction coordinate calculations (M06/6-31G(d,p)) from the [4+2]-cycloaddition transition state to the arene complex. Top: relative energy and RMS gradient. Bottom: distances for the two forming C–C bonds.

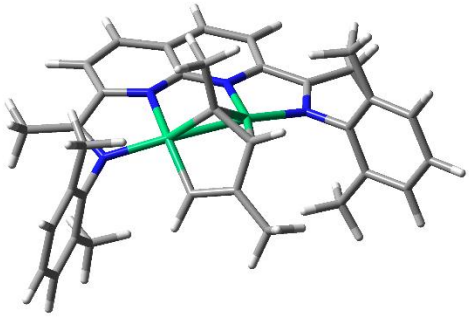

Charge: 0
Multiplicity: 1
Imaginary Frequencies: 0
Energy: –4551.45951010

Ni	-1.16820300	-0.10524300	0.35045200
Ni	1.18072300	0.01219900	0.25484800
N	2.95667400	0.25160900	-0.31206500
N	1.05282200	1.82854400	-0.06977200
N	-1.18365900	1.79610700	0.34978700
N	-3.00670300	0.14223500	-0.04322100
C	4.71495100	1.91896400	-0.80929600
H	5.38086800	1.71326800	0.03807700
H	4.79474100	2.98120500	-1.05157300
H	5.10368100	1.34185800	-1.65755700
C	3.30975300	1.52296000	-0.50404200
C	2.23308200	2.44781000	-0.42212000
C	2.24293500	3.82940200	-0.63552300
H	3.17457300	4.33402800	-0.87992700
C	1.07072000	4.55773700	-0.53858200
H	1.07134500	5.62979900	-0.72281200
C	-0.14966500	3.91742200	-0.22716600
C	-1.42132200	4.52127200	-0.17662900
H	-1.51064700	5.58815900	-0.36903600
C	-2.55332400	3.74405600	0.01870100
H	-3.53891900	4.19857800	-0.04596900
C	-2.43115500	2.36884900	0.21973800
C	-3.45555700	1.38563500	0.12018200
C	-4.91071900	1.71318100	0.17222600
H	-5.43657700	1.36928900	-0.72623700
H	-5.08021400	2.78618400	0.28694400
H	-5.38689300	1.20418200	1.02001500
C	-0.09372600	2.50840800	0.01856000

C	3.93319100	-0.77327400	-0.26703200
C	4.14702500	-1.55860500	-1.40978600
C	5.07512700	-2.59606000	-1.33778600
H	5.25230000	-3.20483600	-2.22341100
C	5.76041800	-2.86340100	-0.15901700
H	6.47689800	-3.68028400	-0.11773800
C	5.51571300	-2.09317900	0.97087200
H	6.03567300	-2.30831100	1.90358100
C	4.60325400	-1.04050800	0.93717900
C	-3.93914100	-0.91162400	-0.23383200
C	-4.38445900	-1.66143900	0.86349800
C	-5.28187100	-2.70268500	0.63411500
H	-5.63490700	-3.28741500	1.48254100
C	-5.71270200	-3.00673700	-0.65106300
H	-6.41209500	-3.82353900	-0.81282000
C	-5.23603500	-2.27348900	-1.72957000
H	-5.55199800	-2.52003800	-2.74237100
C	-4.33948400	-1.22191100	-1.54192500
C	0.15278300	-0.63821100	1.62198600
C	0.90898700	-1.73156000	1.12712100
H	1.71226200	-2.21254100	1.69563800
C	0.19198500	-2.44118200	0.06162900
C	-0.97939400	-1.83892200	-0.26794400
H	-1.64899700	-2.25679200	-1.02971100
C	4.30582200	-0.22759000	2.15912000
H	4.68198400	0.80142800	2.07913300
H	3.22024600	-0.14593800	2.30962700
H	4.75425000	-0.67603400	3.05107600
C	3.36999600	-1.29555800	-2.66305800
H	2.29237700	-1.43374700	-2.49438900
H	3.49389100	-0.26525700	-3.01950400
H	3.67926800	-1.97283500	-3.46550000
C	-3.85358600	-1.38594600	2.23552700
H	-4.40008800	-1.95558900	2.99380000
H	-2.79251100	-1.67004600	2.28565400
H	-3.90104400	-0.32200900	2.50105000
C	-3.78365400	-0.45956100	-2.70608600
H	-4.07444400	0.59906600	-2.69563700
H	-2.68610100	-0.47508800	-2.69220700
H	-4.12568100	-0.88855200	-3.65323400
C	0.75946900	-3.68489100	-0.53922800
C	0.07540200	-0.15978100	3.02401700

H	0.11883500	-4.07436800	-1.33718100
H	1.76111900	-3.50095900	-0.95570100
H	0.88106600	-4.47122200	0.21858700
H	0.97921400	-0.44075200	3.58621700
H	-0.06205100	0.92641900	3.08878400
H	-0.77486500	-0.62905600	3.54156300

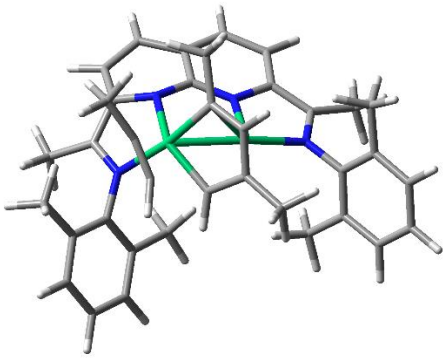

Charge: 0
Multiplicity: 1
Imaginary Frequencies: 1
Energy: –4668.00477695

Ni	-1.21429600	0.10757000	0.83808100
Ni	1.08865900	0.13777000	0.40809500
N	2.81462400	0.25659200	-0.42246300
N	0.84418500	1.82285400	-0.31819300
N	-1.39962800	1.90841400	0.27552900
N	-2.74288400	-0.10433000	-0.40876000
C	4.35486000	1.75826700	-1.63104300
H	4.53407100	1.03850100	-2.43979500
H	5.20718700	1.67132400	-0.94600900
H	4.36287400	2.76179300	-2.06108200
C	3.06430900	1.45263000	-0.94362900
C	1.99481800	2.38402200	-0.86278200
C	1.94989000	3.68973200	-1.34512100
H	2.84873400	4.15140400	-1.74633600
C	0.75769700	4.39573200	-1.34009700
H	0.71497100	5.40583200	-1.74217000
C	-0.43249600	3.79391700	-0.88593300
C	-1.73130100	4.32588400	-1.02592300
H	-1.85385600	5.32034200	-1.44904500
C	-2.82213200	3.47839600	-0.87068900
H	-3.79414400	3.77634200	-1.25844500
C	-2.63805700	2.20491900	-0.33818300
C	-3.36907900	1.04172100	-0.66816500
C	-4.68971300	1.07813400	-1.36756700
H	-4.63123600	0.53279200	-2.31812700
H	-5.01239000	2.09999800	-1.57816500
H	-5.47265100	0.59111000	-0.77402400

C	-0.31818600	2.48358700	-0.29882600
C	3.79156500	-0.76317800	-0.42991400
C	3.70313700	-1.78767400	-1.38590700
C	4.63242600	-2.82580400	-1.34021900
H	4.57013300	-3.61937900	-2.08388700
C	5.61986600	-2.85999800	-0.36379700
H	6.33584200	-3.67804400	-0.33924000
C	5.68267900	-1.84944700	0.58809000
H	6.44377200	-1.87900000	1.36697500
C	4.77323300	-0.79276600	0.57535500
C	-3.22396400	-1.34891200	-0.85942800
C	-4.24818800	-2.05229800	-0.20368300
C	-4.57475300	-3.33354600	-0.65733300
H	-5.36670500	-3.88150100	-0.14640800
C	-3.91399800	-3.90856500	-1.73154200
H	-4.18064100	-4.90859400	-2.06570700
C	-2.91060800	-3.19727500	-2.38267400
H	-2.39363300	-3.63639900	-3.23510900
C	-2.55432200	-1.91975300	-1.96347400
C	0.17649700	0.58853800	2.12599700
C	1.01302600	-0.45016800	2.46909000
H	1.72841800	-0.42684800	3.29452600
C	0.95433600	-1.55090600	1.54244200
C	-0.18856500	-1.50936200	0.70525700
C	4.80099700	0.26214500	1.63957200
H	5.09124700	1.24758800	1.25191700
H	3.80569000	0.39005100	2.08673300
H	5.50908500	-0.00052600	2.43196700
C	2.60428900	-1.77641900	-2.40260200
H	1.62934000	-1.94521000	-1.92215600
H	2.52086800	-0.80982000	-2.91456000
H	2.75317600	-2.55708000	-3.15561600
C	-5.00600400	-1.47281400	0.95556100
H	-4.98575700	-2.14958200	1.81946500
H	-4.59042200	-0.51412400	1.27767300
H	-6.06272200	-1.32053600	0.69763700
C	-1.48941000	-1.13667800	-2.66803400
H	-1.88751000	-0.20063800	-3.08285300
H	-0.68882900	-0.83722600	-1.97582200
H	-1.05214500	-1.71419300	-3.48958700
C	1.89459900	-2.71455200	1.60018900
C	0.15445200	1.89630500	2.84456400

H	1.92740300	-3.24844000	0.64339700
H	2.91945900	-2.40025400	1.83480900
H	1.57670800	-3.42816200	2.37177400
H	0.59430700	1.79420600	3.84649100
H	0.73266900	2.65664000	2.30257000
H	-0.85897000	2.30158100	2.94480200
H	-0.43914700	-2.37033600	0.07785000
C	-1.83473300	-1.50019200	1.96273500
C	-2.18450900	-0.43793400	2.54245100
H	-2.02047600	-2.54602900	1.77691400
C	-2.86995800	0.41142300	3.51495700
H	-3.35393900	1.26062000	3.01484500
H	-3.63363000	-0.14976900	4.06866700
H	-2.15960200	0.82464300	4.24123800

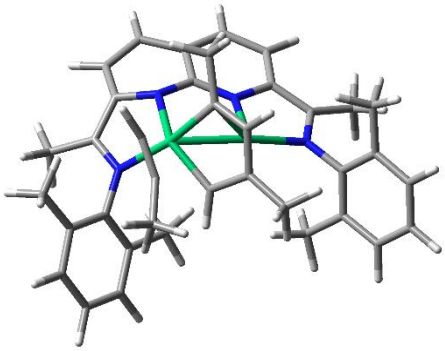

Charge: 0
Multiplicity: 1
Imaginary Frequencies: 1
Energy: –4668.00158962

Ni	-1.18504500	0.16795300	0.89025500
Ni	1.10970500	0.13690400	0.42444100
N	2.81223500	0.24664900	-0.45408800
N	0.92435500	1.88770100	-0.14081000
N	-1.30336800	2.02435200	0.51002300
N	-2.76763200	0.14755100	-0.31552200
C	4.38442900	1.78808800	-1.57494400
H	5.24268300	1.30837700	-1.09228800
H	4.57229700	2.86288400	-1.62644900
H	4.34985500	1.40313900	-2.60322900
C	3.10978300	1.47590100	-0.86125500
C	2.09013300	2.44307000	-0.66177200
C	2.10016700	3.78892600	-1.01996700
H	3.01163800	4.24141300	-1.40294400
C	0.94500600	4.54622400	-0.92087100
H	0.94388900	5.59091100	-1.22463400
C	-0.26493800	3.95973400	-0.49874400
C	-1.53672700	4.56361500	-0.56287400
H	-1.61679900	5.59714100	-0.89189200
C	-2.66501000	3.75782400	-0.46060900
H	-3.62785900	4.13404000	-0.79933700
C	-2.53392400	2.43489900	-0.04793100
C	-3.33396300	1.34531000	-0.45697900
C	-4.67077600	1.51601100	-1.10358100
H	-4.70680700	0.96178100	-2.04963100
H	-4.89187200	2.56513700	-1.31023300
H	-5.47490100	1.11929800	-0.47210500

C	-0.20476200	2.59641200	-0.03499000
C	3.73878800	-0.81282600	-0.55820900
C	3.58089500	-1.76550400	-1.57728800
C	4.45729500	-2.84885400	-1.62018700
H	4.34025400	-3.58842600	-2.41148200
C	5.46140600	-2.99642700	-0.67179600
H	6.13461900	-3.84917800	-0.71704800
C	5.59598500	-2.05417400	0.34071500
H	6.37132300	-2.17133800	1.09698800
C	4.74016100	-0.95634200	0.41860000
C	-3.36764700	-1.02277200	-0.81817000
C	-4.46015700	-1.64839700	-0.19257400
C	-4.91526900	-2.86728000	-0.70328100
H	-5.75598000	-3.35737400	-0.21185300
C	-4.31359800	-3.45870800	-1.80339400
H	-4.67859500	-4.41118400	-2.18080100
C	-3.24714300	-2.81982600	-2.42921100
H	-2.78222100	-3.26531600	-3.30793500
C	-2.76741900	-1.60188200	-1.95804500
C	0.24655900	0.46593000	2.19262900
C	1.05227700	-0.62841700	2.42216600
H	1.77945000	-0.70542000	3.23373900
C	0.92595000	-1.63934600	1.40790300
C	-0.23510700	-1.47870600	0.60799600
C	4.85030600	0.02887400	1.54283000
H	5.18861900	1.01740400	1.20465600
H	3.87443200	0.18697200	2.02234000
H	5.55946100	-0.32039600	2.30006100
C	2.46392700	-1.63555800	-2.56585800
H	1.49123000	-1.79787900	-2.07839600
H	2.41206700	-0.63216100	-3.00568500
H	2.56555700	-2.36621500	-3.37474500
C	-5.14857400	-1.06189500	1.00526300
H	-5.28605300	-1.81925900	1.78728700
H	-4.58560300	-0.23092800	1.43870500
H	-6.15170100	-0.69592900	0.74604200
C	-1.65932800	-0.87955700	-2.66058200
H	-2.00585200	0.08745900	-3.04983800
H	-0.82839100	-0.64538400	-1.98009200
H	-1.27674200	-1.46688400	-3.50225100
C	1.81298800	-2.84444700	1.34780500
C	0.27038200	1.69116000	3.04432800

H	1.77986000	-3.31659200	0.35932000
H	2.85991400	-2.59075500	1.55605400
H	1.49794900	-3.59275300	2.08822300
H	0.81506500	1.49555100	3.97803600
H	0.76911700	2.52669400	2.53660000
H	-0.73755600	2.03939400	3.29562400
H	-0.50828300	-2.26904300	-0.09685500
C	-1.83109000	-1.59582900	1.95004500
C	-2.05929600	-0.50607800	2.54607000
C	-2.12424400	-3.03487800	1.78964900
H	-2.42872900	-3.27590600	0.76441200
H	-1.25067800	-3.64956300	2.03768000
H	-2.94629900	-3.31461900	2.45836500
H	-2.49276200	0.04951000	3.35956800

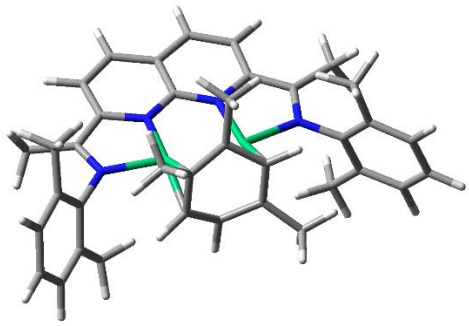

Charge: 0
Multiplicity: 1
Imaginary Frequencies: 0
Energy: –4668.16251770

Ni	-1.25855400	-0.05591800	0.10316200
Ni	1.22828100	-0.06164700	0.03060900
N	3.13436900	0.30164800	-0.01440600
N	1.11709900	1.80294700	-0.00538600
N	-1.15771100	1.79858900	-0.02450700
N	-3.16380300	0.27998600	-0.15218800
C	4.85804400	2.07393600	0.10594300
H	5.37571700	1.62351100	0.96226000
H	4.92449600	3.15853800	0.20554800
H	5.42705500	1.77990000	-0.78480900
C	3.44208400	1.59996800	0.03760800
C	2.33980200	2.47291800	0.04072900
C	2.38183300	3.86432400	0.06765000
H	3.33935700	4.37579700	0.11010300
C	1.21486100	4.60120300	0.03190200
H	1.23862600	5.68843800	0.03816800
C	-0.02757800	3.94323300	-0.02012600
C	-1.27360100	4.59157100	-0.08810700
H	-1.30453200	5.67859600	-0.10057900
C	-2.43462000	3.84639800	-0.16574800
H	-3.39553500	4.34854000	-0.23828300
C	-2.38089900	2.45637400	-0.14209300
C	-3.47355800	1.57380500	-0.24482100
C	-4.87181500	2.05293600	-0.47072800
H	-5.38618900	1.42253300	-1.20450200
H	-4.88954400	3.08086000	-0.83821700
H	-5.46892500	2.01534100	0.44966300

C	-0.02173000	2.50553500	-0.01357300
C	4.21626700	-0.60600600	-0.13728900
C	4.72706900	-0.87030400	-1.42409500
C	5.75418600	-1.79849400	-1.56239700
H	6.14326000	-2.01036900	-2.55754500
C	6.27412200	-2.46093000	-0.45465700
H	7.06847000	-3.19313000	-0.57898100
C	5.78012700	-2.17517500	0.80852200
H	6.19657000	-2.67302800	1.68415100
C	4.75974100	-1.23756200	0.99114700
C	-4.20726100	-0.66443300	-0.32473300
C	-5.07462100	-0.98745900	0.73228200
C	-6.04237100	-1.97321200	0.52800400
H	-6.70568300	-2.23409200	1.35233100
C	-6.16878200	-2.61423900	-0.69546500
H	-6.92446300	-3.38374800	-0.83454100
C	-5.32944300	-2.26086700	-1.74519400
H	-5.43429500	-2.74338000	-2.71619100
C	-4.34913600	-1.28453700	-1.58160700
C	0.11074500	-1.31382400	1.58886300
C	1.25496700	-1.80979000	0.87381600
H	2.17896300	-2.03924500	1.40325500
C	1.13279400	-2.05197600	-0.51189300
C	-0.15534700	-1.84932900	-1.07723800
C	4.31514900	-0.89380000	2.38375700
H	5.12942800	-0.41216200	2.94106000
H	3.46348200	-0.20698500	2.38217900
H	4.03577300	-1.79080600	2.95196200
C	4.15257100	-0.18006200	-2.62430800
H	3.05676900	-0.24705400	-2.64193800
H	4.38648800	0.89278000	-2.63725500
H	4.54479100	-0.61442500	-3.54973400
C	-5.00050100	-0.28944500	2.05840900
H	-5.14895700	-0.99568500	2.88375000
H	-4.04003700	0.21580800	2.20108400
H	-5.78921100	0.47014100	2.14798400
C	-3.49070800	-0.86204300	-2.73526700
H	-3.82146600	0.10348800	-3.14283300
H	-2.44706500	-0.71608800	-2.43343400
H	-3.53312100	-1.59398100	-3.54841000
C	2.16370400	-2.78579400	-1.31137800
C	0.29147000	-0.93309900	3.03042300

H	2.31608100	-2.33540000	-2.29978300
H	3.12928100	-2.84665000	-0.80507900
H	1.81106000	-3.81175300	-1.47801700
H	0.11287700	-1.78532800	3.70261000
H	1.30964100	-0.57220600	3.21228600
H	-0.39300800	-0.12996600	3.32658500
H	-0.26958300	-1.98602900	-2.15176900
C	-1.30256900	-1.98928600	-0.25054400
C	-1.18014100	-1.75936000	1.13993100
H	-2.24296400	-2.34999600	-0.66372300
C	-2.23907000	-2.15555300	2.11837900
H	-2.41545700	-1.38877300	2.88126800
H	-3.18799100	-2.36960500	1.61736000
H	-1.92688200	-3.06847600	2.64521000

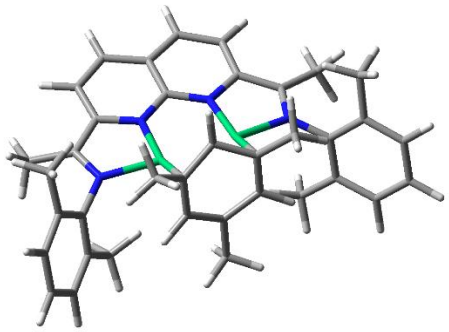

Charge: 0
Multiplicity: 1
Imaginary Frequencies: 0
Energy: –4668.16437521

Ni	-1.24892100	0.01595600	-0.34780500
Ni	1.24892700	0.01598000	-0.34775800
N	3.13807400	0.31955600	-0.00874500
N	1.13713300	1.84346600	-0.01821700
N	-1.13684500	1.84344800	-0.01821100
N	-3.13787800	0.31961500	-0.00823000
C	4.83260400	2.04132900	0.53936200
H	5.20943500	1.46639500	1.39473000
H	4.86916900	3.09956300	0.80404700
H	5.53658700	1.87062900	-0.28453900
C	3.44790300	1.60250000	0.18942400
C	2.36213400	2.49605000	0.10783600
C	2.41217500	3.88487000	0.19403400
H	3.37306000	4.38690100	0.27007300
C	1.24803900	4.62940200	0.17834800
H	1.27818300	5.71445200	0.24601100
C	0.00014900	3.98129400	0.11715600
C	-1.24770800	4.62939400	0.17880000
H	-1.27783800	5.71444000	0.24652500
C	-2.41182400	3.88482800	0.19491300
H	-3.37269700	4.38680800	0.27143200
C	-2.36177400	2.49602100	0.10858200
C	-3.44757500	1.60251400	0.19028600
C	-4.83213400	2.04135000	0.54080100
H	-5.53674600	1.86956200	-0.28232400
H	-4.86879500	3.09982600	0.80447600
H	-5.20809200	1.46710600	1.39702900

C	0.00014700	2.54878900	0.00946300
C	4.13806000	-0.65158000	0.25327300
C	5.09477200	-0.99893300	-0.71430100
C	6.00077200	-2.02185600	-0.42480500
H	6.73381300	-2.29927900	-1.18185400
C	5.97932500	-2.67805800	0.79677400
H	6.68655400	-3.47846300	1.00064200
C	5.05627700	-2.29616600	1.76365400
H	5.04770200	-2.78689000	2.73622000
C	4.13827000	-1.27907000	1.51515900
C	-4.13807500	-0.65144000	0.25325800
C	-4.13845800	-1.27960900	1.51477400
C	-5.05677600	-2.29656300	1.76273700
H	-5.04833800	-2.78781000	2.73504200
C	-5.97992400	-2.67767900	0.79565300
H	-6.68740100	-3.47797500	0.99908800
C	-6.00109100	-2.02090200	-0.42563200
H	-6.73417000	-2.29775200	-1.18285200
C	-5.09477900	-0.99810700	-0.71459100
C	-0.00050400	-2.08356500	0.63245100
C	1.21467600	-2.01871100	-0.09135500
H	2.12161400	-2.43146000	0.35329200
C	1.23423000	-1.58515200	-1.43943400
C	0.00026600	-0.99228000	-1.89267500
C	3.19618600	-0.81536500	2.58433000
H	3.52701900	0.13993900	3.01570000
H	2.19127800	-0.63490300	2.18343900
H	3.13196900	-1.54275300	3.40069800
C	5.18379600	-0.28455000	-2.03127300
H	4.27002000	0.27482800	-2.25297100
H	6.01937300	0.42881700	-2.03518300
H	5.36693500	-0.98877300	-2.85141400
C	-3.19620500	-0.81679700	2.58419500
H	-3.13129700	-1.54519300	3.39961800
H	-2.19153400	-0.63535900	2.18318300
H	-3.52743100	0.13774600	3.01695000
C	-5.18358800	-0.28304900	-2.03122200
H	-6.01843700	0.43117300	-2.03451700
H	-4.26937500	0.27552600	-2.25312500
H	-5.36776500	-0.98674100	-2.85158900
C	2.31604300	-1.92926900	-2.40864200
C	-0.00099100	-2.48523100	2.07729700

H	2.47351500	-1.12592500	-3.13924700
H	3.26423900	-2.14710400	-1.90720100
H	2.02903600	-2.82806700	-2.97118300
H	-0.88792300	-3.08377800	2.31905200
H	0.88414500	-3.08647100	2.31897400
H	0.00033600	-1.62459600	2.75975300
H	0.00064200	-0.59210800	-2.90866500
C	-1.23407500	-1.58488800	-1.44013300
C	-1.21521700	-2.01877900	-0.09215300
C	-2.31558600	-1.92875100	-2.40974000
H	-3.26436500	-2.14510200	-1.90876500
H	-2.47154100	-1.12600400	-3.14131600
H	-2.02921700	-2.82847300	-2.97113300
H	-2.12247500	-2.43150500	0.35185900

APPENDIX B. CHAPTER 2

B.1 General Information

General considerations. All manipulations were carried out using standard Schlenk or glovebox techniques under an atmosphere of N_2. Solvents were dried and degassed by passing through a column of activated alumina and sparging with Ar gas. Deuterated solvents were purchased from Cambridge Isotope Laboratories, degassed, and stored over activated 3 Å molecular sieves prior to use. All other reagents and starting materials were purchased from commercial vendors and used without further purification unless otherwise noted. Liquid reagents were degassed and stored over activated 3 Å molecular sieves prior to use. The [$^{i\text{-Pr}}$NDI]$Ni_2(C_6H_6)$ complex **1** was prepared according to previously reported procedures.[i] Zn powder (325 mesh, 99.9%) was purchased from Strem Chemicals, stored under inert atmosphere, and used without further purification.

Physical methods. ^{1}H, ^{19}F and ^{13}C{^{1}H} NMR spectra were collected at room temperature on a Varian INOVA 300 MHz or a Bruker AV500HD NMR spectrometer. ^{1}H and ^{13}C{^{1}H} NMR spectra are reported in parts per million relative to tetramethylsilane, using the residual solvent resonances as an internal standard. High-resolution mass data were obtained using a Thermo Scientific LTQ Orbitrap XL mass spectrometer or a Thermo Electron Corporation MAT 95XP-Trap mass spectrometer. ATR- IR data were collected on a Thermo Scientific Nicolet Nexus spectrometer containing a MCT* detector and KBr beam splitter with a range of 350–7400 cm^{-1}. UV–vis measurements were acquired on an **Agilent Cary 6000i UV-Vis-NIR Spectrophotometer** using a 1- cm two- window quartz cuvette. Elemental analyses were performed by Midwest Microlab (Indianapolis, IN).

X-ray crystallography. Single-crystal X-ray diffraction studies were carried out at the Purdue X-ray crystallography facility using a Rigaku Rapid II diffractometer or a Bruker AXS D8 Quest CMOS diffractometer.

Procedure for XRD data collected using the Rigaku Rapid II instrument. Single crystal X-ray measurements were conducted on a Rigaku Rapid II curved image plate diffractometer with a Cu-Kα X-ray microsource (λ = 1.54178 Å) with a laterally graded multilayer (Goebel) mirror for monochromatization. Single crystals were mounted on Mitegen microloop mounts using a trace of mineral oil and cooled in-situ to 150(2) K for data collection. Data were collected using the dtrek option of CrystalClear-SM Expert 2.1 b32.[ii] Data were processed using HKL3000 and data were corrected for absorption and scaled using Scalepack.[iii]

Procedure for XRD data collected using the Bruker Quest instrument. Single crystals of were coated with mineral oil or fomblin and quickly transferred to the goniometer head of a Bruker Quest diffractometer with kappa geometry, an I-μ-S microsource X-ray tube, laterally graded multilayer (Goebel) mirror single crystal for monochromatization, a Photon2 CMOS area detector and an Oxford Cryosystems low temperature device. Examination and data collection were performed with Cu Kα radiation (λ = 1.54178 Å) at 100 K. Data were collected, reflections were indexed and processed, and the files scaled and corrected for absorption using APEX3.[4]

Structure Solution and Refinement. The space groups were assigned and the structures were solved by direct methods using XPREP within the SHELXTL suite of programs[iv] and refined by full matrix least squares against F^2 with all reflections using Shelxl2016[v] using the graphical interface Shelxle.[vi] If not specified otherwise H atoms attached to carbon and nitrogen atoms were positioned geometrically and constrained to ride on their parent atoms, with carbon hydrogen bond distances of 0.95 Å for and aromatic C-H, 1.00, 0.99 and 0.98 Å for aliphatic C-H, CH_2 and CH_3 moieties, respectively. Methyl H atoms were allowed to rotate but not to tip to best fit the experimental electron density. U_{iso}(H) values were set to a multiple of U_{eq}(C) with 1.5 for CH_3, and 1.2 for C-H units, respectively. Additional data collection and refinement details, including description of disorder and/or twinning (where present) can be found in Section 9.

B.2 Synthesis and Characterization of Novel 1,1-Dichloroalkenes

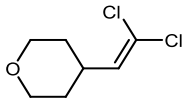

4-(2,2-dichlorovinyl)tetrahydro-2H-pyran.[8] Under an N_2 atmosphere, a 100-mL Schlenk flask was charged with Ph_3P (10.5 g, 40 mmol, 4.0 equiv) and a magnetic stir bar. MeCN (20 mL) was added, and the solution was stirred at 0 °C. Tetrahydro-2H-pyran-4-carbaldehyde (1.14 g, 10 mmol, 1.0 equiv) and CCl_4 (1.9 mL, 20 mmol, 2.0 equiv) were added sequentially by syringe, and stirring was continued at 0 °C. After 5 min, the reaction was allowed to warm to room temperature and monitored by TLC. After full consumption of Ph_3P (approx. 2 h), the reaction mixture was quenched with water (150 mL), and the product was extracted with Et_2O (3 x 100 mL). The combined organic phases were dried over Na_2SO_4 and filtered. The filtrate was evaporated to dryness under reduced pressure. The crude material was purified by column chromatography (SiO_2, 4:1 CH_2Cl_2/hexanes) to provide 4-(2,2-dichlorovinyl)tetrahydro-2H-pyran as a colorless liquid (1.28 g, 71% yield).

^{1}H NMR (500 MHz, $CDCl_3$) δ 5.72 (d, *J* = 9.1 Hz, 1H), 3.99–3.88 (m, 2H), 3.43 (td, *J* = 11.7, 2.3 Hz, 2H), 2.62 (tdt, *J* = 11.3, 8.6, 4.1 Hz, 1H), 1.70–1.56 (m, 2H), 1.54–1.37 (m, 2H).

^{13}C{^{1}H } NMR (125 MHz, $CDCl_3$) δ 133.4, 120.1, 67.4, 36.5, 31.3.

HRMS(APCI) (m/z): $[M + H]^+$ calcd for $C_7H_{10}Cl_2O$: 181.0187; found: 181.0179.

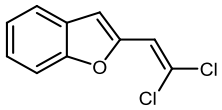

2-(2,2-dichlorovinyl)benzofuran.[vii] Under an N_2 atmosphere, a 100-mL Schlenk flask was charged with Ph_3P (2.6 g, 10 mmol, 1.0 equiv) and a magnetic stir bar. CCl_4 (5.8 mL, 60 mmol, 6.0 equiv) was added by syringe, and the solution was stirred at 60 °C. After 1 h, 2-benzofurancarboxaldehyde (1.46 g, 10 mmol, 1.0 equiv) was added by syringe, and stirring was continued at 60 °C overnight. The reaction mixture was concentrated to dryness under reduced pressure. The crude reaction mixture was directly loaded onto a

SiO_2 column for purification, providing 2-(2,2-dichlorovinyl)benzofuran as a colorless crystalline solid (660 mg, 31% yield).

^{1}H NMR (500 MHz, $CDCl_3$) δ 7.59 (d, *J* = 7.8 Hz, 1H), 7.46 (d, *J* = 8.2 Hz, 1H), 7.37–7.29 (m, 1H), 7.29–7.19 (m, 1H), 7.16 (s, 1H), 6.91 (s, 1H).

^{13}C{^{1}H } NMR (125 MHz, $CDCl_3$) δ 154.3, 150.2, 128.4, 125.5, 123.4, 122.9, 121.6, 119.0, 111.3, 107.7.

HRMS(APCI) (m/z): M^+ calcd for $C_{10}H_6Cl_2O$: 211.9796; found: 211.9785.

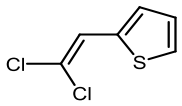

2-(2,2-dichlorovinyl)thiophene [65085-96-3].[3] Under an N_2 atmosphere, a 100-mL Schlenk flask was charged with Ph_3P (2.6 g, 10 mmol, 1.0 equiv) and a magnetic stir bar. CCl_4 (5.8 mL, 60 mmol, 6.0 equiv) was added by syringe, and the solution was stirred at 60 °C. After 1 h, 2-thiophenecarboxaldehyde (1.12 g, 10 mmol, 1.0 equiv) was added by syringe, and stirring was continued at 60 °C overnight. The reaction mixture was concentrated to dryness under reduced pressure. The crude reaction mixture was directly loaded onto a SiO_2 column for purification, providing 2-(2,2-dichlorovinyl)thiophene as a colorless crystalline solid (537 mg, 30% yield).

^{1}H NMR (500 MHz, $CDCl_3$) δ 7.38 (ddd, J = 5.1, 1.2, 0.6 Hz, 1H), 7.20 (ddd, J = 3.7, 1.2, 0.6 Hz, 1H), 7.11–7.02 (m, 2H).

^{13}C{^{1}H } NMR (125 MHz, $CDCl_3$) δ 136.4, 129.5, 127.4, 126.8, 123.0, 118.8.

B.3 Catalyst Comparison Studies

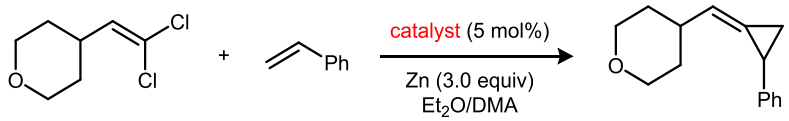

2 **3**

Entry	Catalyst	Conversion	Yield	E/Z ratio
1	[$^{i\text{-Pr}}$NDI]$Ni_2(C_6H_6)$ (**1**)	>99%	94%	1:5
2	[$^{i\text{-Pr}}$NDI]Ni_2Cl_2 (**4**)	93%	87%	1:5
3	[$^{i\text{-Pr}}$NDI] (**5**) + $Ni(DME)Cl_2$	96%	92%	1:5
4	[^{Et}NDI] (**6**) + $Ni(DME)Cl_2$	71%	50%	1.2:1
5	[^{Me}NDI] (**7**) + $Ni(DME)Cl_2$	14%	<2%	-
6	[$^{i\text{-Pr}}$PDI]$NiCl_2$ (**8**)	30%	<2%	-
7	[$^{i\text{-Pr}}$IP]Ni(COD) (**9**)	16%	<2%	-
8	[BiPy]Ni(COD) (**10**)	10%	<2%	-
9	[$^{i\text{-Pr}}$DAD]Ni(COD) (**11**)	<2%	<2%	-

Figure B.1. Catalyst comparison data for the methylenecyclopropanation of styrene.

General Procedure for Entries 1, 2, 6–9. In an N_2-filled glovebox, a 5-mL vial was charged with a magnetic stir bar, the catalyst (5 mol%), and Zn powder (0.60 mmol). A solution of *N*,*N*-dimethylacetamide (200 µL) and Et_2O (500 µL) was added. A solution containing styrene (0.20 mmol), mesitylene (0.20 mmol), and 4-(2,2-dichlorovinyl)tetrahydro-2H-pyran (0.21 mmol) in Et_2O (1.1 mL) was added to the catalyst/reductant mixture. The vial was sealed, and the reaction mixture was stirred at room temperature. After 24 h, an aliquot of the reaction was removed, and the substrate conversion, yield of **3**, and the ratio of E/Z diastereomers were determined by ^{1}H NMR analysis.

General Procedure for Entries 3–5. In an N_2-filled glovebox, a 5-mL vial was charged with a magnetic stir bar, the [NDI] ligand (5 mol%), Ni(DME)Cl_2 (10 mol%), and Zn powder (0.60 mmol). A solution of *N*,*N*-dimethylacetamide (200 µL) and Et_2O (500 µL) was added, and the mixture was stirred at room temperature for 5 min. A solution containing styrene (0.20 mmol), mesitylene (0.20 mmol), and 4-(2,2-dichlorovinyl)tetrahydro-2H-pyran (0.21 mmol) in Et_2O (1.1 mL) was added to the catalyst/reductant mixture. The vial was sealed, and the reaction mixture was stirred at room temperature. After 24 h, an aliquot of the reaction was removed, and the substrate conversion, yield of **3**, and the ratio of E/Z diastereomers were determined by ^{1}H NMR analysis.

B.4 Substrate Scope Studies and Methylenecyclopropane Characterization

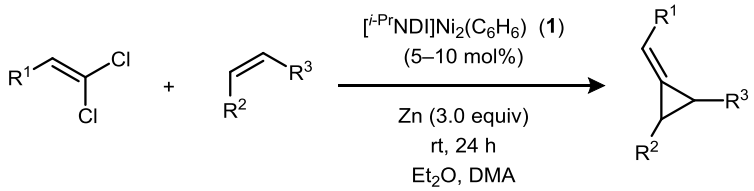

General Procedure. In an N_2-filled glovebox, a 5-mL vial was charged with a magnetic stir bar, the alkene, the 1,1-dichloroalkene, Zn powder (0.60 mmol, 3.0 equiv), *N*,*N*-dimethylacetamide (200 µL), and Et_2O (500 µL). A solution of [$^{i\text{-Pr}}$NDI]$Ni_2(C_6H_6)$ (0.010 mmol, 5 mol%) in Et_2O (1.1 mL) was added. The vial was sealed, and the reaction mixture was stirred at room temperature. After 24 h, the reaction mixture was concentrated under reduced pressure, and the crude residue was directly loaded onto a SiO_2 column for purification. Isolated yields were determined following purification.

For terminal alkene substrates, the E/Z diastereomers were inseparable unless otherwise indicated. Yields, NMR spectroscopy data, and high-resolution mass spectrometry data correspond to the mixture of diastereomers. E/Z ratios were determined by ^{1}H NMR integration.

NOTE: The methylenecyclopropanes described below are sufficiently stable to permit their purification by column chromatography without any special precautions to

protect them from O_2. Following purification, they were immediately pumped into an N_2-filled glovebox for long-term storage. Under air, these methylenecyclopropanes undergo complete decomposition to intractable mixtures of products over the course of several hours to days.

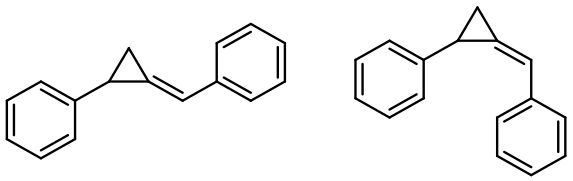

(2-benzylidenecyclopropyl)benzene [201345-00-8] (12). [viii] The reaction was conducted according to the general procedure without modification using (2,2-dichlorovinyl)benzene (38 mg, 0.22 mmol, 1.1 equiv) and styrene (21 mg, 0.20 mmol, 1.0 equiv). The products were isolated as a white solid following column chromatography (SiO_2, hexanes).

Run 1: 36.3 mg (88% yield), Run 2: 35 mg (85% yield) (E/Z = 1:3.1).

12-*E/Z*: ^{1}H NMR (500 MHz, $CDCl_3$) δ 7.66 (d, *J* = 5 Hz, 2H, **12-*E***), 7.54-7.37 (m, 2H, **12–*E/Z***), 7.37–7.27 (m, 4H, **12–*E/Z***), 7.27–7.16 (m, 4H, **12–*E/Z***), 7.03–6.99 (m, 1H, **12-*Z***), 6.99–6.96 (m, 1H, **12-*E***), 2.97 (ddd, *J* = 9.2, 4.9, 2.1 Hz, 1H, **12-*Z***), 2.77 (ddd, *J* = 9.1, 4.9, 1.8 Hz, 1H, **12-*E***), 2.16 (td, *J* = 10, 5.0 Hz, 1H, **12-*E***), 1.90 (td, *J* = 9.1, 2.0 Hz, 1H, **12-*Z***), 1.61 (ddd, *J* = 9.4, 4.9, 2.5 Hz, 1H, **12-*E***), 1.33 (ddd, *J* = 9.0, 4.8, 2.0 Hz, 1H, **12-*Z***).

12-*E*: ^{13}C{^{1}H} NMR (125 MHz, $CDCl_3$) δ 142.2, 137.8, 128.7, 128.5, 127.3, 127.0, 126.6, 126.1, 119.5, 18.1, 16.1.

12-*Z*: ^{13}C{^{1}H} NMR (125 MHz, $CDCl_3$) δ 141.3, 137.4, 128.7, 128.6, 127.6, 127.2, 127.1, 126.5, 126.1, 120.3, 21.6, 13.9.

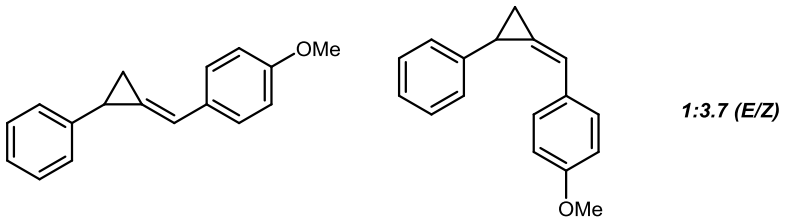

1-methoxy-4-((2-phenylcyclopropylidene)methyl)benzene (13). The reaction was conducted according to the general procedure without modification using 1-(2,2-dichlorovinyl)-4-methoxybenzene (45 mg, 0.22 mmol, 1.1 equiv) and styrene (21 mg, 0.20 mmol, 1.0 equiv). The products were isolated as a colorless oil following column chromatography (SiO_2, 1:4 CH_2Cl_2/hexanes).

Run 1: 43.3 mg (92% yield), Run 2: 44.3 mg (94% yield) (E:Z = 1:3.7).

Scale-up Reaction: In an N_2-filled glovebox, a 100-mg round bottom flask was charged with a magnetic stir bar, 1-(2,2-dichlorovinyl)-4-methoxybenzene (1.12 g, 5.5 mmol, 1.1 equiv), styrene (521 mg, 5.0 mmol, 1.0 equiv), Zn powder (981 mg, 1.5 mmol, 3.0 equiv), *N*,*N*-dimethylacetamide (5 mL), and Et_2O (35 mL). A solution of [$^{i\text{-}Pr}$NDI]$Ni_2(C_6H_6)$ (181 mg, 0.25 mmol, 5 mol%) in Et_2O (5 mL) was added. The reaction vessel was sealed with a septum, and the reaction mixture was stirred at room temperature. After 24 h, the reaction flask was removed from the glovebox and opened to the ambient atmosphere. The reaction mixture was washed with water (20 mL). The aqueous phase was extracted with an additional portion of Et_2O (50 mL). The combined organic phases were dried over Na_2SO_4 and filtered. The filtrate was concentrated to dryness under reduced pressure, and the crude product was purified by column chromatography (SiO_2, 1:4 CH_2Cl_2/hexanes) to afford 1-methoxy-4-((2-phenylcyclopropylidene)methyl)benzene as a colorless liquid (1.16 g, 98% yield, E/Z = 1:3.3).

13-*E*/*Z*: ^{1}H NMR (500 MHz, $CDCl_3$) δ 7.59–7.52 (m, 2H, **13-*E***), 7.37–7.31 (m, 2H, **13-*Z***), 7.31–7.24 (m, 2H), 7.23–7.17 (m, 2H), 7.17–7.11 (m, 2H), 6.96–6.92 (m, 2H, **13-*E***), 6.92–6.87 (m, 1H), 6.84–6.77 (m, 2H, **13-*Z***), 3.85 (s, 3H, **13-*E***), 3.77 (s, 3H, **13-*Z***), 2.90 (ddd, *J* = 9.0, 4.6, 2.1 Hz, 1H, **13-*Z***), 2.71 (ddd, *J* = 8.9, 4.6, 1.7 Hz, 1H, **13-*E***), 2.09 (td, *J* = 9.0, 2.4 Hz, 1H, **13-*E***), 1.85 (td, *J* = 8.9, 2.0 Hz, 1H, **13-*Z***), 1.53 (ddd, *J* = 9.2, 4.7, 2.5 Hz, 1H, **13-*E***), 1.26 (ddd, *J* = 8.8, 4.7, 2.0 Hz, 1H, **13-*Z***).

13-*E*: ^{13}C{^{1}H} NMR (125 MHz, $CDCl_3$) δ 159.0, 142.5, 130.7, 128.5, 128.1, 126.6, 126.3, 126.0, 118.9, 114.1, 55.5, 18.1, 16.0.

13-*Z*: $^{13}C\{^{1}H\}$ NMR (125 MHz, $CDCl_3$) δ 158.8, 141.5, 130.4, 128.7, 128.3, 126.5, 126.0, 125.0, 119.6, 114.1, 55.3, 21.5, 14.0.

HRMS(ESI) (m/z): $[M + H]^+$ calcd for $C_{17}H_{16}O$: 237.1280; found: 237.1272.

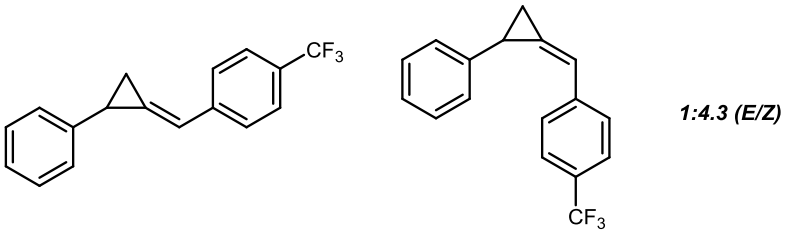

1-((2-phenylcyclopropylidene)methyl)-4-(trifluoromethyl)benzene (14). The reaction was conducted according to the general procedure using 1-(2,2-dichlorovinyl)-4-(trifluoromethyl)benzene (53 mg, 0.22 mmol, 1.1 equiv) and styrene (21 mg, 0.20 mmol, 1.0 equiv). Modifications from the general procedure: 10 mol% instead of 5 mol% catalyst loading. The products were isolated as a colorless oil following column chromatography (SiO_2, hexanes).

Run 1: 37.7 mg (69% yield), Run 2: 40 mg (73% yield) (E:Z = 1:4.3).

14-*E*/*Z*: ^{1}H NMR (500 MHz, $CDCl_3$) δ 7.73–7.60 (m, 4H, **14-*E***), 7.52–7.43 (m, 4H, **14-*Z***), 7.28 (t, *J* = 10 Hz, 2H, **14-*E*/*Z***), 7.24–7.17 (m, 1H, **14-*E*/*Z***), 7.11 (d, *J* = 5 Hz, 2H, **14-*E*/*Z***), 7.0–6.97 (m, 1H, **14-*Z***), 6.97–6.94 (m, 1H, **14-*E***), 2.95 (ddd, *J* = 9.5, 5.1, 2.1 Hz, 1H, **14-*Z***), 2.77 (ddd, *J* = 9.3, 5.2, 1.7 Hz, 1H, **14-*E***), 2.14 (td, *J* = 9.4, 2.4 Hz, 1H, **14-*E***), 1.91 (td, *J* = 9.4, 2.0 Hz, 1H, **14-*Z***), 1.60 (ddd, *J* = 9.6, 5.2, 2.5 Hz, 1H, **14-*E***), 1.34 (ddd, *J* = 9.4, 5.1, 2.0 Hz, 1H, **14-*Z***).

14-*E*/*Z*: $^{13}C\{^{1}H\}$ NMR (125 MHz, $CDCl_3$) δ 141.6, 140.7, 140.6, 131.2, 128.9, 128.8 (q, $^{2}J_{C–F}$ = 33 Hz, **14-*Z***), 128.6, 127.2, 127.1, 126.6, 126.4, 126.3, 125.6 (q, $^{3}J_{C–F}$ = 3.8 Hz, **14-*Z***), 124.4 (q, $^{1}J_{C–F}$ = 270 Hz, **14-*Z***), 119.1, 118.5, 21.7 (**14-*Z***), 18.2 (**14-*E***), 15.9 (**14-*E***), 13.9 (**14-*Z***).

14-*E*: ^{19}F NMR (300 MHz, $CDCl_3$) δ –63.91.

14-*Z*: ^{19}F NMR (300 MHz, $CDCl_3$) δ –63.97.

HRMS(APCI): $[M + H]^+$ calcd for $C_{17}H_{13}F_3$: 275.1048; found: 275.1034.

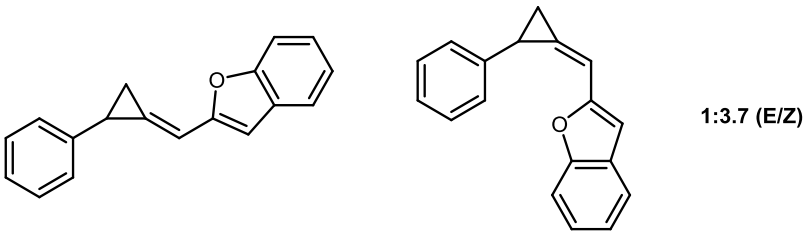

2-((2-phenylcyclopropylidene)methyl)benzofuran (15). The reaction was conducted according to the general procedure without modification using 2-(2,2-dichlorovinyl)benzofuran (47 mg, 0.22 mmol, 1.1 equiv) and styrene (21 mg, 0.20 mmol, 1.0 equiv). The products were isolated as a pale yellow oil following column chromatography (SiO_2, 5:1 CH_2Cl_2/hexanes).

Run 1: 27 mg (55% yield), Run 2: 25.1 mg (51% yield) (E:Z = 1:3.7).

15-*E/Z*: ^{1}H NMR (300 MHz, $CDCl_3$) δ 7.74–7.56 (m, 3H, **15-*E***), 7.55–7.42 (m, 3H, **15-*Z***), 7.41–7.24 (m, 3H, **15-*E/Z***), 7.24–7.15 (m, 2H, **15-*E/Z***), 7.14–7.06 (m, 2H, **15-*E/Z***), 7.01–6.96 (m, 1H, **15-*Z***), 6.96–6.93 (m, 1H, **15-*E***), 2.94 (ddd, *J* = 9.6, 5.2, 2.0 Hz, 1H, **15-*Z***), 2.80–2.72 (m, 1H, **15-*E***), 2.14 (td, *J* = 9.5, 2.4 Hz, 1H, **15-*E***), 1.90 (td, *J* = 9.4, 2.0 Hz, 1H, **15-*Z***), 1.60 (ddd, *J* = 9.7, 5.1, 2.5 Hz, 1H, **15-*E***), 1.39–1.29 (m, 1H, **15-*Z***).

15-*E/Z*: $^{13}C\{^1H\}$ NMR (125 MHz, $CDCl_3$) δ 140.7, 140.6, 131.2, 128.9, 128.7, 128.6, 127.2, 127.1, 127.1, 126.8, 126.6, 126.4, 126.3, 125.6, 125.6, 119.1 (**15-*Z***), 118.5 (**15-*E***), 21.7 (**15-*Z***), 18.2 (**15-*E***), 15.9 (**15-*E***), 13.9 (**15-*Z***).

HRMS(APCI) (m/z): $[M + H]^+$ calcd for $C_{18}H_{14}O$: 247.1123; found: 247.1109.

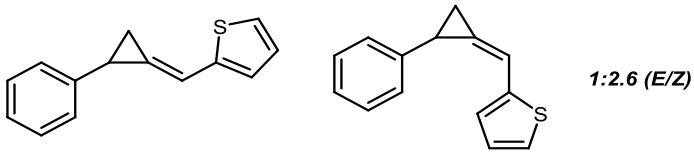

2-((2-phenylcyclopropylidene)methyl)thiophene (16). The reaction was conducted according to the general procedure without modification using 2-(2,2-dichlorovinyl)thiophene (39 mg, 0.22 mmol, 1.1 equiv) and styrene (21 mg, 0.20 mmol, 1.0 equiv). The products were isolated as a pale orange oil following column chromatography (SiO_2, 9:1 CH_2Cl_2/hexanes).

Run 1: 27 mg (64% yield), Run 2: 25 mg (59% yield) (E:Z = 1:2.6).

16-*E*/*Z*: ^{1}H NMR (500 MHz, $CDCl_3$) δ 7.39–7.30 (m, 3H, **16-*E*/*Z***), 7.30–7.23 (m, 2H, **16-*E*/*Z***), 7.23–7.16 (m, 2H, **16-*E*/*Z***), 7.16–7.08 (m, 1H, **16-*E*/*Z***), 7.06–6.97 (m, 1H, **16-*E*/*Z***), 2.94–2.84 (m, 1H, **16-*E*/*Z***), 2.07 (td, *J* = 9.2, 2.4 Hz, 1H, **16-*E***), 2.01 (td, *J* = 9.1, 1.9 Hz, 1H, **16-*Z***), 1.52 (ddd, *J* = 9.5, 4.9, 2.4 Hz, 1H, **16-*E***), 1.50–1.42 (m, 1H, **16-*Z***).

16-*E*/*Z*: $^{13}C\{^{1}H\}$ NMR (125 MHz, $CDCl_3$) δ 143.3 (**16-*E***), 142.7 (**16-*Z***), 141.9 (**16-*E***), 140.8 (**16-*Z***), 128.6, 128.5, 127.3, 127.2, 127.1, 126.6, 126.4, 126.2, 126.1, 125.2, 125.1, 125.0, 124.7, 114.0 (**16-*Z***), 113.8 (**16-*E***), 21.5 (**16-*Z***), 20.3 (**16-*E***), 16.1 (**16-*E***), 15.4 (**16-*Z***).

HRMS(ESI) (m/z): $[M + H]^+$ calcd for $C_{14}H_{12}S$: 213.0738; found: 213.0932.

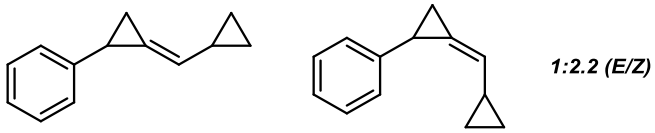

(2-(cyclopropylmethylene)cyclopropyl)benzene (17). The reaction was conducted according to the general procedure without modification using (2,2-dichlorovinyl)cyclopropane (30 mg, 0.22 mmol, 1.1 equiv) and styrene (21 mg, 0.20 mmol, 1.0 equiv). The products were isolated as a colorless oil following column chromatography (SiO_2, hexanes).

Run 1: 23 mg (68% yield), Run 2: 22.5 mg (66% yield) (E:Z = 1:2.2).

17-E/*Z* : ^{1}H NMR (500 MHz, $CDCl_3$): δ 7.45–7.22 (m, 2H, **17-E/*Z***), 7.22–7.06 (m, 3H, **17-E/*Z***), 5.57–5.48 (m, 1H, **17-E/*Z***), 2.67 (ddd, *J* = 8.7, 4.5, 2.1 Hz, 1H, **17-*Z***), 2.56 (ddd, *J* = 8.6, 4.6, 1.7 Hz, 1H, **17-*E***), 1.78 (td, *J* = 8.5, 2.4 Hz, 1H, **17-*E***), 1.71 (td, *J* = 8.4, 2.0 Hz, 1H, **17-*Z***), 1.68–1.60 (m, 1H, **17-*E***), 1.57–1.46 (m, 1H, **17-*Z***), 1.22 (ddd, *J* = 8.5, 4.5, 2.4 Hz, 1H, **17-*E***), 1.14 (ddd, *J* = 8.2, 4.5, 2.0 Hz, 1H, **17-*Z***), 0.84–0.75 (m, 2H, **17-*E***), 0.74–0.64 (m, 2H, **17-*Z***), 0.58–0.49 (m, 2H, **17-*E***), 0.49–0.33 (m, 2H, **17-*Z***).

17-E/*Z* : $^{13}C\{^{1}H\}$ NMR (126 MHz, $CDCl_3$) δ 142.9 (**17-*E***), 142.7 (**17-*Z***), 128.5 (**17-*Z***), 128.4 (**17-*E***), 126.5, 125.8 (**17-*E***), 125.8 (**17-*Z***), 123.9, 123.9, 123.6 (**17-*Z***), 123.4 (**17-*E***), 20.1 (**17-*Z***), 19.6 (**17-*E***), 15.0 (**17-*Z***), 14.3 (**17-*E***), 13.4 (**17-*Z***), 13.2 (**17-*E***), 6.8, 6.7, 6.6.

HRMS(APCI) (m/z): $[M + H]^+$ calcd for $C_{13}H_{14}$: 171.1174; found: 171.1162.

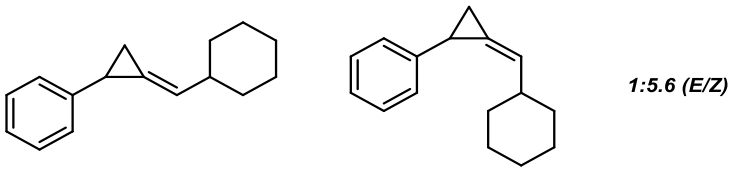

(2-(cyclohexylmethylene)cyclopropyl)benzene (18). The reaction was conducted according to the general procedure without modification using (2,2-dichlorovinyl)cyclohexane (38 mg, 0.21 mmol, 1.05 equiv) and styrene (21 mg, 0.20 mmol, 1.0 equiv). The products were isolated as a pale yellow oil following column chromatography (SiO_2, hexanes).

Run 1: 40.2 mg (95% yield), Run 2: 40 mg (94% yield) (E:Z = 1:5.6).

18-*E/Z*: ^{1}H NMR (500 MHz, $CDCl_3$) δ 7.32–7.23 (dd, *J* = 9.1, 6.2 Hz, 2H, **18-*E/Z***), 7.21–7.08 (m, 3H, **18-*E/Z***), 5.94–84 (m, 1H, **18-*E/Z***), 2.61 (ddt, *J* = 8.0, 4.4, 1.6 Hz, 1H, **18-*Z***), 2.52 (ddt, *J* = 8.1, 4.6, 1.5 Hz, 1H, **18-*E***), 2.34–2.24 (m, 1H, **18-*E***), 2.23–2.10 (m, 1H, **18-*Z***), 1.94–1.56 (m, 6H, **18-*E/Z***), 1.42–1.02 (m, 6H, **18-*E/Z***).

18-*E*: ^{13}C{^{1}H} NMR (125 MHz, $CDCl_3$) δ 143.1, 128.4, 126.4, 125.7, 125.6, 124.1, 40.6, 33.2, 33.1, 26.4, 18.8, 14.9.

18-*Z*: ^{13}C{^{1}H} NMR (125 MHz, $CDCl_3$) δ 143.2, 128.4, 126.2, 126.1, 125.6, 123.6, 40.8, 33.0, 32.8, 26.3, 26.2, 20.6, 14.7.

HRMS(EI) (m/z): M^+ calcd for $C_{16}H_{20}$: 212.1560; found: 212.1564.

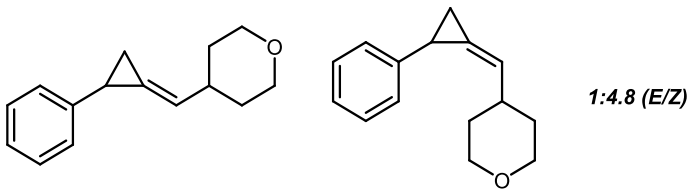

4-((2-phenylcyclopropylidene)methyl)tetrahydro-2H-pyran (3). The reaction was conducted according to the general procedure without modification using 4-(2,2-dichlorovinyl)tetrahydro-2H-pyran (38 mg, 0.21 mmol, 1.05 equiv) and styrene (21 mg, 0.20 mmol, 1.0 equiv). The products were isolated as a pale yellow oil following column chromatography (SiO_2, hexanes).

Run 1: 42 mg (98% yield), Run 2: 40.1 mg (94% yield) (E:Z = 1:4.8).

3-*E/Z*: δ 7.33–7.21 (m, 2H, **3-*E/Z***), 7.21–7.12 (m, 1H, **3-*E/Z***), 7.11–7.03 (m, 2H, **3-*E/Z***), 5.94–5.90 (m, 1H, **3-*E***), 5.90–5.84 (m, 1H, **3-*Z***), 4.08–3.96 (m, 2H, **3-*E***), 3.96–3.81 (m, 2H, **3-*Z***), 3.56–3.43 (m, 2H, **3-*E***), 3.42–3.27 (m, 2H, **3-*Z***), 2.68–2.57 (m, 1H, **3-*Z***), 2.56–2.48 (m, 1H, **3-*E***), 2.45–2.31 (m, 1H, **3-*E/Z***), 1.83–1.43 (m, 5H, **3-*E/Z***), 1.25–1.20 (m, 1H, **3-*E***), 1.17–1.09 (m, 1H, **3-*Z***).

3-*E*: $^{13}C\{^{1}H\}$ NMR (125 MHz, $CDCl_3$) δ 142.6, 128.4, 126.4, 125.9, 125.4, 123.7, 67.9, 37.7, 32.8, 32.7, 18.7, 14.7.

3-*Z*: $^{13}C\{^{1}H\}$ NMR (125 MHz, $CDCl_3$) δ 142.8, 128.5, 126.0, 125.8, 125.1, 124.0, 67.9, 37.9, 32.5, 32.5, 20.6, 14.6.

HRMS(ESI) (m/z): $[M + H]^+$ calcd for $C_{15}H_{18}O$: 215.1436; found: 215.1432.

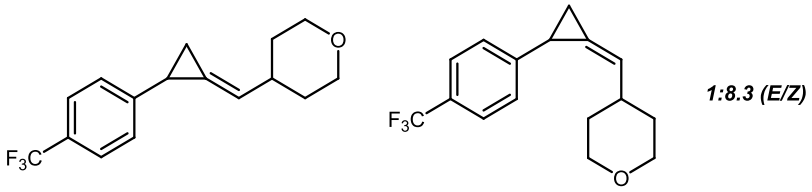

4-((2-(4-(trifluoromethyl)phenyl)cyclopropylidene)methyl)tetrahydro-2H-pyran (19). The reaction was conducted according to the general procedure without modification using 4-(2,2-dichlorovinyl)tetrahydro-2H-pyran (38 mg, 0.21 mmol, 1.05 equiv) and 1-(trifluoromethyl)-4-vinylbenzene (34 mg, 0.20 mmol, 1.0 equiv). The products were isolated as a pale yellow oil following column chromatography (SiO_2, 4:1 CH_2Cl_2/hexanes).

Run 1: 55.8 mg (99% yield), Run 2: 55.3 mg (98% yield) (E:Z = 1:8.3).

19-*E/Z*: ^{1}H NMR (300 MHz, $CDCl_3$) δ 7.49 (d, *J* = 8.1 Hz, 2H, **19-*E/Z***), 7.16 (d, *J* = 8.1 Hz, 2H, **19-*E/Z***), 6.08–5.79 (m, 1H, **19-*E/Z***), 4.10–3.99 (m, 2H, **19-*E***), 3.98–3.82 (m, 2H, **19-*Z***), 3.58–3.46 (m, 2H, **19-*E***), 3.46–3.22 (m, 2H, **19-*Z***), 2.78–2.63 (m, 1H, **19-*Z***), 2.63–2.55 (m, 1H, **19-*E***), 2.49–2.25 (m, 1H, **19-*E/Z***), 2–1.40 (m, 5H, **19-*E/Z***), 1.28–1.12 (m, 1H, **19-*E/Z***).

19-*Z*: $^{13}C\{^{1}H\}$ NMR (125 MHz, $CDCl_3$) δ 147.3, 128.0 (q, $^{2}J_{C–F}$ = 33 Hz), 126.2, 125.5 (q, $^{3}J_{C–F}$ = 3.8 Hz), 124.5, 124.5 (q, $^{1}J_{C–F}$ = 271 Hz), 124.3, 67.8, 37.9, 32.4, 32.4, 20.4, 15.2.

19-*E*: ^{19}F NMR (300 MHz, $CDCl_3$) δ –63.82.

19-*Z*: ^{19}F NMR (300 MHz, $CDCl_3$) δ –63.78.

HRMS(ESI) (m/z): $[M + H]^+$ calcd for $C_{16}H_{17}F_3O$: 283.1310; found: 283.0003.

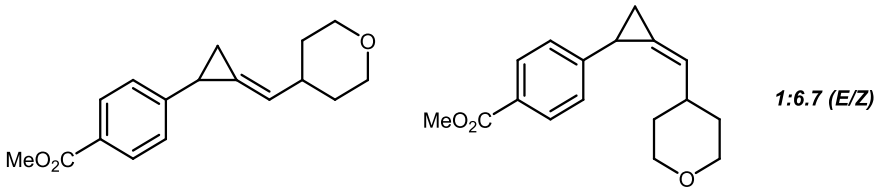

methyl 4-(2-((tetrahydro-2H-pyran-4-yl)methylene)cyclopropyl)benzoate (20). The reaction was conducted according to the general procedure without modification using 4-(2,2-dichlorovinyl)tetrahydro-2H-pyran (38 mg, 0.21 mmol, 1.05 equiv) and methyl 4-vinylbenzoate (32 mg, 0.20 mmol, 1.0 equiv). The products were isolated as a pale yellow oil following column chromatography (SiO_2, 10:1 CH_2Cl_2/EtOAc).

Run 1: 39.8 mg (73% yield), Run 2: 48 mg (88% yield) (E:Z = 1:6.7).

20-*E/Z*: ^{1}H NMR (300 MHz, $CDCl_3$) δ 7.90 (d, *J* = 7.9 Hz, 2H, **20-*E/Z***), 7.11 (d, *J* = 7.9 Hz, 2H, **20-*E/Z***), 5.97–5.82 (m, 1H, **20-*E/Z***), 4.09–3.78 (m, 2H, **20-*E/Z***), 3.91 (s, 3H, **20-*E/Z***), 3.57–3.44 (m, 2H, **20-*E***), 3.43–3.22 (m, 2H, **20-*Z***), 2.74–2.62 (m, 1H, **20-*Z***), 2.62–2.54 (m, 1H, **20-*E***), 2.45–2.27 (m, 1H, **20-*E/Z***), 1.98–1.39 (m, 5H, **20-*E/Z***), 1.37–1.15 (m, 1H, **20-*E/Z***).

20-*Z*: ^{13}C{^{1}H} NMR (125 MHz, $CDCl_3$) δ 167.1, 148.7, 129.9, 127.7, 125.8, 124.9, 124.3, 67.8, 52.0, 37.9, 32.4, 20.6, 15.1.

HRMS(ESI) (m/z): $[M + H]^+$ calcd for $C_{17}H_{20}O_3$: 273.1491; found: 273.1479.

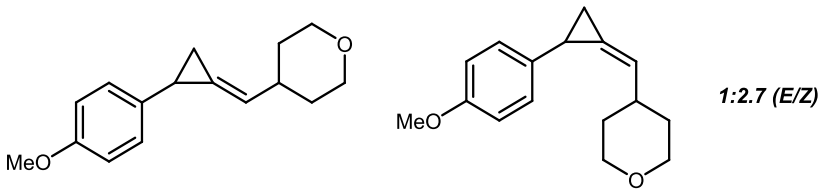

4-((2-(4-methoxyphenyl)cyclopropylidene)methyl)tetrahydro-2H-pyran (21). The reaction was conducted according to the general procedure without modification using 4-(2,2-dichlorovinyl)tetrahydro-2H-pyran (38 mg, 0.21 mmol, 1.05 equiv) and 4-vinylanisole (27 mg, 0.20 mmol, 1.0 equiv). The products were isolated as a pale yellow oil following column chromatography (SiO_2, 9:1 CH_2Cl_2/EtOAc).

Run 1: 40 mg (82% yield), Run 2: 47 mg (96% yield) (E:Z = 1:2.7).

21-*E/Z*: ^{1}H NMR (300 MHz, $CDCl_3$) δ 7.06 (d, *J* = 8.4 Hz, 2H, **21-*E***), 7.01 (d, *J* = 8.4 Hz, 2H, **21-*Z***), 6.81 (d, *J* = 8.3 Hz, 2H, **21-*E/Z***), 5.98–5.80 (m, 1H, **21-*E/Z***), 4.12–3.99 (m, 2H, **21-*E***), 3.98–3.88 (m, 2H, **21-*Z***), 3.81 (s, 3H, **21-*E/Z***), 3.59–3.46 (m, 2H, **21-*E***), 3.46–3.28 (m, 2H, **21-*Z***), 2.73–2.57 (m, 1H, **21-*Z***), 2.57–2.49 (m, 1H, **21-*E***), 2.49–2.30 (m, 1H, **21-*E/Z***), 1.97–1.43 (m, 5H, **21-*E/Z***), 1.27–1.16 (m, 1H, **21-*E***), 1.16–1.04 (m, 1H, **21-*Z***).

21-*E*: ^{13}C{^{1}H} NMR (125 MHz, $CDCl_3$) δ 158.0, 134.4, 127.5, 125.5, 123.6, 113.9, 68.0, 55.4, 37.8, 32.8, 32.7, 17.9, 14.3.

21-*Z*: ^{13}C{^{1}H} NMR (125 MHz, $CDCl_3$) δ 157.9, 134.7, 127.0, 125.3, 124.0, 114.0, 67.9, 55.4, 37.9, 32.6, 32.5, 19.9, 14.2.

HRMS(ESI) (m/z): $[M + H]^+$ calcd for $C_{16}H_{20}O_2$: 245.1542; found: 245.1536.

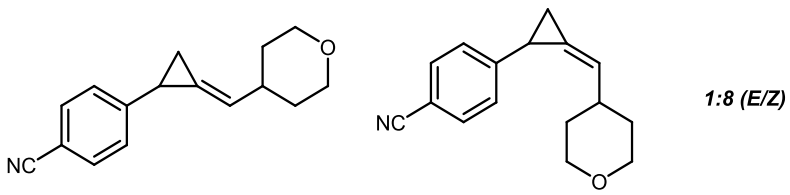

4-(2-((tetrahydro-2H-pyran-4-yl)methylene)cyclopropyl)benzonitrile (22). The reaction was conducted according to the general procedure without modification using 4-(2,2-dichlorovinyl)tetrahydro-2H-pyran (38 mg, 0.21 mmol, 1.05 equiv) and 4-vinylbenzonitrile (26 mg, 0.20 mmol, 1.0 equiv). The products were isolated as a pale

yellow solid following column chromatography (SiO_2, 10:1 CH_2Cl_2/EtOAc). Single crystals of **22-*Z*** suitable for X-ray diffraction analysis were obtained from concentrated MeOH solutions at room temperature.

Run 1: 35 mg (73% yield), Run 2: 35.8 mg (75% yield) (E:Z = 1:8).

22-*E/Z*: ^{1}H NMR (500 MHz, $CDCl_3$) δ 7.53 (d, *J* = 5 Hz, 2H, **22-*E/Z***), 7.19–7.10 (m, 2H, **22-*E/Z***), 5.95–5.85 (m, 1H, **22-*E/Z***), 4.04–3.95 (m, 2H, **22-*E***), 3.93–3.81 (m, 2H, **22-*Z***), 3.53–3.41 (m, 2H, **22-*E***), 3.32 (qd, *J* = 11.5, 2.7 Hz, 2H, **22-*Z***), 2.62 (ddd, *J* = 8.2, 4.2, 1.9 Hz, 1H, **22-*Z***), 2.57–2.49 (m, 1H, **22-*E***), 2.31 (dq, *J* = 10.6, 5.6 Hz, 1H, **22-*E/Z***), 1.92–1.85 (m, 1H, **22-*E***), 1.80 (tt, *J* = 8.8, 1.8 Hz, 1H, **22-*Z***), 1.69–1.33 (m, 4H, **22-*E/Z***), 1.31–1.25 (m, 1H, **22-*E***), 1.20 (ddt, *J* = 8.4, 4.1, 1.8 Hz, 1H, **22-*Z***).

22-*Z*: $^{13}C\{^1H\}$ NMR (125 MHz, $CDCl_3$) δ 149.1, 132.4, 126.6, 124.7, 124.3, 119.2, 109.4, 67.7, 37.9, 32.3, 32.3, 20.7, 15.5.

HRMS(ESI) (m/z): $[M + Na]^+$ calcd for $C_{16}H_{17}NO$: 262.1208; found: 262.1205.

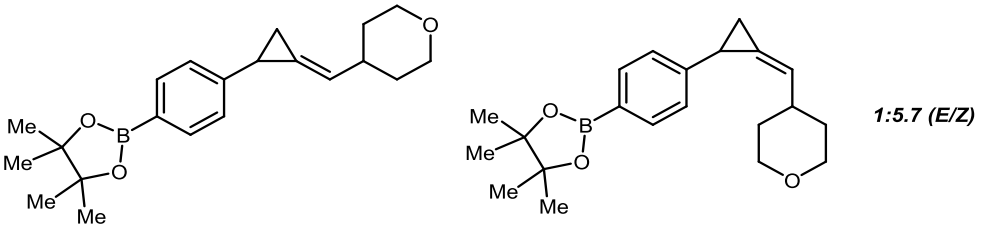

4,4,5,5-tetramethyl-2-(4-(2-((tetrahydro-2H-pyran-4-yl)methylene)cyclopropyl)phenyl)-1,3,2-dioxaborolane (23). The reaction was conducted according to the general procedure without modification using 4-(2,2-dichlorovinyl)tetrahydro-2H-pyran (38 mg, 0.21 mmol, 1.05 equiv) and 4,4,5,5-tetramethyl-2-(4-vinylphenyl)-1,3,2-dioxaborolane (46 mg, 0.20 mmol, 1.0 equiv). The products were isolated as a pale yellow oil following column chromatography (SiO_2, 9:1 CH_2Cl_2/EtOAc).

Run 1: 51 mg (75% yield), Run 2: 54.4 mg (80% yield) (E:Z = 1:5.7).

23-*E*/*Z*: ^{1}H NMR (300 MHz, $CDCl_3$) δ 7.70 (d, *J* = 7.6 Hz, 2H), 7.08 (d, *J* = 9 Hz, 2H), 5.95–5.80 (m, 1H), 4.07–3.98 (m, 2H, **23-*E***), 3.97–3.80 (m, 2H, **23-*Z***), 3.58–3.44 (m, 2H, **23-*E***), 3.44–3.25 (m, 2H, **23-*Z***), 2.72–2.58 (m, 1H, **23-*Z***), 2.60–2.52 (m, 1H, **23-*E***), 2.48–2.27 (m, 1H), 1.91–1.69 (m, 1H), 1.69–1.45 (m, 4H), 1.39 (s, 12H), 1.27–1.12 (m, 1H).

23-*E*: $^{13}C\{^{1}H\}$ NMR (125 MHz, $CDCl_3$) δ 146.2, 135.0, 125.7, 123.7, 83.7, 67.8, 37.7, 32.8, 32.7, 25.0, 19.0, 14.9.

23-*Z*: $^{13}C\{^{1}H\}$ NMR (125 MHz, $CDCl_3$) δ 146.4, 135.0, 125.4, 125.2, 124.0, 83.8, 67.8, 37.9, 32.4, 32.4, 25.0, 25.0, 20.8, 14.8.

HRMS(ESI) (m/z): M^+ calcd for $C_{21}H_{29}BO_3$: 340.2325; found: 340.2315.

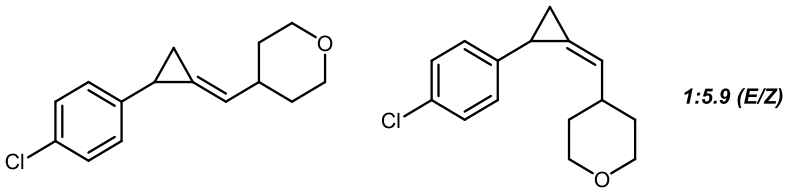

4-((2-(4-chlorophenyl)cyclopropylidene)methyl)tetrahydro-2H-pyran (24). The reaction was conducted according to the general procedure without modification using 4-(2,2-dichlorovinyl)tetrahydro-2H-pyran (38 mg, 0.21 mmol, 1.05 equiv) and 4-vinylbenzyl chloride (28 mg, 0.20 mmol, 1.0 equiv). The products were isolated as a colorless oil following column chromatography (SiO_2, 9:1 CH_2Cl_2/hexanes).

Run 1: 40.7 mg (82% yield), Run 2: 41.6 mg (84% yield) (E:Z = 1:5.9).

24-*E/Z*: ^{1}H NMR (500 MHz, $CDCl_3$) δ 7.33–7.17 (m, 2H, **24-*E/Z***), 7.11–6.95 (m, 2H, **24-*E/Z***), 6.00–5.88 (m, 1H, **24-*E/Z***), 4.12–4.01 (m, 2H, **24-*E***), 4.01–3.82 (m, 2H, **24-*Z***), 3.59–3.48 (m, 2H, **24-*E***), 3.47–3.27 (m, 2H, **24-*Z***), 2.72–2.56 (m, 1H, **24-*Z***), 2.56–2.49 (m, 1H, **24-*E***), 2.49–2.28 (m, 1H, **24-E/*Z***), 1.90–1.42 (m, 5H, **24-E/*Z***), 1.28–1.20 (m, 1H, **24-*E***), 1.20–1.08 (m, 1H, **24-*Z***).

24-*E*: $^{13}C\{^{1}H\}$ NMR (125 MHz, $CDCl_3$) δ 141.1, 131.5, 128.5, 127.7, 124.9, 124.1, 67.9, 37.7, 32.8, 32.6, 18.1, 14.8.

24-*Z*: $^{13}C\{^{1}H\}$ NMR (125 MHz, $CDCl_3$) δ 141.5, 131.3, 128.6, 127.3, 124.8, 124.3, 67.8, 37.9, 32.4, 20.0, 14.7.

HRMS(EI) (m/z): M^+ calcd for $C_{15}H_{17}ClO$: 248.0962; found: 248.0968.

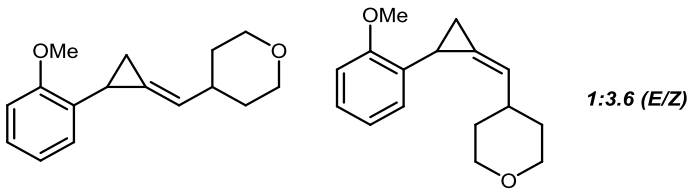

4-((2-(2-methoxyphenyl)cyclopropylidene)methyl)tetrahydro-2H-pyran (25). The reaction was conducted according to the general procedure without modification using 4-(2,2-dichlorovinyl)tetrahydro-2H-pyran (38 mg, 0.21 mmol, 1.05 equiv) and 2-vinylanisole (27 mg, 0.20 mmol, 1.0 equiv). The products were isolated as a pale yellow oil following column chromatography (SiO_2, 9:1 CH_2Cl_2/EtOAc).

Run 1: 34.1 mg (70% yield), Run 2: 35.5 mg (73% yield) (E:Z = 1:3.6).

25-*E/Z*: ^{1}H NMR (500 MHz, $CDCl_3$) δ 7.21–7.12 (m, 1H, **25-*E/Z***), 6.93–6.79 (m, 3H, **25-*E/Z***), 5.95– (m, 1H, **25-*E***), 5.90–5.84 (m, 1H, **25-*Z***), 4.04–3.97 (m, 2H, **25-*E***), 3.96–3.82 (m, 2H, **25-*Z***), 3.89 (s, 3H, **25-*Z***), 3.88 (s, 3H, **25-*E***), 3.48 (tdd, *J* = 11.6, 2.4, 1.2 Hz, 2H, **25-*E***), 3.37 (tdd, *J* = 11.6, 5.6, 2.5 Hz, 2H, **25-*Z***), 3.03–2.92 (m, 1H, **25-*Z***), 2.80 (ddt, *J* = 8.6, 5.1, 1.6 Hz, 1H, **25-*E***), 2.56–2.47 (m, 1H, **25-*E***), 2.47–2.33 (m, 1H, **25-*Z***), 1.87–1.45 (m, 5H, **25-*E/Z***), 1.17–1.10 (m, 1H, **25-*E***), 1.09–1.01 (m, 1H, **25-*Z***).

25-*E*: ^{13}C{^{1}H} NMR (125 MHz, $CDCl_3$) δ 158.4, 130.4, 126.9, 125.9, 125.0, 123.7, 120.6, 110.3, 68.0, 55.6, 37.8, 32.9, 32.7, 13.6, 13.1.

25-*Z*: ^{13}C{^{1}H} NMR (125 MHz, $CDCl_3$) δ 157.9, 130.8, 126.7, 125.4, 124.9, 124.1, 120.8, 110.3, 67.9, 55.6, 37.9, 32.6, 32.5, 14.5, 13.8.

HRMS(ESI) (m/z): $[M + H]^+$ calcd for $C_{16}H_{20}O_2$: 245.1542; found: 245.1537.

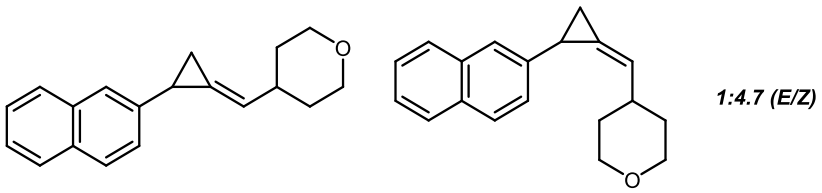

4-((2-(naphthalen-2-yl)cyclopropylidene)methyl)tetrahydro-2H-pyran (26). The reaction was conducted according to the general procedure without modification using 4-(2,2-dichlorovinyl)tetrahydro-2H-pyran (38 mg, 0.21 mmol, 1.05 equiv) and 2-

vinylnaphthalene (31 mg, 0.20 mmol, 1.0 equiv). The products were isolated as a white solid following column chromatography (SiO_2, 9:1 CH_2Cl_2/hexanes).

Run 1: 52.3 (99% yield), Run 2: 50.8 mg (96% yield) (E:Z = 1:4.7).

26-*E/Z*: ^{1}H NMR (300 MHz, $CDCl_3$) δ 7.89–7.70 (m, 3H, **26-*E/Z***), 7.61 (s, 1H, **26-*E***), 7.59 (s, 1H, **26-*Z***), 7.54–7.35 (m, 2H, **26-*E/Z***), 7.23 (d, *J* = 9 Hz, 1H, **26-*E***), 7.18 (d, *J* = 7.18 Hz, 1H, **26-*Z***), 6.04-5.9 (m, 1H, **26-*E/Z***), 4.13–3.98 (m, 2H, **26-*E***), 3.98–3.80 (m, 2H, **26-*Z***), 3.61–3.45 (m, 2H, **26-*E***), 3.44–3.20 (m, 2H, **26-*Z***), 2.86–2.74 (m, 1H, **26-*Z***), 2.74–2.67 (m, 1H, **26-*E***), 2.66–2.50 (m, 1H, **26-*E***), 2.50–2.28 (m, 1H, **26-*Z***), 1.96–1.42 (m, 5H, **26-*E/Z***), 1.39–1.31 (m, 1H, **26-*E***), 1.31–1.20 (m, 1H, **26-*Z***).

26-*Z*: $^{13}C\{^1H\}$ NMR (126 MHz, $CDCl_3$) δ 140.4, 133.7, 132.2, 128.2, 127.8, 127.4, 126.2, 125.2, 125.2, 124.5, 124.4, 124.3, 67.9, 38.0, 32.5, 32.5, 20.8, 14.6.

HRMS(ESI) (m/z): $[M + H]^+$ calcd for $C_{19}H_{20}O$: 265.1593; found: 265.1591.

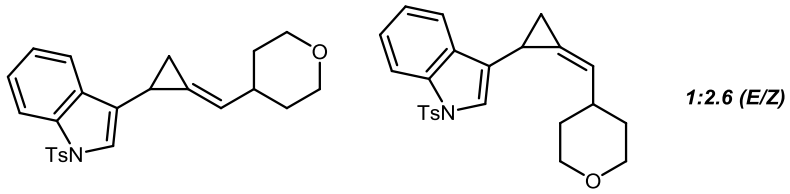

3-(2-((tetrahydro-2H-pyran-4-yl)methylene)cyclopropyl)-1-tosyl-1H-indole (27). The reaction was conducted according to the general procedure without modification using 4-(2,2-dichlorovinyl)tetrahydro-2H-pyran (38 mg, 0.21 mmol, 1.05 equiv) and 1-tosyl-3-vinyl-1H-indole (59 mg, 0.20 mmol, 1.0 equiv). The products were isolated as a yellow-brown oil following column chromatography (SiO_2, 9:1 CH_2Cl_2/EtOAc).

Run 1: 53 mg (65% yield), Run 2: 54.5 mg (67% yield) (E:Z = 1:2.6).

27-E/*Z*: ^{1}H NMR (300 MHz, $CDCl_3$) δ 8.01–7.90 (m, 1H), 7.77–7.65 (m, 2H), 7.60–7.51 (m, 1H), 7.35–7.13 (m, 5H), 6.03–5.96 (m, 1H, **27-*E***), 5.96 – 5.88 (m, 1H, **27-*Z***), 4.02 (dt, *J* = 11.2, 3.1 Hz, 2H, **27-*E***), 3.89 (ddt, J = 11.1, 6.6, 3.3 Hz, 2H, **27-*Z***), 3.51 (td, J = 11.5, 2.6 Hz, 2H, **27-*E***), 3.35 (dtd, J = 14.0, 11.0, 3.1 Hz, 2H, **27-*Z***), 2.67 (dd, J = 8.9, 4.6 Hz, 1H, **27-*Z***), 2.53 (dd, J = 9.5, 5.1 Hz, 1H, **27-*E***), 2.44 (m, 1H), 2.35 (s, 3H), 1.88–1.48 (m, 5H), 1.39–1.21 (m, 1H).

27-E/*Z*: $^{13}C\{^1H\}$ NMR (126 MHz, $CDCl_3$) δ 144.9, 135.6, 135.5, 135.4, 135.3, 130.9, 130.5, 129.9, 126.8, 126.8, 124.9, 124.8, 124.6, 124.3, 124.2, 123.6, 123.2, 123.1,

123.0, 122.3, 121.7, 119.8, 120.0, 114.0, 113.8, 67.9 (**27-*E***), 67.8 (**27-*Z***), 38.1 (**27-*Z***), 37.7 (**27-*E***), 32.7 (**27-*E***), 32.6 (**27-*E***), 32.5 (**27-*Z***), 21.6, 12.7 (**27-*Z***), 12.4 (**27-*E***), 11.6 (**27-*Z***), 9.6 (**27-*E***).

HRMS(ESI) (m/z): $[M + H]^+$ calcd for $C_{24}H_{25}NO_3S$: 408.1634; found: 408.1629.

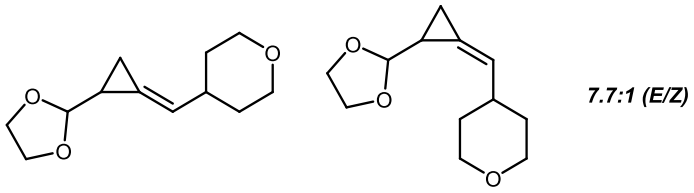

4-((2-(1,3-dioxolan-2-yl)cyclopropylidene)methyl)tetrahydro-2H-pyran (28). The reaction was conducted using 4-(2,2-dichlorovinyl)tetrahydro-2H-pyran (38 mg, 0.21 mmol, 1.05 equiv) and 2-vinyl-1,3-dioxolane (20 mg, 0.20 mmol, 1.0 equiv). Modifications from the general procedure: 10 mol% instead of 5 mol% catalyst loading and 48 h instead of 24 h reaction time. The products were isolated as a brown solid following column chromatography (SiO_2, 9:1 CH_2Cl_2/EtOAc). Single crystals of **28-*E*** suitable for X-ray diffraction analysis were obtained from concentrated $CHCl_3$ solutions at room temperature.

Run 1: 22.2 mg (53% yield), Run 2: 19.8 mg (47% yield) (E:Z = 7.7:1).

28-*E*: ^{1}H NMR (300 MHz, $CDCl_3$) δ 5.89 (dq, *J* = 6.3, 2.2 Hz, 1H), 4.42 (d, *J* = 6.4 Hz, 1H), 4.03–3.97 (m, 2H), 3.97–3.92 (m, 2H), 3.89–3.82 (m, 2H), 3.43 (td, *J* = 11.6, 2.4 Hz, 2H), 2.41 (ddddd, *J* = 15.0, 9.9, 5.6, 3.7, 1.8 Hz, 1H), 1.75–1.61 (m, 3H), 1.61–1.50 (m, 2H), 1.39 (tt, *J* = 8.7, 1.9 Hz, 1H), 1.17 (dddd, *J* = 8.8, 4.2, 2.4, 1.5 Hz, 1H).

28-*E*: $^{13}C\{^1H\}$ NMR (126 MHz, $CDCl_3$) δ 124.6, 119.8, 106.8, 67.9, 65.3, 65.1, 37.7, 32.6, 32.6, 16.7, 6.6.

HRMS(ESI) (m/z): $[M + H]^+$ calcd for $C_{12}H_{18}O_3$: 211.1334; found: 211.1328.

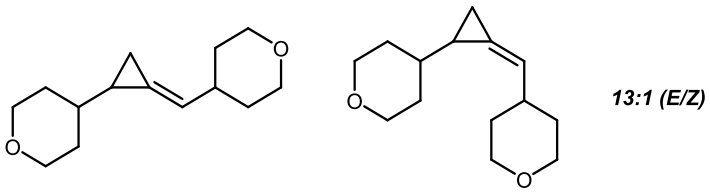

4-((2-(tetrahydro-2H-pyran-4-yl)cyclopropylidene)methyl)tetrahydro-2H-pyran (29). The reaction was conducted using 4-(2,2-dichlorovinyl)tetrahydro-2H-pyran (38 mg, 0.21 mmol, 1.05 equiv) and 4-vinyltetrahydro-2H-pyran (22 mg, 0.20 mmol, 1.0 equiv). Modifications from the general procedure: 48 h instead of 24 h reaction time. The products were isolated as a brown oil following column chromatography (SiO_2, 9:1 CH_2Cl_2/EtOAc).

Run 1: 26.5 mg (60% yield), Run 2: 22.7 mg (51% yield) (E:Z = 13:1).

29-*E*: ^{1}H NMR (500 MHz, $CDCl_3$) δ 5.71 (dq, *J* = 6.3, 2.1 Hz, 1H), 3.93 (dtd, *J* = 10.5, 5.7, 5.0, 2.2 Hz, 4H), 3.47–3.37 (m, 2H), 3.31 (td, *J* = 11.7, 2.4 Hz, 2H), 2.37 (tdd, *J* = 10.5, 6.7, 3.0 Hz, 1H), 1.66 (dtq, *J* = 11.1, 4.2, 2.2 Hz, 3H), 1.62–1.48 (m, 3H), 1.48–1.34 (m, 2H), 1.26–1.14 (m, 2H), 1.08 (dpd, *J* = 14.8, 7.6, 7.0, 4.4 Hz, 1H), 0.87–0.74 (m, 1H).

29-*E*: ^{13}C{^{1}H} NMR (125 MHz, $CDCl_3$) δ 124.7, 122.0, 68.1, 68.1, 68.0, 38.7, 37.8, 32.9, 32.8, 32.2, 32.2, 19.6, 7.5.

HRMS(ESI) (m/z): $[M + H]^+$ calcd for $C_{14}H_{22}O_2$: 223.1698; found: 223.1695.

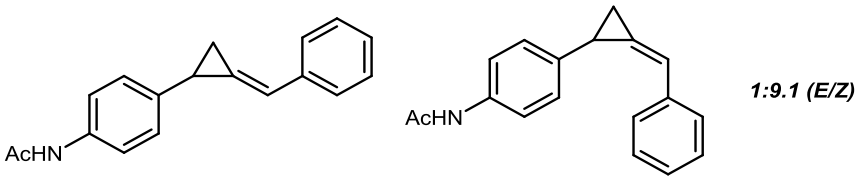

N-(4-(2-benzylidenecyclopropyl)phenyl)acetamide (30). The reaction was conducted using (2,2-dichlorovinyl)benzene (38 mg, 0.22 mmol, 1.1 equiv) and *N*-(4-vinylphenyl)acetamide (32 mg, 0.20 mmol, 1.0 equiv). Modifications from the general procedure: 10 mol% instead of 5 mol% catalyst loading. The products were isolated as a pale yellow solid following column chromatography (SiO_2, 9:1 EtOAc/CH_2Cl_2). Single

crystals suitable for X-ray diffraction analysis were obtained from concentrated MeCN solutions at room temperature.

Run 1: 51.5 mg (98% yield), Run 2: 50.5 mg (96% yield) (E:Z = 1:9.1).

30-*Z*: ^{1}H NMR (300 MHz, $CDCl_3$) δ 7.36 (dd, *J* = 7.6, 4.5 Hz, 4H), 7.23 (t, *J* = 7.1 Hz, 2H), 7.15 (dd, *J* = 8.9, 5.4 Hz, 2H), 7.07 (d, *J* = 8.2 Hz, 2H), 6.92 (s, 1H), 2.91 (dd, *J* = 10.0, 5.5 Hz, 1H), 2.22 (s, 3H), 1.87 (t, *J* = 9.0 Hz, 1H), 1.28 (dd, J = 12.5, 6.3 Hz, 1H).

30-*Z*: ^{13}C{^{1}H} NMR (125 MHz, $CDCl_3$) δ 168.7, 137.3, 137.2, 136.1, 128.6, 127.6, 127.1, 127.0, 126.9, 120.5, 120.2, 24.5, 21.1, 13.8.

HRMS(ESI) (m/z): $[M + Na]^+$ calcd for $C_{18}H_{17}NO$: 286.1208; found: 286.1196.

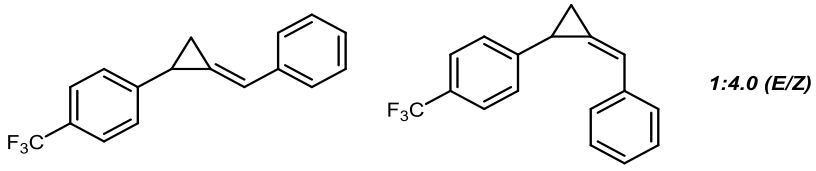

1-(2-benzylidenecyclopropyl)-4-(trifluoromethyl)benzene (31). The reaction was conducted using (2,2-dichlorovinyl)benzene (38 mg, 0.22 mmol, 1.1 equiv) and 1-(trifluoromethyl)-4-vinylbenzene (35 mg, 0.20 mmol, 1.0 equiv). Modifications from the general procedure: 10 mol% instead of 5 mol% catalyst loading. The products were isolated as a colorless oil following column chromatography (SiO_2, hexanes).

Run 1: 45 mg (82% yield), Run 2: 43.9 mg (80% yield) (E:Z = 1:4.0).

31-*E/Z*: ^{1}H NMR (300 MHz, $CDCl_3$) δ 7.63 (d, *J* = 9 Hz, 2H, **31-*E***), 7.54 (d, *J* = 9 Hz, 2H, **31-*Z***), 7.44–7.32 (m, 2H, **31-*E/Z***), 7.31–7.13 (m, 5H, **31-*E/Z***), 7.05–6.98 (m, 1H, **31-*Z***), 6.98–6.92 (m, 1H, **31-*E***), 3.10–2.93 (m, 1H, **31-*Z***), 2.86–2.78 (m, 1H, **31-*E***), 2.26 (td, *J* = 9.5, 2.6 Hz, 1H, **31-*E***), 2.0 (td, *J* = 8.8, 1.9 Hz, 1H, **31-*Z***), 1.72–1.63 (m, 1H, **31-*E***), 1.48–1.22 (m, 1H, **31-*Z***).

31-*Z*: ^{13}C{^{1}H} NMR (126 MHz, $CDCl_3$) δ 145.6, 137.0, 128.7, 128.4 (q, $^{2}J_{C–F}$ = 33 Hz), 127.4, 127.1, 126.7, 126.5, 125.7 (q, $^{3}J_{C–F}$ = 3.8 Hz), 124.5 (q, $^{1}J_{C–F}$ = 272 Hz), 120.7, 21.4, 14.4.

31-*Z*: ^{19}F NMR (300 MHz, $CDCl_3$) δ –63.80.

HRMS(APCI) (m/z): $[M + H]^+$ calcd for $C_{17}H_{13}F_3$: 275.1048; found: 275.1035.

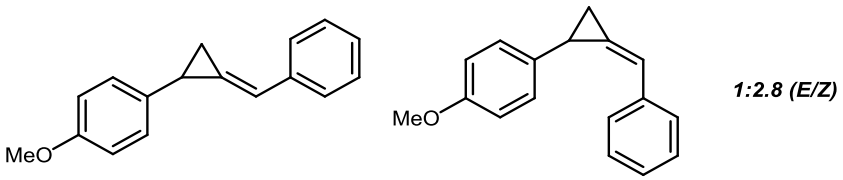

1-(2-benzylidenecyclopropyl)-4-methoxybenzene (32). The reaction was conducted according to the general procedure without modification using (2,2-dichlorovinyl)benzene (38 mg, 0.22 mmol, 1.1 equiv) and 4-vinylanisole (27 mg, 0.20 mmol, 1.0 equiv). The products were isolated as a pale yellow oil following column chromatography (SiO_2, 2:3 CH_2Cl_2/hexanes).

Run 1: 37.8 mg (80% yield), Run 2: 36.7 mg (78% yield) (E:Z = 1:2.8).

32-*E/Z*: ^{1}H NMR (500 MHz, $CDCl_3$) δ 7.64 (d, *J* = 8.1 Hz, 2H, **32-*E***), 7.45–7.41 (m, 2H, **32-*Z***), 7.39 (d, *J* = 7.9 Hz, 2H, **32-*E***), 7.32–7.25 (m, 1H/2H, **32-*E*/*Z***), 7.23–7.17 (m, 1H, **32-*Z***), 7.16 (d, *J* = 8.7 Hz, 2H, **32-*E***), 7.09 (d, *J* = 8.7 Hz, 2H, **32-*Z***), 6.96 (m, 1H, **32-*E*/*Z***), 6.89–6.82 (m, 2H, **32-*E*/*Z***), 3.81 (s, 3H, **32-*E***), 3.79 (s, 3H, **32-*Z***), 2.92 (ddd, *J* = 9.1, 4.9, 2.1 Hz, 1H, **32-*Z***), 2.71 (ddd, *J* = 9.0, 5.0, 1.8 Hz, 1H, **32-*E***), 2.09 (td, *J* = 9.2, 2.4 Hz, 1H, **32-*E***), 1.83 (td, *J* = 9.0, 2.0 Hz, 1H, **32-*Z***), 1.51 (ddd, *J* = 9.3, 5.0, 2.5 Hz, 1H, **32-*E***), 1.23 (ddd, *J* = 8.9, 4.9, 2.0 Hz, 1H, **32-*Z***).

32-*E*: $^{13}C\{^1H\}$ NMR (125 MHz, $CDCl_3$) δ 158.1, 137.9, 134.0, 129.0, 128.7, 127.7, 127.2, 127.0, 119.5, 114.0, 55.4, 17.3, 15.7.

32-*Z*: $^{13}C\{^1H\}$ NMR (125 MHz, $CDCl_3$) δ 158.1 137.5, 133.1, 128.6, 128.0, 127.6, 127.2, 127.0, 120.3, 114.2, 55.3, 20.9, 13.6.

HRMS(ESI) (m/z): $[M + H]^+$ calcd for $C_{17}H_{16}O$: 237.1280; found: 237.1277.

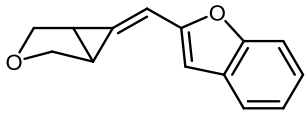

2-((3-oxabicyclo[3.1.0]hexan-6-ylidene)methyl)benzofuran (33). The reaction was conducted using 2-(2,2-dichlorovinyl)benzofuran (43 mg, 0.20 mmol, 1.0 equiv) and 2,5-dihydrofuran (140 mg, 2.0 mmol, 10 equiv). Modifications from the general procedure: 10 mol% instead of 5 mol% catalyst loading. The product was isolated as a pale yellow solid following column chromatography (SiO_2, 3:2 CH_2Cl_2/hexanes).

Run 1: 30 mg (71% yield), Run 2: 34.8 mg (82% yield).

^{1}H NMR (300 MHz, $CDCl_3$) δ 7.56–7.49 (m, 1H), 7.44 (dq, *J* = 8.2, 0.9 Hz, 1H), 7.30–7.15 (m, 2H), 6.76 (d, *J* = 1.5 Hz, 1H), 6.62 (s, 1H), 4.33 (d, *J* = 8.0 Hz, 1H), 4.17 (d, *J* = 8.1 Hz, 1H), 4.02–3.85 (m, 2H), 2.53 (ddd, *J* = 7.2, 3.4, 1.8 Hz, 1H), 2.32 (ddd, *J* = 7.1, 3.2, 1.1 Hz, 1H).

^{13}C{^{1}H} NMR (125 MHz, $CDCl_3$) δ 155.1, 155.0, 131.6, 129.2, 124.2, 122.8, 120.9, 111.1, 110.3, 103.6, 71.82, 71.6, 23.2, 21.2.

HRMS(ESI) (m/z): calcd for $C_{14}H_{13}O_2$: 213.0916; found: 213.0912.

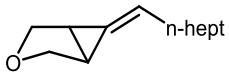

6-octylidene-3-oxabicyclo[3.1.0]hexane (34). The reaction was conducted using 1,1-dichlorononon-1-ene (39 mg, 0.20 mmol, 1.0 equiv) and 2,5-dihydrofuran (140 mg, 2.0 mmol, 10 equiv). Modifications from the general procedure: 10 mol% instead of 5 mol% catalyst loading. The product was isolated as a pale yellow oil following column chromatography (SiO_2, 3:2 CH_2Cl_2/hexanes).

Run 1: 28 mg (72% yield), Run 2: 30 mg (77% yield).

^{1}H NMR (300 MHz, $CDCl_3$) δ 5.82 (t, *J* = 6.5 Hz, 1H), 4.04 (t, *J* = 7.6 Hz, 2H), 3.80 (dt, *J* = 6.8, 2.7 Hz, 2H), 2.27–2.05 (m, 4H), 1.56–1.24 (m, 13H), 1.01–0.87 (m, 3H).

^{13}C{^{1}H} NMR (125 MHz, $CDCl_3$) δ 124.9, 121.3, 71.3, 71.2, 32.0, 31.9, 29.9, 29.4, 29.4, 22.8, 21.0, 20.9, 14.3.

HRMS(APCI) (m/z): $[M + H]^+$ calcd for $C_{13}H_{22}O$: 195.1749; found: 195.1735.

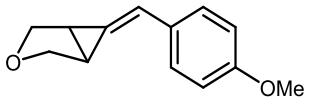

6-(4-methoxybenzylidene)-3-oxabicyclo[3.1.0]hexane (35). The reaction was conducted using 1-(2,2-dichlorovinyl)-4-methoxybenzene (41 mg, 0.20 mmol, 1.0 equiv) and 2,5-dihydrofuran (140 mg, 2.0 mmol, 10 equiv). Modifications from the general procedure: 10 mol% instead of 5 mol% catalyst loading. The product was obtained as a pale brown oil following column chromatography (SiO_2, 3:2 EtOAc/CH_2Cl_2).

Run 1: 31 mg (77% yield), Run 2: 32.2 mg (80% yield).

^{1}H NMR (300 MHz, $CDCl_3$) δ 7.40 (d, *J* = 8.6 Hz, 2H), 6.87 (d, *J* = 8.6 Hz, 2H), 6.72 (s, 1H), 4.25 (d, *J* = 7.8 Hz, 1H), 4.12 (d, *J* = 8.1 Hz, 1H), 3.91 (ddd, *J* = 15.3, 8.2, 3.4 Hz, 2H), 3.84 (s, 3H), 2.52-2.44 (m, 1H), 2.24 (dd, *J* = 7.1, 3.2 Hz, 1H).

^{13}C{^{1}H} NMR (125 MHz, $CDCl_3$) δ 158.9, 130.5, 128.0, 125.1, 120.2, 114.1, 71.4, 70.9, 55.4, 22.6, 19.7.

HRMS(ESI) (m/z): $[M + H]^+$ calcd for $C_{13}H_{14}O$: 203.1072; found: 203.1066.

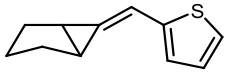

2-(((bicyclo[3.1.0]hexan-6-ylidene)methyl)thiophene (36). The reaction was conducted using 2-(2,2-dichlorovinyl)thiophene (36 mg, 0.20 mmol, 1.0 equiv) and cyclopentene (136 mg, 2.0 mmol, 10 equiv). Modifications from the general procedure: 10 mol% instead of 5 mol% catalyst loading. The product was isolated as a pale brown oil following column chromatography (SiO_2, hexanes).

Run 1: 34.9 mg (99% yield), Run 2: 35 mg (99% yield).

^{1}H NMR (300 MHz, $CDCl_3$) δ 6.97 (s, 1H), 6.92 (d, *J* = 4.5 Hz, 1H), 6.90–6.83 (m, 2H), 2.30 (dd, *J* = 12.0, 7.2 Hz, 1H), 2.10–2.03 (m, 1H), 2.01–1.88 (m, 2H), 1.88–1.66 (m, 2H), 1.61–1.45 (m, 1H), 1.37–1.16 (m, 1H).

^{13}C{^{1}H} NMR (125 MHz, $CDCl_3$) δ 144.2, 133.2, 127.2, 124.0, 123.9, 114.0, 30.2, 29.1, 22.8, 21.7, 21.3.

HRMS(ESI) (m/z): $[M + H]^+$ calcd for $C_{11}H_{12}S$: 177.0738; found: 177.0735.

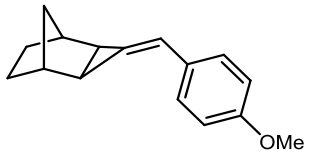

3-(4-methoxybenzylidene)tricyclo[3.2.1.02,4]octane [607020-85-8] (37).[ix] The reaction was conducted using 1-(2,2-dichlorovinyl)-4-methoxybenzene (41 mg, 0.20 mmol, 1.0 equiv) and norbornene (75 mg, 0.80 mmol, 4 equiv). Modifications from the general procedure: 10 mol% instead of 5 mol% catalyst loading, 60 °C instead of room temperature. The product was isolated as a colorless oil following column chromatography (SiO_2, 1:5 CH_2Cl_2/hexanes).

Run 1: 39.3 mg (87% yield), Run 2: 38 mg (84% yield).

^{1}H NMR (500 MHz, $CDCl_3$) δ 7.44 (d, *J* = 10 Hz, 2H), 6.88 (d, *J* = 10 Hz, 2H), 6.60 (s, 1H), 3.82 (s, 3H), 2.62 (s, 1H), 2.50 (s, 1H), 1.65–1.53 (m, 3H), 1.52–1.43 (m, 2H), 1.34 (d, *J* = 10 Hz, 1H), 1.03 (d, *J* = 10 Hz, 1H), 0.82 (d, *J* = 10 Hz, 1H).

^{13}C{^{1}H} NMR (125 MHz, $CDCl_3$) δ 158.6, 131.3, 128.2, 127.6, 118.9, 114.0, 55.4, 38.5, 38.1, 31.0, 29.0, 28.8, 23.0, 19.5.

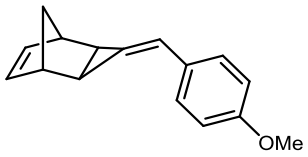

3-(4-methoxybenzylidene)tricyclo[3.2.1.02,4]oct-6-ene [1195789-82-2] (38). [x] The reaction was conducted using 1-(2,2-dichlorovinyl)-4-methoxybenzene (41 mg, 0.20 mmol, 1.0 equiv) and norbornadiene (92 mg, 1 mmol, 5.0 equiv). Modifications from the general procedure: 10 mol% instead of 5 mol% catalyst loading. The product was isolated as a colorless oil following column chromatography (SiO_2, 1:5 CH_2Cl_2/hexanes).

Run 1: 23.7 mg (53% yield), Run 2: 24.1 mg (54% yield).

^{1}H NMR (300 MHz, $CDCl_3$) δ 7.45 (d, *J* = 9 Hz, 2H), 6.88 (d, *J* = 8.6 Hz, 2H), 6.51 (s, 1H), 6.43 (bs, 2H), 3.85 (s, 3H), 3.23 (s, 1H), 3.11 (s, 1H), 1.88 (d, *J* = 7.7 Hz, 1H), 1.66 (d, *J* = 8.0 Hz, 1H), 1.19 (d, *J* = 8.3 Hz, 1H), 1.01 (d, *J* = 8.6 Hz, 1H).

^{13}C{^{1}H} NMR (125 MHz, $CDCl_3$) δ 158.7, 139.9, 139.4, 138.9, 131.0, 127.8, 116.7, 114.1, 55.5, 45.2, 44.5, 42.7, 28.4, 25.1.

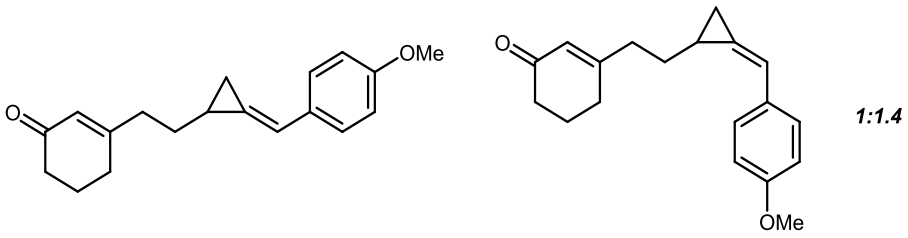

3-(2-(2-(4-methoxybenzylidene)cyclopropyl)ethyl)cyclohex-2-en-1-one (39). The reaction was conducted according to the general procedure without modification using 3-(but-3-en-1-yl)cyclohex-2-en-1-one (30.0 mg, 0.20 mmol, 1.0 equiv) and (2,2-dichlorovinyl)benzene (38.2 mg, 0.22 mmol, 1.10 equiv). The product was isolated as a yellow oil following column chromatography (SiO_2, 2:3 CH_2Cl_2/hexanes).

38.0 mg, 67% yield (ratio of stereoisomer = 1:1.4).

39-*E/Z*: ^{1}H NMR (500 MHz, $CDCl_3$) δ 7.45 (d, *J* = 8.8 Hz, 2H, **39-major**), 7.35 (d, *J* = 8.7 Hz, 2H, **39-minor**), 6.87 (d, *J* = 8.8 Hz, 2H), 6.71 (q, J = 2.0 Hz, 1H, **39-major**), 6.66 (q, J = 1.8 Hz, 1H, **39-minor**), 5.93 (s, 1H, **39-major**), 5.91 (s, 1H, **39-minor**), 3.82 (s, 3H, **39-minor**), 3.81 (s, 3H, **39-major**), 2.41–2.27 (m, 6H), 2.21–2.12 (m, 1H, **39-major**), 2.04–1.95 (m, 2H), 1.76 (dddq, J = 11.0, 6.5, 4.4, 2.1 Hz, 1H, **39-minor**), 1.72–1.53 (m, 3H), 1.48 (dddd, J = 11.5, 8.7, 4.6, 1.7 Hz, 1H, **39-major**), 1.36–1.24 (m, 1H), 1.07 (ddd, J = 8.9, 4.6, 2.3 Hz, 1H, **39-major**), 0.84 (ddd, J = 8.7, 4.8, 1.9 Hz, 1H, **39-minor**).

39-*E/Z*: $^{13}C\{^1H\}$ NMR (125 MHz, $CDCl_3$) δ 199.8, 165.9, 165.8, 158.7, 158.6, 130.8, 130.7, 127.8, 127.7, 126.5, 126.3, 126.0, 125.9, 118.7, 117.6, 114.0, 113.9, 55.3, 37.9, 37.4, 37.3, 37.1, 30.7, 29.8, 29.7, 29.5, 22.7, 16.3, 12.8, 10.7, 7.5.

HRMS(ESI) (m/z): $[M + H]^+$ calcd for $C_{19}H_{22}O$: 283.1698; found: 283.1693.

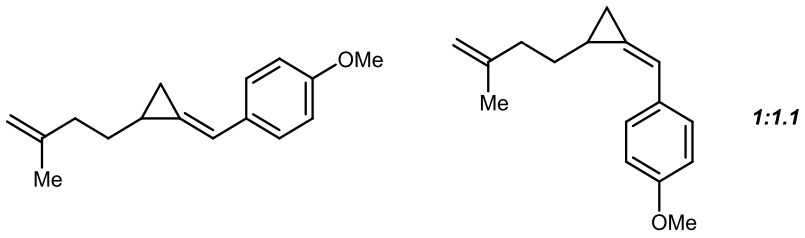

1-methoxy-4-((2-(3-methylbut-3-en-1-yl)cyclopropylidene)methyl)benzene (40). The reaction was conducted according to the general procedure without modification using 2-methyl-1,5-hexadiene (19.2 mg, 0.20 mmol, 1.0 equiv) and (2,2-dichlorovinyl)benzene (38.2 mg, 0.22 mmol, 1.10 equiv). The product was isolated as a colorless oil following column chromatography (SiO_2, 1:4 CH_2Cl_2/hexanes).

43.5 mg, 95% yield (ratio of stereoisomer = 1:1.1).

40-*E/Z*: ^{1}H NMR (500 MHz, $CDCl_3$) δ 7.47 (d, *J* = 8.8 Hz, 2H), 7.39 (d, *J* = 8.8 Hz, 2H), 6.88 (dd, *J* = 8.9, 2.4 Hz, 2H), 6.72 (q, *J* = 2.0 Hz, 1H), 6.65 (q, *J* = 1.8 Hz, 1H), 4.77–4.70 (m, 2H), 3.82 (s, 3H), 3.81 (s, 3H), 2.24–2.15 (m, 2H), 2.16–2.08 (m, 1H), 1.81–1.69 (m, 3H), 1.65–1.43 (m, 2H), 1.29 (tdd, *J* = 8.7, 2.1, 1.1 Hz, 1H), 1.22–1.12 (m, 1H), 1.09–1.02 (m, 1H), 0.83 (ddd, *J* = 8.6, 4.9, 1.9 Hz, 1H).

40-*E/Z*: $^{13}C\{^1H\}$ NMR (125 MHz, $CDCl_3$) δ 158.5, 145.7, 131.2, 131.0, 127.8, 127.6, 127.5, 118.1, 117.0, 113.9, 113.9, 110.0, 55.3, 37.6, 36.9, 31.5, 30.3, 22.6, 22.5, 16.7, 13.1, 10.6, 7.5.

HRMS(ESI) (m/z): $[M + H]^+$ calcd for $C_{16}H_{20}O$: 229.1593; found: 229.1590.

B.5 Reactions with Ethylene

General procedures for reactions with ethylene. In an N_2-filled glovebox, a 25-mL Schlenk tube was charged with a magnetic stir bar, the [$^{i\text{-Pr}}$NDI]$Ni_2(C_6H_6)$ catalyst **1** (0.010 mmol, 0.050 equiv), Zn powder (0.60 mmol, 3.0 equiv), DMA (200 µL), and Et_2O (1.6 mL). The reaction mixture was frozen in the glovebox cold well at liquid N_2 temperatures. The 1,1-dichloroalkene (0.20 mmol, 1.0 equiv) was added. The Schlenk tube was sealed, removed from the glove box, and immediately placed in liquid N_2. The Schlenk tube was connected to a Schlenk line, the N_2 atmosphere was evacuated, and the reaction vessel was back-filled with ethylene (1 atm). The reaction was stirred at room temperature.

After 24 h, the reaction mixture was concentrated under reduced pressure, and the crude residue was directly loaded onto a SiO_2 column for purification. Isolated yields were determined following purification.

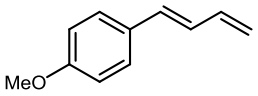

(*E*)-1-(buta-1,3-dien-1-yl)-4-methoxybenzene [32507-39-4] (41).[xi] According to the general procedure, ethylene was (1 atm) reacted with 1-(2,2-dichlorovinyl)-4-methoxybenzene (41 mg, 0.2 mmol, 1.0 equiv). Isolated yields were determined by following column chromatography (SiO_2, 1:3 CH_2Cl_2/hexanes).

Run 1: 78% yield, Run 2: 78% yield.

^{1}H NMR (500 MHz, $CDCl_3$) δ 7.35 (d, *J* = 8.7 Hz, 2H), 6.87 (d, *J* = 8.8 Hz, 2H), 6.68 (dd, *J* = 15.5, 10.5 Hz, 1H), 6.58–6.45 (m, 2H), 5.29 (d, *J* = 15.3 Hz, 1H), 5.13 (d, *J* = 8.5 Hz, 1H), 3.82 (s, 3H).

^{13}C{^{1}H} NMR (125 MHz, $CDCl_3$) δ 159.4, 137.5, 132.5, 130.1, 127.8, 116.6, 114.2, 55.4.

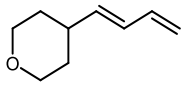

(*E*)-4-(buta-1,3-dien-1-yl)tetrahydro-2H-pyran [1646529-61-4] (42). [xii] According to the general procedure, ethylene was (1 atm) reacted with 4-(2,2-dichlorovinyl)tetrahydro-2H-pyran (36 mg, 0.2 mmol, 1.0 equiv). Isolated yields were determined by following column chromatography (SiO_2, 19:1 CH_2Cl_2/EtOAc hexanes).

Run 1: 76% yield, Run 2: 80% yield.

^{1}H NMR (300 MHz, $CDCl_3$) δ 6.64 (dt, *J* = 16.7, 10.5 Hz, 1H), 5.96 (t, *J* = 10.9 Hz, 1H), 5.42–5.04 (m, 3H), 4.11–3.87 (m, 2H), 3.47 (td, *J* = 11.5, 2.7 Hz, 2H), 2.86–2.64 (m, 1H), 1.73–1.41 (m, 4H).

^{13}C{^{1}H} (126 MHz, $CDCl_3$) δ 136.7, 132.2, 128.5, 117.8, 67.6, 34.2, 32.9.

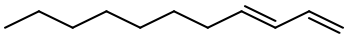

(*E*)-undeca-1,3-diene [79309-74-3] (43).[xiii] According to the general procedure, ethylene was (1 atm) reacted with 1,1-dichlorononon-1-ene (39 mg, 0.2 mmol, 1.0 equiv). Isolated yields were determined by following column chromatography (SiO_2, hexanes).

Run 1: 74% yield, Run 2: 74% yield (E:Z = 8.3:1).

43-*E*: ^{1}H NMR (500 MHz, $CDCl_3$) δ 6.71–6.57 (m, 1H), 6.04–5.94 (m, 1H), 5.46 (dt, *J* = 10.9, 7.8 Hz, 1H), 5.18 (dd, *J* = 16.9, 2.0 Hz, 1H), 5.08 (dd, *J* = 10.2, 2.1 Hz, 1H), 2.19 (qd, *J* = 7.5, 1.6 Hz, 2H), 1.35 – 1.12 (m, 10H), 0.89 (t, *J* = 6.8 Hz, 3H).

43-*E*: ^{13}C{^{1}H} (125 MHz, $CDCl_3$) δ 133.2, 132.5, 129.3, 116.8, 32.0, 29.8, 29.4, 29.4, 27.9, 22.8, 14.3.

B.6 Assignment of E/Z Sterechemistry in Methylenecyclopropane Products

The assignments of alkene stereochemistry in products **3** and **12–32** were made using a combination of X-ray crystallography, ^{1}H NMR analysis, and NOE analysis. Each of the product classes are discussed separately below.

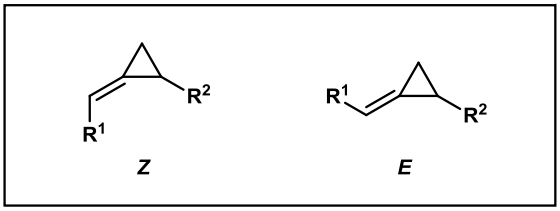

Product Class: R^1 = aryl, R^2 = aryl — Products **12–16**, **30–32**

For these methylenecyclopropanes, the *Z*-stereoisomer is the major product.

The ^{1}H NMR signals for the *E* and *Z* stereoisomers of **12** (aryl = phenyl) were previously assigned in the literature[xiv] and are consistent with our data.

Single crystals were obtained for a representative member of the class, compound **30**, which affords high diastereoselectivity. The XRD structure shows *Z*-stereochemistry, and the ^{1}H NMR spectrum was obtained for the pure major diastereomer.

NOE data were obtained for a representative member of the class, compound **31**, which has sufficiently resolved ^{1}H NMR signals to permit the detection of key exchange interactions (Figure S2).

All other members of this class were assigned by comparison of the ^{1}H NMR spectra. The most reliable signal for stereochemical assignment is the cyclopropyl methine proton. The $^{4}J_{HH}$ coupling constant is larger for the *Z*-isomer than for the *E*-isomer.

Examples:

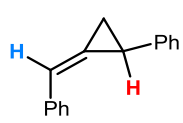

12-Z

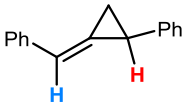

12-E

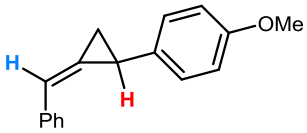

32-Z

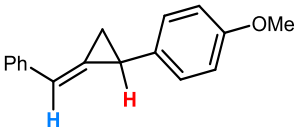

32-Z

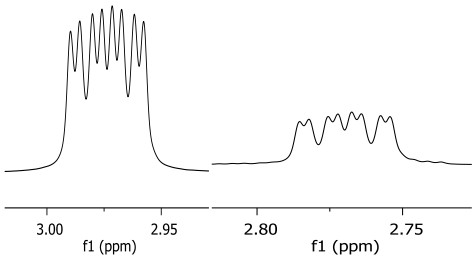

ddd, *J* = 9.2, 4.9, **2.1** Hz

ddd, *J* = 9.1, 4.9, **1.8** Hz

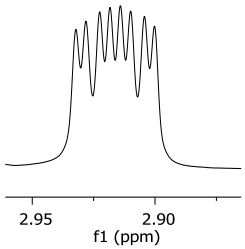

ddd, *J* = 9.1, 4.9, **2.1** Hz

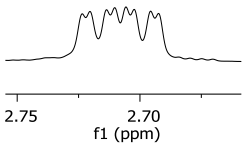

ddd, *J* = 9.0, 5.0, **1.8** Hz

Product Class: R^1 = branched alkyl (eg. THP), R^2 = aryl — Products **3**, **17–27**

For these methylenecyclopropanes, the *Z*-stereoisomer is the major product.

Single crystals were obtained for a representative member of the class, compound **22**, which affords high diastereoselectivity. The XRD structure shows Z-stereochemistry.

NOE data were obtained for representative members of the class, compounds **20** and **26**, which has sufficiently resolved ^{1}H NMR signals to permit the detection of key exchange interactions (Figures S3 and S4).

All other members of this class were assigned by comparison of the ^{1}H NMR spectra. For THP-containing products, the most reliable signals for stereochemical

assignment are the protons adjacent to the THP oxygen, which show distinct splitting patterns for the E and Z stereoisomers.

The related products **17** and **18** were assigned by analogy.

Examples:

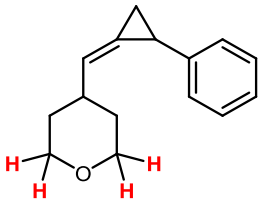

3

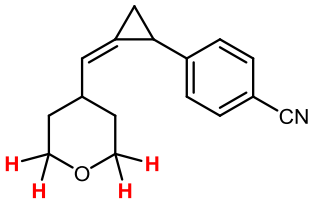

22

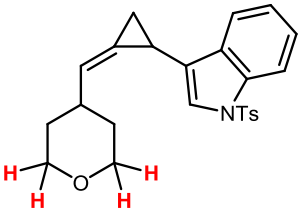

27

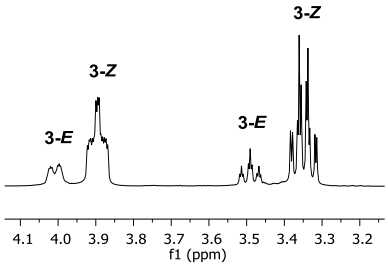

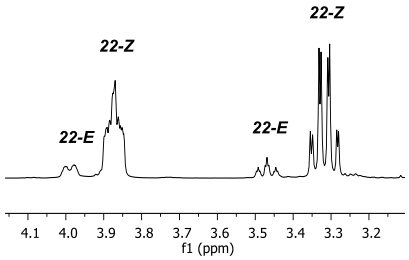

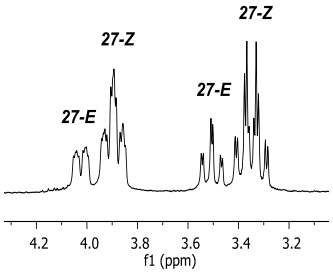

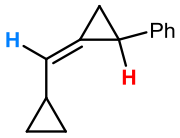

17-Z

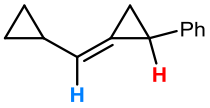

17-E

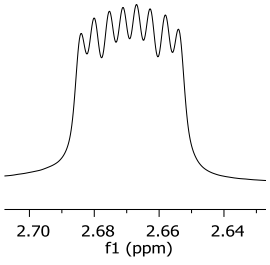

ddd, *J* = 8.7, 4.5, **2.1** Hz

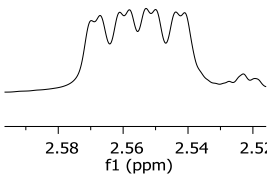

ddd, *J* = 8.6, 4.6, **1.7** Hz

	R^1 = branched alkyl	
Product Class:	(eg. THP)	Products **28** and **29**
	R^2 = branched alkyl	

For these methylenecyclopropanes, the E-stereoisomer is the major product.

Single crystals were obtained for a representative member of the class, compound **28**, which affords high diastereoselectivity. The XRD structure shows E-stereochemistry, and the ^{1}H NMR spectrum was obtained for the pure major diastereomer.

NOE data were obtained for a representative member of the class, compound **28**, which has sufficiently resolved ^{1}H NMR signals to permit the detection of key exchange interactions (Figure S4).

The related product **29** was assigned by analogy.

Product Class:	R^1 = aryl	Products **39** and **40**
	R^2 = linear alkyl	

These methylenecyclopropanes are formed in a near 1:1 mixture of E- and Z-stereoisomers. The ^{1}H NMR resonances that correspond to each stereoisomer are left unassigned.

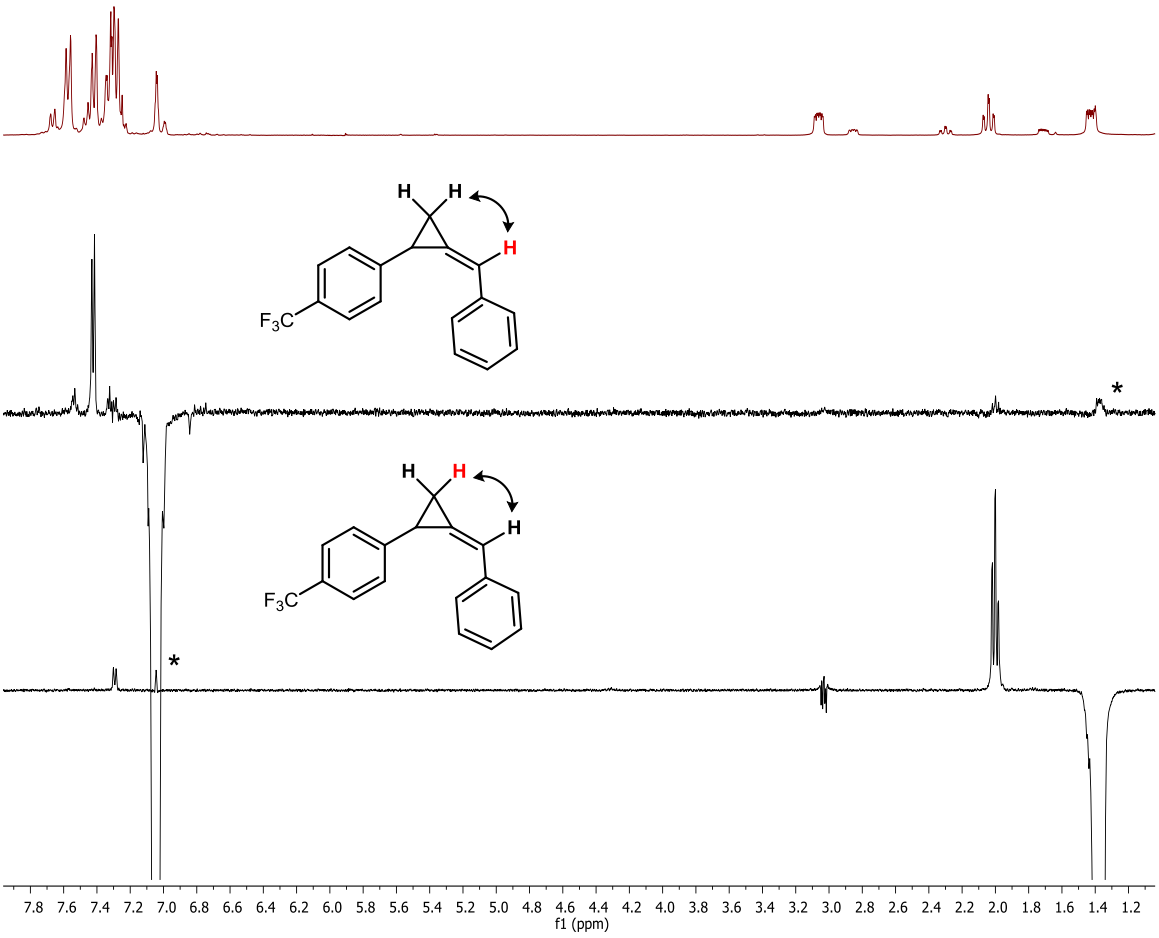

Figure B.2. NOE data for **31** highlighting exchange interactions relevant to the assignment of the alkene stereochemistry. The irradiated proton is shown in red (negative phase), and an asterisk is placed next to the exchange interaction indicated by the double-headed arrow.

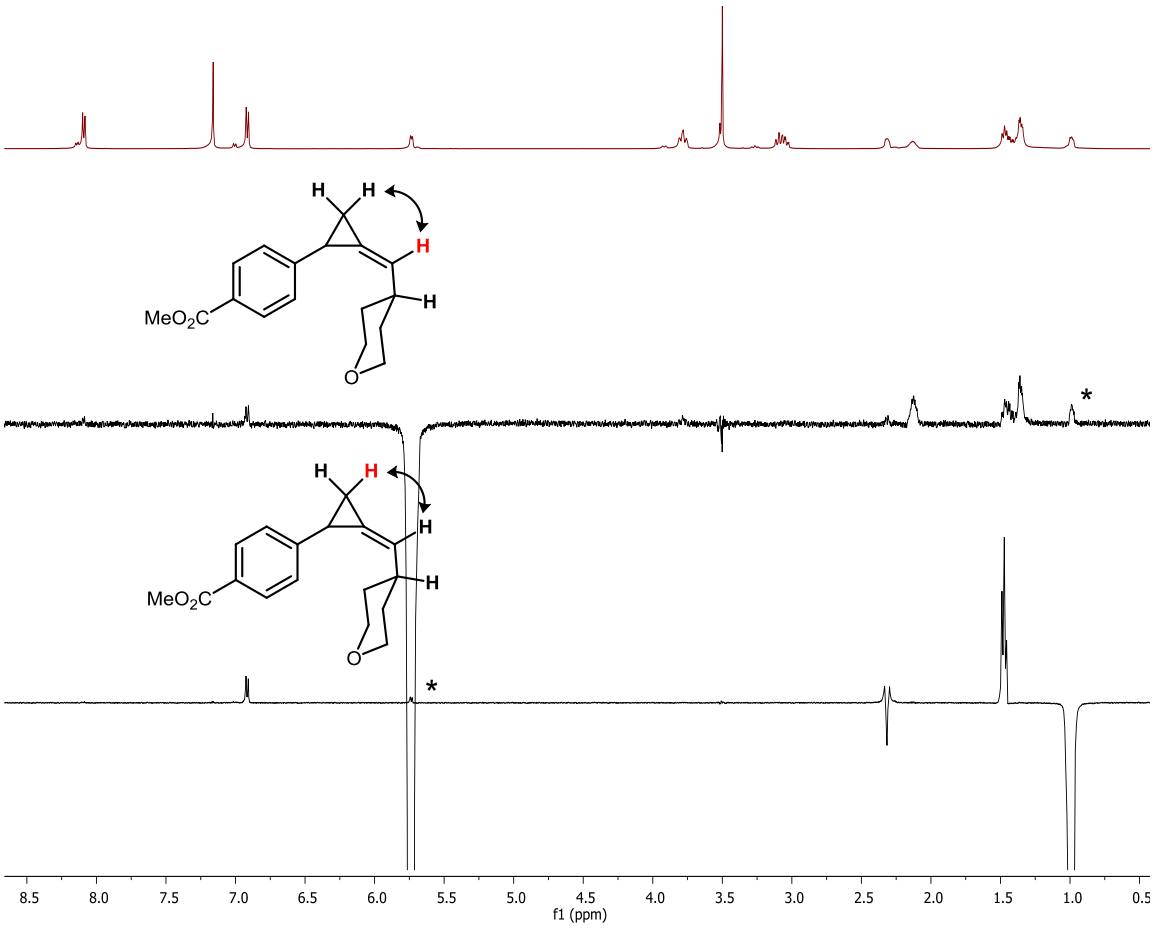

Figure B.3. NOE data for **20** highlighting exchange interactions relevant to the assignment of the alkene stereochemistry. The irradiated proton is shown in red (negative phase), and an asterisk is placed next to the exchange interaction indicated by the double-headed arrow.

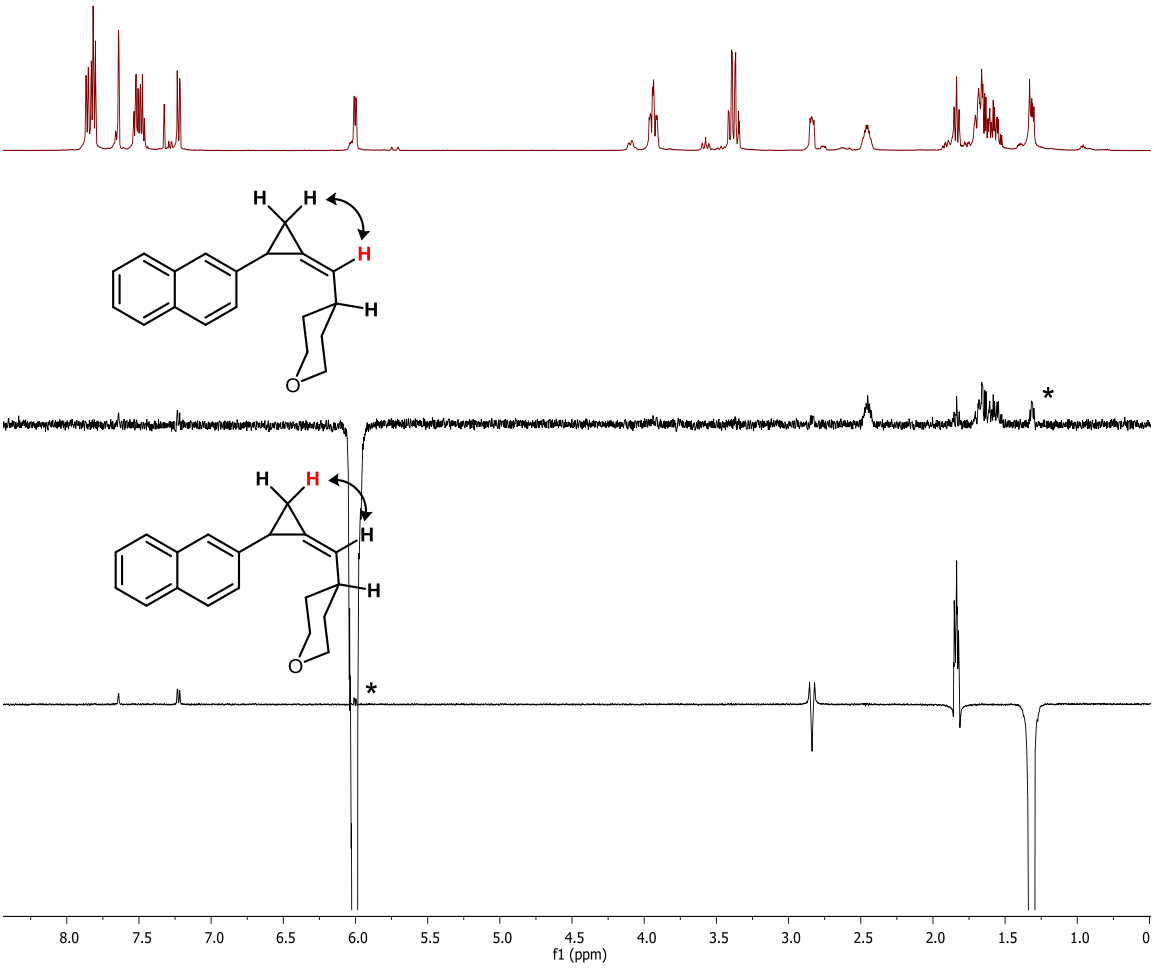

Figure B.4. NOE data for **26** highlighting exchange interactions relevant to the assignment of the alkene stereochemistry. The irradiated proton is shown in red (negative phase), and an asterisk is placed next to the exchange interaction indicated by the double-headed arrow.

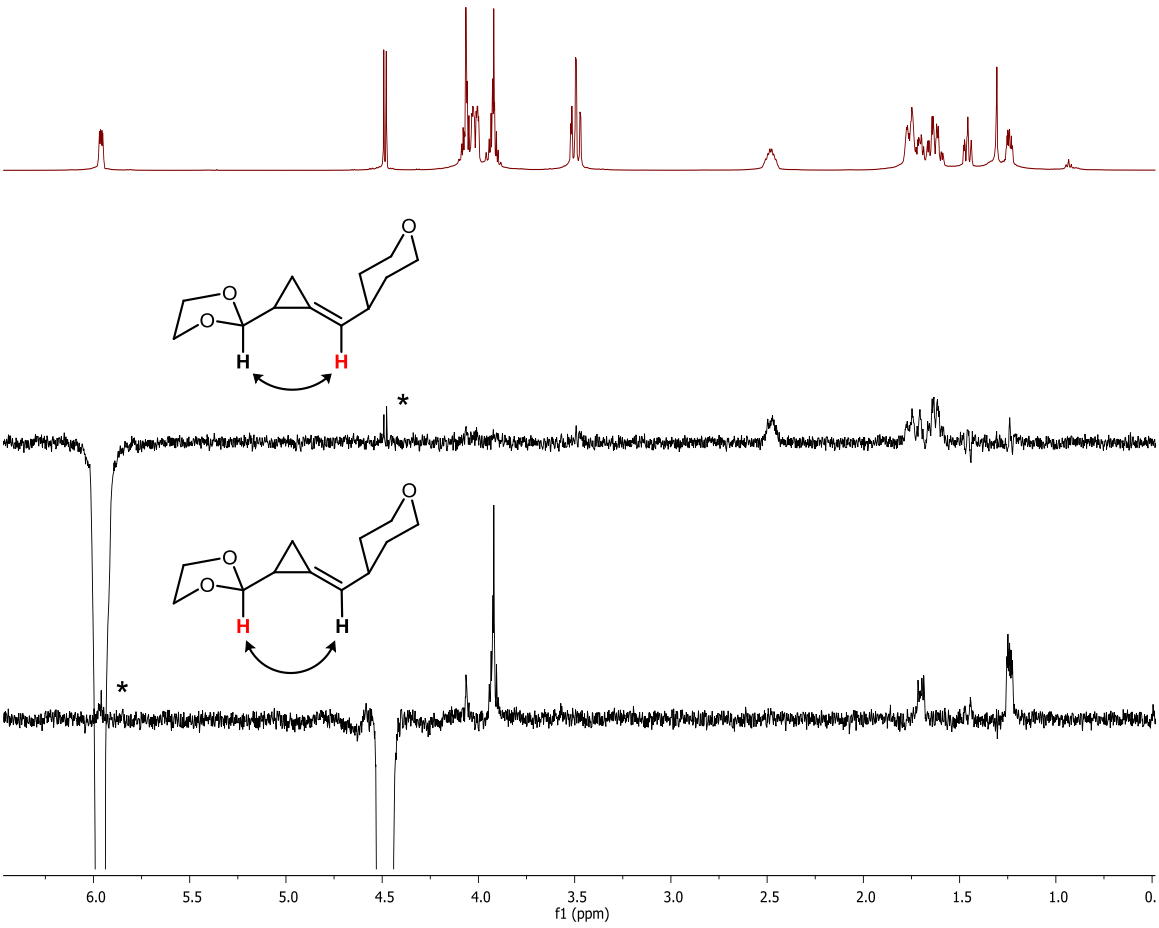

Figure B.5. NOE data for **28** highlighting exchange interactions relevant to the assignment of the alkene stereochemistry. The irradiated proton is shown in red (negative phase), and an asterisk is placed next to the exchange interaction indicated by the double-headed arrow.

B.7 Mechanistic Studies

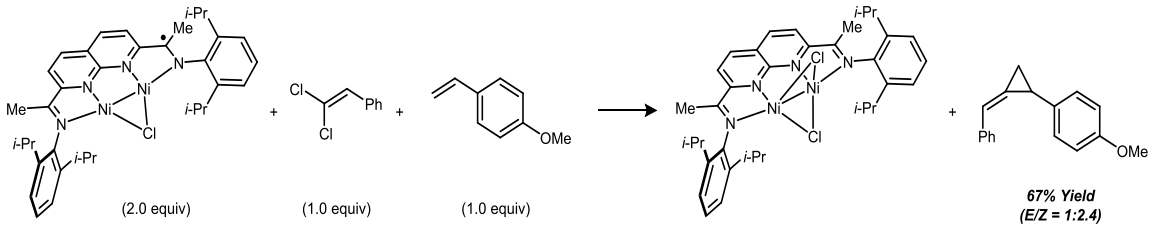

Stoichiometric methylenecyclopropanation in the absence of Zn. In an N_2-filled glovebox, the [$^{i\text{-Pr}}$NDI]Ni_2Cl complex **44** (20.6 mg, 0.030 mmol, 2.0 equiv) was dissolved Et_2O (0.6 mL), generating a dark purple solution. A solution of (2,2-dichlorovinyl)benzene (2.6 mg, 0.015 mmol, 1.0 equiv) and 1-methoxy-4-vinylbenzene (2.0 mg, 0.015 mmol, 1.0 equiv) dissolved in DMA (0.20 mL) and ether (1.0 mL) was added. The reaction mixture was stirred at room temperature, resulting in a color change to dark green. After 1 h, the reaction vessel was removed from the glovebox, opened to atmosphere, and concentrated under reduced pressure. Mesitylene (4.3 mg, 5.0 μL) was added as a ^{1}H NMR integration standard, and an aliquot of this solution was filtered through a short plug of SiO_2, eluting with $CDCl_3$ (approx. 1.5 mL). The product mixture was analyzed by ^{1}H NMR spectroscopy.

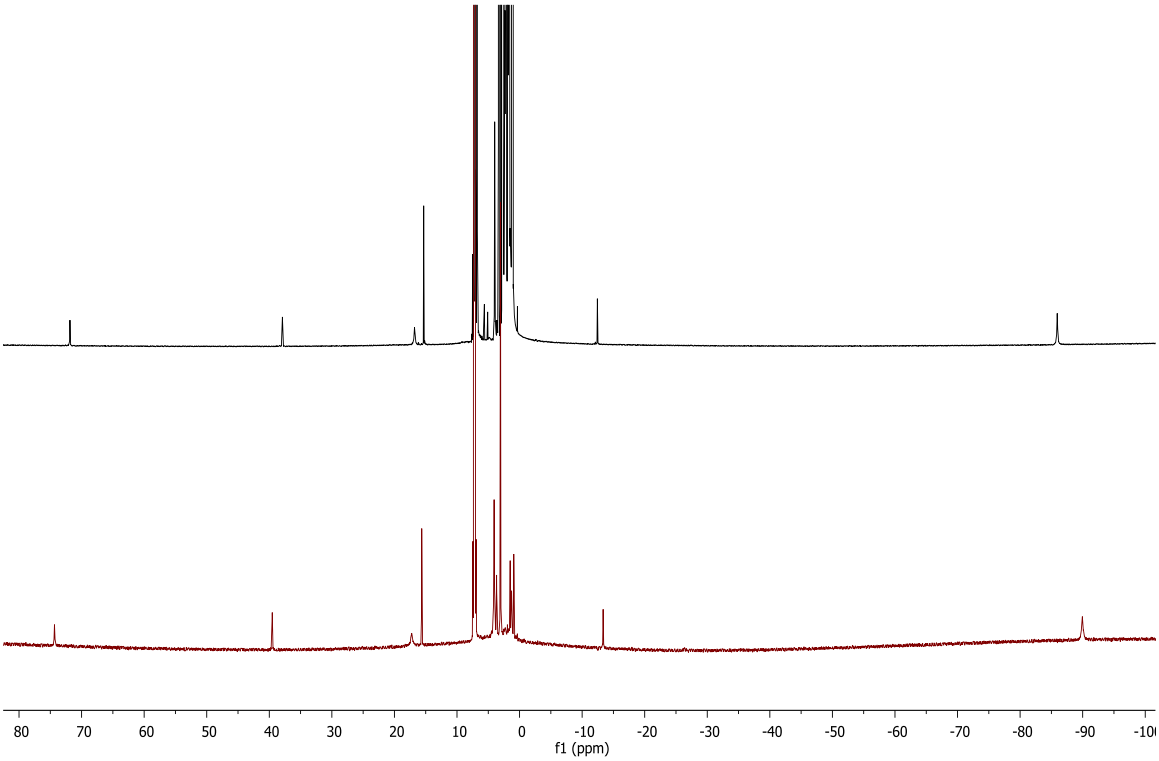

Figure B.6. ^{1}H NMR detection of the [$^{i\text{-Pr}}$NDI]Ni$_2$Cl$_2$ complex **4** from the stoichiometric methylenecyclopropanation (top, black). A comparison ^{1}H NMR spectrum for isolated **4** (bottom, red).

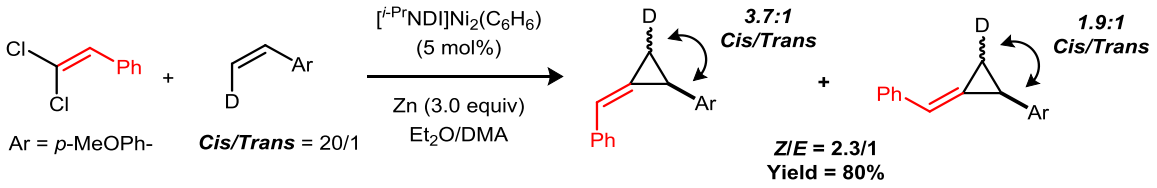

Stereoselectivity Under Catalytic Conditions. In an N$_2$-filled glovebox, a 5-mL vial was charged with a magnetic stir bar, (*Z*)-1-methoxy-4-(vinyl-2-*d*)benzene (28 mg, 0.20 mmol, 1.0 equiv), (2,2-dichlorovinyl)benzene (38 mg, 0.22 mmol, 1.1 equiv), Zn powder (0.6 mmol, 3 equiv), DMA (200 µL), and Et$_2$O (500 µL). A solution of [$^{i\text{-Pr}}$NDI]Ni$_2$(C$_6$H$_6$) (0.01 mmol, 0.05 equiv) in Et$_2$O (1.1 mL) was added. The vial was sealed, and the reaction mixture was stirred at room temperature. After 24 h, the reaction mixture was concentrated under reduced pressure, and the crude residue was directly loaded onto a SiO$_2$ column for purification (4:1 hexane/CH$_2$Cl$_2$). Isolated yields and ratios of stereoisomers were determined following purification.

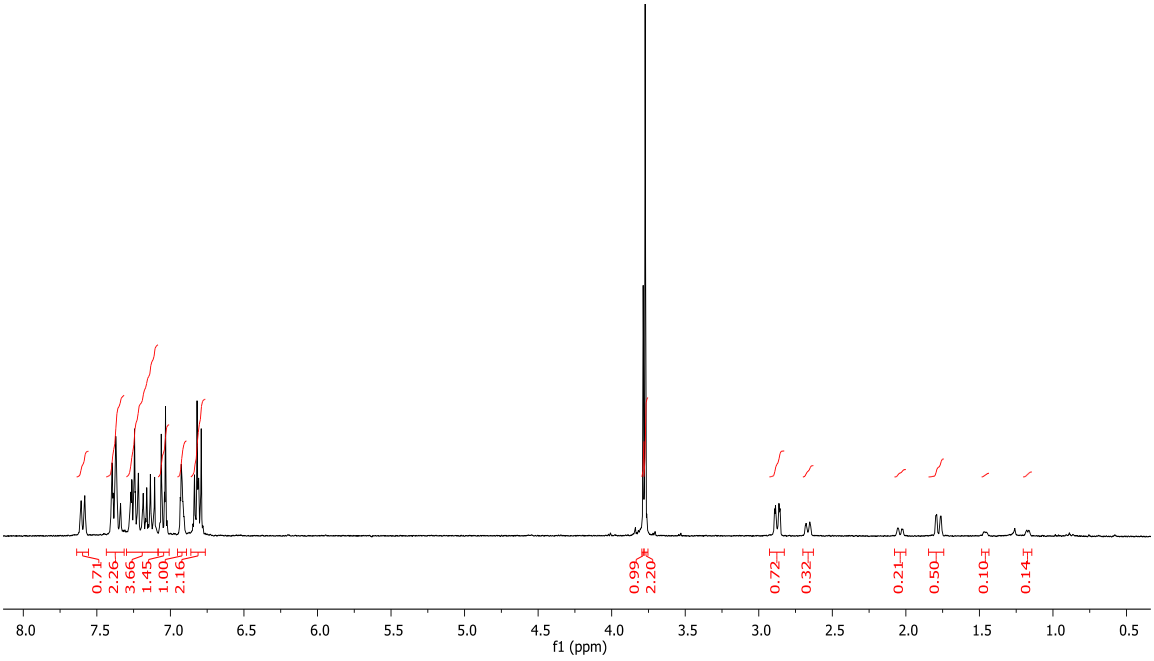

Figure B.7. ^{1}H NMR data for the mixture of stereoisomers of **32** formed using (*Z*)-1-methoxy-4-(vinyl-2-*d*)benzene.

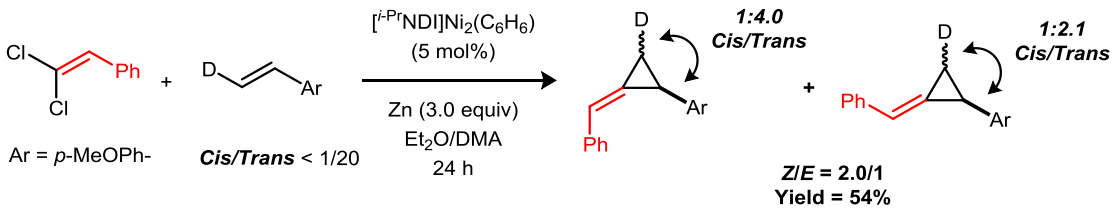

Stereoselectivity Under Catalytic Conditions. In an N_2-filled glovebox, a 5-mL vial was charged with a magnetic stir bar, (*E*)-1-methoxy-4-(vinyl-2-*d*)benzene (28 mg, 0.20 mmol, 1.0 equiv), (2,2-dichlorovinyl)benzene (38 mg, 0.22 mmol, 1.1 equiv), Zn powder (0.6 mmol, 3 equiv), DMA (200 µL), and Et_2O (500 µL). A solution of [$^{i\text{-}Pr}$NDI]$Ni_2(C_6H_6)$ (0.01 mmol, 0.05 equiv) in Et_2O (1.1 mL) was added. The vial was sealed, and the reaction mixture was stirred at room temperature. After 24 h, the reaction mixture was concentrated under reduced pressure, and the crude residue was directly loaded onto a SiO_2 column for purification (4:1 hexane/CH_2Cl_2). Isolated yields and ratios of stereoisomers were determined following purification.

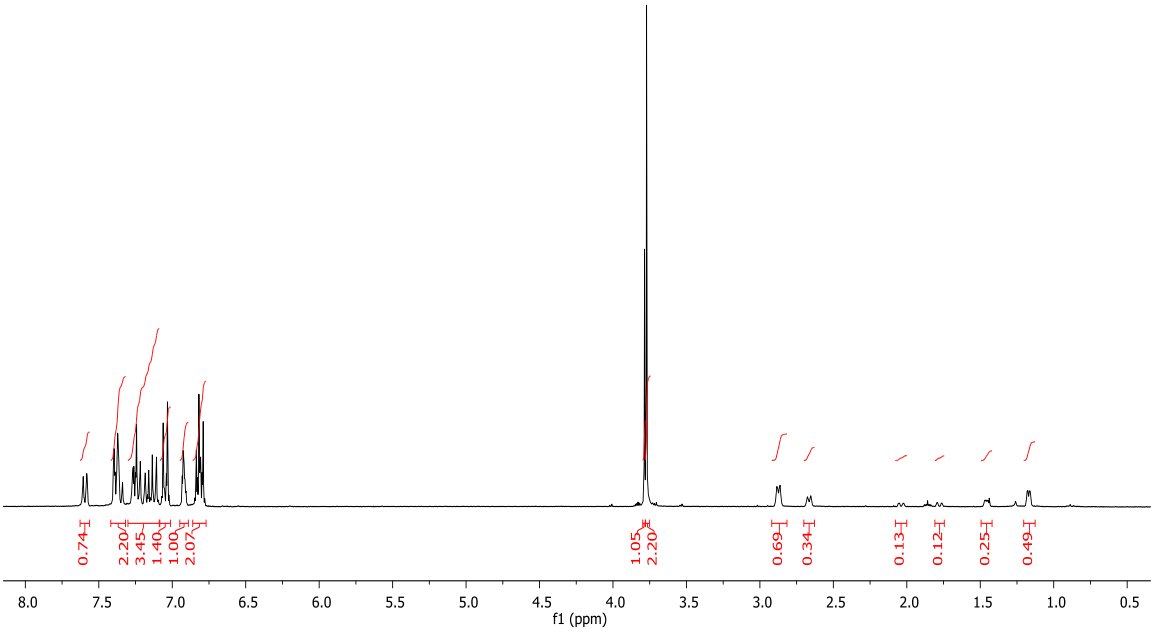

Figure B.8. ^{1}H NMR data for the mixture of stereoisomers of **32** formed using (*E*)-1-methoxy-4-(vinyl-2-*d*)benzene.

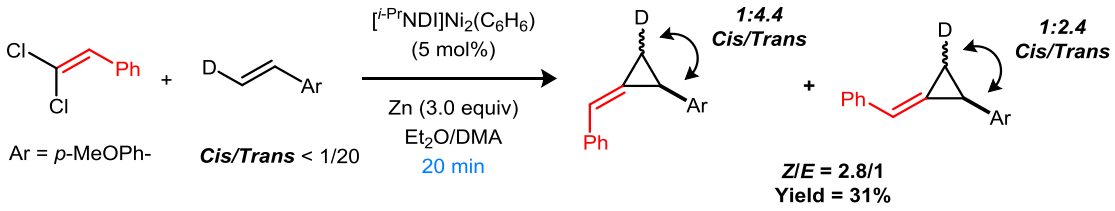

Starting Material Stereochemistry at Partial Conversions. The procedure above was repeated, stopping the reaction after 20 min in order to examine the stereochemistry of the recovered starting material. (*E*)-1-Methoxy-4-(vinyl-2-*d*)benzene was recovered in 60% yield with no erosion of stereochemistry.

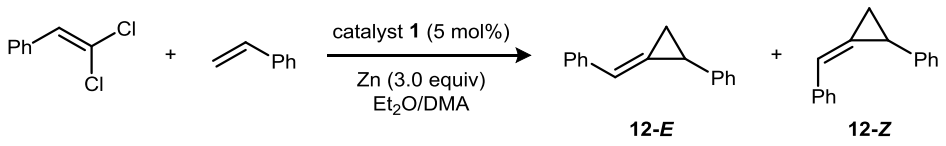

Product E/Z ratio monitored as a function of conversion

Dependence of product E/Z ratio on conversion. In order to test for a catalyst-promoted E/Z isomerization of the product or a selective ring-opening of one product isomer, the E/Z ratio for product **12** was monitored as a function of conversion.

The reaction was conducted according to the general procedure without modification using (2,2-dichlorovinyl)benzene (38 mg, 0.22 mmol, 1.1 equiv) and styrene (21 mg, 0.20 mmol, 1.0 equiv).

Reaction Time: 30 min, 55% conversion of styrene. E/Z = 1:3.3

Reaction Time: 2 h, 75% conversion of styrene. E/Z = 1:3.1

Reaction Time: 24 h, 93% conversion of styrene. E/Z = 1:3.1

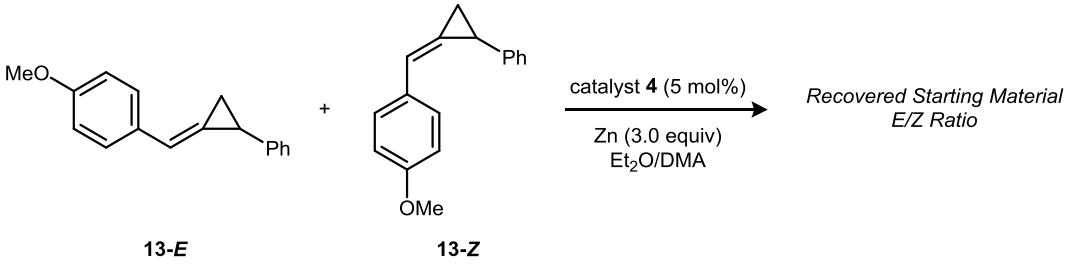

Resubjecting Product 13-*E*/*Z* to the Standard Catalytic Conditions. In order to probe the stability of the product under the reaction conditions, the isolated product **13-E/Z** was resubjected to the standard reaction conditions.

In an N_2-filled glovebox, a 5-mL vial was charged with a magnetic stir bar, 1-methoxy-4-((2-phenylcyclopropylidene)methyl)benzene (**13-*E*/*Z***, 47.2 mg, 0.2 mmol, ***E*/*Z*** = 1:3.3, 1.0 equiv), Zn powder (40 mg, 0.60 mmol, 3.0 equiv), *N*,*N*-dimethylacetamide (200 µL), and Et_2O (500 µL). A solution of [$^{i\text{-Pr}}$NDI]Ni_2Cl_2 (7.2 mg, 0.010 mmol, 5 mol%) in Et_2O (1.1 mL) was added. The vial was sealed, and the reaction mixture was stirred at room temperature for 24 h. After 24 h, the vial was taken out from the glovebox and the reaction mixture was concentrated under reduced pressure. The crude material was purified by column chromatography (SiO_2, 1:4 CH_2Cl_2/hexanes) to afford 1-methoxy-4-((2-phenylcyclopropylidene)methyl)benzene (43 mg, 91% recovery) with ***E*/*Z*** = 1:5.0.

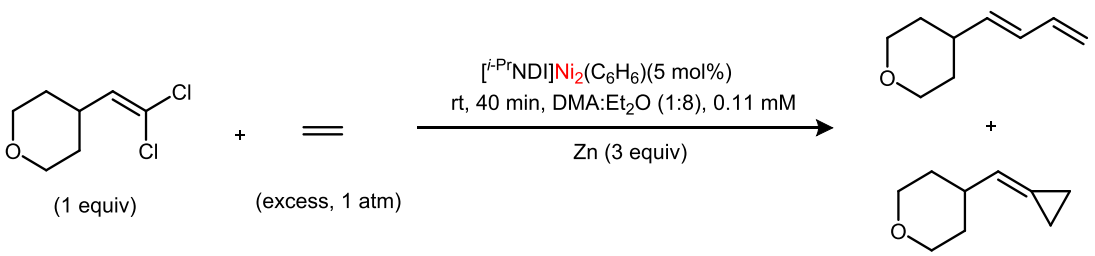

Tandem methylenecyclopropanation–isomerization reactions: detection of the methylenecyclopropane intermediate. In an N_2-filled glovebox, a 25-mL Schlenk tube was charged with a magnetic stir bar, the [$^{i\text{-Pr}}$NDI]$Ni_2(C_6H_6)$ catalyst **1** (0.010 mmol, 0.050 equiv), Zn powder (0.60 mmol, 3.0 equiv), DMA (200 µL), and Et_2O (1.6 mL). The reaction mixture was frozen in the glovebox cold well at liquid N_2 temperatures. 4-(2,2-Dichlorovinyl)tetrahydro-2H-pyran (36 mg, 0.2 mmol, 1.0 equiv) was added. The Schlenk tube was sealed, removed from the glove box, and immediately placed in liquid N_2. The Schlenk tube was connected to a Schlenk line, the N_2 atmosphere was evacuated, and the reaction vessel was back-filled with ethylene (1 atm). The reaction was stirred at room temperature. After 40 min, the reaction mixture was concentrated under reduced pressure, and the crude residue was directly loaded onto a SiO_2 column for purification. Following column chromatography, a mixture of the 1,3-diene **42** and methylenecyclopropane was characterized by ^{1}H NMR spectroscopy.

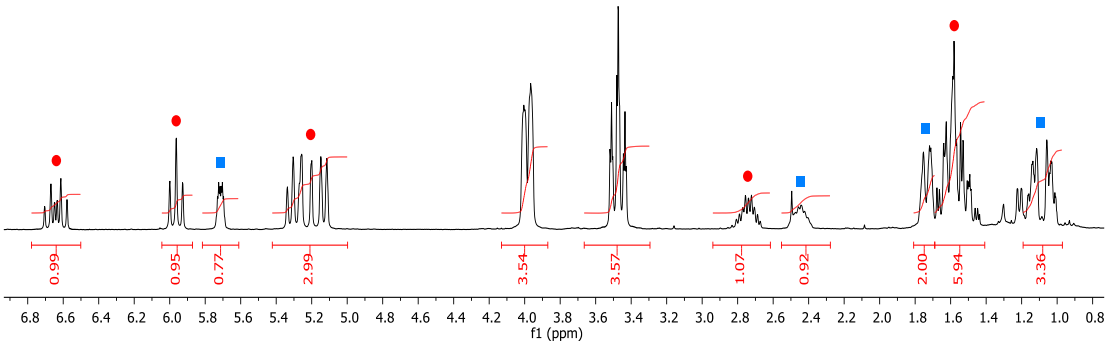

Figure B.9. ^{1}H NMR spectrum for the mixture containing the 1,3-diene (red circles) and methylenecyclopropane (blue squares) products.

B.8 Characterization of Complex 47

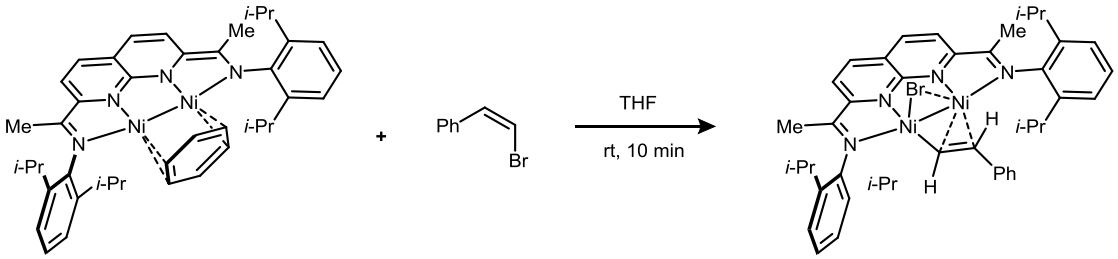

In an N_2-filled glovebox, the ($^{i\text{-Pr}}$NDI)$Ni_2(C_6H_6)$ complex **1** (44 mg, 0.060 mmol, 1.0 equiv) was dissolved in THF (1.0 mL) to generate a dark brown solution. A solution of (*Z*)-(2-bromovinyl)benzene (0.60 mL, 0.10 M) in THF was added, resulting in a color change to purple then indigo. After stirring for 10 min, the reaction mixture was concentrated to approx. 0.50 mL under reduced pressure then filtered through a glass fiber pad to remove any insoluble impurities. Complex **47** was obtained as a brown-green crystalline solid (13.7 mg, 27 % yield) from the filtrate by slow diffusion of pentane vapor at –30 °C over 16 h. Single crystals obtained by this procedure were suitable for XRD analysis.

^{1}H NMR (300 MHz, THF-d_8) δ 34.36, 32.67, 13.76, 11.71, 8.35, 7.06, 5.21, 4.99, 3.26, 2.89, 2.55, 2.11, 1.82.

UV–Vis (THF, nm {M^{-1} cm^{-1}}):268 {33,000}, 353 {sh}, 471 {sh}, 585 {sh}, 631 {sh}, 796 {sh}.

μ_{eff} = 1.83 μ_B (Evans method, 295 K, C_6H_6).

Anal. Calcd. for **47** ($C_{44}H_{51}BrN_4Ni_2$): C 63.43, H 6.17, N 6.72; found: C 63.72, H 6.23, N 6.60.

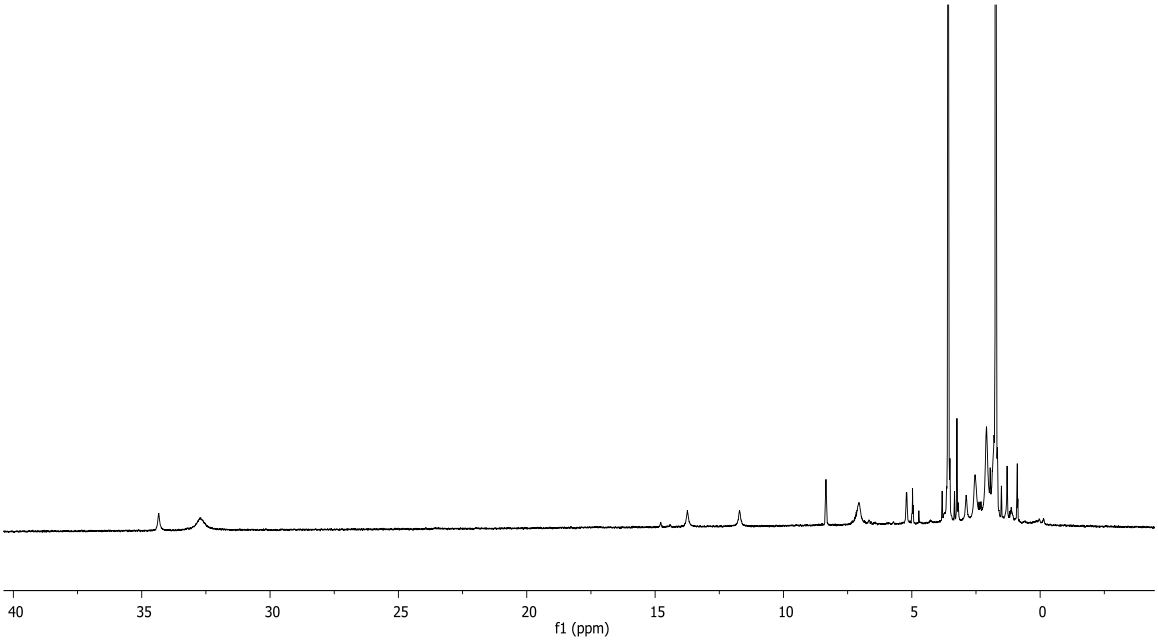

Figure B.10. ^{1}H NMR spectrum (THF-d_8, room temperature) for **47**.

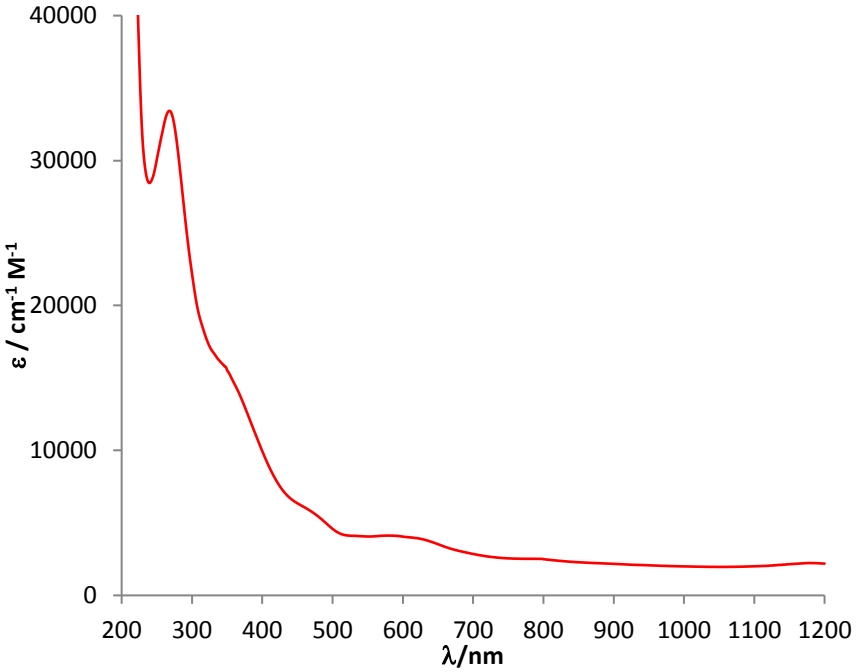

Figure B.11. UV-Vis-NIR spectrum for **47** in THF (0.040 mM) at room temperature.

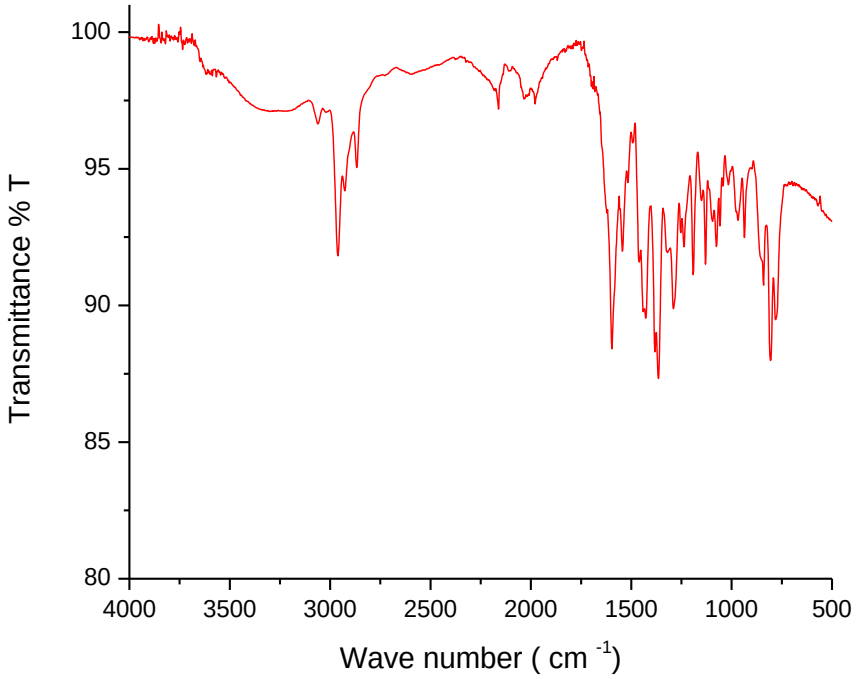

Figure B.12. ATR-IR spectrum for **47**.

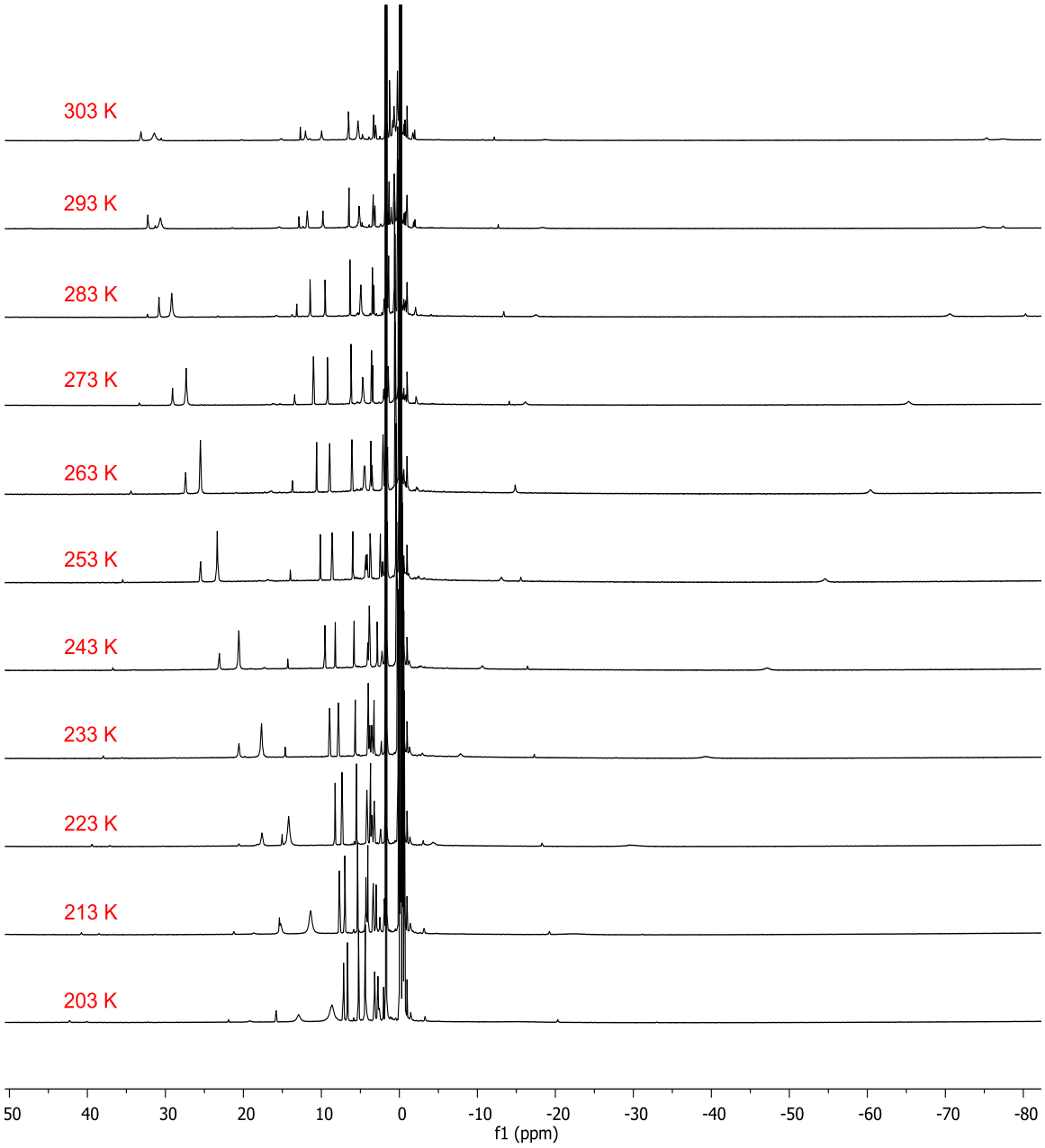

Figure B.13. ^{1}H VT-NMR spectra for **47** over a temperature range of 203–303 K.

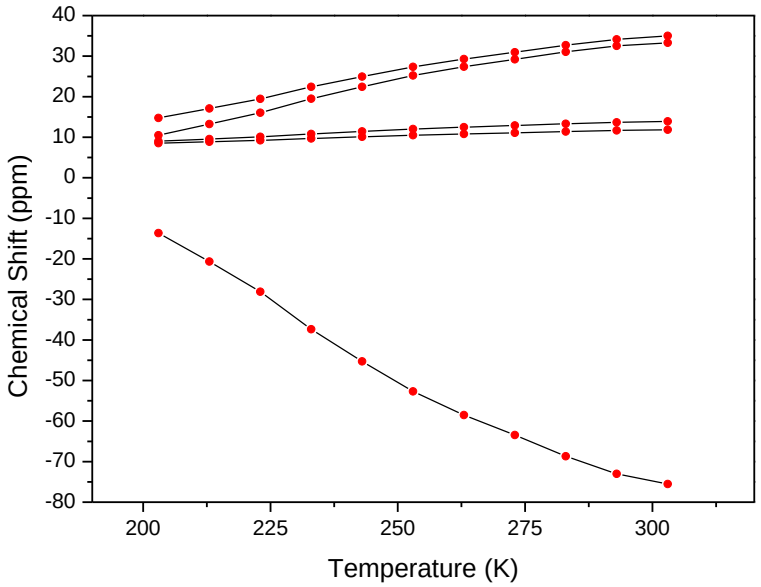

Figure B.14. Selected ^{1}H NMR peaks for **47** are plotted as a function of temperature (red points), and each set of points was fit (black lines) to the Boltzmann function for a spin-crossover system according to the equation shown below.

$$chemical\ shift = a + \frac{b}{T * (1 + e^{\left(\frac{c}{8.314*T} - \frac{d}{8.314}\right)})}$$

a = chemical shift for the diamagnetic state

b = fitting constant

c = enthalpy of spin-crossover event in units of J/mol

d = entropy of spin-crossover event in units of J/mol·K

Curve	Adj. R^2	a	b	c	d
1	0.99951	1.01654	14639.03	13298.72	49.72218
2	0.99948	5.8751	14498.62	12288.66	44.22822
3	0.99936	7.23334	2513.489	12179.55	42.04741
4	0.9995	7.09212	3434.173	12619.98	45.06768
5	0.99931	12.74163	-42194.5	12735.01	46.58308

ΔH = 12,600 J/mol, ΔS = 46 ± 1 J/mol·K

B.9 XRD Data

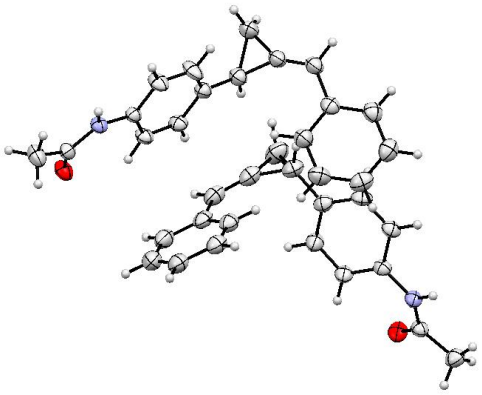

Crystal data	
Chemical formula	$C_{18}H_{17}NO$
M_r	263.32
Crystal system, space group	Triclinic, $P\bar{1}$
Temperature (K)	150
a, *b*, *c* (Å)	9.4236 (8), 11.2688 (10), 14.0432 (12)
α, β, γ (°)	77.633 (5), 82.697 (5), 79.523 (6)
V (Å^3)	1426.3 (2)
Z	4
Radiation type	Cu *K*α
□ (mm^{-1})	0.59
Crystal size (mm)	0.30 × 0.21 × 0.02
Data collection	
Diffractometer	Bruker AXS D8 Quest CMOS diffractometer
Absorption correction	Multi-scan *SADABS* 2016/2: Krause, L., Herbst-Irmer, R., Sheldrick G.M. & Stalke D., J. Appl. Cryst. 48 (2015) 3-10
T_{min}, T_{max}	0.540, 0.754
No. of measured, independent and observed [$I > 2\square(I)$] reflections	14713, 5735, 4670
R_{int}	0.047
$(\sin \square/\square)_{max}$ (Å^{-1})	0.639
Refinement	
$R[F^2 > 2\square(F^2)]$, $wR(F^2)$, *S*	0.048, 0.130, 1.05

No. of reflections	5735
No. of parameters	369
No. of restraints	2
H-atom treatment	H atoms treated by a mixture of independent and constrained refinement
□ρ_{max},□□ρ_{min} (e Å^{-3})	0.22, -0.18

Computer programs: Apex3 v2016.9-0 (Bruker, 2016), *SAINT* V8.37A (Bruker, 2016), *SHELXS97* (Sheldrick, 2008), *SHELXL2016*/6 (Sheldrick, 2015, 2016), SHELXLE Rev714 (Hübschle *et al.*, 2011).

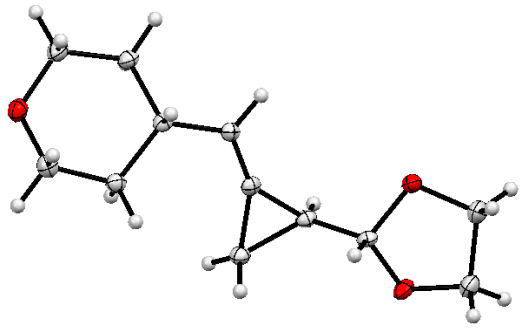

Crystal data	
Chemical formula	$C_{12}H_{18}O_3$
M_r	210.26
Crystal system, space group	Monoclinic, $P2_1/n$
Temperature (K)	100
a, *b*, *c* (Å)	10.9372 (3), 4.3348 (1), 22.8813 (7)
b (°)	94.6511 (10)
V (Å^3)	1081.24 (5)
Z	4
Radiation type	Cu $K\alpha$
μ (mm^{-1})	0.74
Crystal size (mm)	0.54 × 0.32 × 0.10
Data collection	
Diffractometer	Bruker AXS D8 Quest CMOS diffractometer
Absorption correction	Multi-scan *SADABS* 2016/2: Krause, L., Herbst-Irmer, R., Sheldrick G.M. & Stalke D., J. Appl. Cryst. 48 (2015) 3-10
T_{min}, T_{max}	0.550, 0.754
No. of measured, independent and observed [$I > 2s(I)$] reflections	11358, 2291, 2156
R_{int}	0.050
(sin q/l)$_{max}$ (Å^{-1})	0.639
Refinement	
$R[F^2 > 2s(F^2)]$, $wR(F^2)$, S	0.036, 0.091, 1.05
No. of reflections	2291
No. of parameters	136
H-atom treatment	H-atom parameters constrained
$\Delta\rho_{max}$,$\Delta\rho_{min}$ (e Å^{-3})	0.32, -0.18

Computer programs: Apex3 v2016.9-0 (Bruker, 2016), *SAINT* V8.37A (Bruker, 2016),

SHELXS97 (Sheldrick, 2008), *SHELXL2016*/6 (Sheldrick, 2015, 2016), SHELXLE Rev714 (Hübschle *et al.*, 2011).

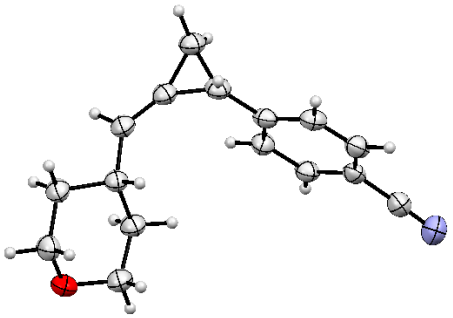

Crystal data	
Chemical formula	$C_{16}H_{17}NO$
M_r	239.30
Crystal system, space group	Monoclinic, $P2_1/c$
Temperature (K)	150
a, b, c (Å)	7.3009 (7), 6.1456 (5), 28.818 (2)
□ (°)	93.188 (5)
V (Å^3)	1291.02 (19)
Z	4
Radiation type	Cu K□
□ (mm^{-1})	0.60
Crystal size (mm)	0.11 × 0.09 × 0.03
Data collection	
Diffractometer	Bruker AXS D8 Quest CMOS diffractometer
Absorption correction	Multi-scan TWINABS 2012/1: Krause, L., Herbst-Irmer, R., Sheldrick G.M. & Stalke D., J. Appl. Cryst. 48 (2015) 3-10
T_{min}, T_{max}	0.481, 0.754
No. of measured, independent and observed [I > 2□(I)] reflections	8625, 3402, 3002
R_{int}	0.073
(sin □□□)$_{max}$ (Å^{-1})	0.638
Refinement	
R[F^2 > 2□(F^2)], wR(F^2), S	0.065, 0.168, 1.12
No. of reflections	3402
No. of parameters	164
H-atom treatment	H-atom parameters constrained
Δρ$_{max}$, Δρ$_{min}$ (e Å^{-3})	0.26, -0.22

Computer programs: Apex3 v2016.9-0 (Bruker, 2016), *SAINT* V8.37A (Bruker, 2016),

SHELXS97 (Sheldrick, 2008), *SHELXL2016*/6 (Sheldrick, 2015, 2016), SHELXLE Rev714 (Hübschle *et al.*, 2011).

The crystal under investigation was found to be non-merohedrally twinned. The orientation matrices for the two components were identified using the program Cell_Now, with the two components being related by a 180 degree rotation around the reciprocal c-axis. The two components were integrated using Saint and corrected for absorption using twinabs, resulting in the following statistics:

1328 data (699 unique) involve domain 1 only, mean I/sigma 21.0
1331 data (696 unique) involve domain 2 only, mean I/sigma 23.5
6067 data (2217 unique) involve 2 domains, mean I/sigma 35.8
3 data (3 unique) involve 3 domains, mean I/sigma 93.3

The exact twin matrix identified by the integration program was found to be
-1.00012 0.00016 -0.00054
-0.00014 -1.00000 -0.00012
0.43061 -0.00268 1.00012
The structure was solved using direct methods with only the non-overlapping reflections of component 1. The structure was refined using the hklf 5 routine with all reflections of component 1 (including the overlapping ones), resulting in a BASF value of 0.526(2).

The R_{int} value given is for all reflections and is based on agreement between observed single and composite intensities and those calculated from refined unique intensities and twin fractions (TWINABS (Sheldrick, 2012)).

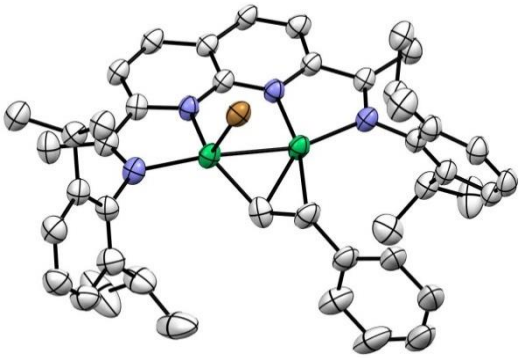

Crystal data	
Chemical formula	$C_{44}H_{51}BrN_4Ni_2 \cdot 1.264(C_4H_8O) \cdot 0.368(C_5H_{12})$
M_r	950.86
Crystal system, space group	Monoclinic, $P2_1/c$
Temperature (K)	100
a, b, c (Å)	19.3774 (7), 15.9602 (6), 15.4736 (6)
β (°)	101.395 (3)
V (Å^3)	4691.2 (3)
Z	4
Radiation type	Cu $K\alpha$
μ (mm^{-1})	2.30
Crystal size (mm)	0.21 × 0.18 × 0.04
Data collection	
Diffractometer	Rigaku Rapid II curved image plate diffractometer
Absorption correction	Multi-scan *SCALEPACK* (Otwinowski & Minor, 1997)
T_{min}, T_{max}	0.750, 0.914
No. of measured, independent and observed [$I > 2\sigma(I)$] reflections	53493, 8895, 7580
R_{int}	0.096
$(\sin \theta/\lambda)_{max}$ (Å^{-1})	0.618
Refinement	
$R[F^2 > 2\sigma(F^2)]$, $wR(F^2)$, S	0.073, 0.202, 1.07
No. of reflections	8895
No. of parameters	701
No. of restraints	526
H-atom treatment	H-atom parameters constrained

Computer programs: *CrystalClear*-SM Expert 2.1 b32 (Rigaku, 2014), *HKL-3000* (Otwinowski & Minor, 1997), *SHELXS97* (Sheldrick, 2008), *SHELXL2014*/7 (Sheldrick, 2014), SHELXLE Rev714 (Hübschle *et al.*, 2011).

A solvate THF molecule was refined as disordered. Another solvate occupied area of the structure is disordered around an inversion center. The area was modeled as being occupied by either two THF molecules (related to each other by inversion), or two pairs of pentane molecules disordered around the inversion center (each two being symmetry equivalent).

All THF molecules were restrained to have similar geometries. All pentane molecules were restrained to have similar geometries, and C-C bonds and 1,3 C...C distances were restrained to 1.50(2) and 2.50(2) Angstrom respectively. Uij components of ADPs of disordered atoms were restrained to be similar for atoms closer to each other than 1.7 Angstrom, and pentane ADPs were restrained to be close to isotropic.

Subject to these conditions the occupancy ratio for the first THF molecule refined to 0.623(10) to 0.377(10). The occupancies for the other type of THF molecule and of the two independent pentane moieties refined to 0.264(3), 0.1744(16) and 0.1936(16).

B.10 NMR Data for 1,1-Dichloroalkenes, Methylenecyclopropanes, and Dienes

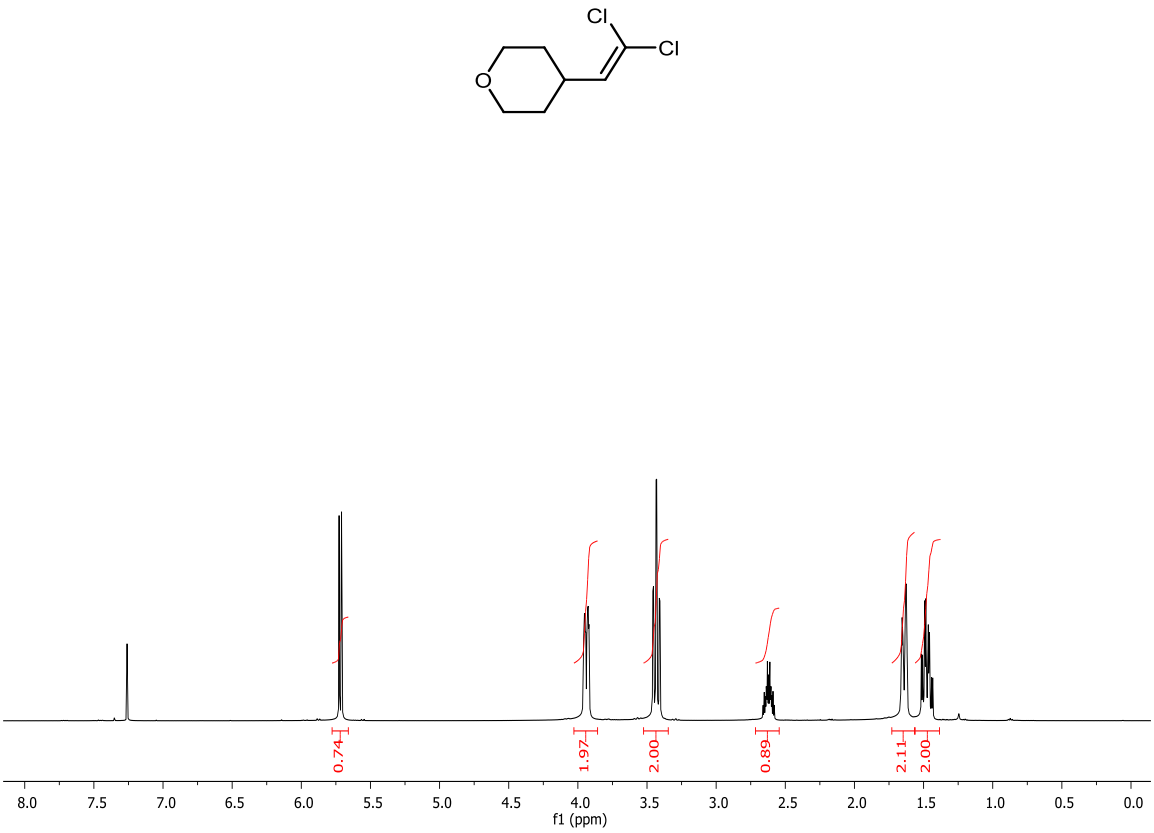

Figure B.15. ^{1}H NMR spectrum for 4-(2,2-dichlorovinyl)tetrahydro-2H-pyran in $CDCl_3$.

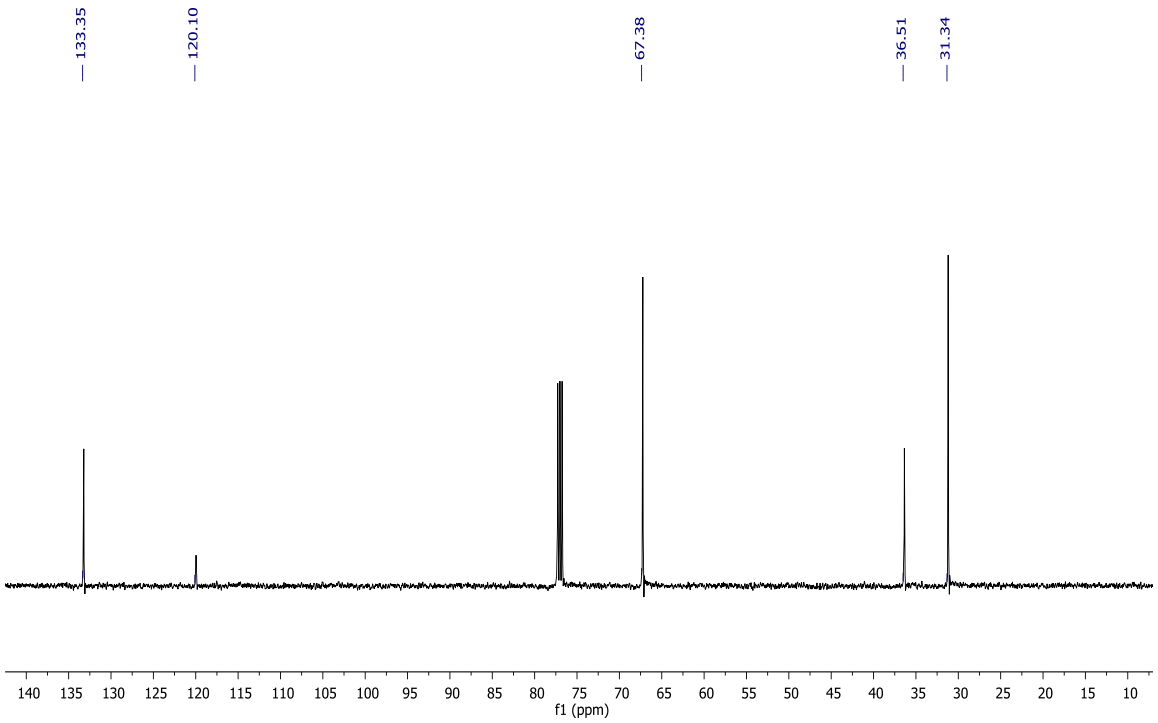

Figure B.16. $^{13}C\{^{1}H\}$ NMR spectrum for 4-(2,2-dichlorovinyl)tetrahydro-2H-pyran in $CDCl_3$.

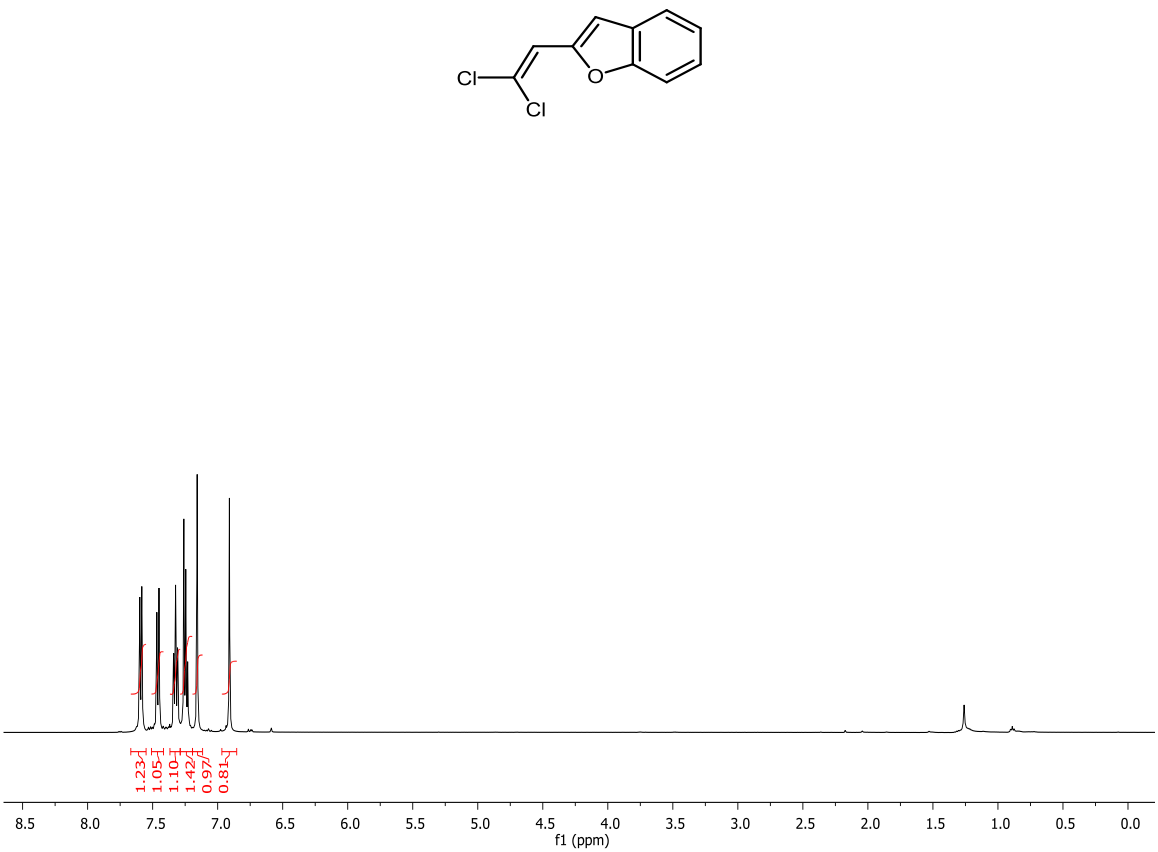

Figure B.17. ^{1}H NMR spectrum for 2-(2,2-dichlorovinyl)benzofuran in $CDCl_3$.

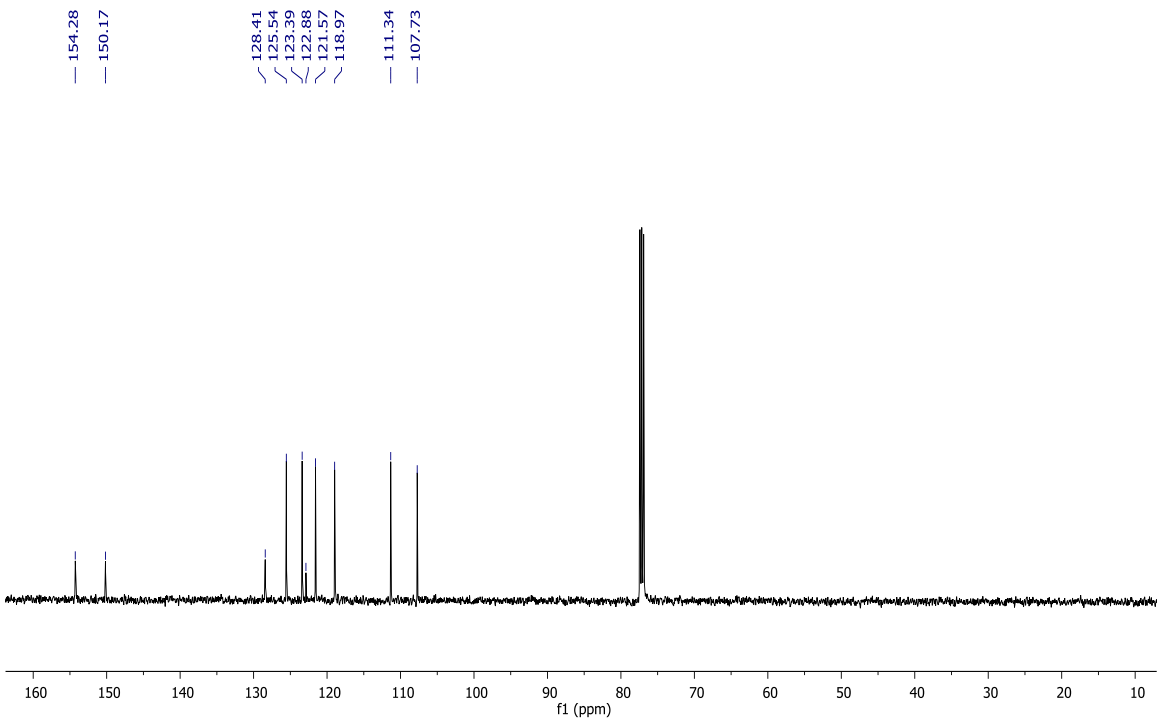

Figure B.18. $^{13}C\{^{1}H\}$ NMR spectrum for 2-(2,2-dichlorovinyl)benzofuran in $CDCl_3$.

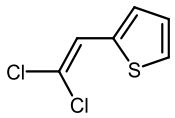

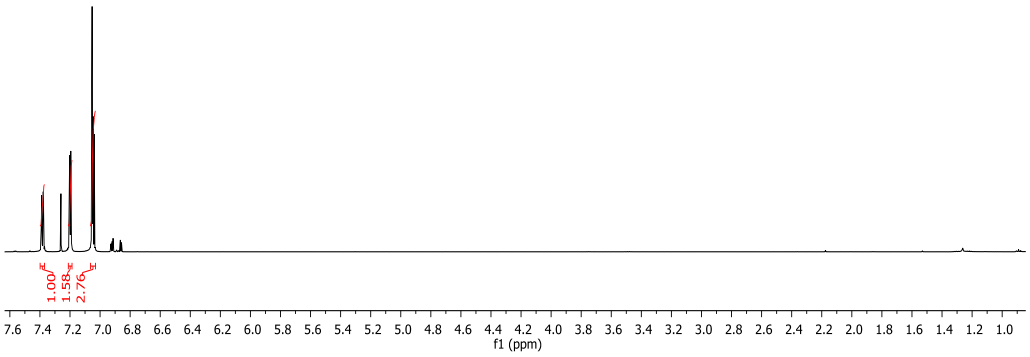

Figure B.19. ^{1}H NMR spectrum for 2-(2,2-dichlorovinyl)thiophene in $CDCl_3$.

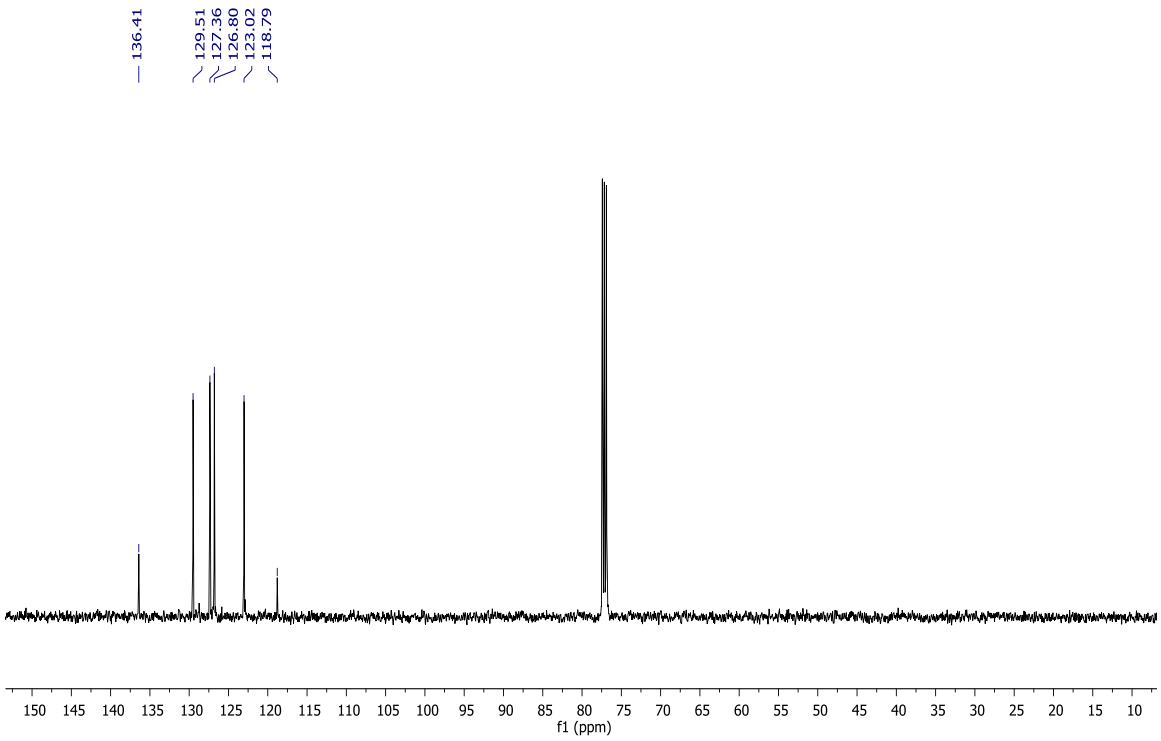

Figure B.20. $^{13}C\{^{1}H\}$ NMR spectrum for 2-(2,2-dichlorovinyl)thiophene in $CDCl_3$.

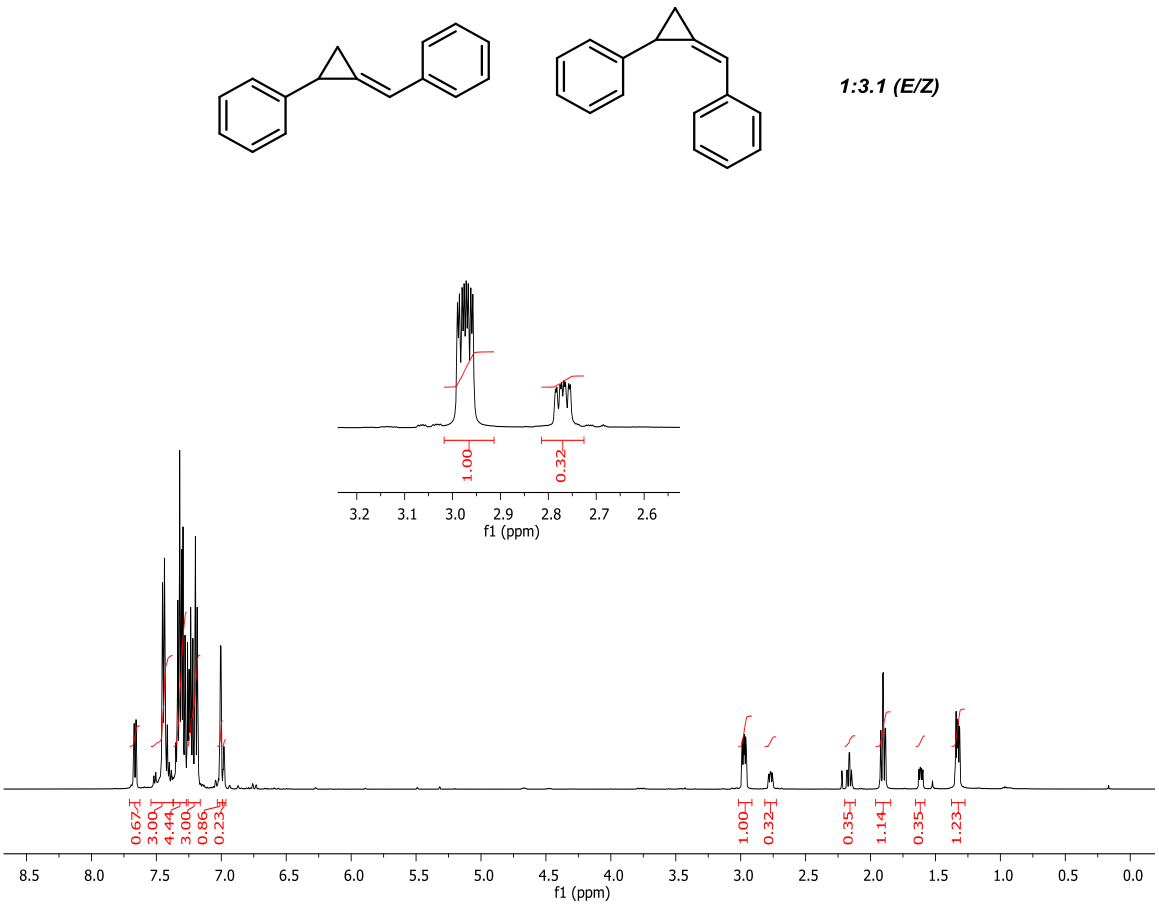

Figure B.21. ^{1}H NMR spectrum for **12** in $CDCl_3$.

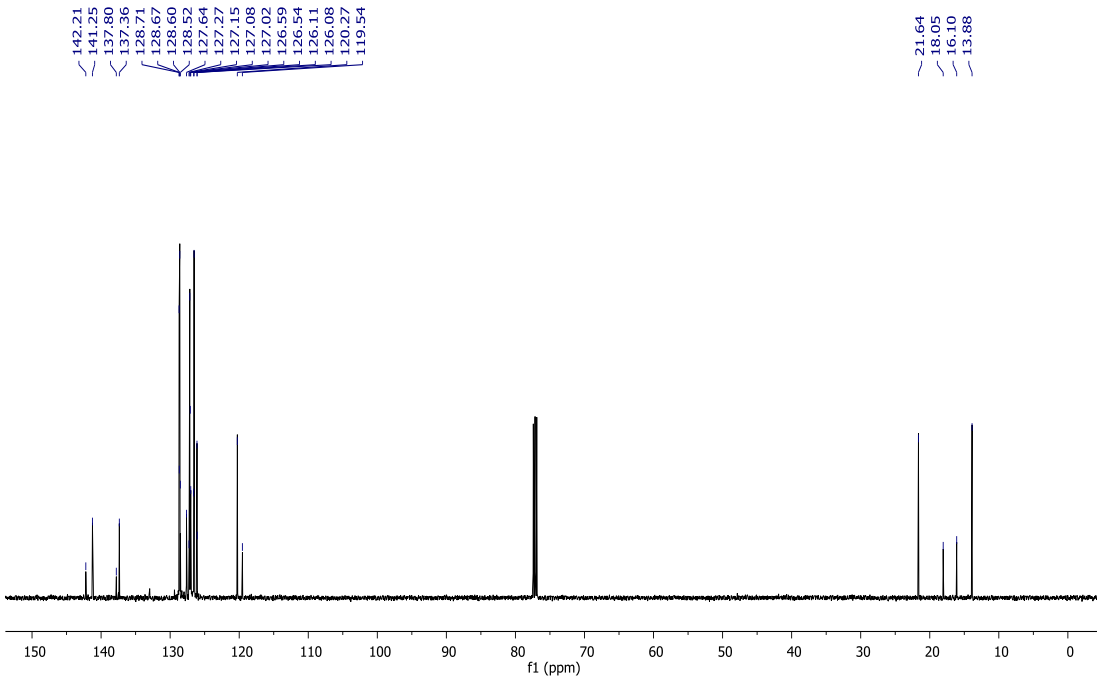

Figure B.22. $^{13}C\{^{1}H\}$ NMR spectrum for **12** in $CDCl_3$.

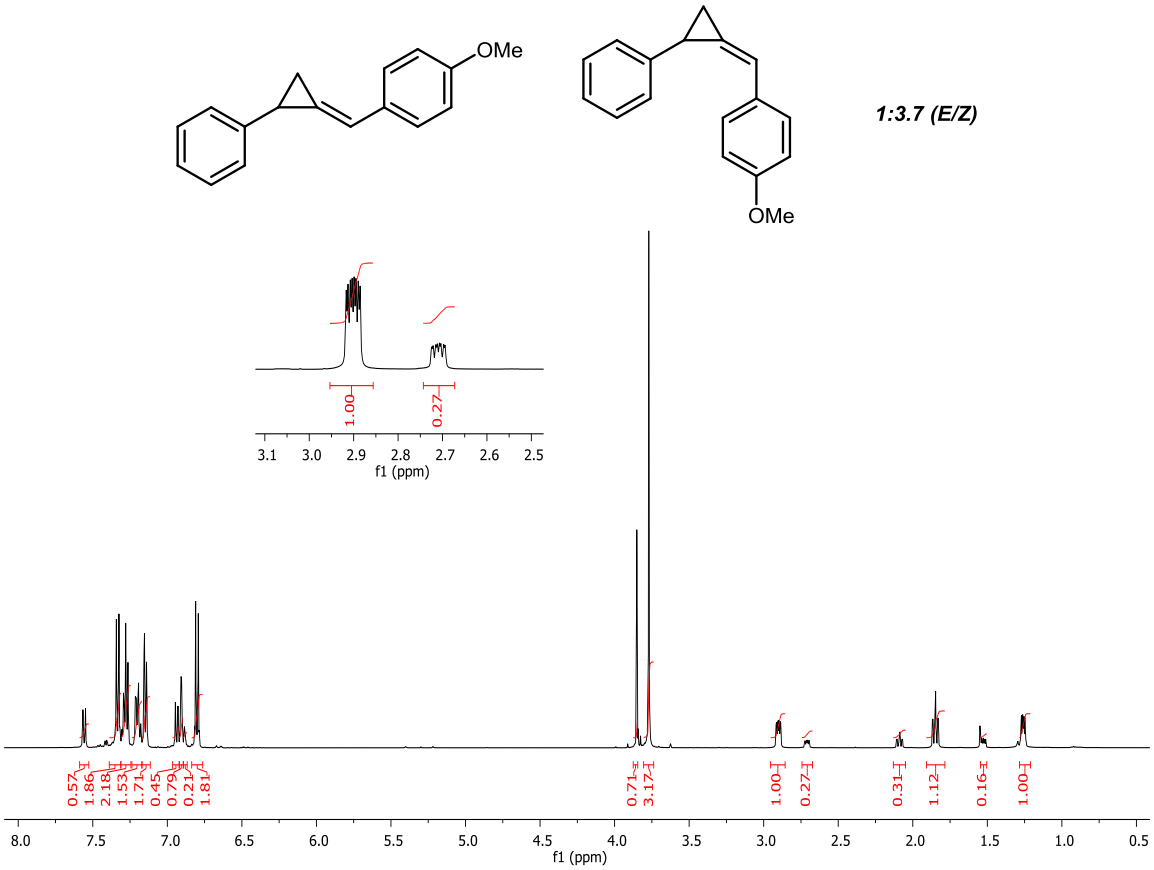

Figure B.23. ^{1}H NMR spectrum for **13** in $CDCl_3$.

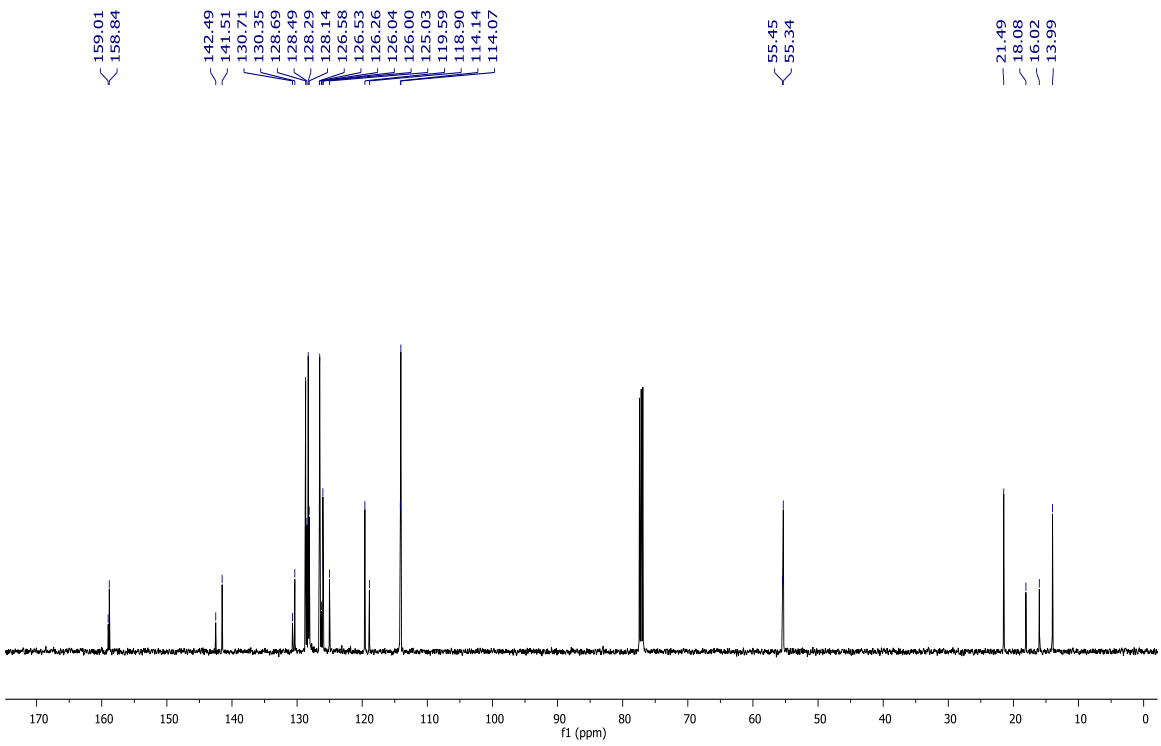

Figure B.24. $^{13}C\{^{1}H\}$ NMR spectrum for **13** in $CDCl_3$.

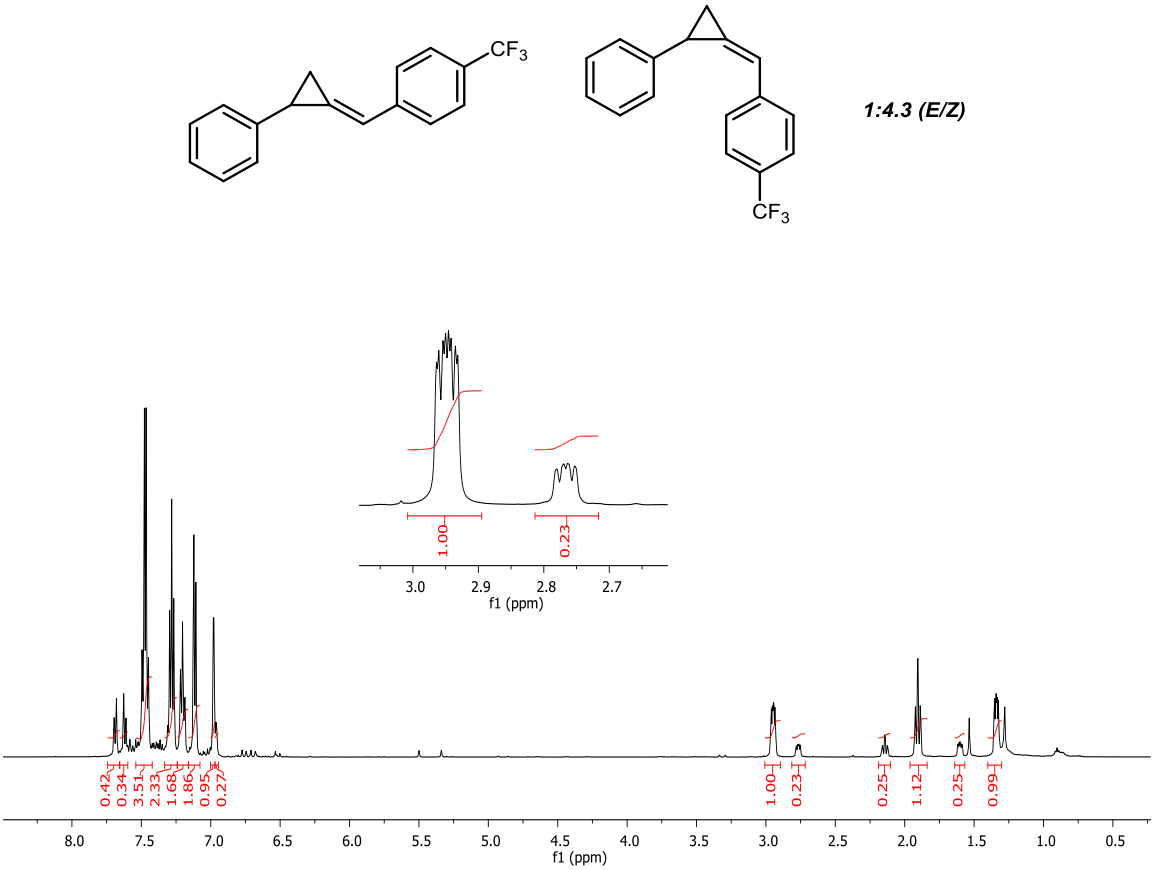

Figure B.25. ^{1}H NMR spectrum for **14** in $CDCl_3$.

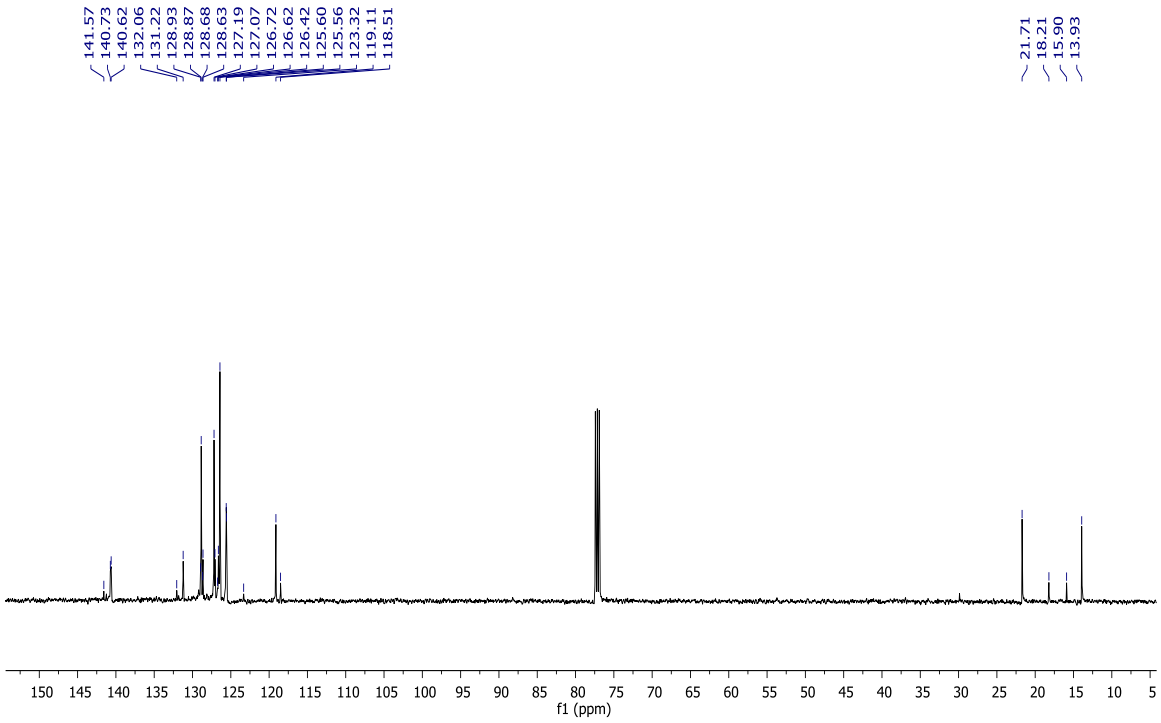

Figure B.26. $^{13}C\{^{1}H\}$ NMR spectrum for **14** in $CDCl_3$.

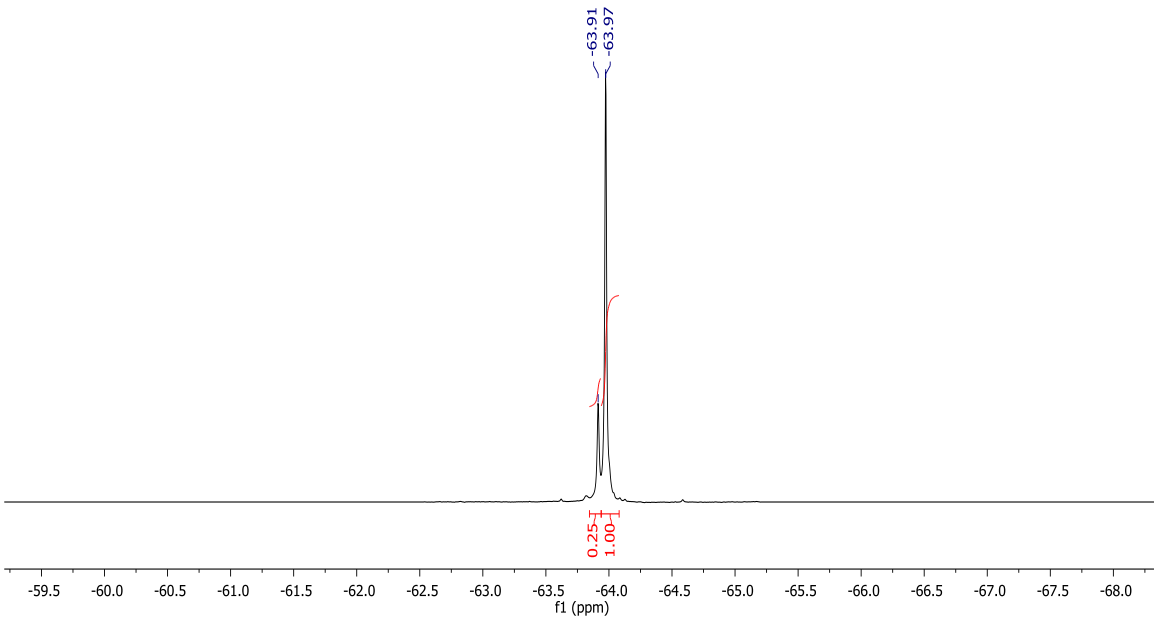

Figure B.27. ^{19}F NMR spectrum for **14** in $CDCl_3$.

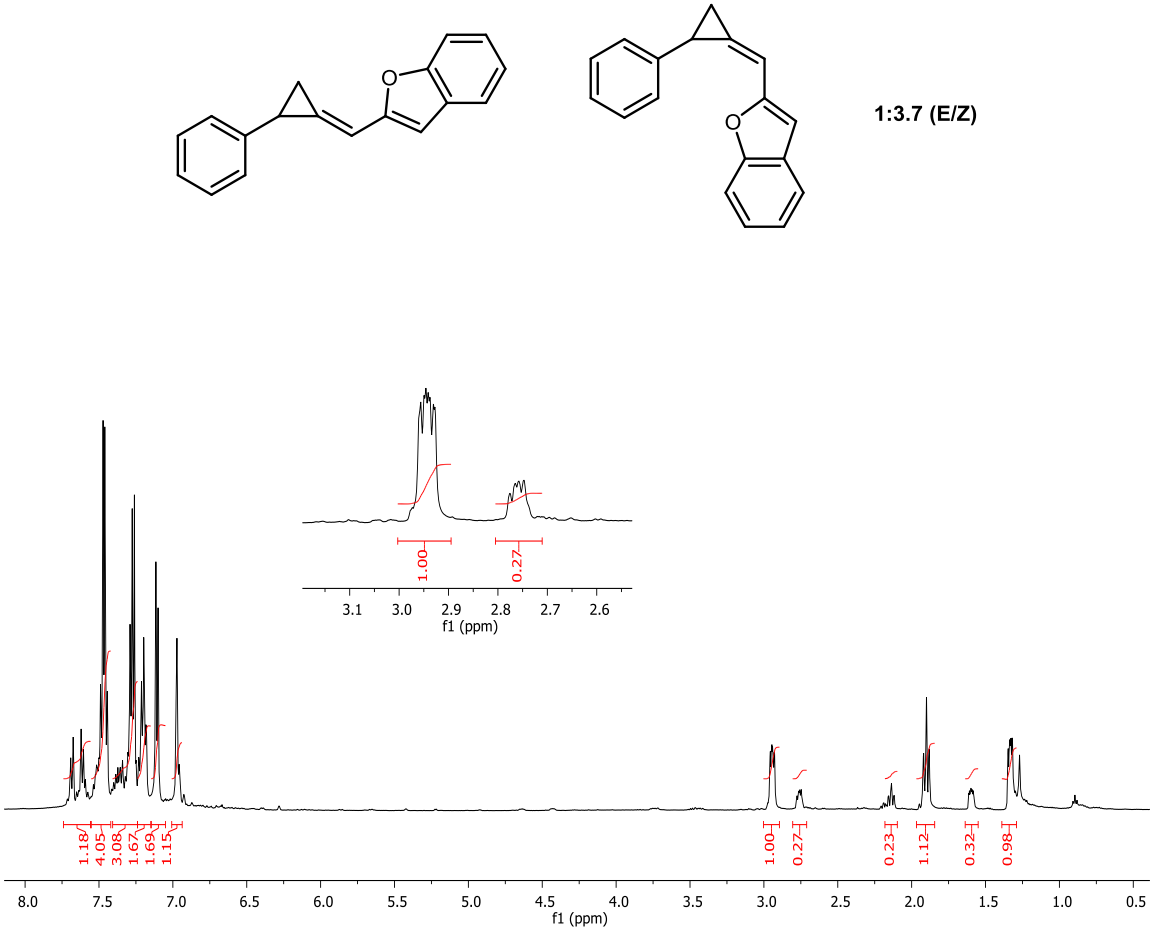

Figure B.28. ^{1}H NMR spectrum for **15** in $CDCl_3$.

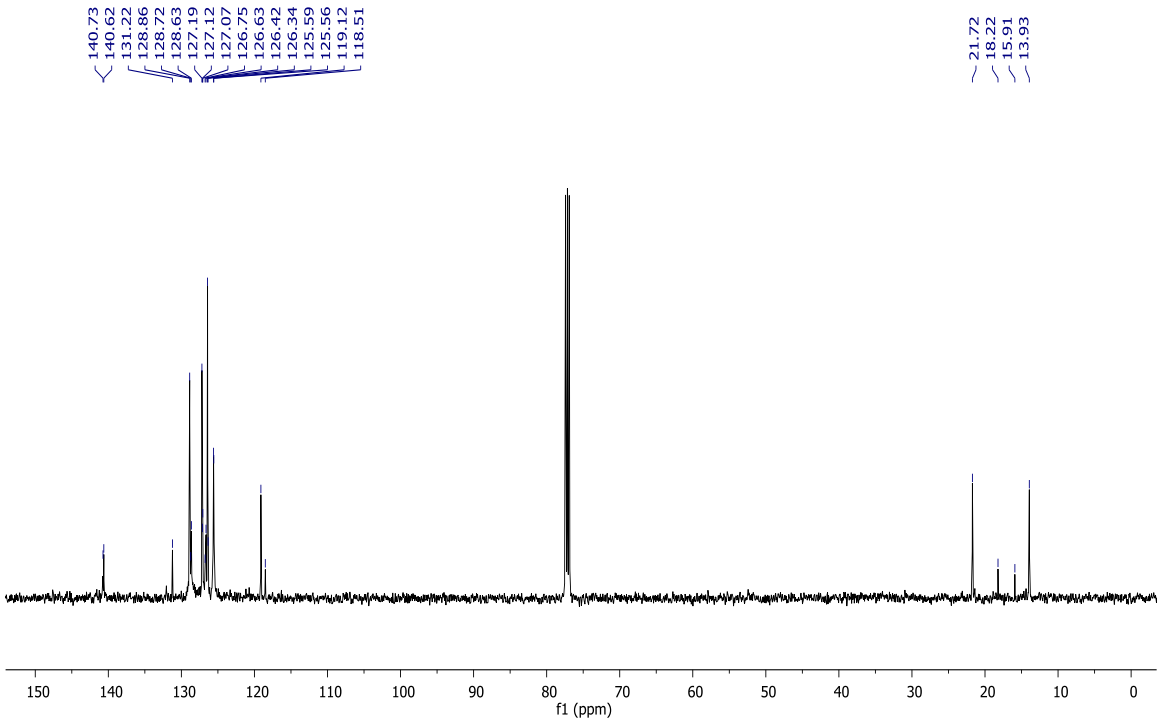

Figure B.29. $^{13}C\{^{1}H\}$ NMR spectrum for **15** in $CDCl_3$.

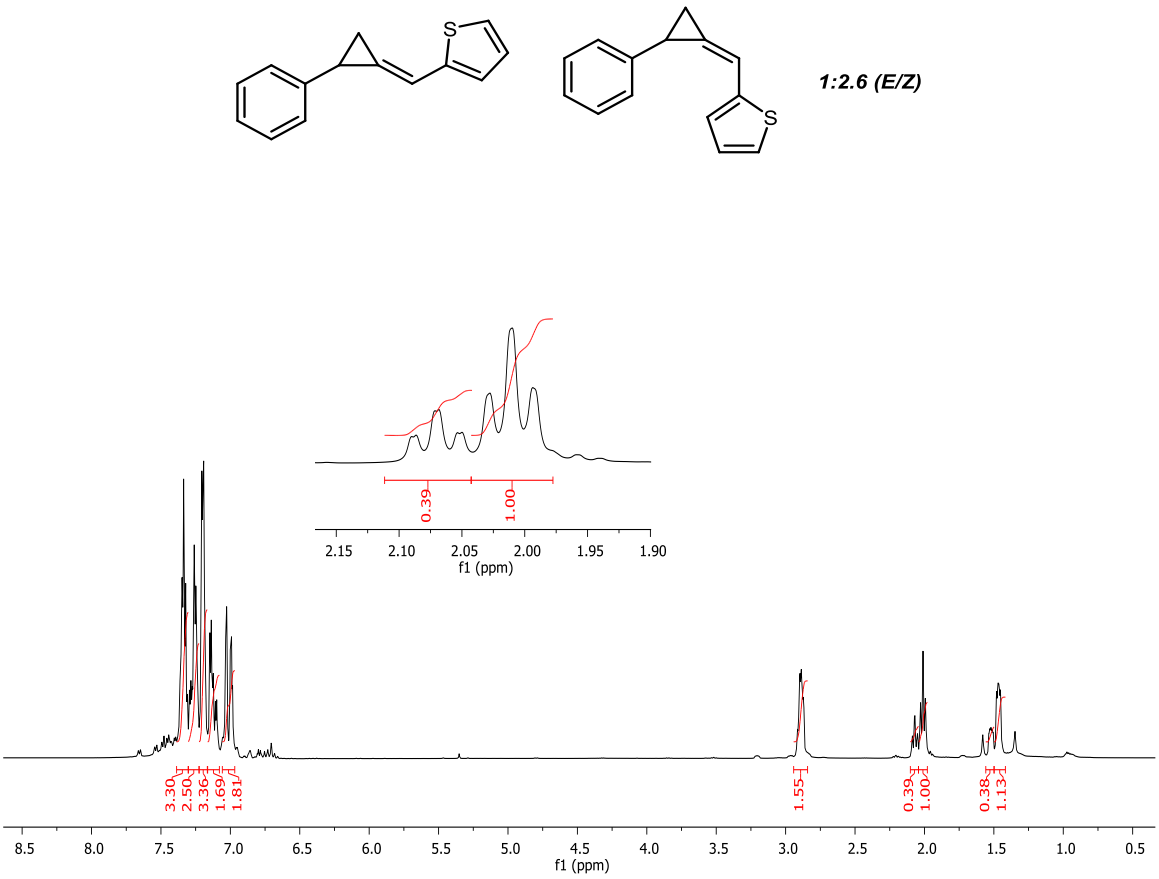

Figure B.30. ^{1}H NMR spectrum for **16** in $CDCl_3$.

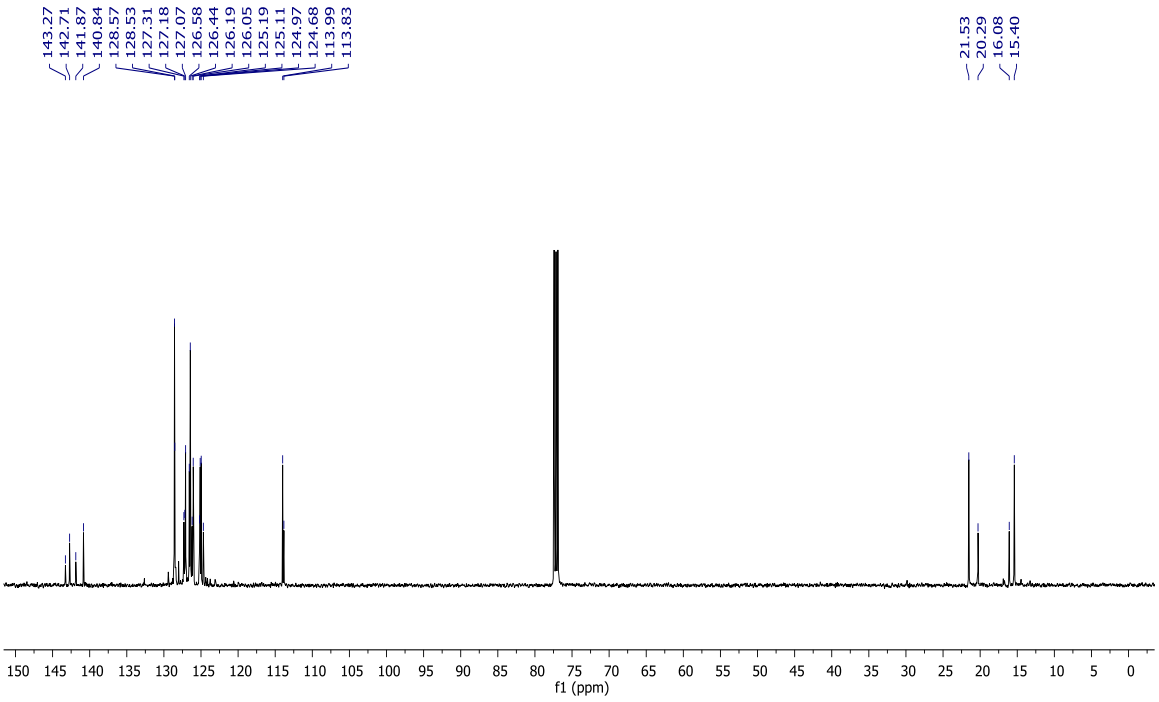

Figure B.31. $^{13}C\{^{1}H\}$ NMR spectrum for **16** in $CDCl_3$.

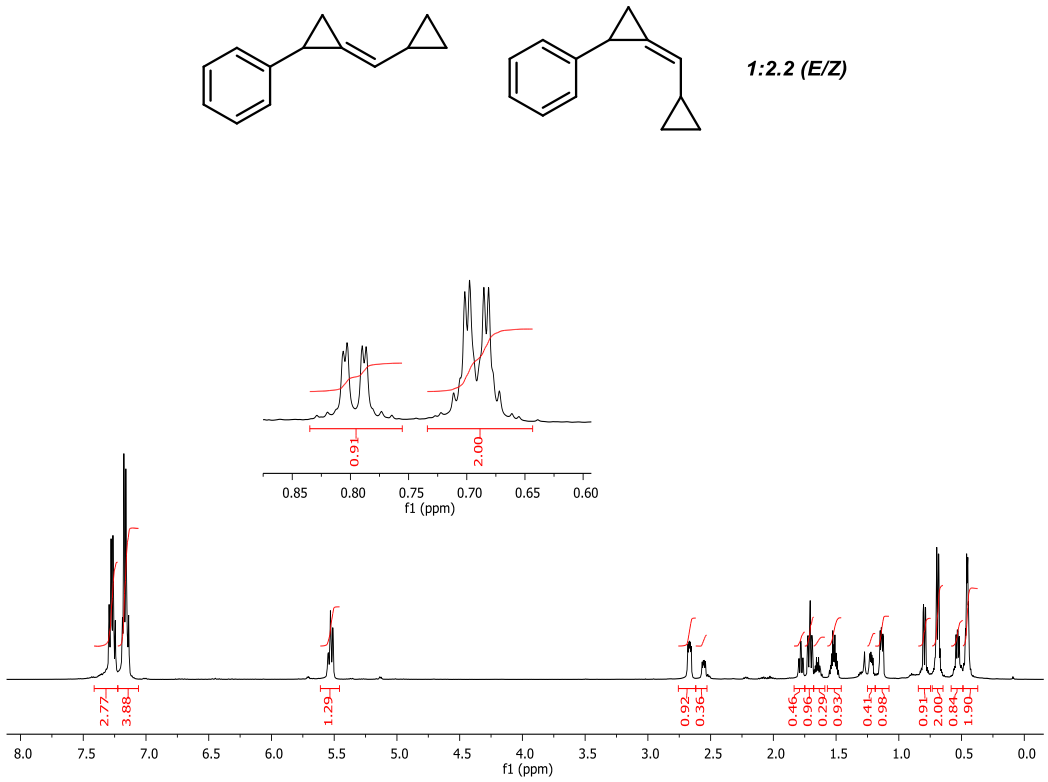

Figure B.32. ^{1}H NMR spectrum for **17** in $CDCl_3$.

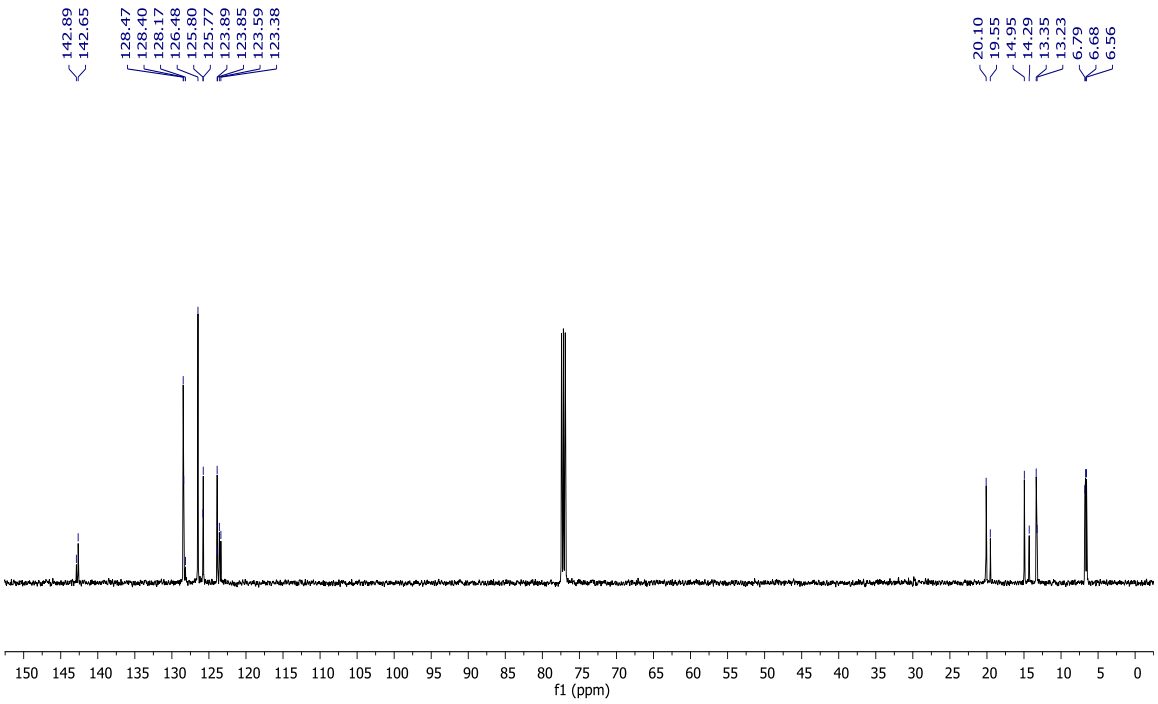

Figure B.33. $^{13}C\{^{1}H\}$ NMR spectrum for **17** in $CDCl_3$.

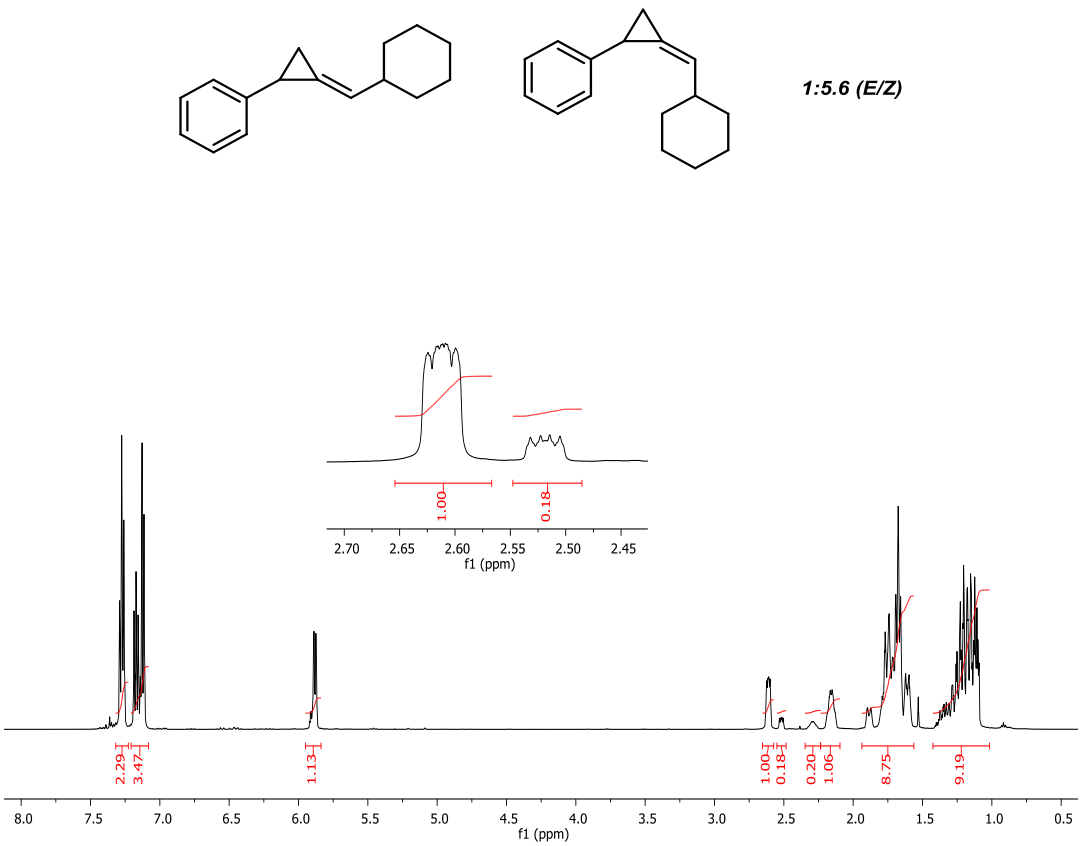

Figure B.34. ^{1}H NMR spectrum for **18** in $CDCl_3$.

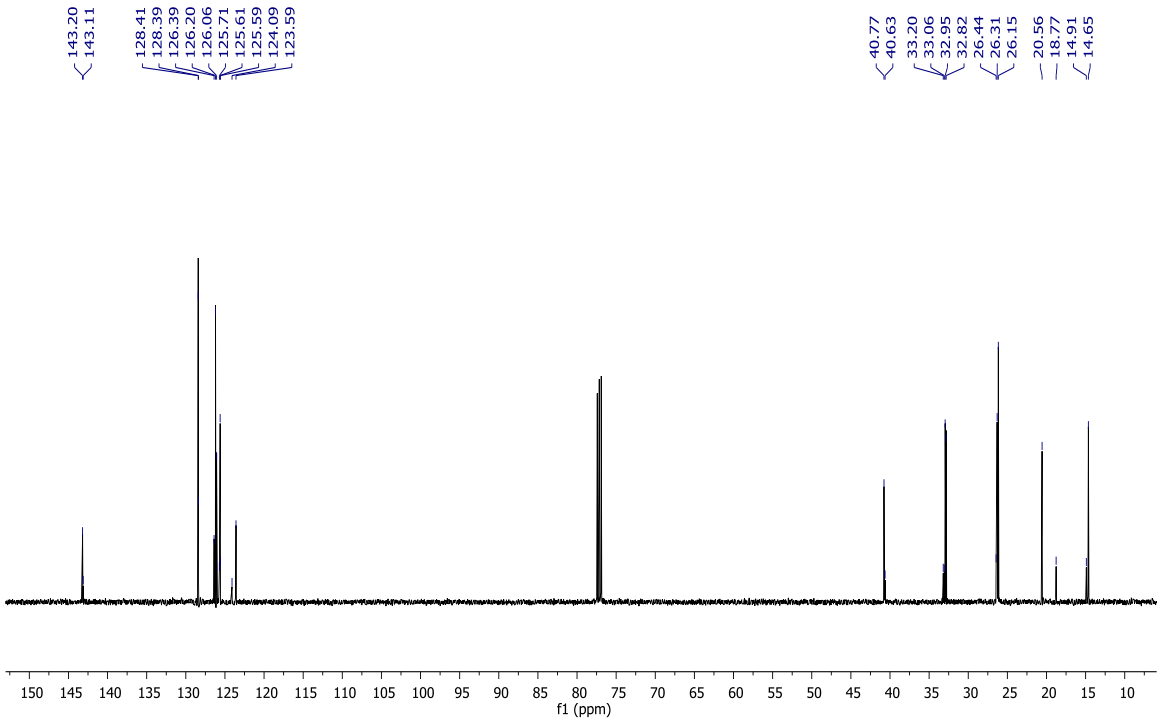

Figure B.35. $^{13}C\{^{1}H\}$ NMR spectrum for **18** in $CDCl_3$.

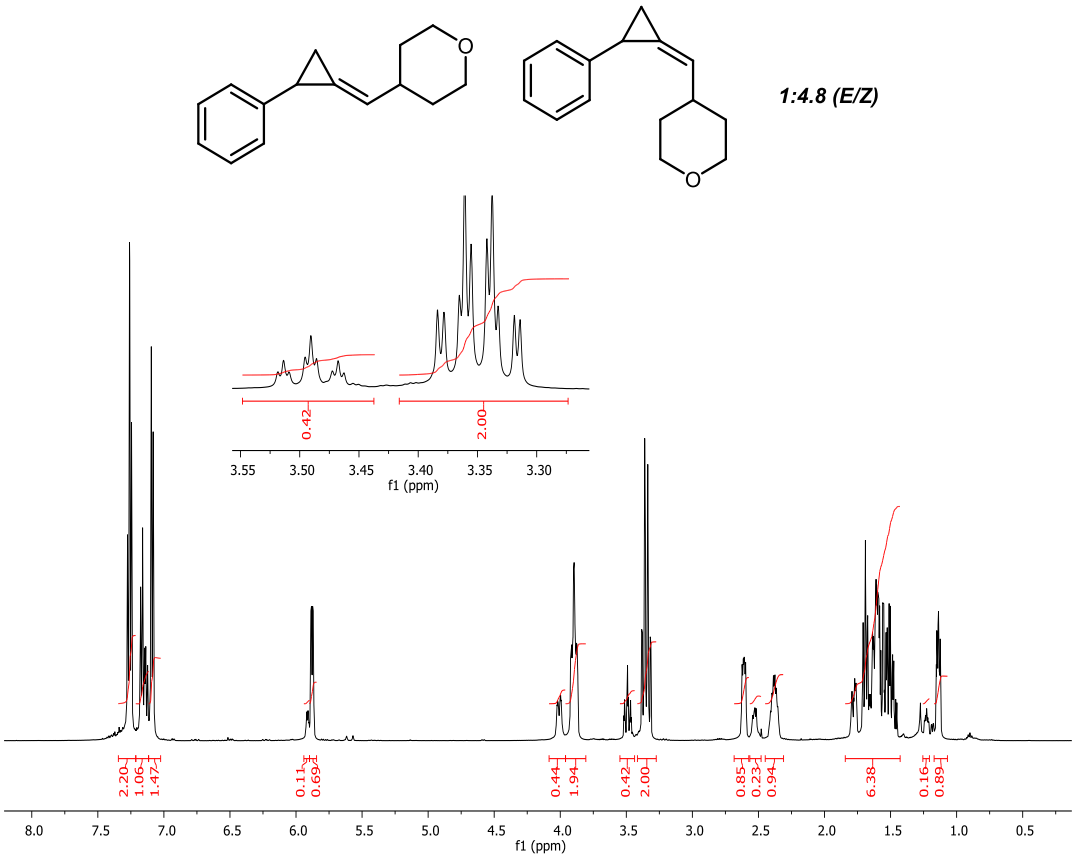

Figure B.36. ^{1}H NMR spectrum for **3** in $CDCl_3$.

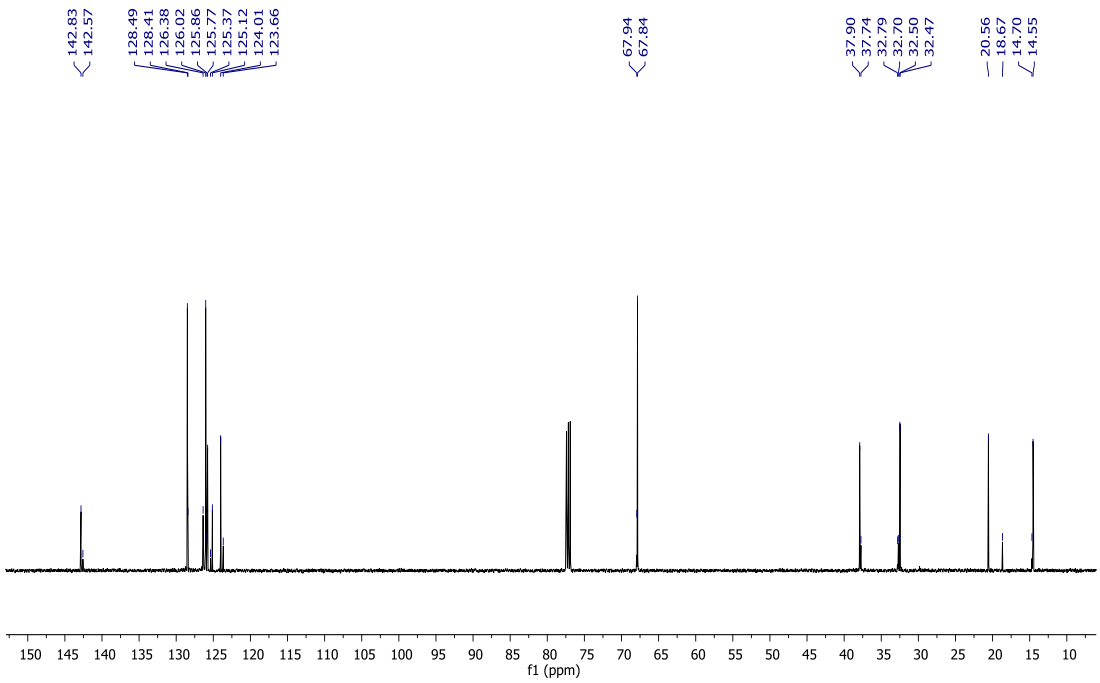

Figure B.37. $^{13}C\{^{1}H\}$ NMR spectrum for **3** in $CDCl_3$.

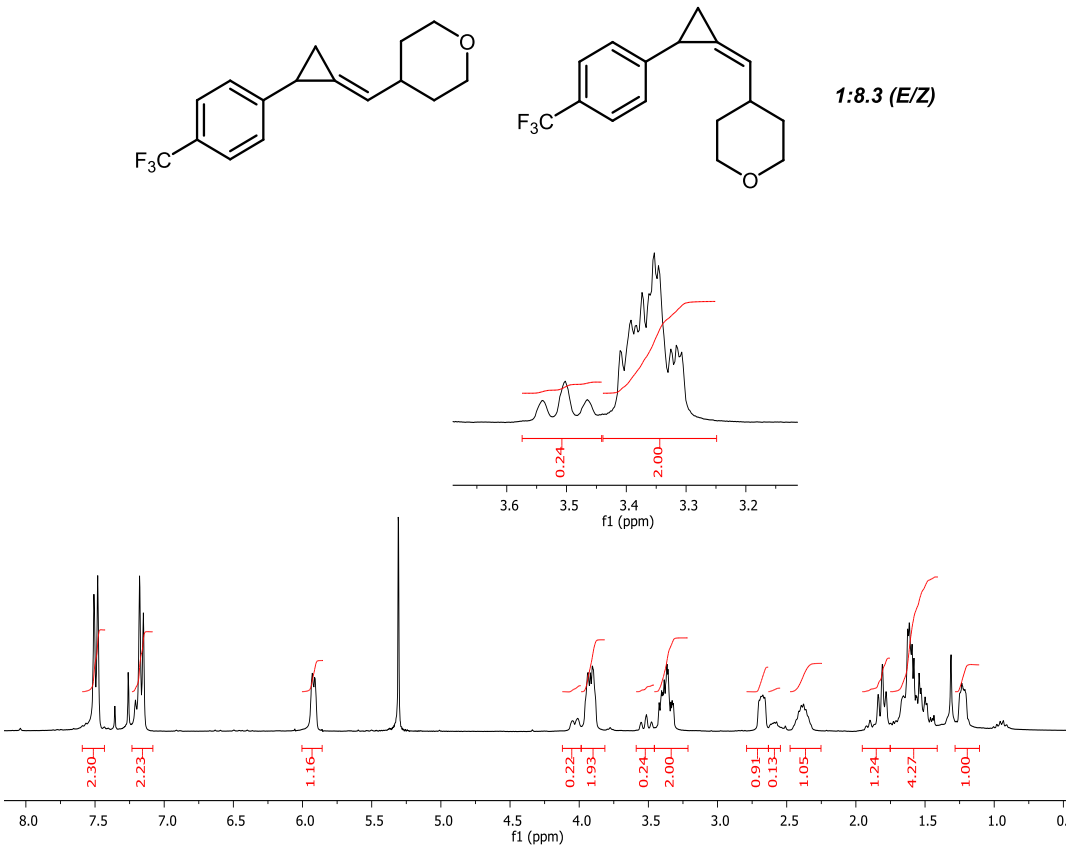

Figure B.38. ^{1}H NMR spectrum for **19** in $CDCl_3$.

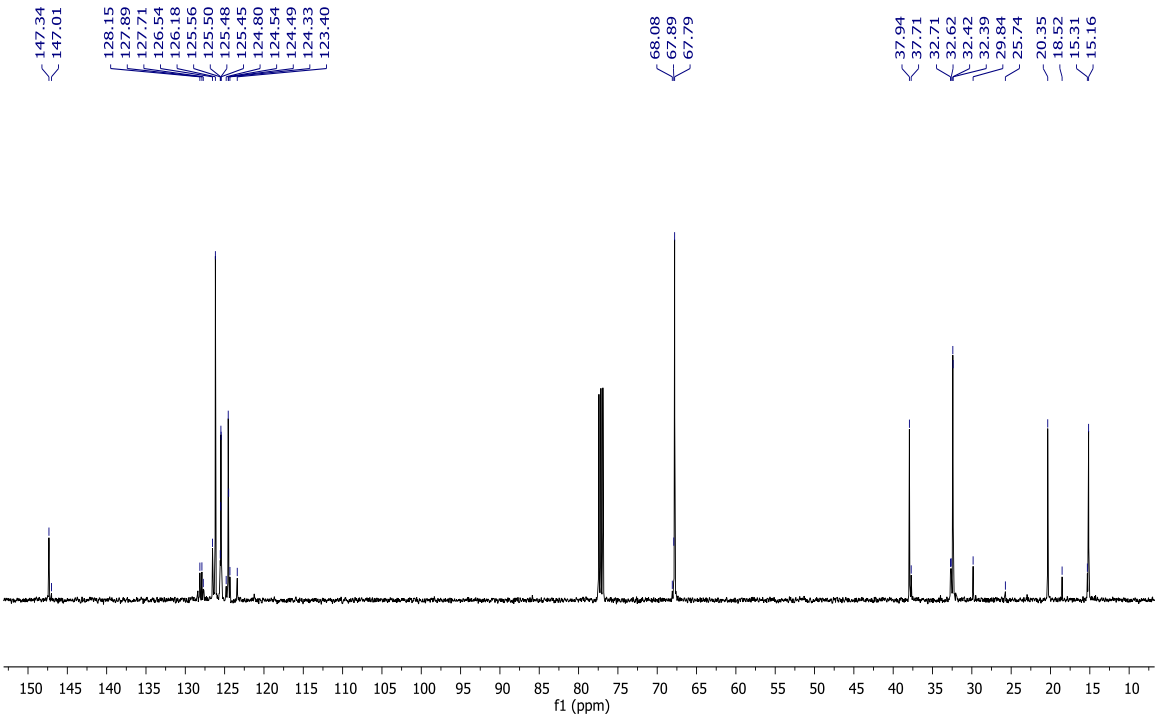

Figure B.39. $^{13}C\{^{1}H\}$ NMR spectrum for **19** in $CDCl_3$.

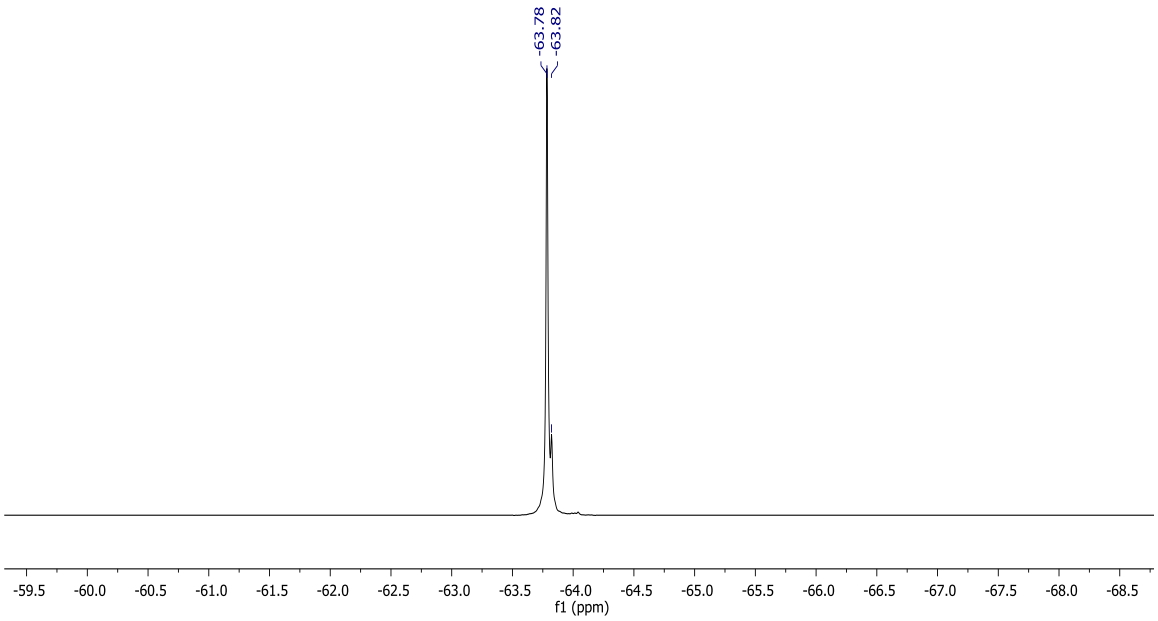

Figure B.40**.** ^{19}F NMR spectrum for **19** in $CDCl_3$.

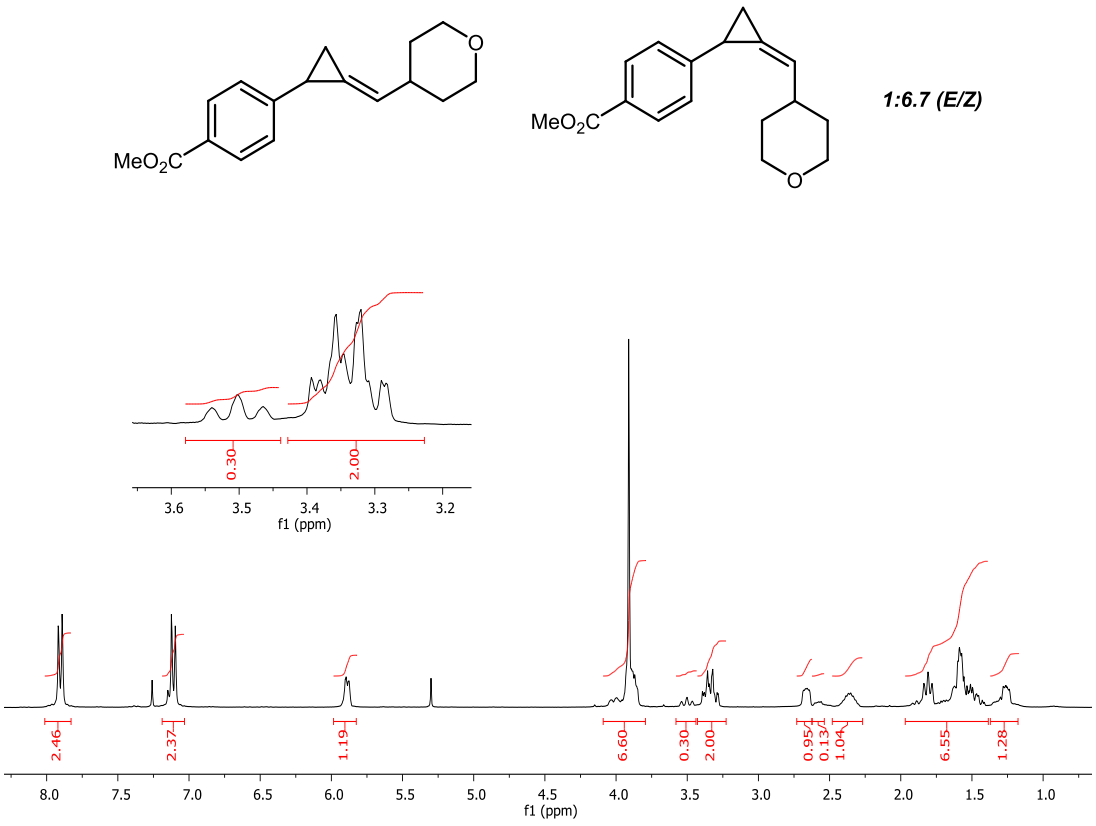

Figure B.41. ^{1}H NMR spectrum for **20** in $CDCl_3$.

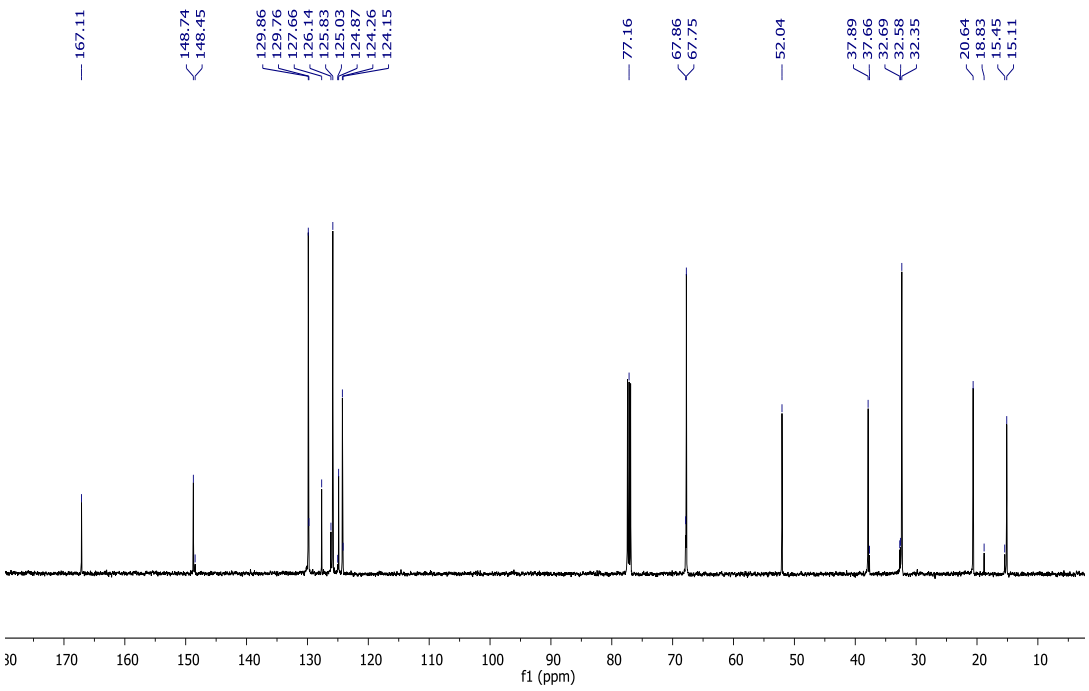

Figure B.42. $^{13}C\{^{1}H\}$ NMR spectrum for **20** in $CDCl_3$.

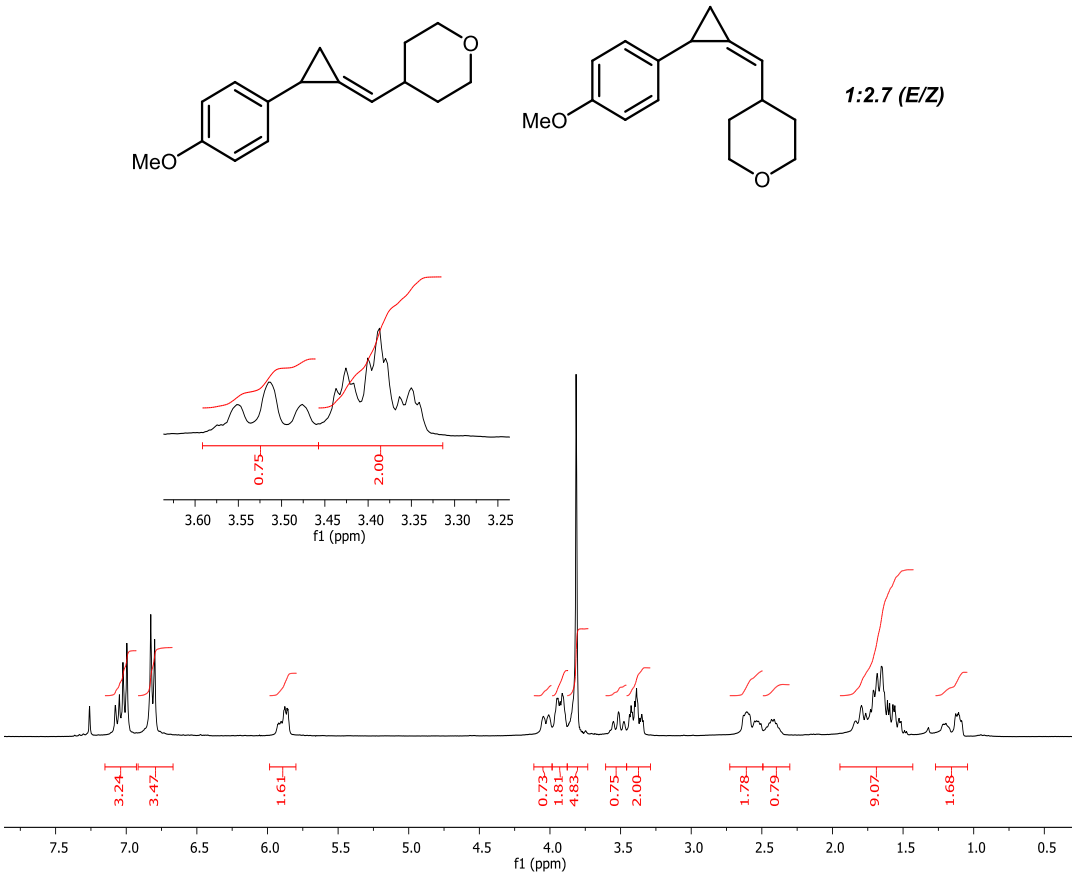

Figure B.43. ^{1}H NMR spectrum for **21** in $CDCl_3$.

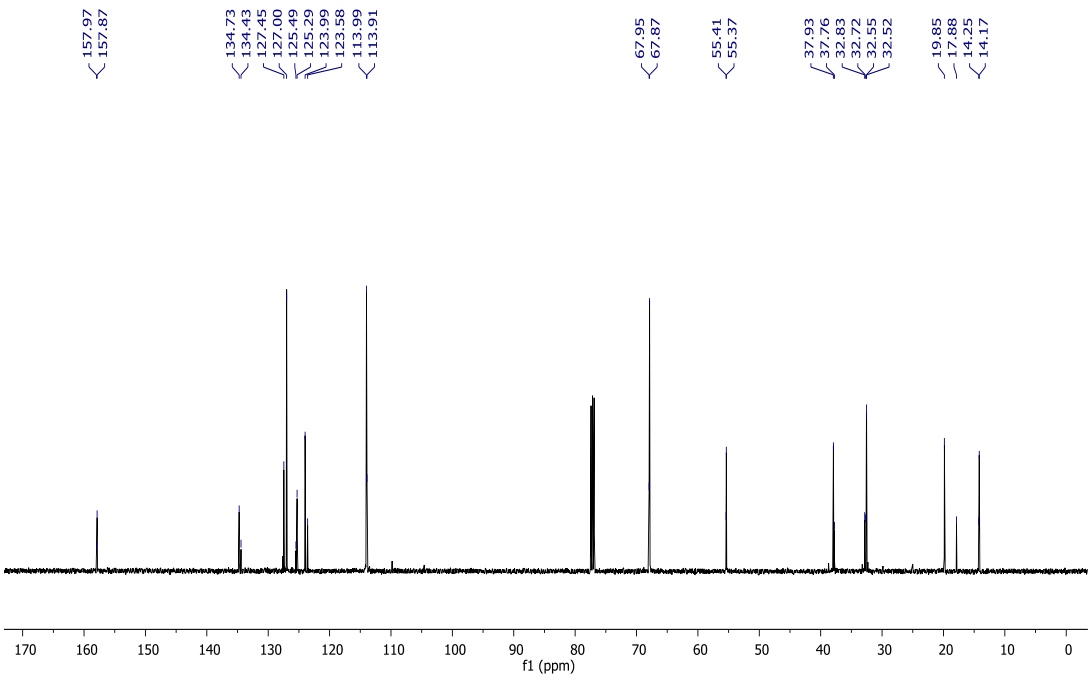

Figure B.44. $^{13}C\{^{1}H\}$ NMR spectrum for **21** in $CDCl_3$.

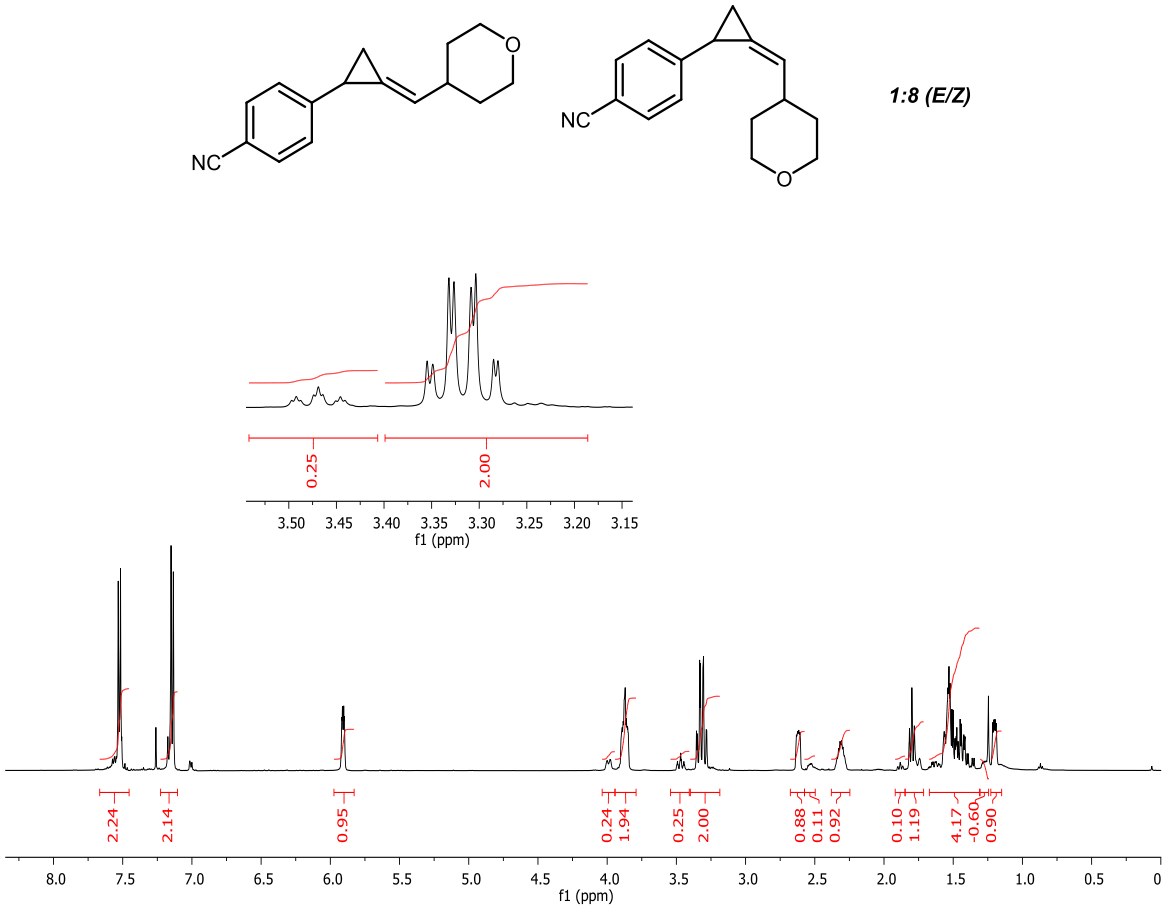

Figure B.45. ^{1}H NMR spectrum for **22** in $CDCl_3$.

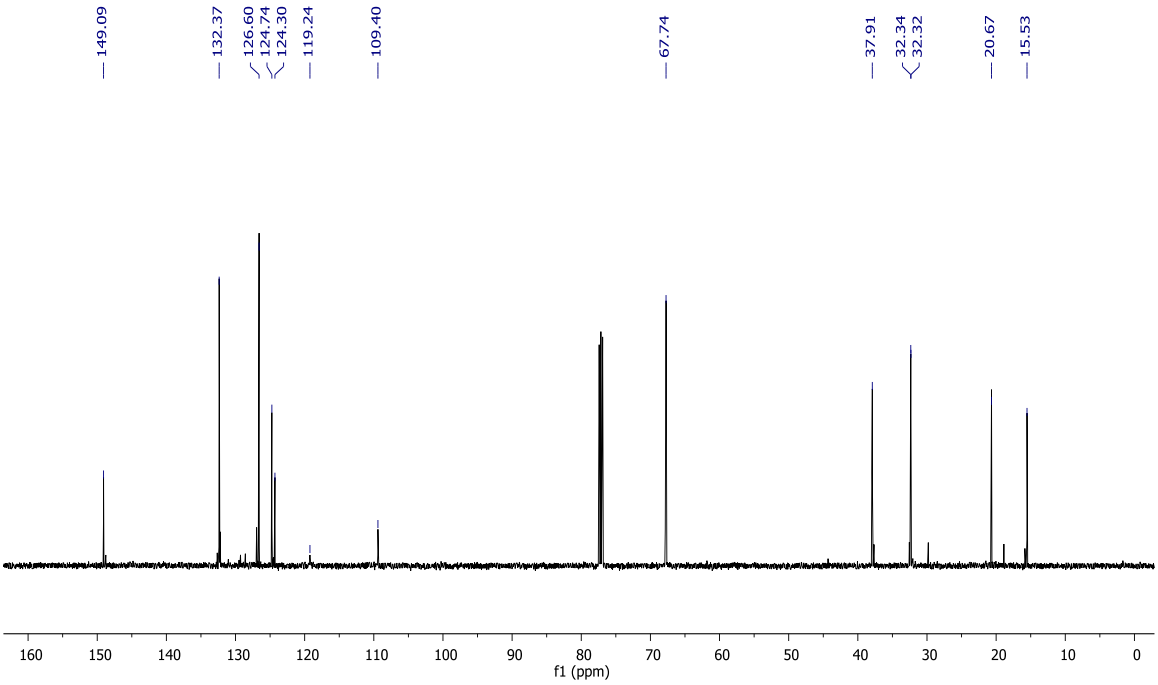

Figure B.46. $^{13}C\{^{1}H\}$ NMR spectrum for **22** in $CDCl_3$.

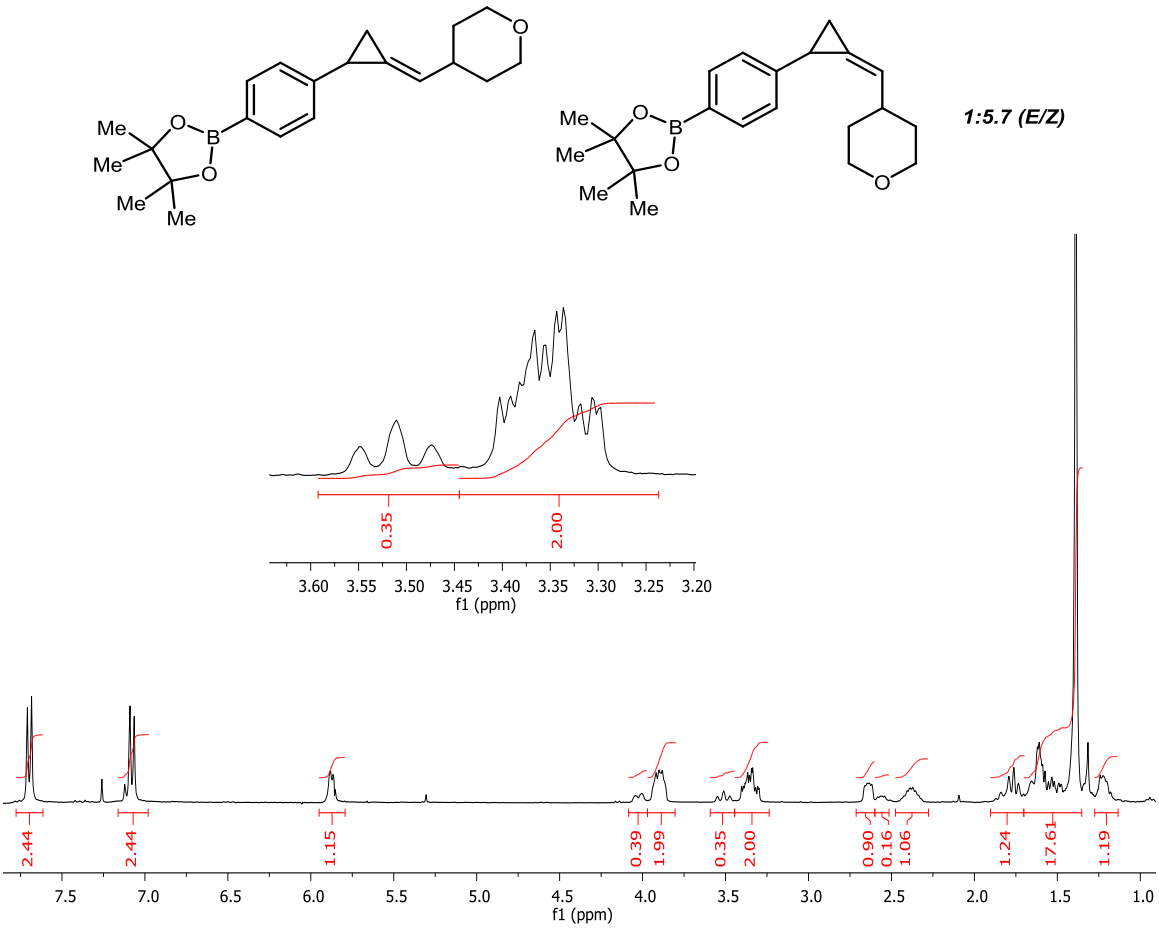

Figure B.47. ^{1}H NMR spectrum for **23** in $CDCl_3$.

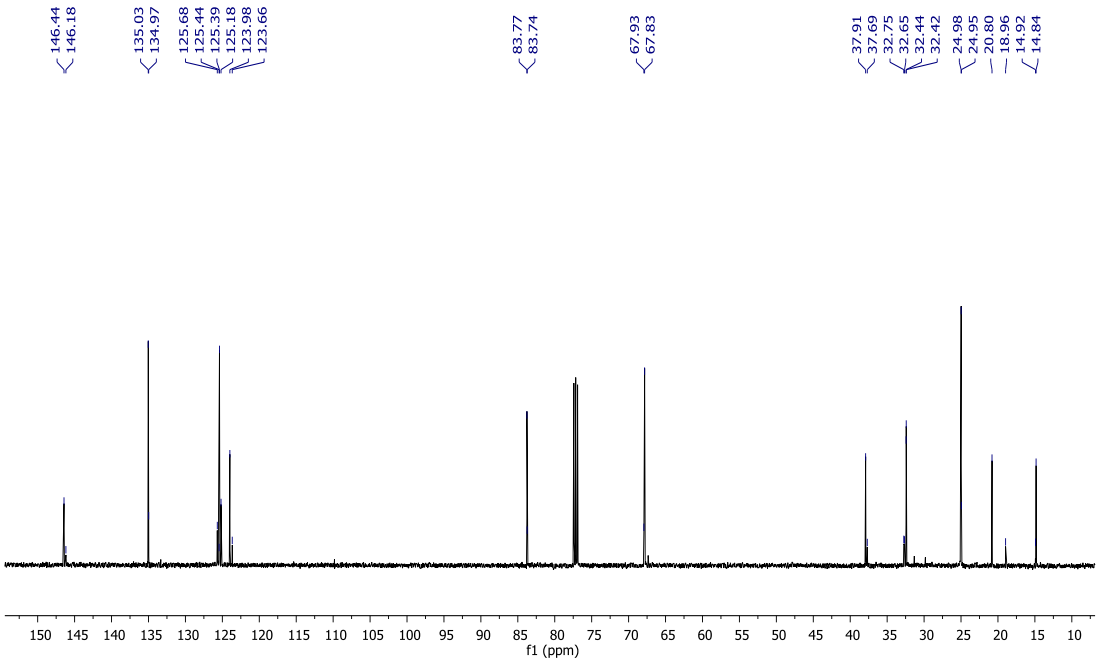

Figure B.48. $^{13}C\{^{1}H\}$ NMR spectrum for **23** in $CDCl_3$.

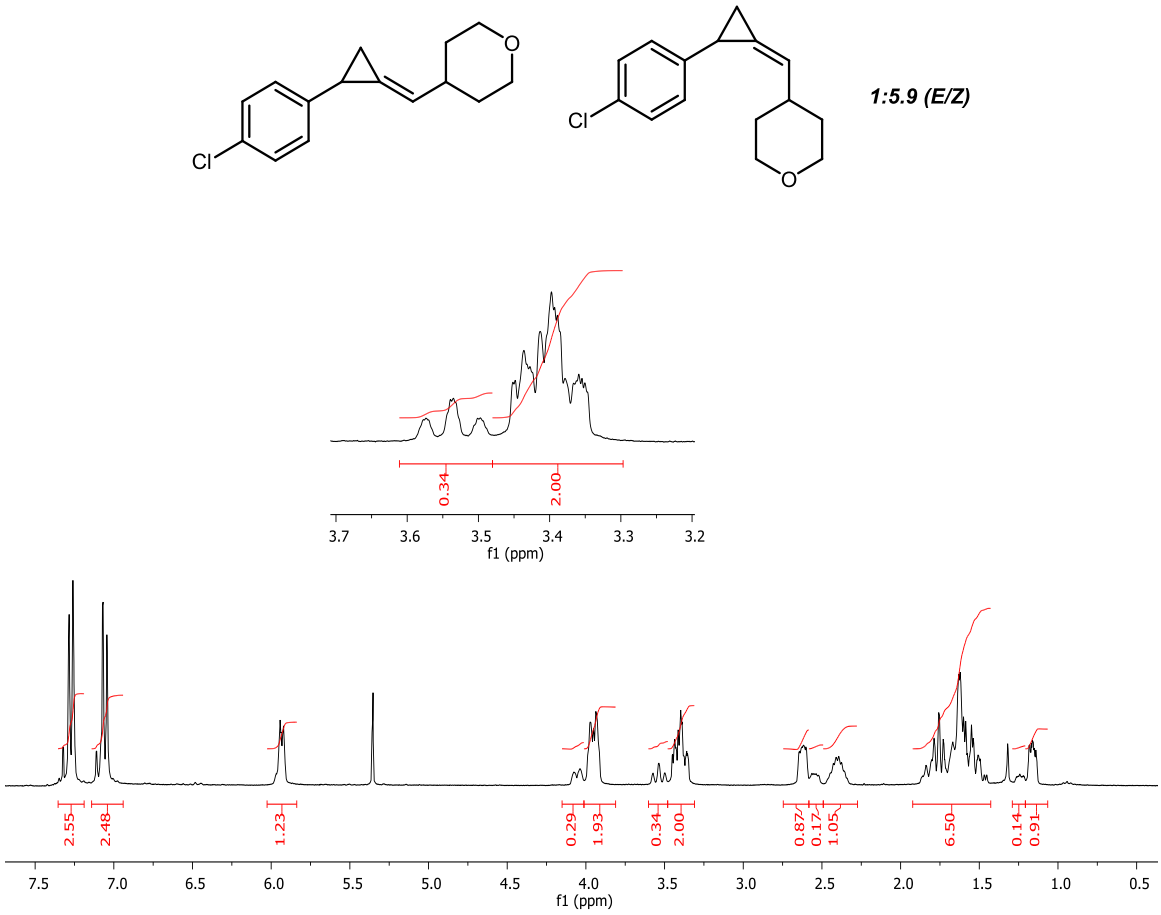

Figure B.49. ^{1}H NMR spectrum for **24** in $CDCl_3$.

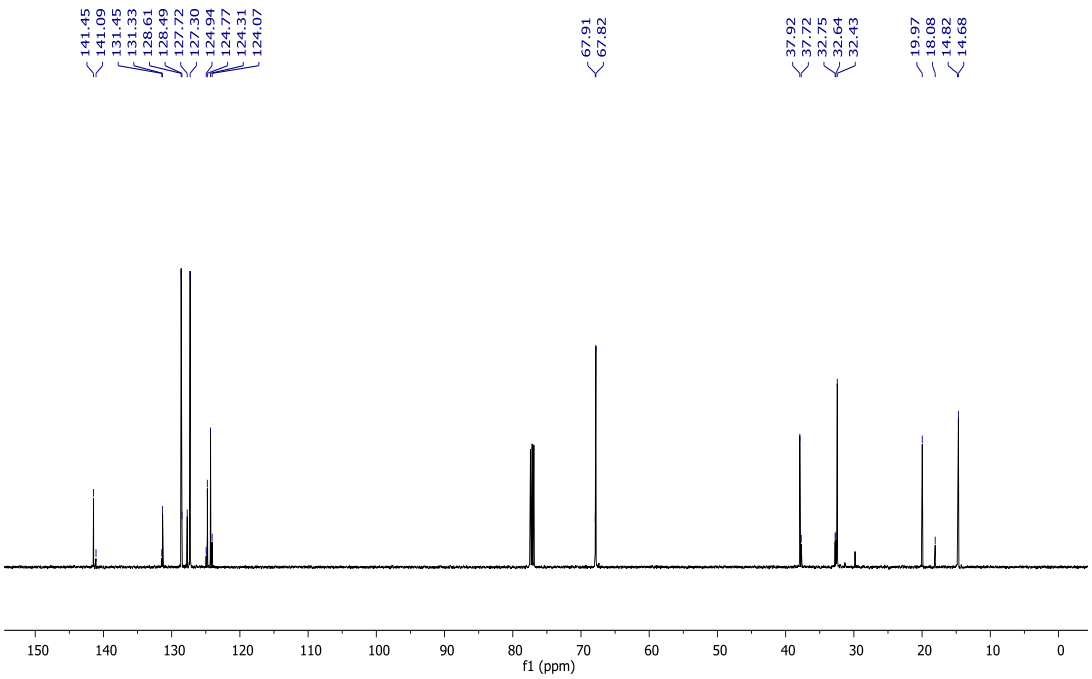

Figure B.50. $^{13}C\{^{1}H\}$ NMR spectrum for **24** in $CDCl_3$.

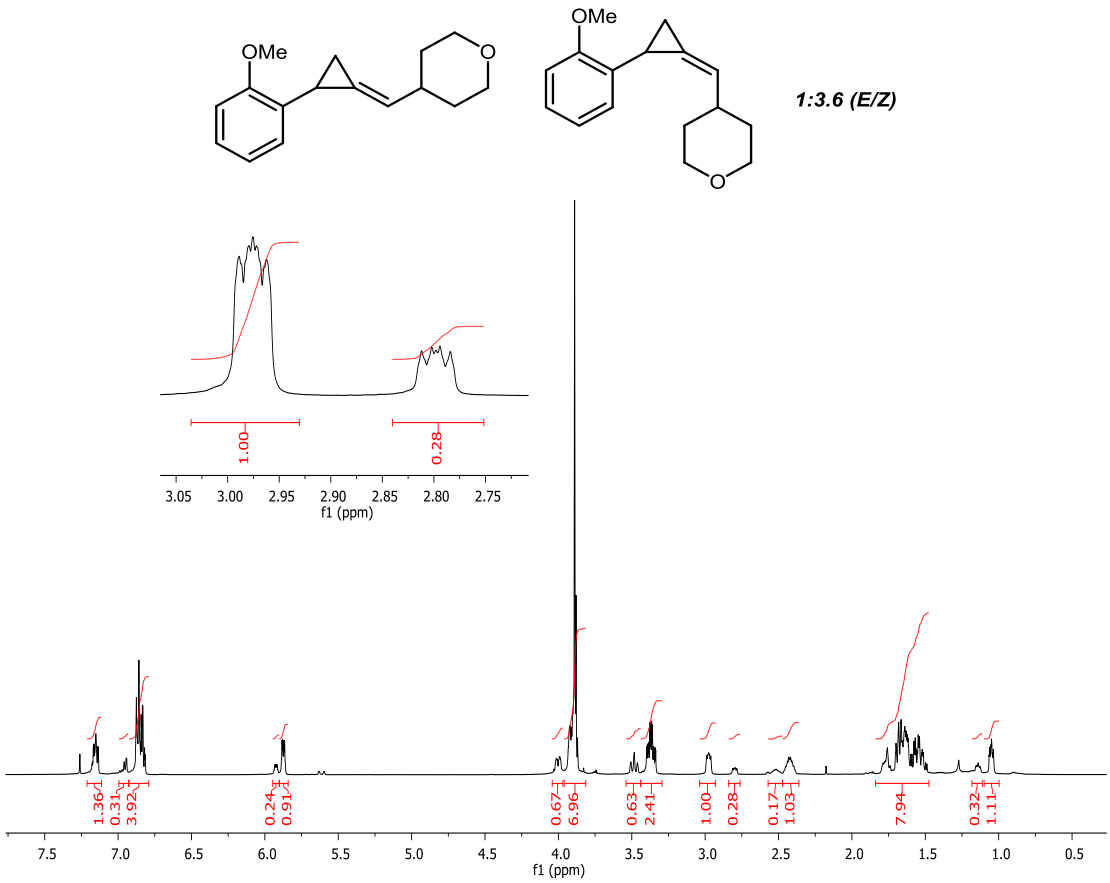

Figure B.51. ^{1}H NMR spectrum for **25** in $CDCl_3$.

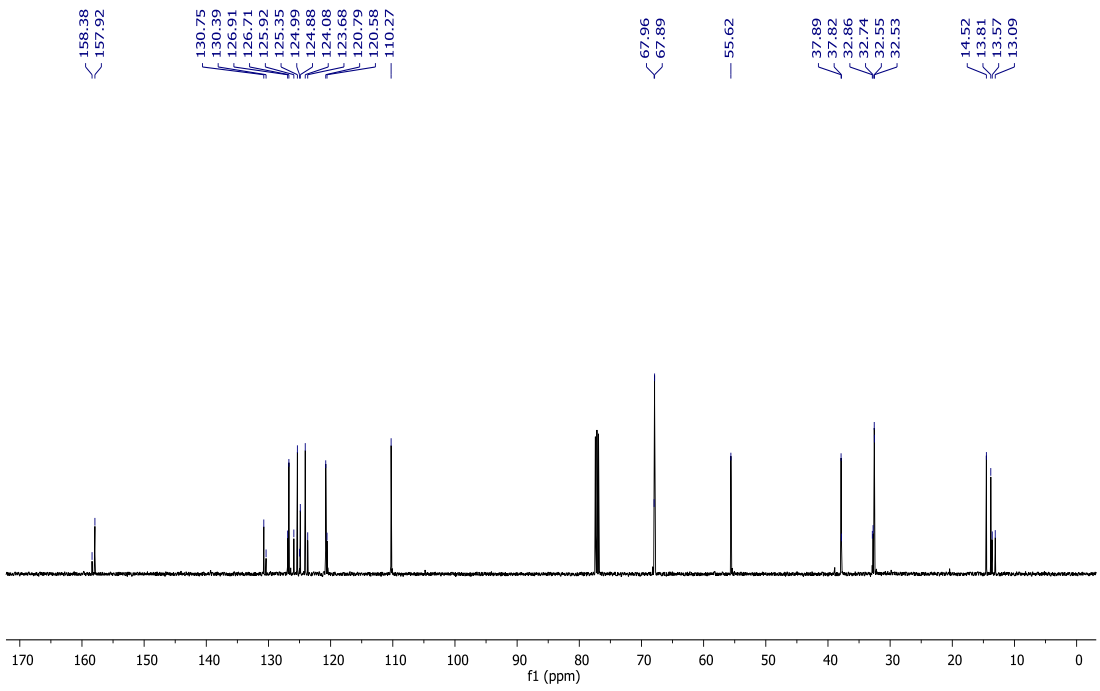

Figure B.52. $^{13}C\{^{1}H\}$ NMR spectrum for **25** in $CDCl_3$.

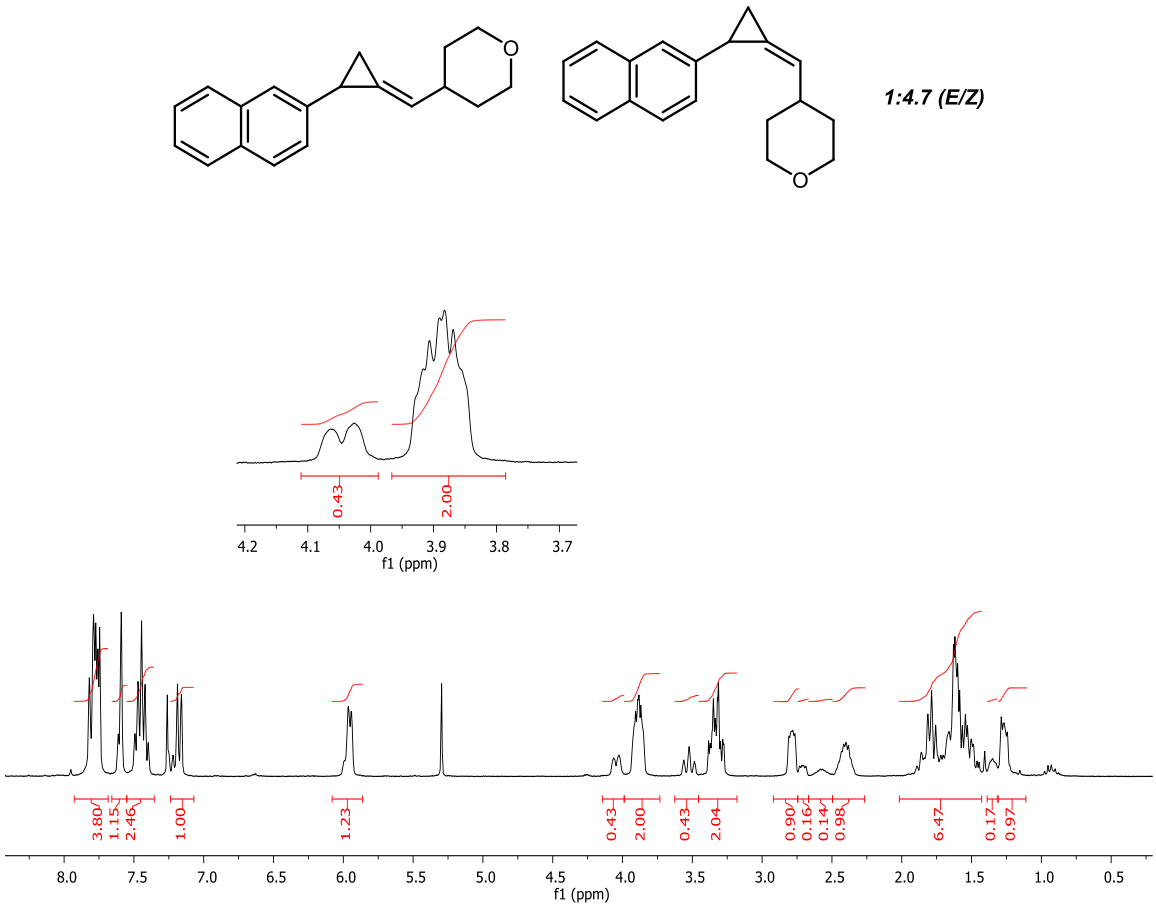

Figure B.53. ^{1}H NMR spectrum for **26** in $CDCl_3$.

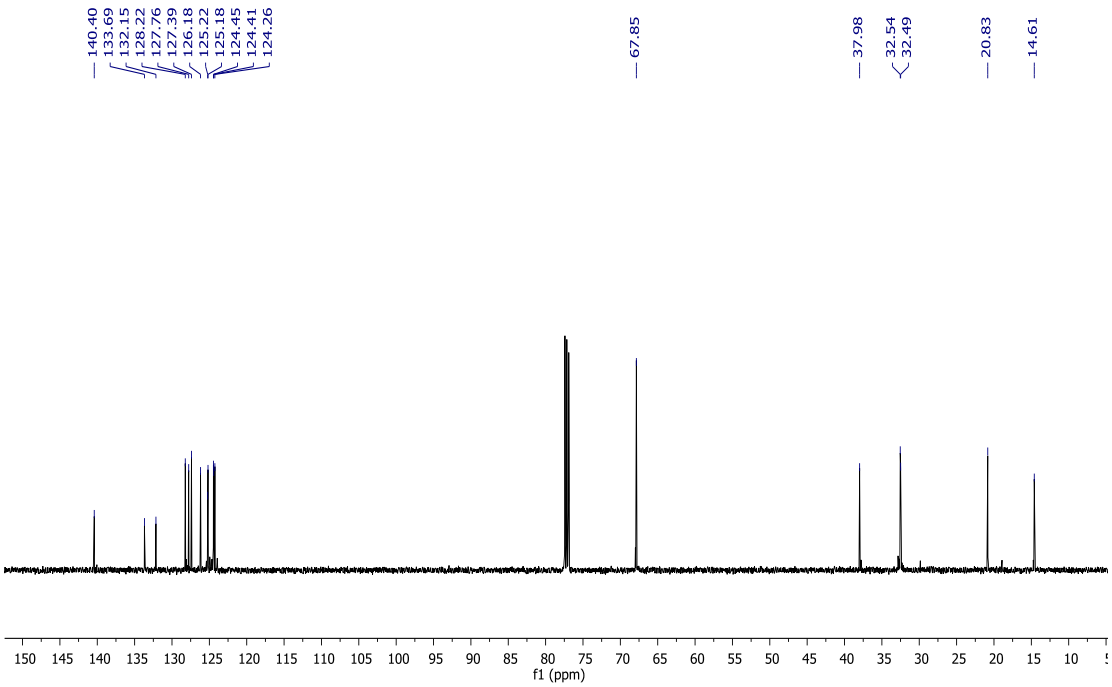

Figure B.54. $^{13}C\{^{1}H\}$ NMR spectrum for **26** in $CDCl_3$.

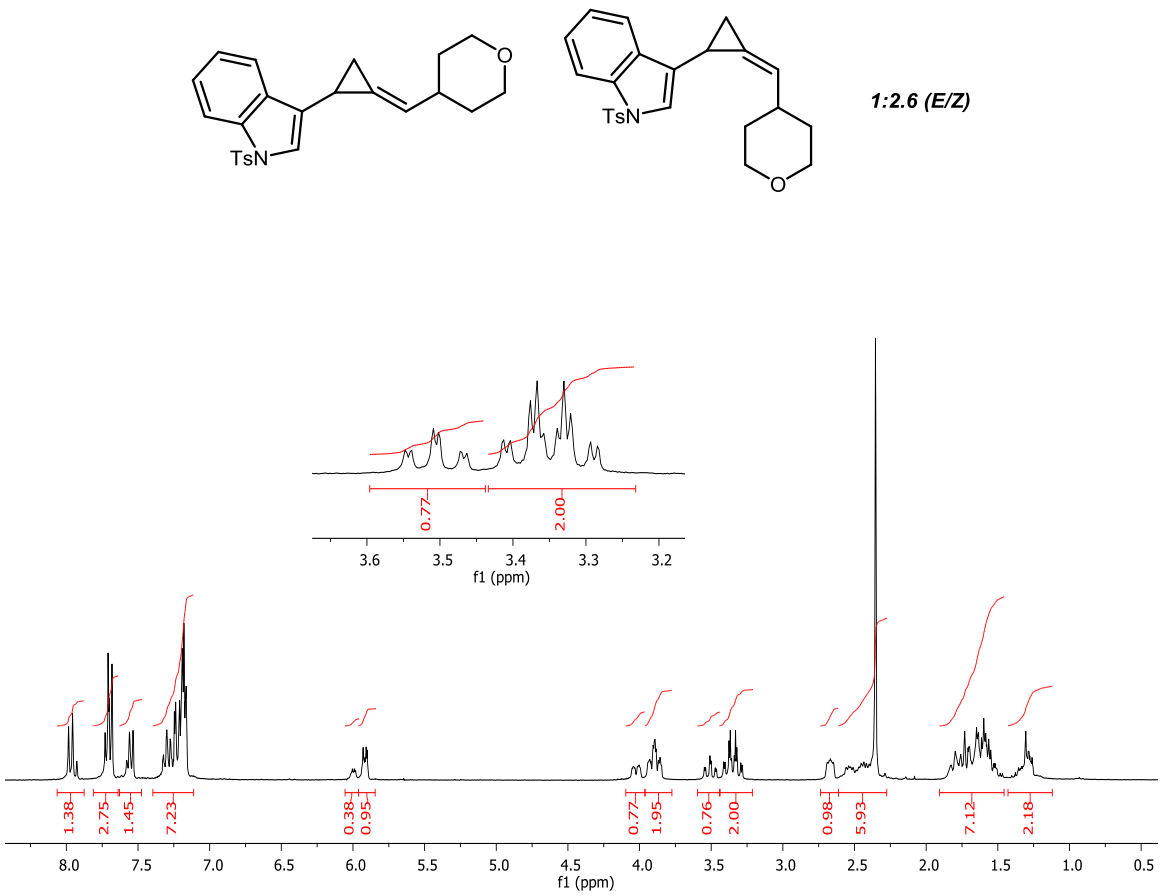

Figure B.55. ^{1}H NMR spectrum for **27** in $CDCl_3$.

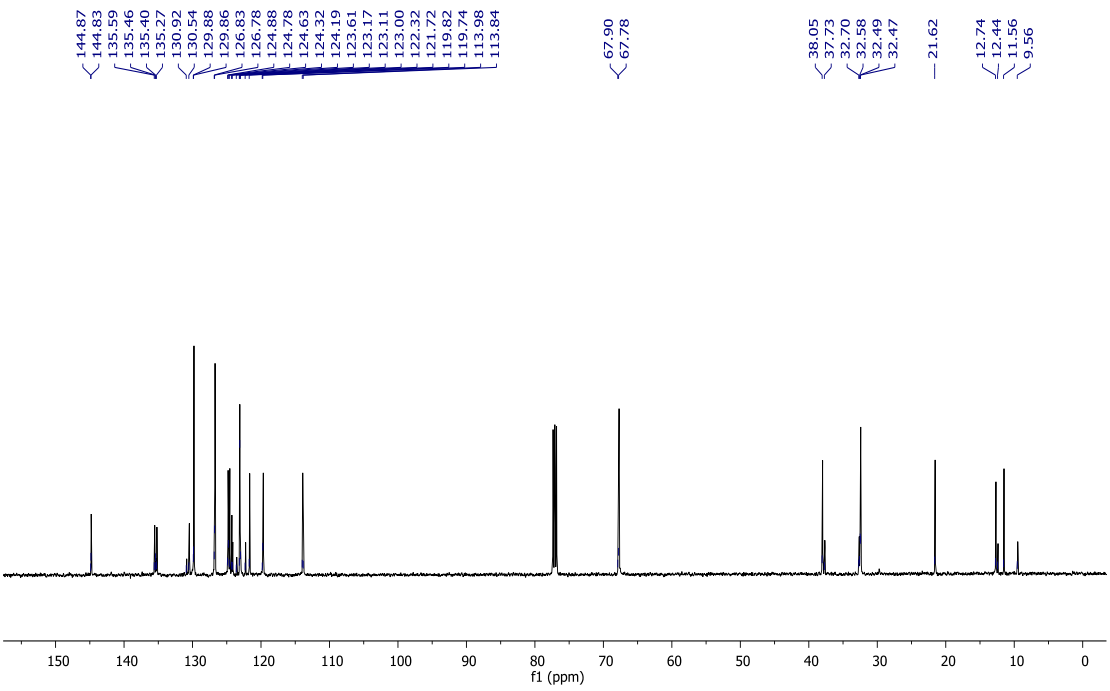

Figure B.56. $^{13}C\{^{1}H\}$ NMR spectrum for **27** in $CDCl_3$.

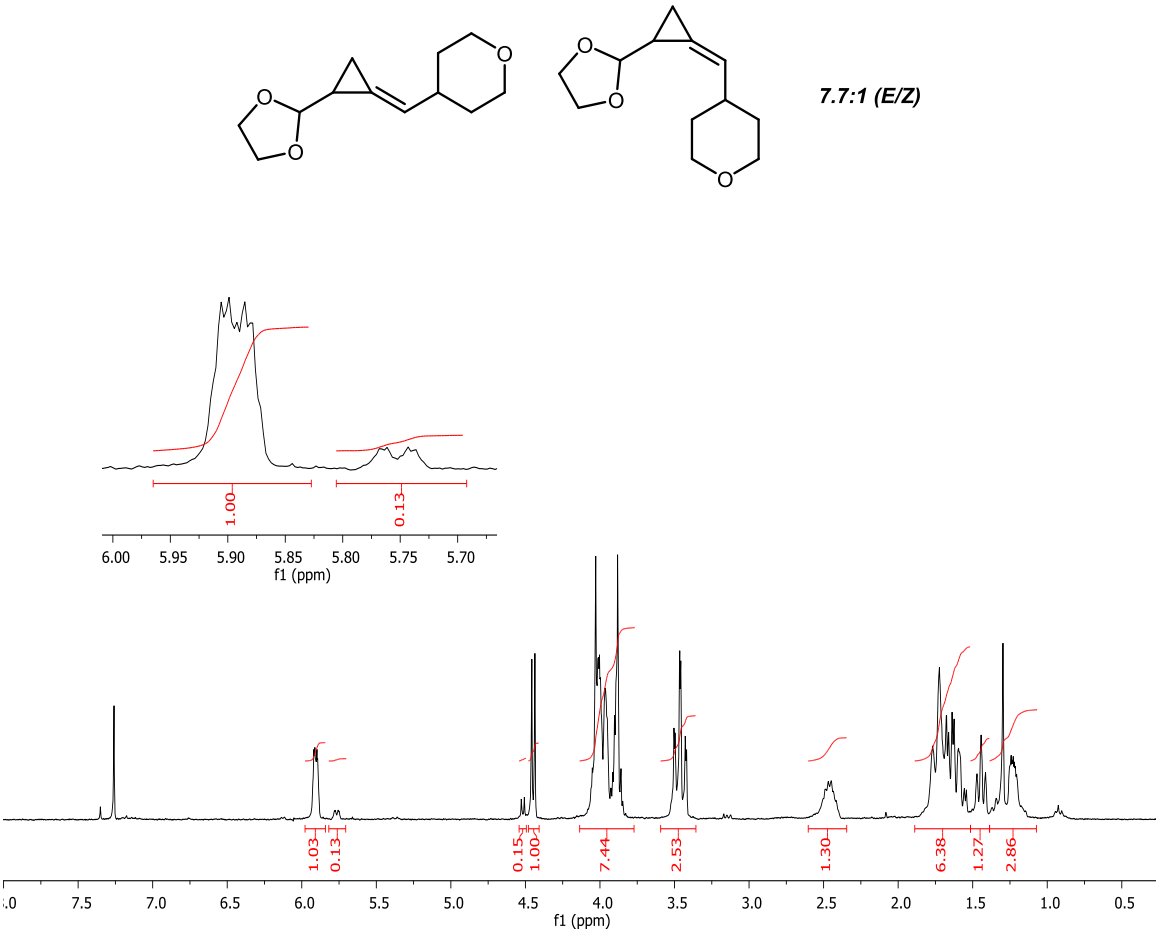

Figure B.57. ^{1}H NMR spectrum for **28** in $CDCl_3$.

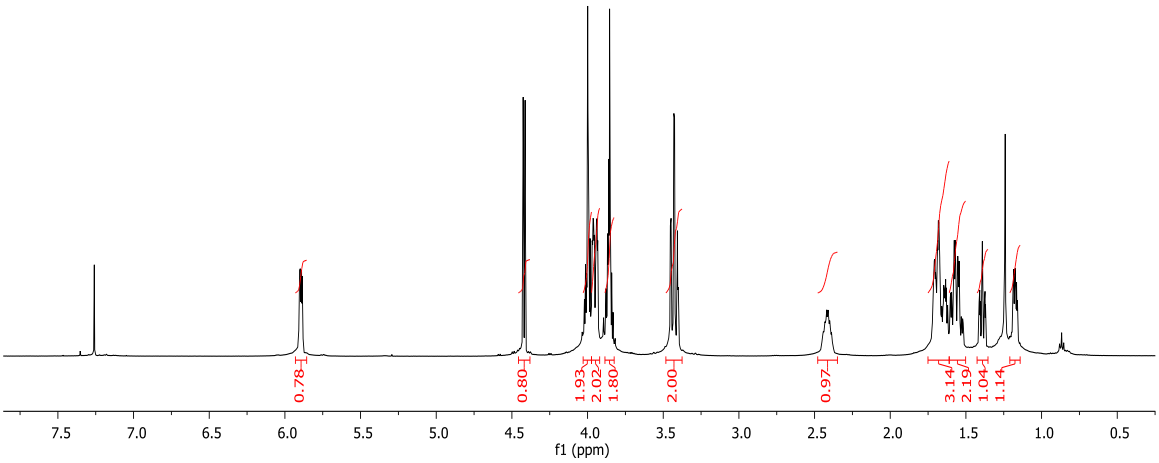

Figure B.58. ^{1}H NMR spectrum for single crystals of **28-*E*** in $CDCl_3$.

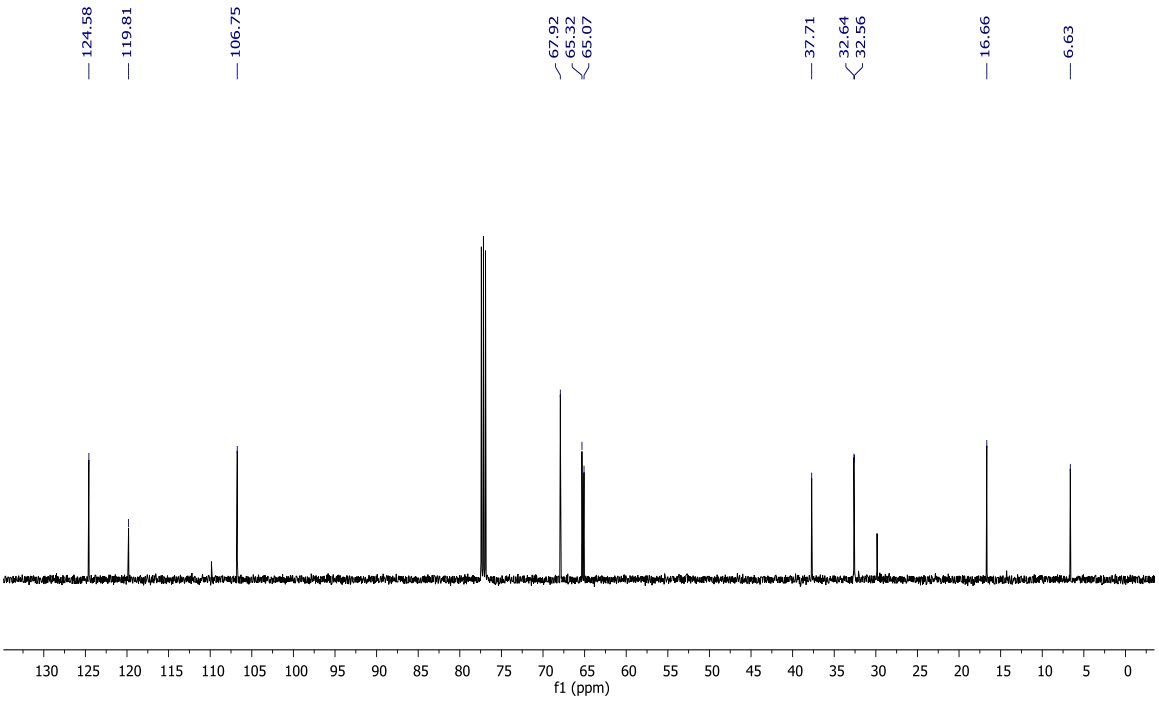

Figure B.59. $^{13}C\{^{1}H\}$ NMR spectrum for **28** in $CDCl_3$.

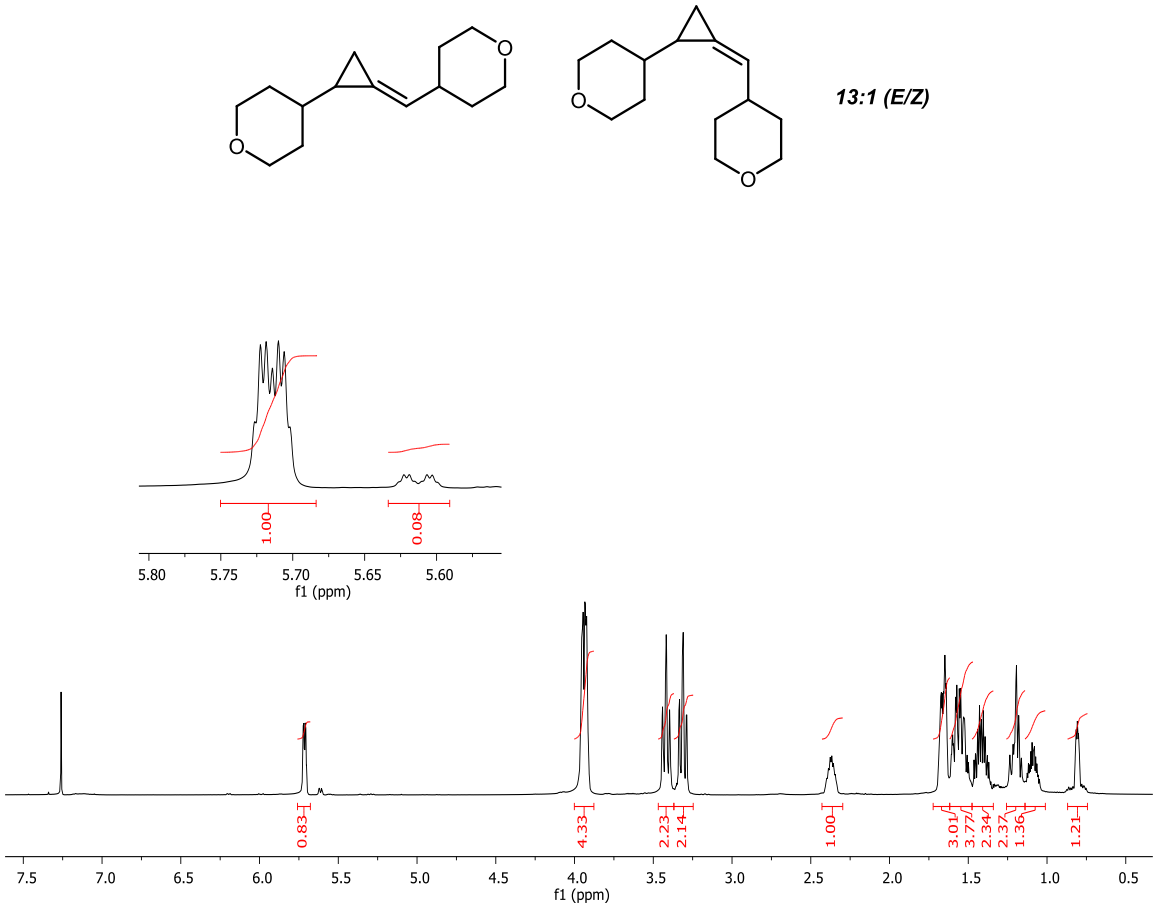

Figure B.60. ^{1}H NMR spectrum for **29** in $CDCl_3$.

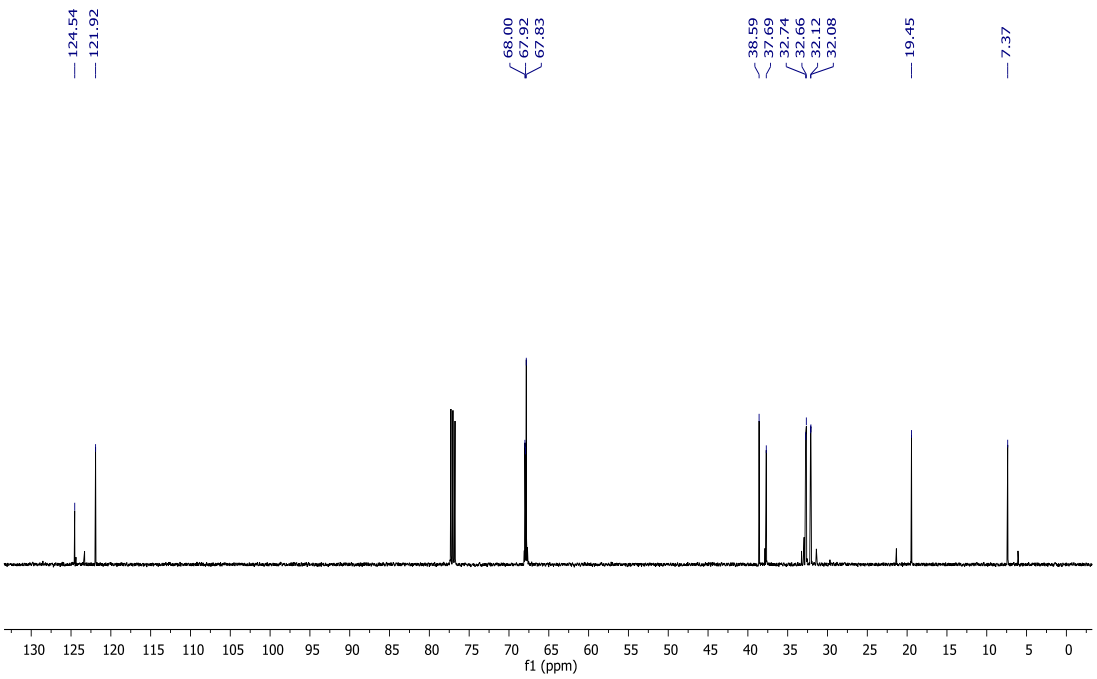

Figure B.61. $^{13}C\{^{1}H\}$ NMR spectrum for **29** in $CDCl_3$.

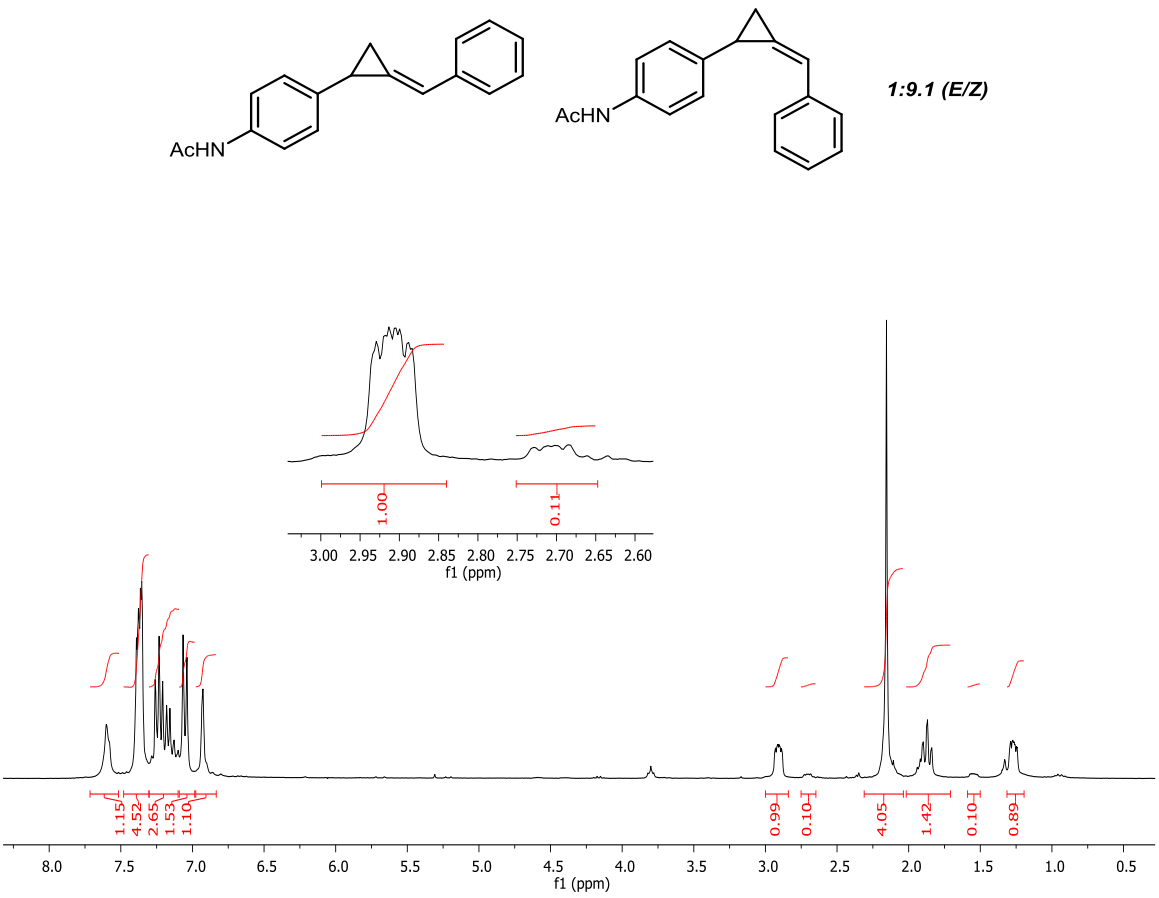

Figure B.62. ^{1}H NMR spectrum for **30** in $CDCl_3$.

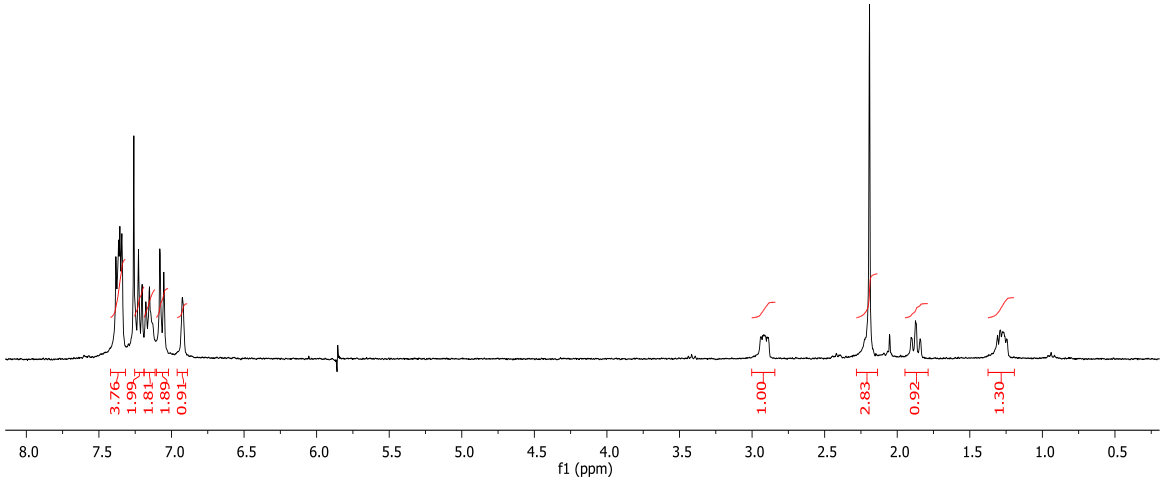

Figure B.63. ^{1}H NMR spectrum for single crystals of **30-*Z*** in $CDCl_3$.

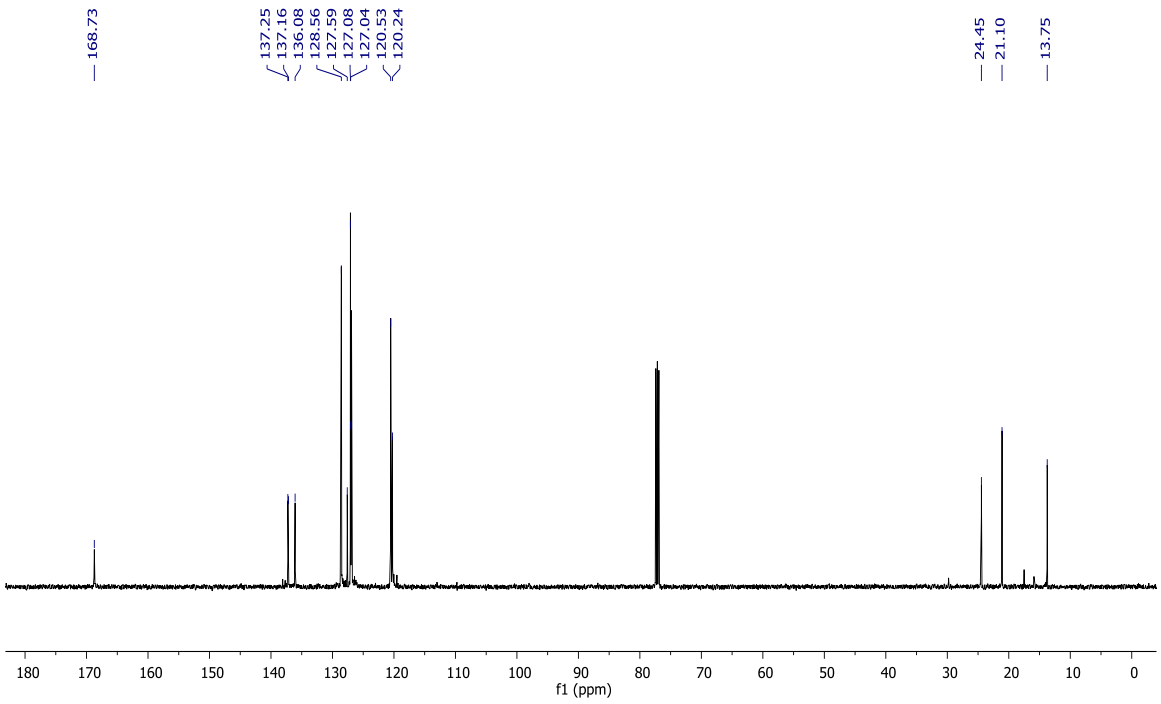

Figure B.64. $^{13}C\{^{1}H\}$ NMR spectrum for **30** in $CDCl_3$.

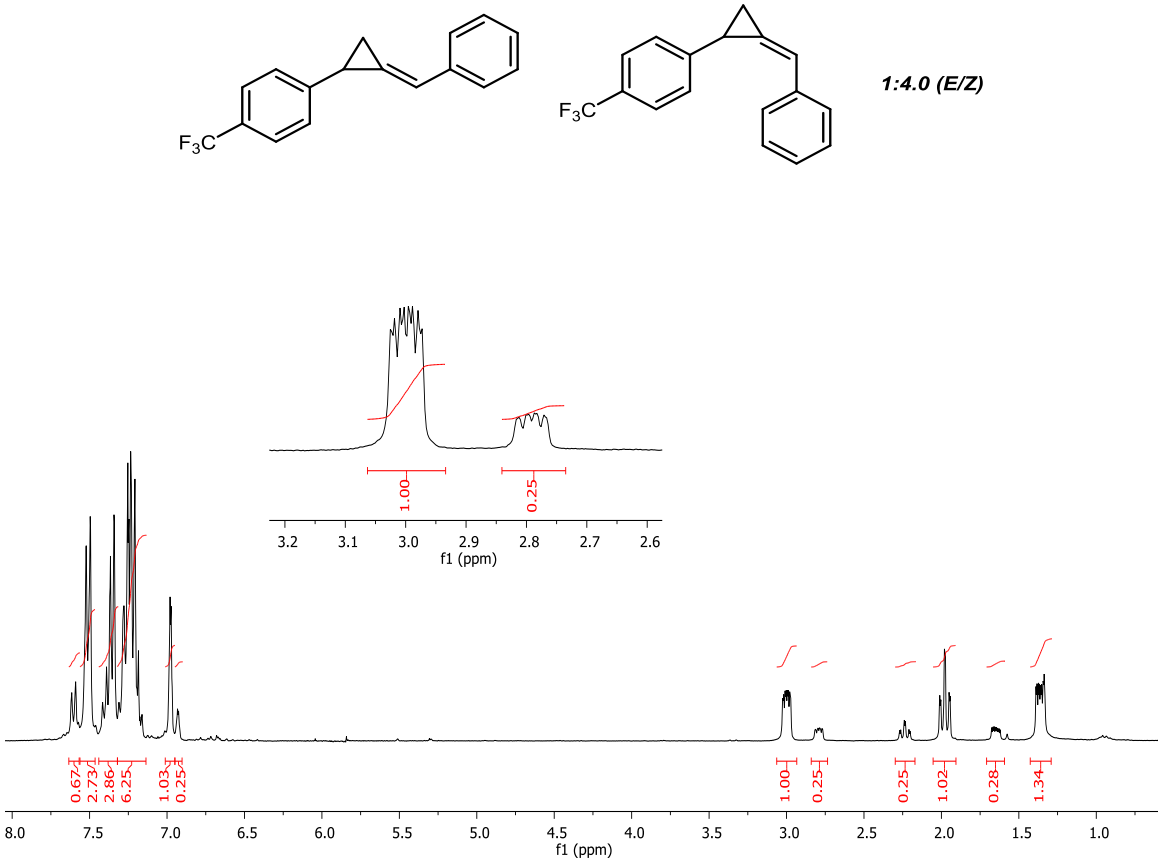

Figure B.65. ^{1}H NMR spectrum for **31** in $CDCl_3$.

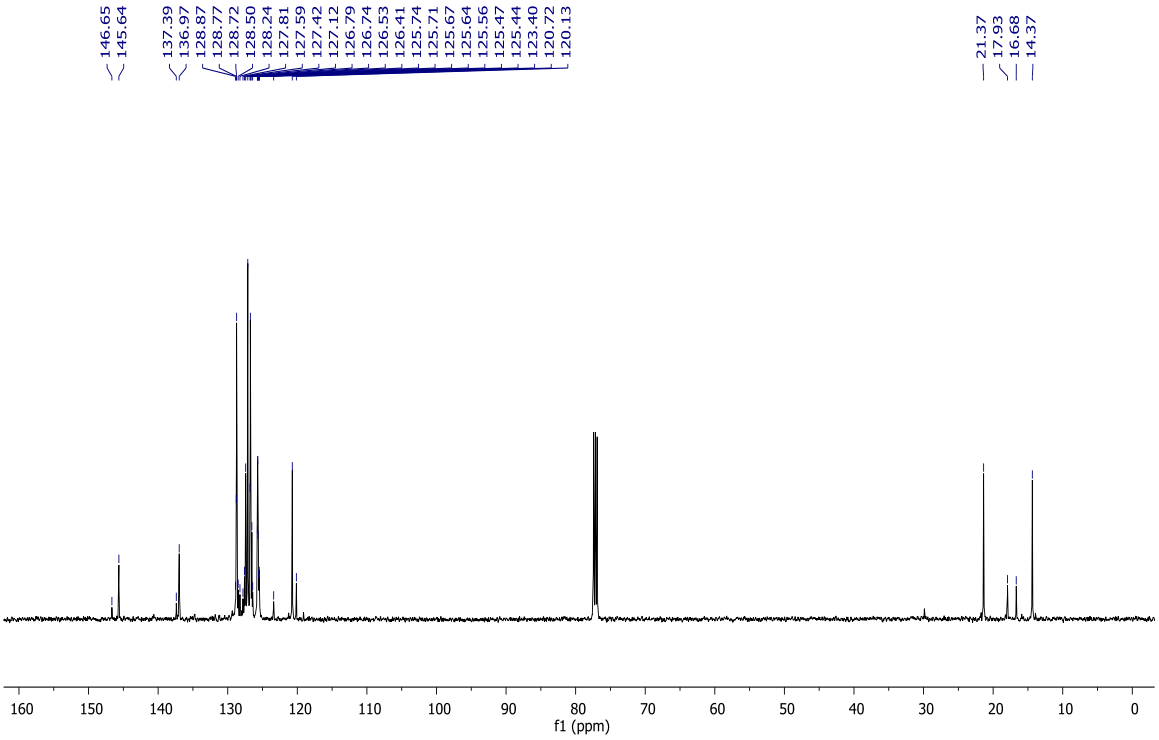

Figure B.66. $^{13}C\{^{1}H\}$ NMR spectrum for **31** in $CDCl_3$.

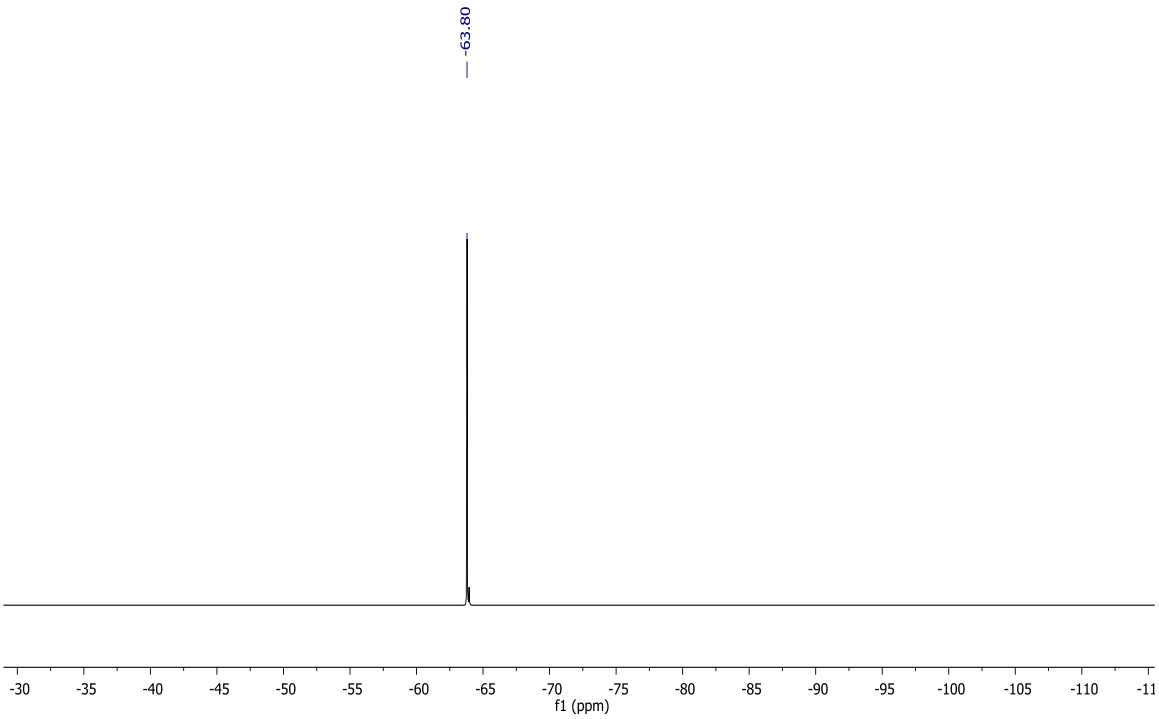

Figure B.67. ^{19}F NMR spectrum for **31** in $CDCl_3$.

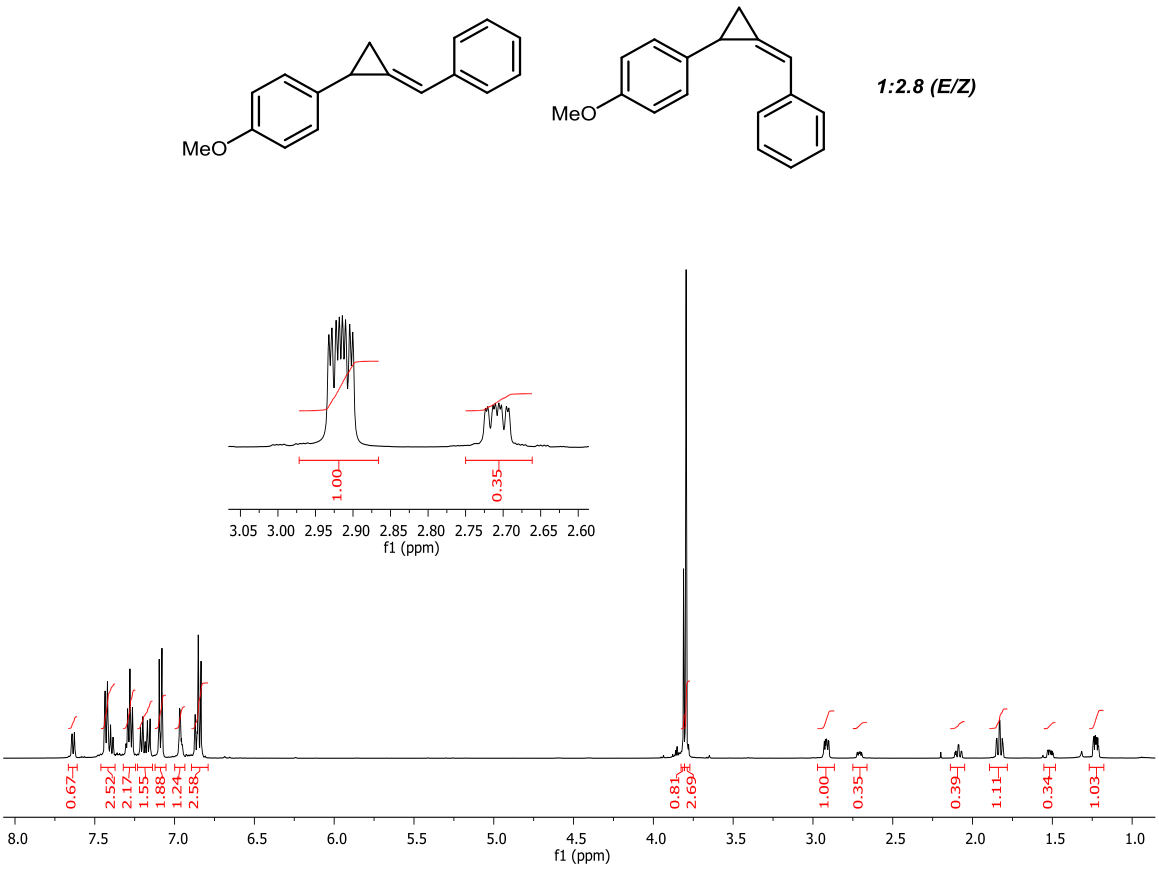

Figure B.68. ^{1}H NMR spectrum for 32 in $CDCl_3$.

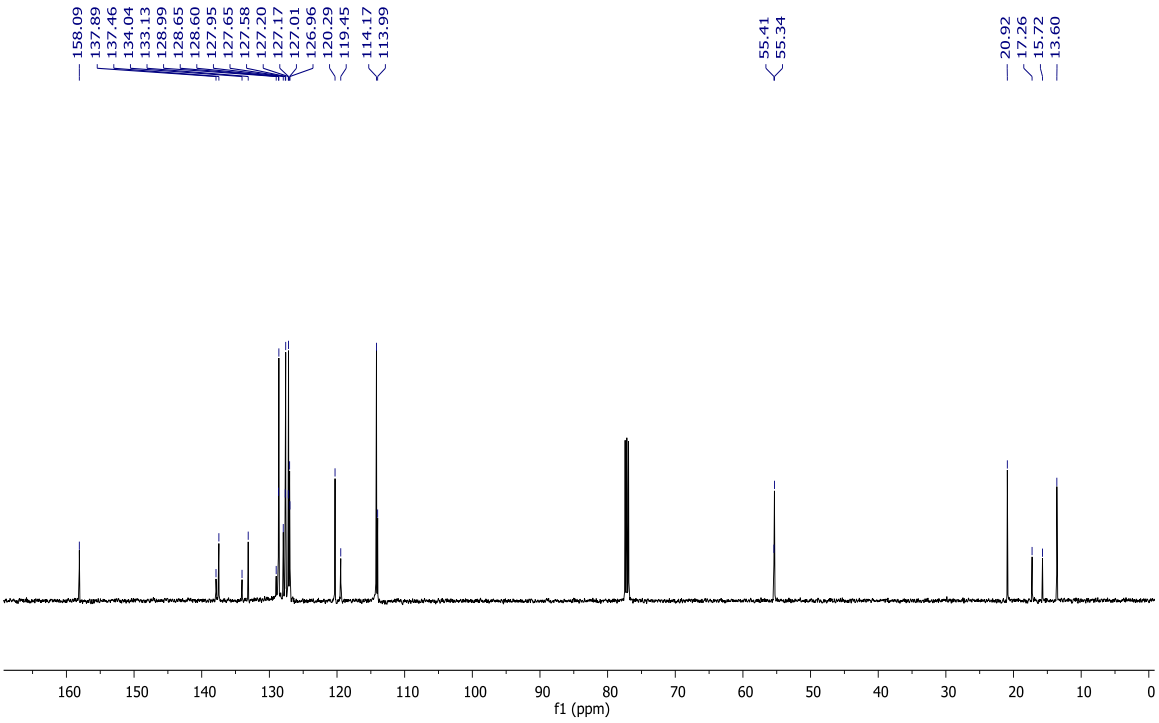

Figure B.69. $^{13}C\{^{1}H\}$ NMR spectrum for **32** in $CDCl_3$.

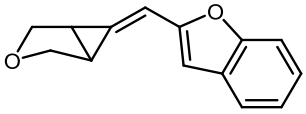

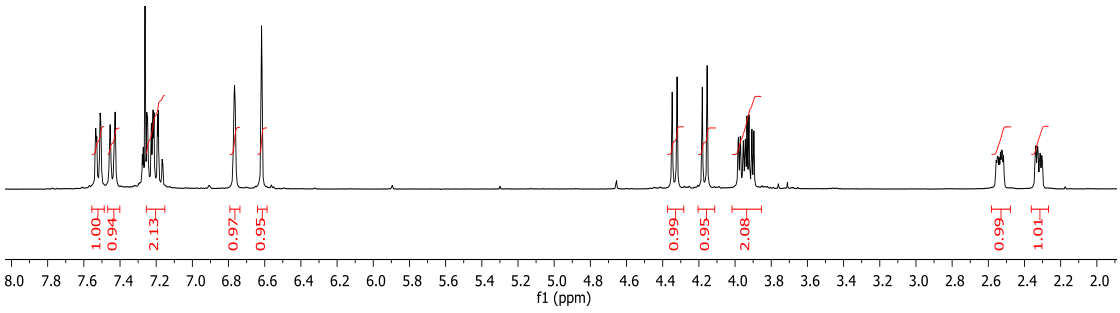

Figure B.70. ^{1}H NMR spectrum for **33** in $CDCl_3$

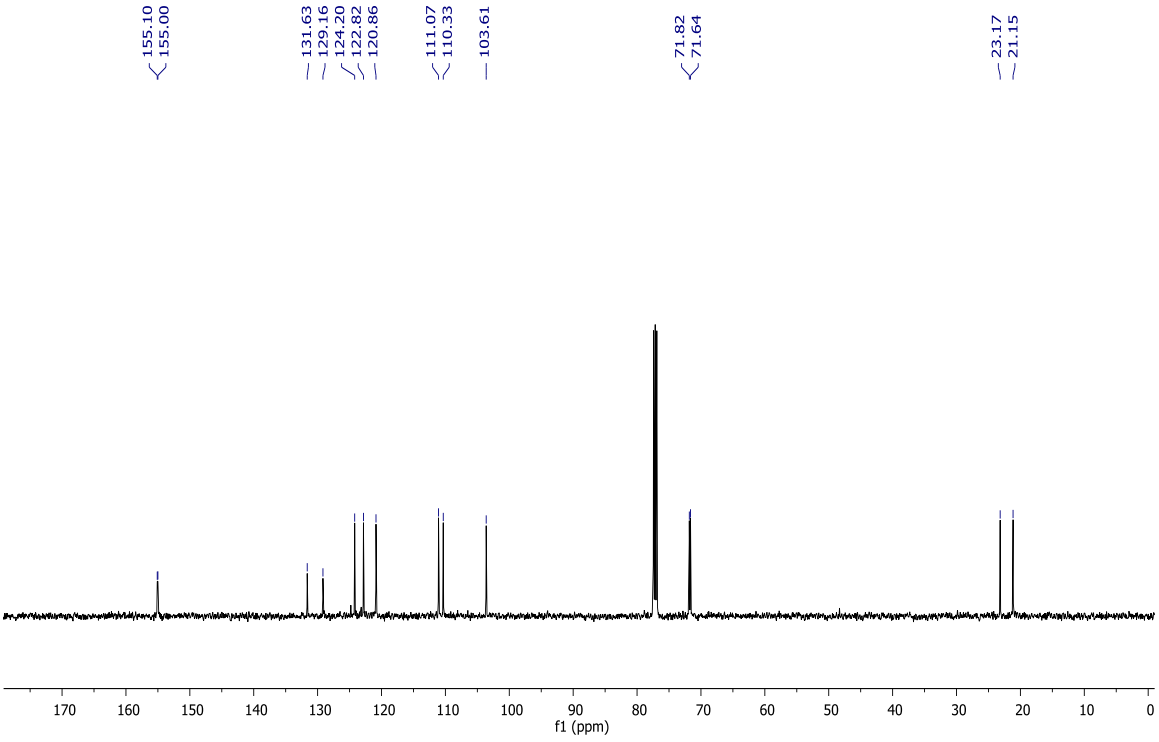

Figure B.71. $^{13}C\{^{1}H\}$ NMR spectrum for **33** in $CDCl_3$

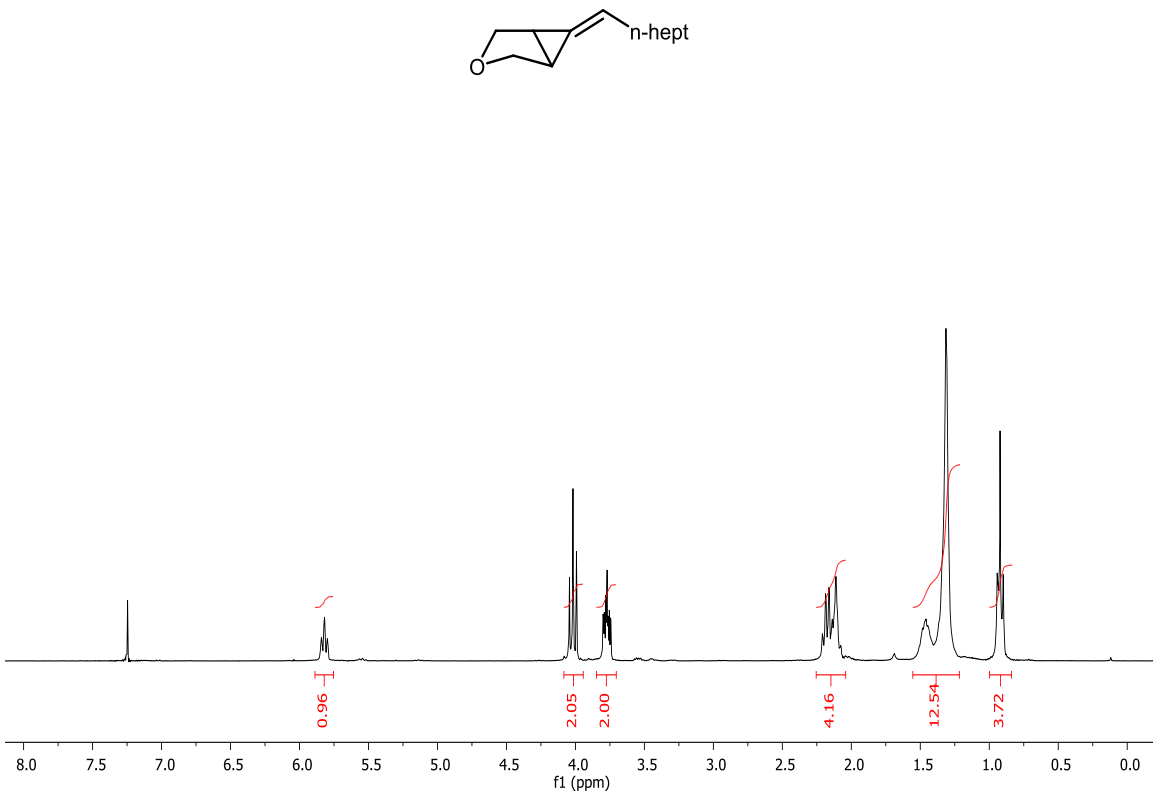

Figure B.72. ^{1}H NMR spectrum for **34** in $CDCl_3$.

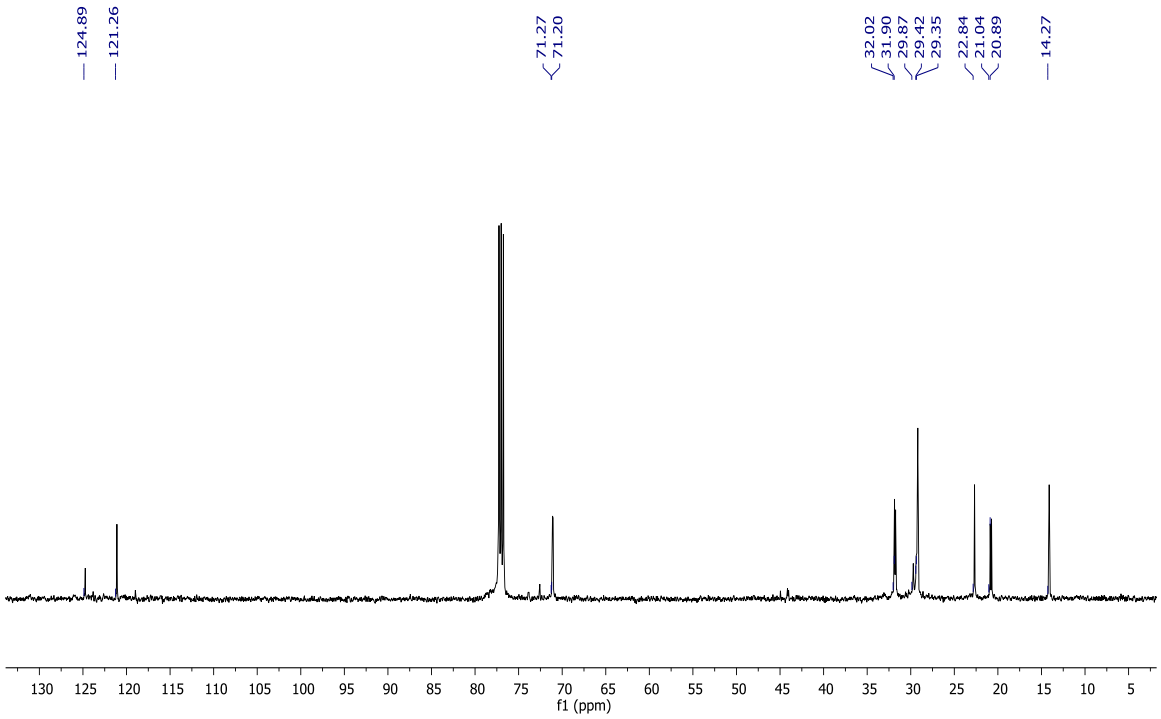

Figure B.73. $^{13}C\{^{1}H\}$ NMR spectrum for **34** in $CDCl_3$.

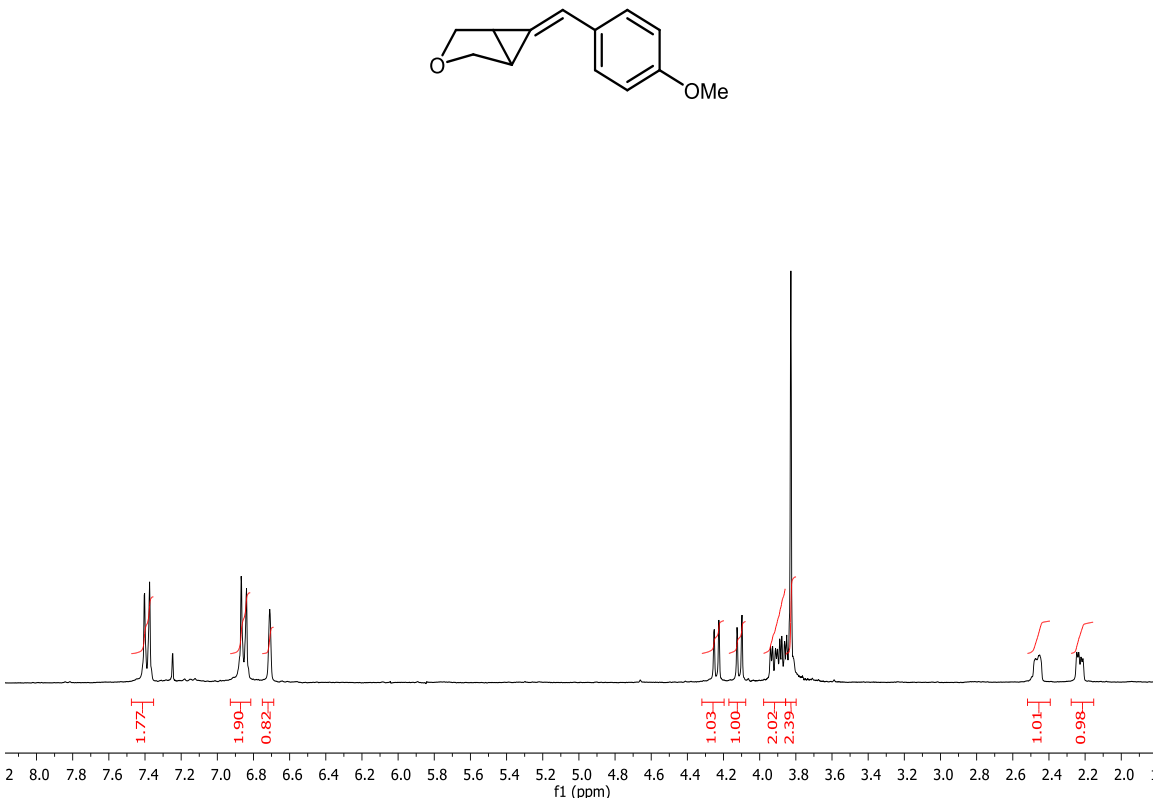

Figure B.74. ^{1}H NMR spectrum for **35** in $CDCl_3$.

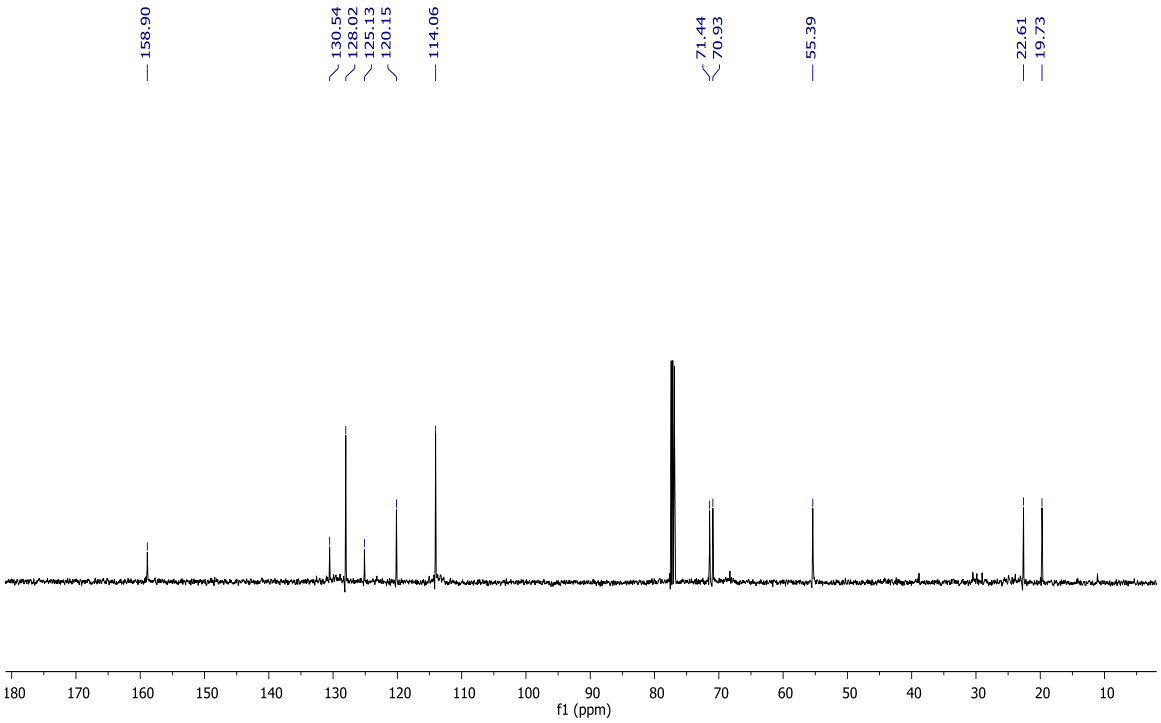

Figure B.75. $^{13}C\{^{1}H\}$ NMR spectrum for **35** in $CDCl_3$.

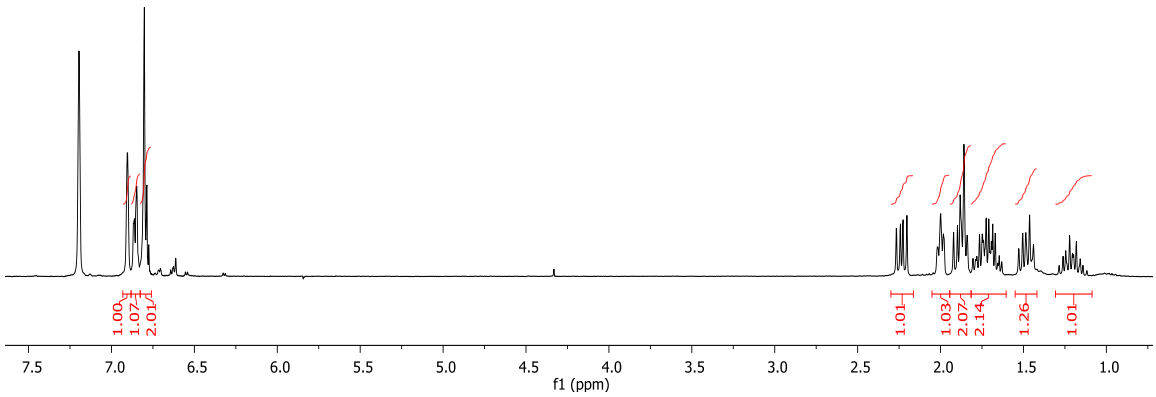

Figure B.76. ^{1}H NMR spectrum for **36** in $CDCl_3$.

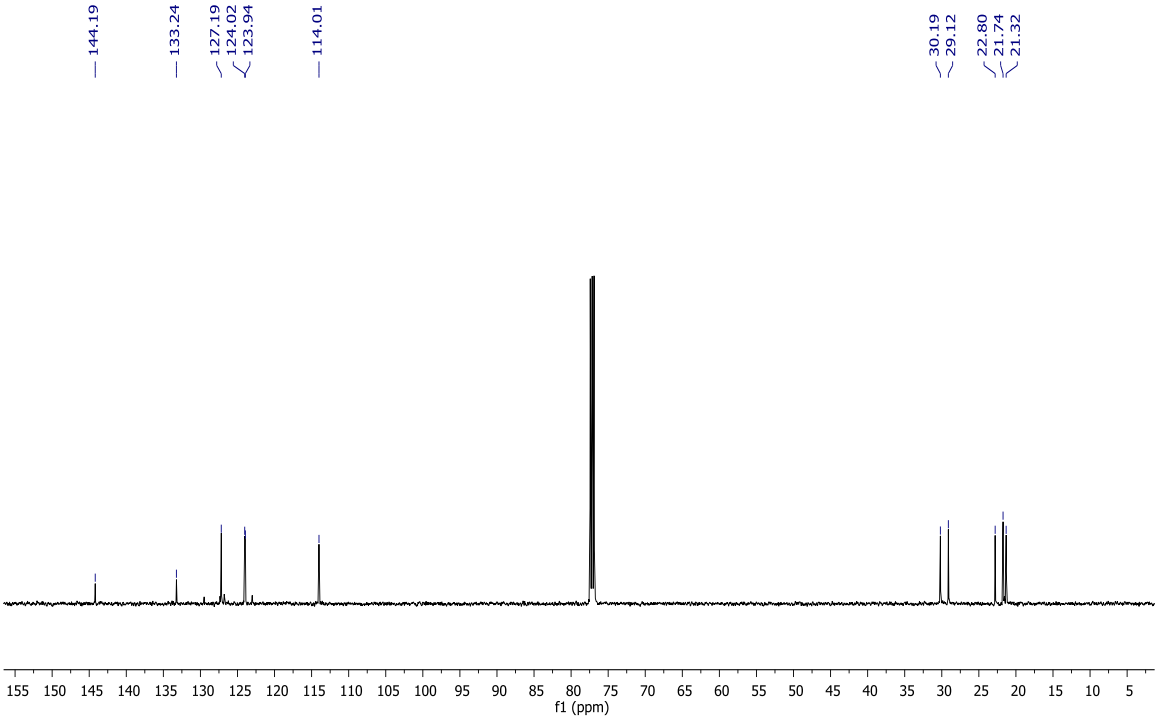

Figure B.77. $^{13}C\{^{1}H\}$ NMR spectrum for **36** in $CDCl_3$.

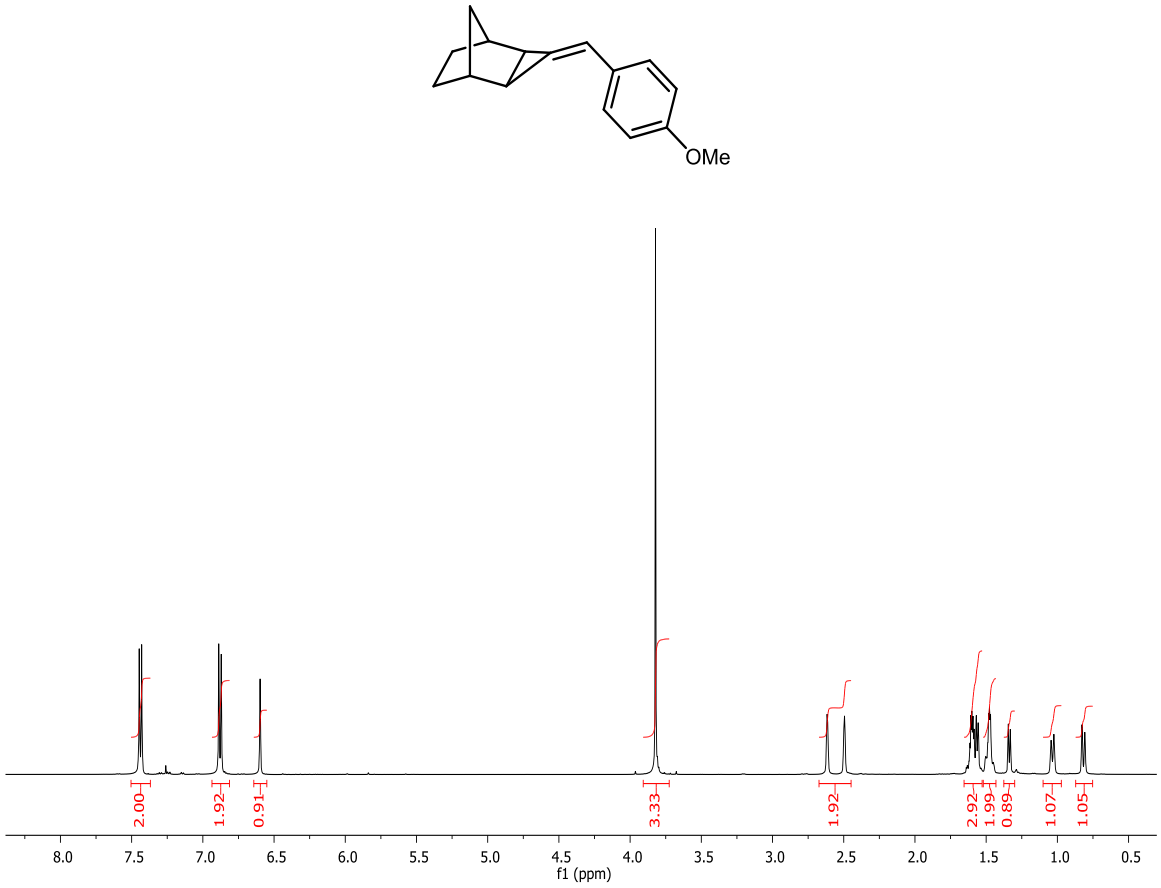

Figure B.78. ^{1}H NMR spectrum for **37** in $CDCl_3$.

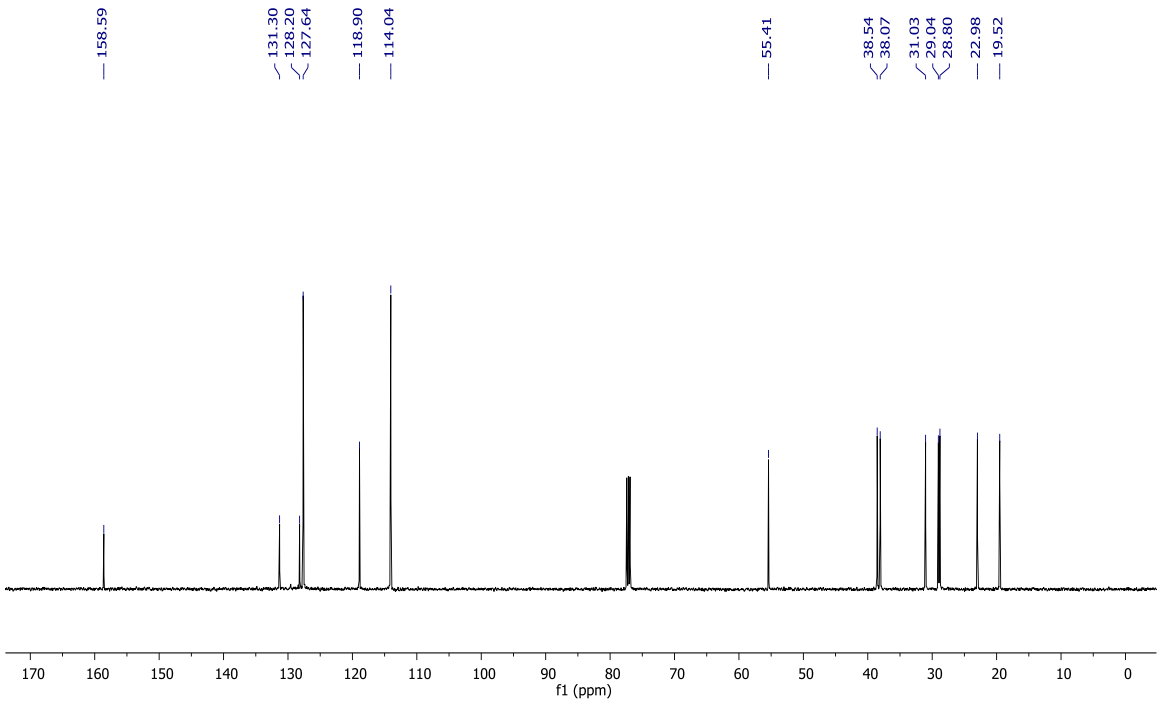

Figure B.79. $^{13}C\{^{1}H\}$ NMR spectrum for **37** in $CDCl_3$

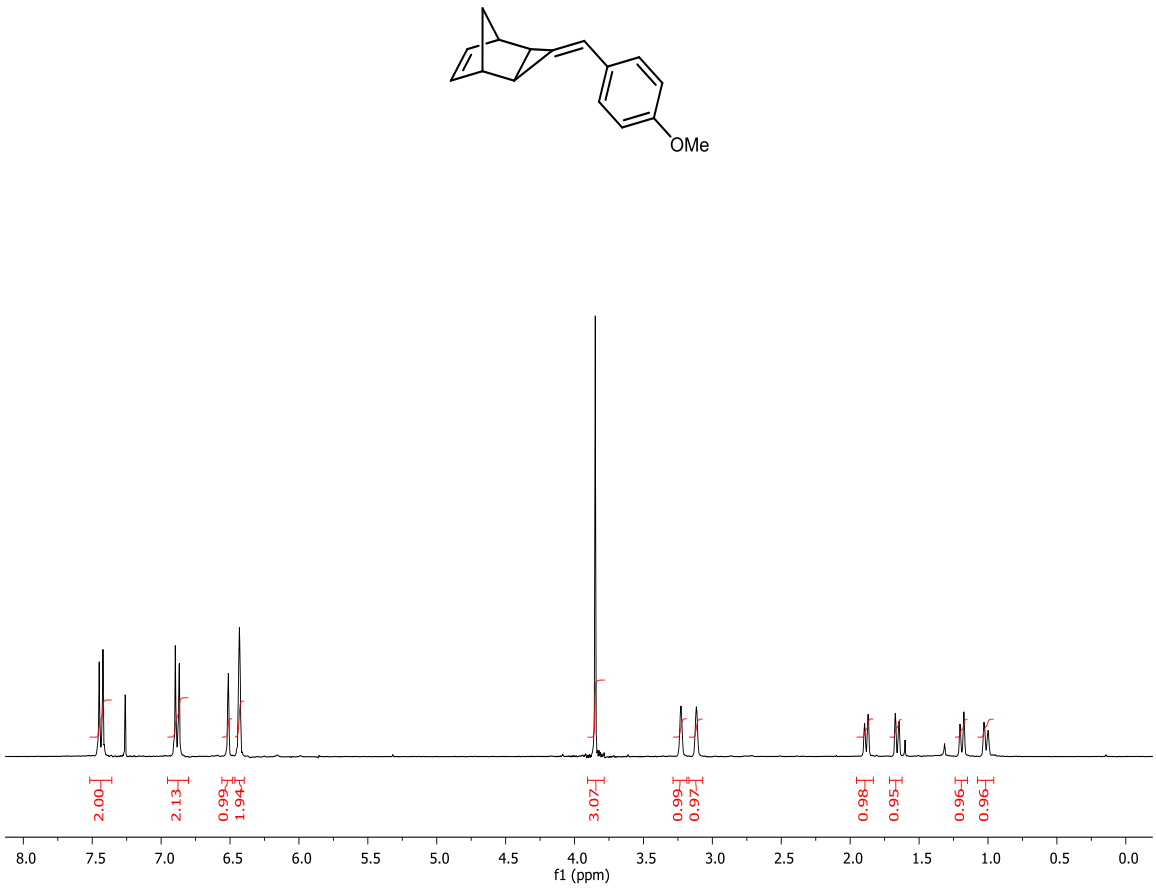

Figure B.80. ^{1}H NMR spectrum for **38** in $CDCl_3$.

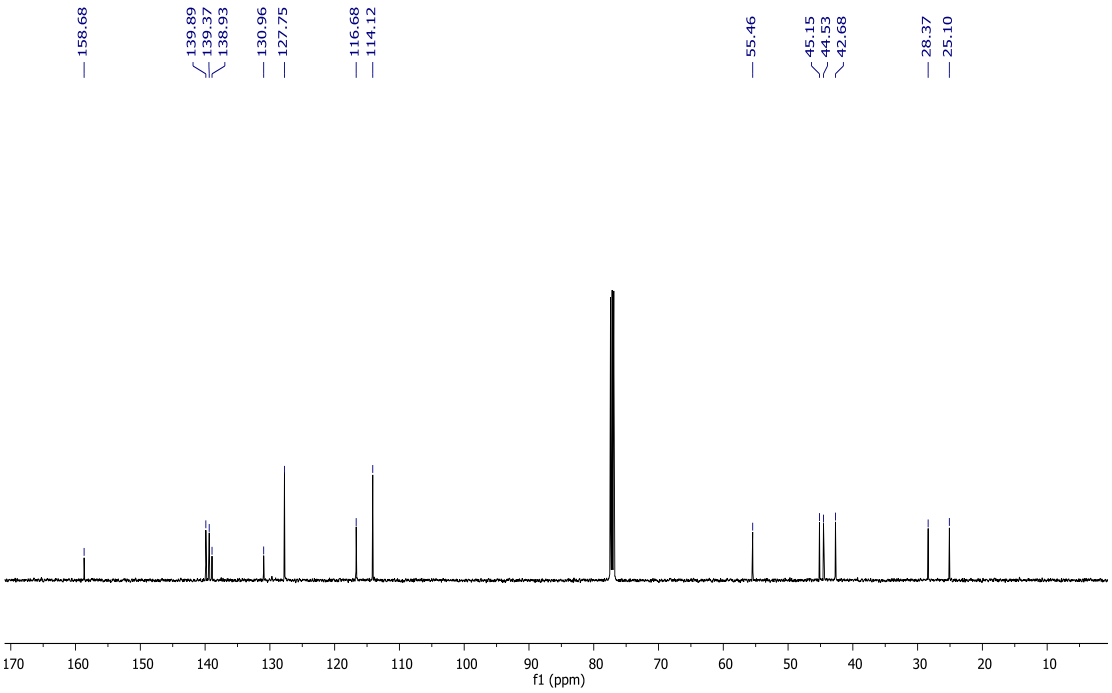

Figure B.81. $^{13}C\{^{1}H\}$ NMR spectrum for **38** in $CDCl_3$.

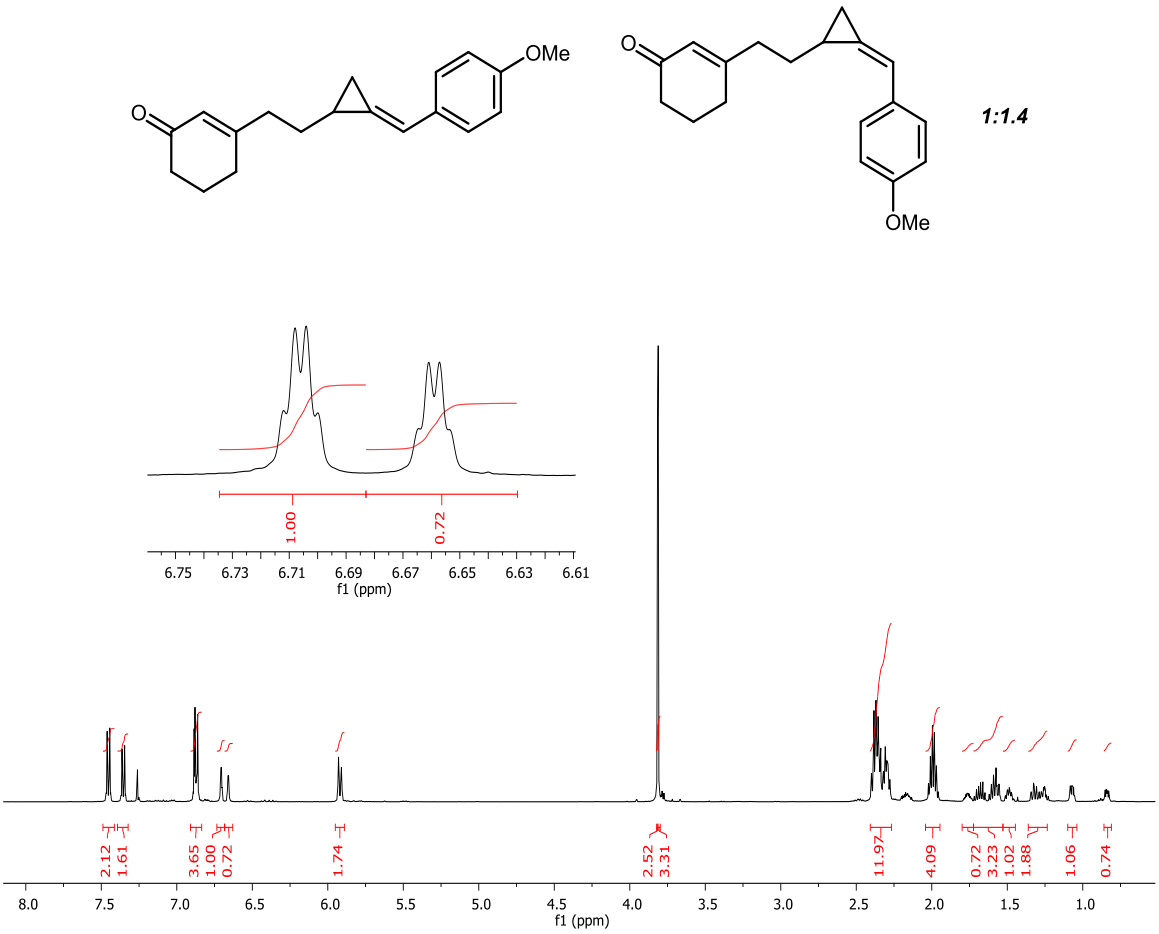

Figure B.82. ^{1}H NMR spectrum for **39** in $CDCl_3$.

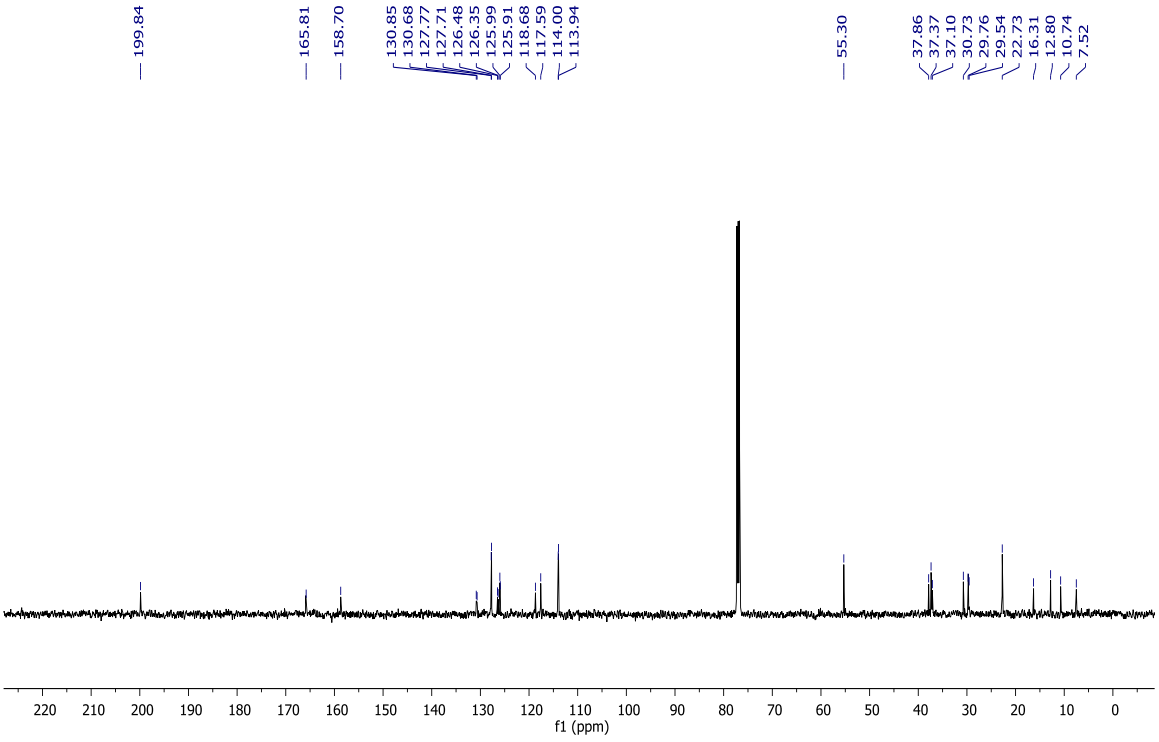

Figure B.83. $^{13}C\{^{1}H\}$ NMR spectrum for **39** in $CDCl_3$.

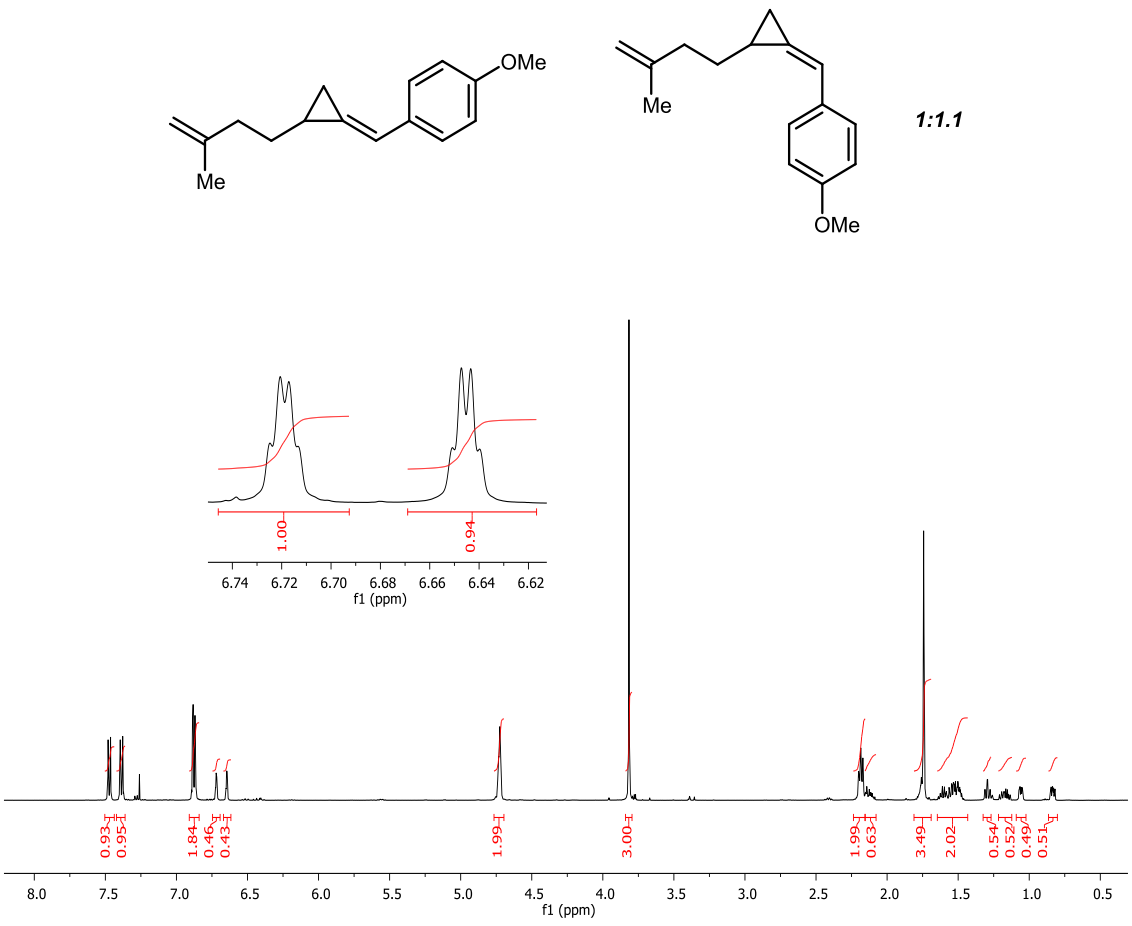

Figure B.84. ^{1}H NMR spectrum for **40** in $CDCl_3$.

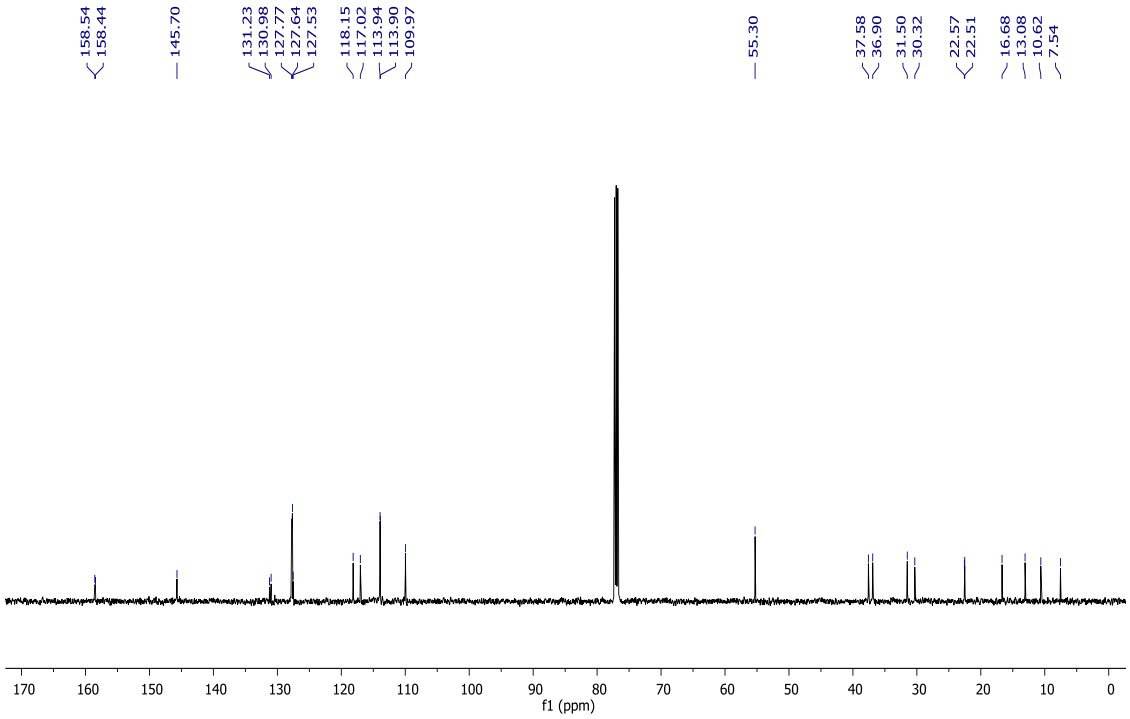

Figure B.85. $^{13}C\{^{1}H\}$ NMR spectrum for **40** in $CDCl_3$.

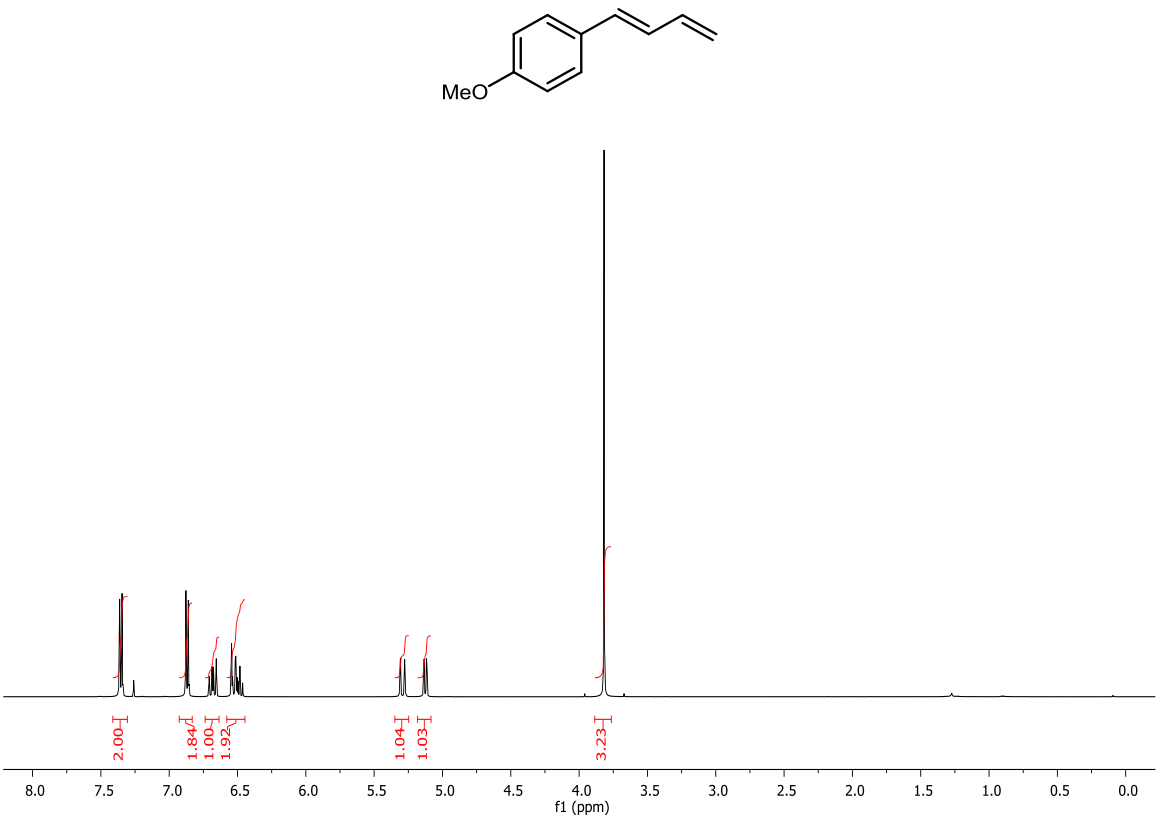

Figure B.86. ^{1}H NMR spectrum for **41** in $CDCl_3$.

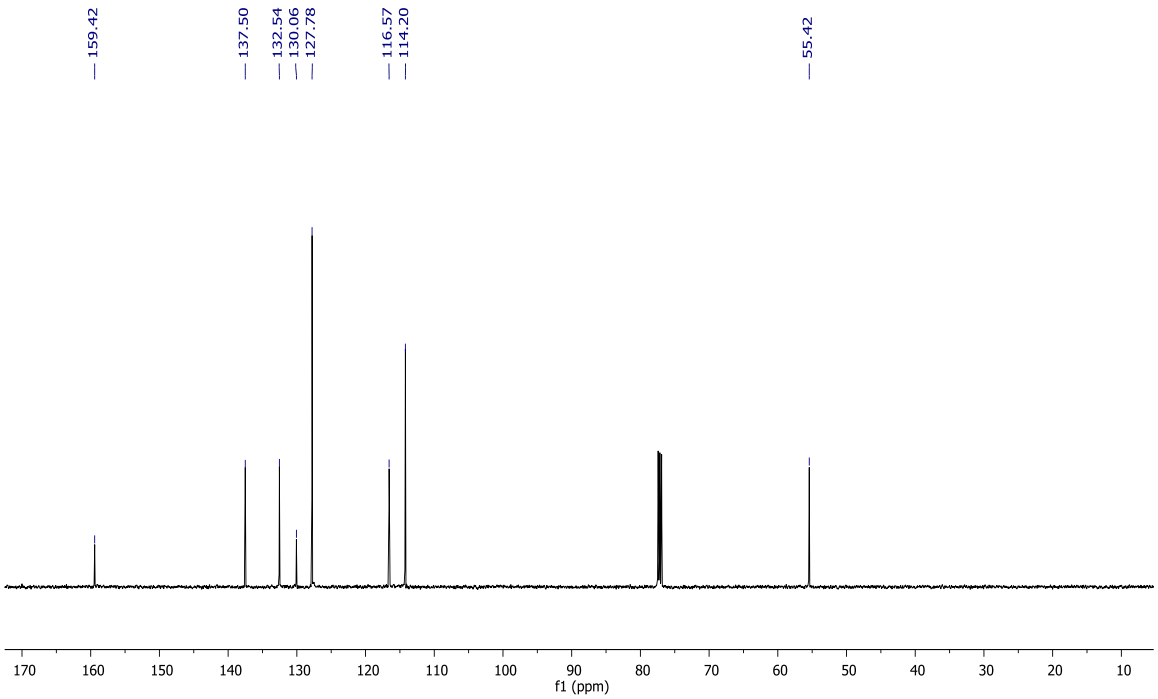

Figure B.87. $^{13}C\{^{1}H\}$ NMR spectrum for **41** in $CDCl_3$.

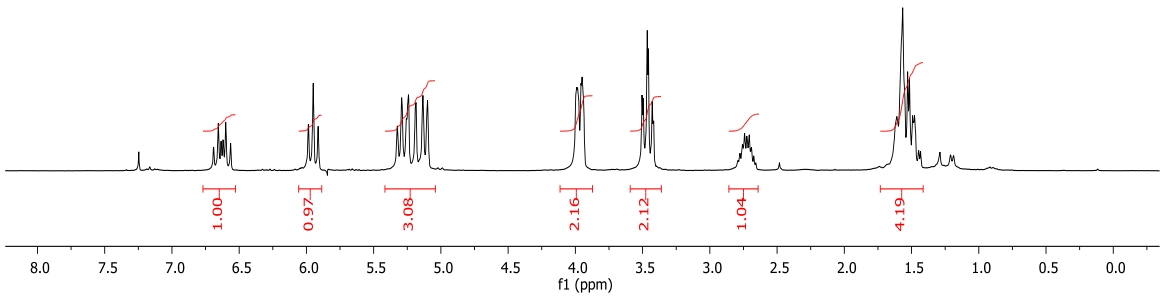

Figure B.88. ^{1}H NMR spectrum for **42** in $CDCl_3$.

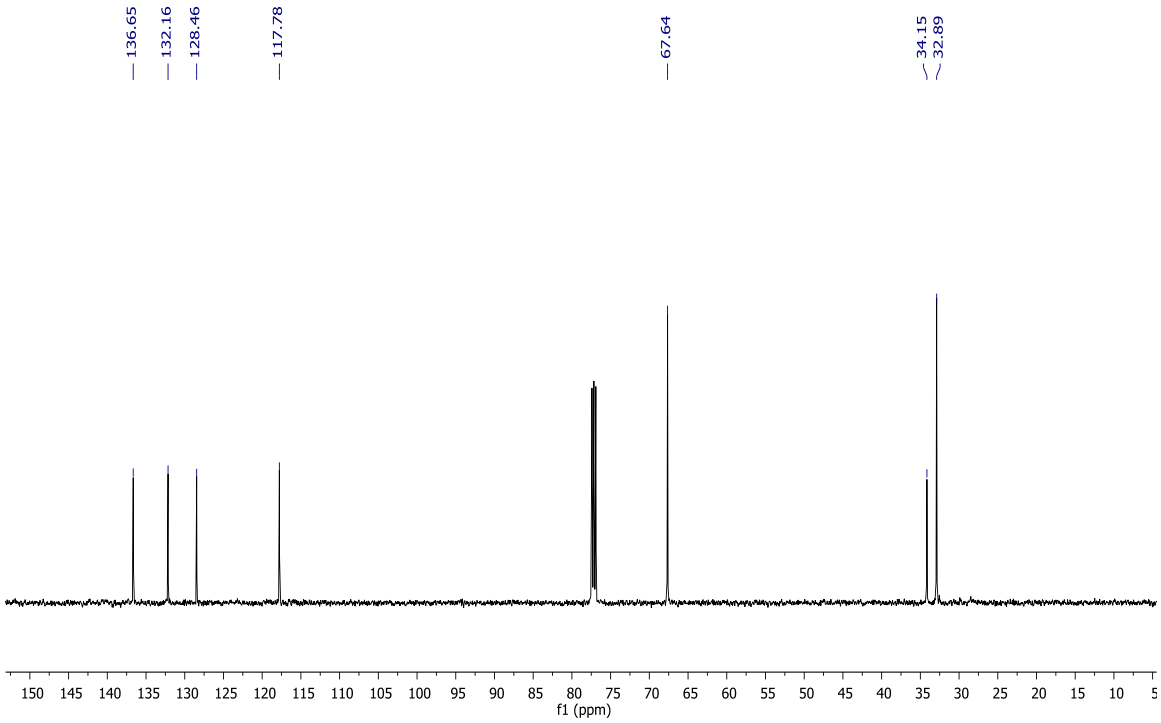

Figure B.89. $^{13}C\{^{1}H\}$ NMR spectrum for **42** in $CDCl_3$.

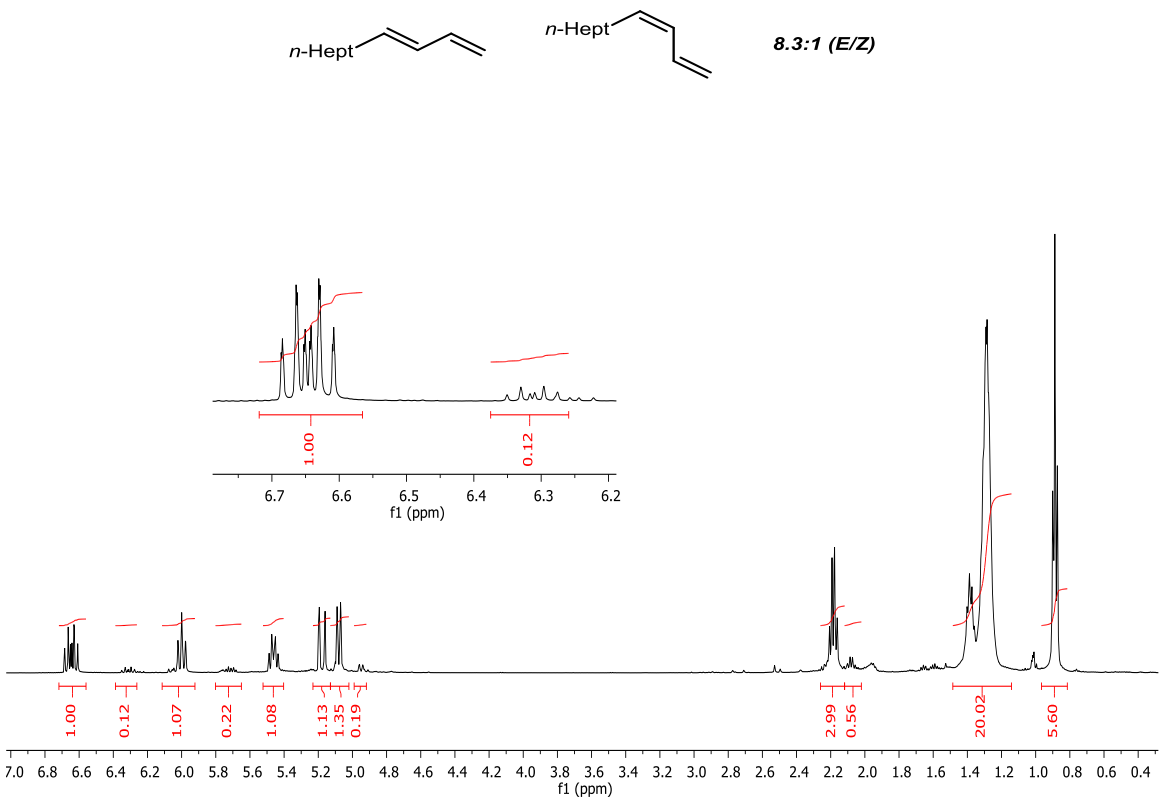

Figure B.90. ^{1}H NMR spectrum for **43** in $CDCl_3$.

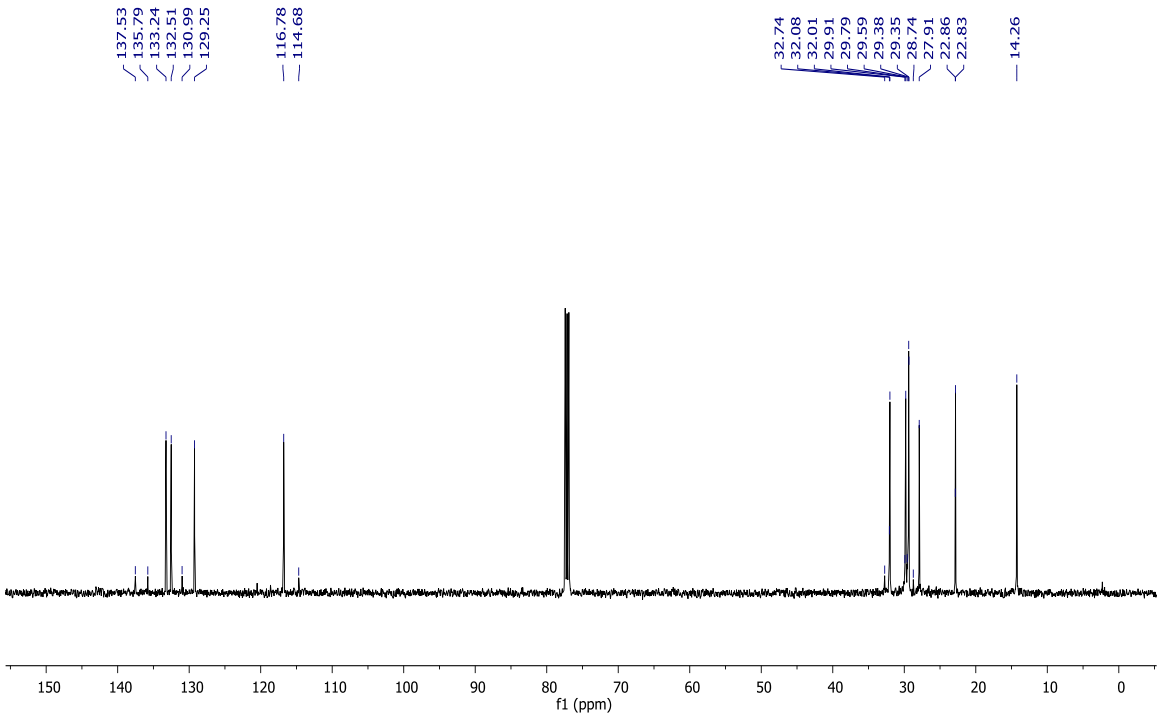

Figure B.91. $^{13}C\{^{1}H\}$ NMR spectrum for **43** in $CDCl_3$.

B.11 DFT Calculations

Computational Methods. Geometry optimizations were performed using the Gaussian09 software package.[xv] All geometries were fully optimized at the BP86/6-311G(d,p) level of DFT. Stationary points were verified by frequency analysis.

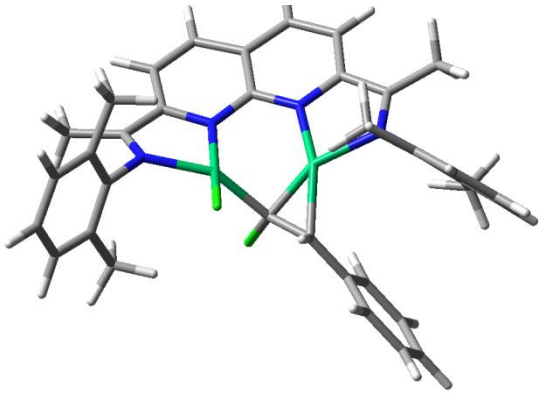

Charge: 0

Multiplicity: 1

Imaginary Frequencies: 0

Energy: –5549.38523891

Free Energy (298 K): –5548.869070

Ni	1.05614100	0.35227600	0.08480000
Ni	-1.49340200	-0.13508200	0.03734600
N	-3.40351600	0.06151500	0.12430700
N	-1.60352100	1.67562300	-0.59481900
N	0.60895000	2.16431700	-0.11530100
N	2.69450000	1.06307300	0.79491400
C	-5.32464600	1.21524500	-0.97896400
H	-5.59692700	0.40503600	-1.67520500
H	-5.53366200	2.17163000	-1.47523600
H	-5.98884000	1.11215700	-0.10592900
C	-3.88078700	1.09812100	-0.57612000

C	-2.89449600	2.10881700	-0.84237700
C	-3.16236000	3.45033800	-1.17840100
H	-4.18364800	3.75109700	-1.41645800
C	-2.14660700	4.39632900	-1.14327700
H	-2.35404600	5.44729900	-1.35872800
C	-0.84074100	4.00617800	-0.75205400
C	-0.61083700	2.60954400	-0.48294500
C	0.25217200	4.89499900	-0.56783200
H	0.10507500	5.96206000	-0.75236300
C	1.47971600	4.41772200	-0.12191600
H	2.31460200	5.10396200	0.03245200
C	1.64590600	3.04003000	0.11919800
C	2.83887200	2.37994200	0.61256900
C	4.08300300	3.15571100	0.94871700
H	3.82815800	4.08567200	1.48062000
H	4.64409300	3.43649600	0.04084300
H	4.75021200	2.56038800	1.58686400
C	-4.31519500	-0.98305000	0.49807200
C	-4.61526300	-2.03327700	-0.39914400
C	-5.53578100	-3.00909700	0.01482000
H	-5.77270800	-3.83254300	-0.66530200
C	-6.13379900	-2.95063400	1.27802200
H	-6.84603700	-3.72209900	1.58212400
C	-5.80148700	-1.91714800	2.15939300
H	-6.24686100	-1.88293000	3.15805700
C	-4.88400500	-0.92107400	1.79047600
C	3.74444700	0.24087300	1.29898400
C	4.93844200	0.00709900	0.57311000
C	5.90159700	-0.84749500	1.13910600
H	6.82067400	-1.04609000	0.57973400
C	5.69821600	-1.45014400	2.38161700

H	6.46196000	-2.10866000	2.80328600
C	4.49991500	-1.23124100	3.07250000
H	4.32535400	-1.71944600	4.03568300
C	3.50176800	-0.40369600	2.54261200
C	0.03379700	-0.74580800	-0.92570800
C	1.10575600	-1.56800300	-0.43729200
H	0.84500500	-2.14621900	0.45751300
C	2.18665400	-2.18823400	-1.23467100
C	2.72010400	-3.42050900	-0.79245800
H	2.30463500	-3.88105100	0.10855300
C	3.75170300	-4.06042200	-1.48562300
H	4.13866100	-5.01559400	-1.11962900
C	4.28642700	-3.48255800	-2.64481500
H	5.08913700	-3.98251100	-3.19342800
C	3.77970200	-2.25390600	-3.09260200
H	4.19019700	-1.78962500	-3.99408700
C	2.75222200	-1.61141700	-2.39469400
H	2.37732600	-0.65195500	-2.75649900
C	-4.48229000	0.17177000	2.75119000
H	-4.91903000	-0.00254400	3.74540300
H	-3.38483500	0.20641100	2.84970300
H	-4.80608600	1.17001400	2.40853300
C	-3.90780300	-2.15107900	-1.72738500
H	-3.92853500	-1.21409900	-2.30726600
H	-2.84393800	-2.40101200	-1.57551900
H	-4.35855700	-2.94381700	-2.34215200
C	5.18713600	0.60367200	-0.79359900
H	5.82547200	1.50338300	-0.73603900
H	5.70370400	-0.12550800	-1.43504700
H	4.25086500	0.88338700	-1.29612700
C	2.18730100	-0.21282000	3.25796200

H	1.98025300	0.84918200	3.46779400
H	1.34926800	-0.57762800	2.63623800
H	2.17297400	-0.76468100	4.20902900
Cl	-1.47918100	-1.88946300	1.32432500
Cl	-0.33129100	-0.56947600	-2.68079700

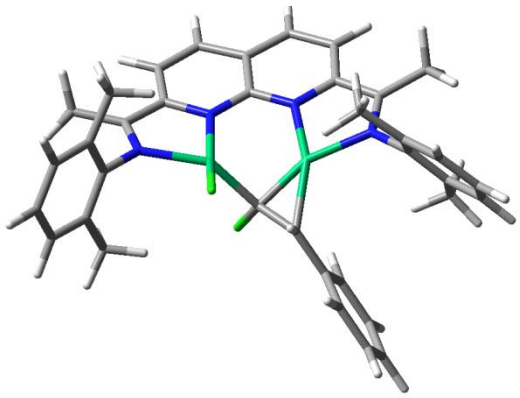

Charge: 0

Multiplicity: 3

Imaginary Frequencies: 0

Energy: –5549.37694191

Free Energy (298 K): –5548.864586

Ni	1.15597500	0.32047700	0.07374800
Ni	-1.47664500	-0.10513400	0.16943200
N	-3.45190400	0.07731600	0.06324100
N	-1.55388600	1.71559000	-0.47762100
N	0.70542800	2.13174400	-0.15305800
N	2.84878700	1.05468000	0.68816600
C	-5.31568400	1.52205100	-0.77086400
H	-5.93589800	0.62164500	-0.67446000
H	-5.44568000	1.93417600	-1.78367800
H	-5.69467500	2.27346500	-0.05693900
C	-3.86751600	1.20234700	-0.50433500
C	-2.81957300	2.14681700	-0.82696500
C	-3.03104800	3.43886200	-1.34631200
H	-4.03859600	3.74398500	-1.63449900
C	-1.97311800	4.33115100	-1.45345700
H	-2.12839000	5.34119500	-1.84013400
C	-0.67578800	3.93792900	-1.02760800

C	-0.50909100	2.58350200	-0.56265800
C	0.46314700	4.78339100	-1.02408300
H	0.36460100	5.81035500	-1.38429600
C	1.68599500	4.31068700	-0.55441300
H	2.56111000	4.96310800	-0.53593400
C	1.79325400	2.97994200	-0.11749000
C	2.98440300	2.34976600	0.43346500
C	4.21874300	3.15456500	0.73673200
H	3.97263300	4.01245900	1.38344900
H	4.66519100	3.56002900	-0.18707900
H	4.97205900	2.53846200	1.24482800
C	-4.39413600	-0.89890800	0.51852100
C	-4.73387400	-1.98180000	-0.32421700
C	-5.64633800	-2.93351900	0.15844000
H	-5.91759400	-3.77660900	-0.48391500
C	-6.19379500	-2.82501000	1.44089400
H	-6.89577200	-3.58101100	1.80224000
C	-5.82347500	-1.75964000	2.26771500
H	-6.22961400	-1.68503800	3.28086100
C	-4.91961000	-0.78137000	1.82596900
C	3.86782700	0.28144400	1.32346900
C	5.02186800	-0.12667500	0.61182800
C	5.96931500	-0.91574300	1.28540100
H	6.86090100	-1.24449100	0.74347000
C	5.78250100	-1.29287700	2.61844600
H	6.53275300	-1.90529300	3.12502400
C	4.62137100	-0.90359900	3.29487100
H	4.46124600	-1.21331100	4.33177800
C	3.64081300	-0.12462500	2.66219600
C	-0.01536100	-0.74944300	-0.85254700
C	1.03601400	-1.62403300	-0.46063600

H	0.85570400	-2.09254400	0.51716300
C	1.97868300	-2.38464400	-1.30825800
C	2.42730200	-3.64081900	-0.84037200
H	2.05282400	-4.01057900	0.11859900
C	3.32315700	-4.41687700	-1.58170500
H	3.64522400	-5.38801800	-1.19570100
C	3.80566700	-3.95389500	-2.81307800
H	4.50372800	-4.55942700	-3.39707400
C	3.38576400	-2.70248700	-3.28573400
H	3.76094600	-2.32503400	-4.24129000
C	2.49110300	-1.92525600	-2.54315200
H	2.18202500	-0.95112600	-2.92654400
C	-4.48378400	0.34722800	2.72937300
H	-4.83026600	0.17859400	3.75933400
H	-3.38465200	0.42606700	2.74003700
H	-4.87960500	1.32341300	2.39764000
C	-4.11012200	-2.12018500	-1.69168600
H	-4.34593500	-1.26365500	-2.34593500
H	-3.01093900	-2.16730900	-1.61962600
H	-4.46187600	-3.03513700	-2.19007100
C	5.20743100	0.22373400	-0.84575300
H	5.42341200	1.29510600	-0.99959200
H	6.04339400	-0.34708000	-1.27487000
H	4.30095200	-0.01724600	-1.42358200
C	2.35936000	0.24266200	3.37245700
H	2.13160500	1.31710600	3.29166700
H	1.49789400	-0.29690100	2.93853300
H	2.41344400	-0.02170600	4.43867000
Cl	-1.44627700	-1.75351700	1.60277400
Cl	-0.44612300	-0.54004700	-2.59329900

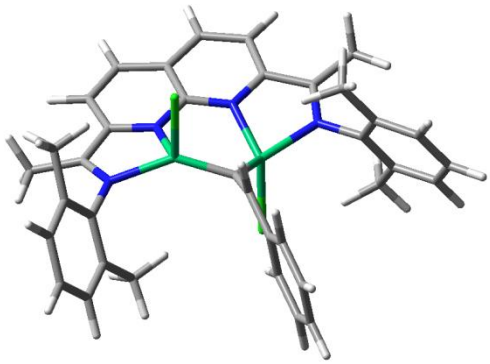

Charge: 0

Multiplicity: 3

Imaginary Frequencies: 0

Energy: –5549.36035636

Free Energy (298 K): –5548.852311

Ni	1.23961100	0.39284100	-0.42135500
Ni	-1.35184700	0.30462600	0.45924100
N	-3.19703100	0.50942900	-0.16983700
N	-1.28240700	2.15550900	-0.18276100
N	1.00802400	2.29584200	-0.04334000
N	3.07524700	0.87118200	0.03851100
C	-4.98628000	2.13051700	-0.84893700
H	-5.62049800	1.24094800	-0.96051600
H	-4.99301800	2.68820300	-1.79952100
H	-5.43854800	2.78145500	-0.08129300
C	-3.58497600	1.73922100	-0.46752800
C	-2.50556100	2.71504900	-0.42783800
C	-2.64609000	4.11235500	-0.59193400
H	-3.63238900	4.53623400	-0.78963500
C	-1.53990400	4.93971500	-0.45759500
H	-1.64213100	6.02475900	-0.53958200
C	-0.25887900	4.37428700	-0.21640200

C	-0.17939500	2.94238900	-0.14441800
C	0.95020300	5.10086800	-0.04223600
H	0.92741000	6.19332500	-0.06328800
C	2.14528500	4.42163300	0.15431900
H	3.07717500	4.97092400	0.30091000
C	2.16225100	3.00898500	0.12082600
C	3.33560700	2.15782900	0.22545200
C	4.69518300	2.71885900	0.54147800
H	4.67577500	3.29246700	1.48284500
H	5.03207800	3.40425300	-0.25469100
H	5.43502300	1.91369400	0.63922600
C	-4.09071600	-0.60609700	-0.19042800
C	-3.98290200	-1.51117900	-1.27650700
C	-4.82176600	-2.63643200	-1.28216000
H	-4.74978700	-3.34266500	-2.11423800
C	-5.72824100	-2.86741900	-0.24262600
H	-6.36594900	-3.75502700	-0.25954000
C	-5.80426800	-1.97092300	0.82817700
H	-6.49897900	-2.15980200	1.65185000
C	-4.99167700	-0.82648200	0.88096100
C	4.08223500	-0.13302700	0.19561500
C	4.90121000	-0.49108700	-0.90266700
C	5.84042300	-1.51734100	-0.71173700
H	6.47756400	-1.80925500	-1.55159500
C	5.96501800	-2.16723300	0.52062700
H	6.69658100	-2.96989700	0.64428000
C	5.14545100	-1.79595600	1.59113500
H	5.23645800	-2.30598400	2.55452700
C	4.19111300	-0.77557800	1.45368200
C	0.10873300	-0.77876200	0.40526100
C	0.07843700	-2.00502000	0.97949000

H	-0.14918700	-1.96342300	2.05794800
C	0.29874700	-3.33722800	0.42337400
C	0.27486300	-4.44860600	1.29950200
H	0.10018400	-4.28192700	2.36653400
C	0.47347900	-5.74462400	0.81711800
H	0.45320800	-6.59055100	1.50956200
C	0.69573600	-5.95888500	-0.55036100
H	0.84994300	-6.97239900	-0.92999000
C	0.71476300	-4.86427000	-1.42965300
H	0.88590100	-5.02467100	-2.49760200
C	0.51480300	-3.56647800	-0.95682300
H	0.53019600	-2.71933200	-1.64743500
C	-5.05549900	0.11441200	2.06110000
H	-5.64595700	-0.33131400	2.87494300
H	-4.04798800	0.34190300	2.44685700
H	-5.53258300	1.07485100	1.79729300
C	-2.99947100	-1.26428600	-2.39510100
H	-3.30986000	-0.41765100	-3.03190500
H	-1.99962800	-1.00997500	-2.00761400
H	-2.90528200	-2.15150900	-3.03689800
C	4.76387800	0.20165400	-2.23688000
H	5.01610800	1.27434000	-2.17005700
H	5.43576400	-0.25338700	-2.97911300
H	3.72978300	0.13293400	-2.61375900
C	3.30933000	-0.36595100	2.60928200
H	3.62362400	0.60288200	3.03619700
H	2.26209200	-0.24725900	2.29038800
H	3.34825300	-1.11244500	3.41540100
Cl	-1.36706700	0.50801900	2.70030700
Cl	1.12163900	-0.37137100	-2.50694100

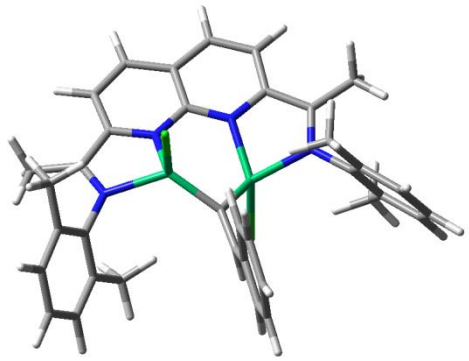

Charge: 0

Multiplicity: 5

Imaginary Frequencies: 0

Energy: –5549.34323365

Free Energy (298 K): –5548.839546

Ni	-1.26035900	-0.32146100	-0.53475200
Ni	1.26214900	-0.47829600	0.61518400
N	3.14545800	-0.62530200	-0.02055800
N	1.18225300	-2.20648700	-0.29827400
N	-1.09317500	-2.24935600	-0.21238000
N	-3.08512300	-0.71782500	0.17435300
C	4.90250200	-2.20961200	-0.83719400
H	5.55837800	-1.32919400	-0.84443700
H	4.92384000	-2.67523700	-1.83529800
H	5.31698200	-2.94187600	-0.12334400
C	3.49687200	-1.82964000	-0.45631000
C	2.40331200	-2.77740700	-0.56221600
C	2.48855700	-4.14724600	-0.87988400
H	3.46070600	-4.59404600	-1.09794800
C	1.33754300	-4.93755500	-0.88946000
H	1.40375300	-6.00572700	-1.10993800

C	0.06780700	-4.35538600	-0.62126700
C	0.05252300	-2.93931400	-0.38071000
C	-1.18768300	-5.01993400	-0.56211200
H	-1.23125200	-6.10111700	-0.71463000
C	-2.35311300	-4.30018300	-0.28899900
H	-3.31169800	-4.81802300	-0.21652000
C	-2.29681900	-2.90276700	-0.12463200
C	-3.40107700	-2.00546400	0.17122800
C	-4.77308700	-2.53748300	0.48728300
H	-4.72636700	-3.27205500	1.30734800
H	-5.20229900	-3.05079800	-0.38969500
H	-5.45147900	-1.72585800	0.78044000
C	4.06201000	0.46336800	0.07699200
C	4.03566500	1.44061200	-0.95030700
C	4.89571700	2.54351000	-0.83795900
H	4.88197900	3.30565700	-1.62227600
C	5.75387800	2.67904900	0.25826900
H	6.41209100	3.54846000	0.33391700
C	5.76051000	1.70718800	1.26405300
H	6.42435500	1.81736200	2.12654000
C	4.91935200	0.58409200	1.19936800
C	-3.99294100	0.30718200	0.57685400
C	-4.94161600	0.83445600	-0.33610000
C	-5.76407800	1.88376000	0.10685000
H	-6.49805000	2.30345100	-0.58717600
C	-5.65340600	2.39790700	1.40234000
H	-6.29884100	3.22040800	1.72133500
C	-4.71038000	1.86352400	2.28638600
H	-4.61972300	2.26386400	3.30032900
C	-3.86466000	0.81397500	1.89593500
C	-0.02463500	0.81299800	0.24185900

C	0.05859500	2.09780600	0.64446900
H	0.24707400	2.20395900	1.72613400
C	-0.05311000	3.34708900	-0.10642800
C	0.01358700	4.57165300	0.59888200
H	0.13542000	4.55561900	1.68582700
C	-0.07877700	5.79104500	-0.07654700
H	-0.02776100	6.72757700	0.48524000
C	-0.23560200	5.81296500	-1.46953900
H	-0.30816000	6.76638900	-1.99931900
C	-0.29879600	4.60363200	-2.18009000
H	-0.42431100	4.61304800	-3.26607200
C	-0.20407200	3.38109800	-1.51334100
H	-0.26388200	2.44433200	-2.07217000
C	4.91739800	-0.44619500	2.30284400
H	5.54089700	-0.10991400	3.14393600
H	3.89594600	-0.62485100	2.67759200
H	5.31677400	-1.41700800	1.96117700
C	3.10878100	1.28653600	-2.13088400
H	3.41424500	0.44941000	-2.78226500
H	2.08007900	1.06738200	-1.80225000
H	3.09211000	2.20128200	-2.73984300
C	-5.06393100	0.30479900	-1.74397300
H	-5.35870000	-0.75831300	-1.76133100
H	-5.82452200	0.87010700	-2.30204000
H	-4.10602200	0.37970700	-2.28539400
C	-2.85596700	0.22736400	2.85337500
H	-3.14623200	-0.78818800	3.17475800
H	-1.86010200	0.13617700	2.39203000
H	-2.76371300	0.84855300	3.75563800
Cl	1.24852800	-0.36769600	2.82988100
Cl	-1.53692100	0.21421900	-2.67038600

B.12 References

(1) Zhou, Y.-Y.; Hartline, D. R.; Steiman, T. J.; Fanwick, P. E.; Uyeda, C. *Inorg. Chem.* **2014**, *53*, 11770–11777.

(2) Rigaku Corp., The Woodlands, Texas, USA.

(3) Otwinowski, Z.; Minor, W. *Methods Enzymol.* **1997**, *276*, 307–326.

(4) Bruker (2016). Apex3 v2016.9-0, Saint V8.34A, SAINT V8.37A, Bruker AXS Inc.: Madison (WI), USA, 2013/2014.

(5) (a) SHELXTL suite of programs, Version 6.14, 2000-2003, Bruker Advanced X-ray Solutions, Bruker AXS Inc., Madison, Wisconsin: USA; (b) Sheldrick, G. M. *Acta Crystallogr A.* **2008**, *64*, 112–122.

(6) (a) Sheldrick, G. M. University of Göttingen, Germany, **2016**; (b) Sheldrick, G. M. *Acta Crystallogr Sect C Struct Chem.* **2015**, *71*, 3–8.

(7) Hübschle, C. B.; Sheldrick, G. M.; Dittrich, B. *J. Appl. Crystallogr.* **2011**, *44*, 1281–1284.

(8) Synthesis was conducted according to a previously reported procedure: Burton, G.; Elder, J. S.; Fell, S. C. M.; Stachulski, A. V. *Tetrahedron Lett.* **1988,** *29*, 3003–3006.

(9) Synthesis was conducted according to a previously reported procedure: Rabinowitz, R.; Marcus, R. *J. Am. Chem. Soc.* **1962**, *84*, 1312.

(10) Ikeda, H.; Nomura, T.; Akiyama, K.; Oshima, M.; Roth, H. D.; Tero-Kubota, S.; Miyashi, T. *J. Am. Chem. Soc.* **2005**, *127*, 14497–1085.

(11) Mao, J.; Bao, W. *Org. Lett*. **2014**, *16*, 2646–2649.

(12) Gatineau, D.; Moraleda, D.; Naubron, J.–V.; Bürgi, T.; Giordano, L.; Buono, G. *Tetrahedron: Asymmetry*. **2009**, *20*, 1912–1917.

(13) Shi, M.; Wang, Bao–Yu.; Huang, J.–W. *J. Org. Chem*. **2005**, *70*, 5606–5610.

(14) Chen, T–Y.; Tsutsumi, R.; Montgomery, T. P.; Volchkov, I.; Krische, M. J. *J. Am. Chem. Soc*. **2015**, *137*, 1798–1801.

(15) Soengas, R. G.; Rodríguez-Solla, H.; Díaz-Pardo, A.; Acúrcio, R.; Concellón, C.; del Amo, V.; Silva, A. M. S. *Eur. J. Org. Chem.* **2015**, 2524–2530.

(16) (a) Witt, O.; Mauser, H.; Friedl, T.; Wilhelm, D.; Clark, T. *J. Org. Chem.* **1998**, *63*, 959–967. (b) Ikeda, H.; Nomura, T.; Akiyama, K.; Oshima, M.; Roth, H. D.; Tero-Kubota, S.; Miyashi, T. *J. Am. Chem. Soc.* **2005**, *127*, 14497–14504.

(17) Gaussian 09, Revision **D.01**, Frisch, M. J.; Trucks, G. W.; Schlegel, H. B.; Scuseria, G. E.; Robb, M. A.; Cheeseman, J. R.; Scalmani, G.; Barone, V.; Mennucci, B.; Petersson, G. A.; Nakatsuji, H.; Caricato, M.; Li, X.; Hratchian, H. P.; Izmaylov, A. F.; Bloino, J.; Zheng, G.; Sonnenberg, J. L.; Hada, M.; Ehara, M.; Toyota, K.; Fukuda, R.; Hasegawa, J.; Ishida, M.; Nakajima, T.; Honda, Y.; Kitao, O.; Nakai, H.; Vreven, T.; Montgomery, J. A., Jr.; Peralta, J. E.; Ogliaro, F.; Bearpark, M.; Heyd, J. J.; Brothers, E.; Kudin, K. N.; Staroverov, V. N.; Kobayashi, R.; Normand, J.; Raghavachari, K.; Rendell, A.; Burant, J. C.; Iyengar, S. S.; Tomasi, J.; Cossi, M.; Rega, N.; Millam, N. J.; Klene, M.; Knox, J. E.; Cross, J. B.; Bakken, V.; Adamo, C.; Jaramillo, J.; Gomperts, R.; Stratmann, R. E.; Yazyev, O.; Austin, A. J.; Cammi, R.; Pomelli, C.; Ochterski, J. W.; Martin, R. L.; Morokuma, K.; Zakrzewski, V. G.; Voth, G. A.; Salvador, P.; Dannenberg, J. J.; Dapprich, S.; Daniels, A. D.; Farkas, Ö.; Foresman, J. B.; Ortiz, J. V.; Cioslowski, J.; Fox, D. J. Gaussian, Inc., Wallingford CT, 2009.

VITA

Sudipta was born and raised in Srirampore, West Bengal, in the north-eastern part of India. She received her bachelor's degree in Chemistry with first class from Raja Peary Mohan College Uttarpara under the Calcutta University in 2010. Later on, she moved to Bombay to pursue her master's degree in Chemistry. Sudipta received her M.Sc. degree in Chemistry from the Indian Institute of Technology Bombay (IIT) in 2012, where she conducted research with Professor I. N. N. Namboothiri. During her master's, she worked on a variety of different methodology projects including the applications of Morita-Baylis-Hillman (MBH) adducts to explore the scope of [3,3]-Sigmatropic Rearrangement with trimethyl orthoacetate. After completion of her master's study, Sudipta worked with Professor K. P. Kaliappan in IIT Bombay as a Research Assistant for 7 months where she worked on the synthesis of the natural product 'Dolabriferol'. In 2013 Sudipta came to the United States to pursue her PhD and joined Professor Christopher Uyeda's research group at Purdue University in the same year. In Professor Chris Uyeda's lab, she worked on a variety of different dinuclear Nickel catalyzed cycloaddition reactions including alkyne cyclotrimerizations and reductive vinylidene transfer reactions. Sudipta graduated from Purdue in August 2018 and accepted a medicinal chemist position in a pharmaceutical company in New Jersey.

PUBLICATIONS

JACS
JOURNAL OF THE AMERICAN CHEMICAL SOCIETY
Communication
pubs.acs.org/JACS

Evaluating the Effect of Catalyst Nuclearity in Ni-Catalyzed Alkyne Cyclotrimerizations

Sudipta Pal and Christopher Uyeda*

Department of Chemistry, Purdue University, West Lafayette, Indiana 47907, United States

Supporting Information

ABSTRACT: An evaluation of catalyst nuclearity effects in Ni-catalyzed alkyne oligomerization reactions is presented. A dinuclear complex, featuring a Ni–Ni bond supported by a naphthyridine–diimine (NDI) ligand, promotes rapid and selective cyclotrimerization to form 1,2,4-substituted arene products. Mononickel congeners bearing related N-donor chelates (2-iminopyridines, 2,2′-bipyridines, or 1,4,-diazadienes) are significantly less active and yield complex product mixtures. Stoichiometric reactions of the dinickel catalyst with hindered silyl acetylenes enable characterization of the alkyne complex and the metallacycle that are implicated as catalytic intermediates. Based on these experiments and supporting DFT calculations, the role of the dinuclear active site in promoting regioselective alkyne coupling is discussed. Together, these results demonstrate the utility of exploring nuclearity as a parameter for catalyst optimization.

Transition-metal catalysts containing polynuclear active sites are underdeveloped alternatives to mononuclear catalysts for organic transformations.[1] Polynuclear complexes have the potential to exhibit unique catalytic properties by binding substrates and delocalizing redox activity across multiple metals. Platforms featuring direct metal–metal bonds are particularly well-suited to capitalize on these cooperative processes due to the enforced proximity of the metals and the strong electronic coupling between them. Consequently, ligands that support reactive metal–metal bonds have emerged as synthetic targets. The resulting complexes have been demonstrated to engage organic and small inorganic molecules in well-defined stoichiometric reactions.[2] Despite these advances, the cooperativity effects attributed to metal–metal bonds have rarely been evaluated in a catalytic process.[3] Such studies would complement those characterizing dinuclear effects in catalyst systems where direct metal–metal interactions either are not relevant[4] or are formed transiently.[5]

Dinuclear complexes of naphthyridine–diimine (NDI) ligands are versatile platforms to study stoichiometric and catalytic redox processes at discrete metal–metal bonds.[6] The [$^{i\text{-Pr}}$NDI]Ni$_2$(C$_6$H$_6$) complex (**1**) is an analog of known mononickel complexes bearing N-donor chelates (e.g., 2-iminopyridines, 2,2′-bipyridines, and 1,4-diazadienes), providing an opportunity to probe nuclearity effects within a family of related catalysts (Scheme 1). Here, we report a comparative study of mono- and dinickel catalysts in the oligomerization of terminal alkynes. Whereas mononuclear [N,N]Ni catalysts **2**–**4** uniformly yield complex product mixtures, the dinuclear catalyst **1** promotes rapid and selective cyclotrimerizations to form 1,2,4-trisubstituted arenes (Figure 1). Stoichiometric reactivity studies, combined with DFT calculations, provide insight into this nuclearity effect.

Scheme 1. Mononuclear and Dinuclear Ni Complexes of Chelating N-Donor Ligands

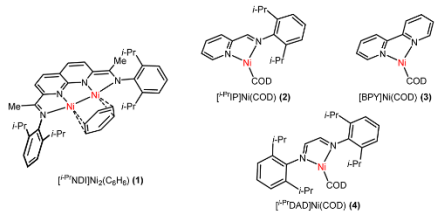

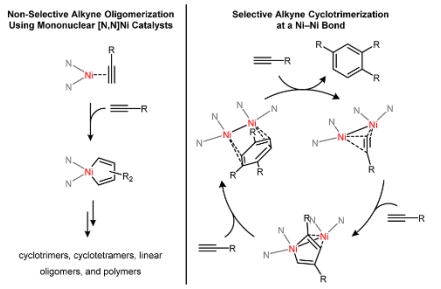

Figure 1. Mononuclear and dinuclear pathways for alkyne oligomerizations using Ni catalysts.

Catalyst Comparison Studies. Transition-metal-catalyzed cycloadditions are direct and efficient routes to cyclic organic molecules;[7] however, complex selectivity considerations must be addressed in order to obtain high yields of a single product. Among the catalysts that have been surveyed in alkyne oligomerization reactions, the low-valent Ni catalysts initially reported by Reppe are unusual in the breadth of accessible

Received: May 13, 2015
Published: June 11, 2015

DOI: 10.1021/jacs.5b04990
J. Am. Chem. Soc. 2015, 137, 8042–8045

products.[8] Simple Ni(0) sources such as $Ni(COD)_2$,[9] activated Ni metal,[10] and combinations of divalent Ni halide salts and reductants[11] convert terminal alkynes to mixtures of cyclic (arene and cyclooctatetraene regioisomers) and acyclic (oligomers and polymers) products. Supporting ligands have been effectively utilized to improve the selectivity of these reactions.[12] For example, phosphine-ligated complexes generally yield benzene derivatives,[12a−g] whereas 1,4-diazadiene complexes favor cyclooctatetraenes.[12h−j]

In order to assess the viability of using catalyst nuclearity to control selectivity in these reactions, terminal alkyne substrates with diverse electronic properties were selected for comparison studies (Figure 2). For ethyl propiolate, all examined

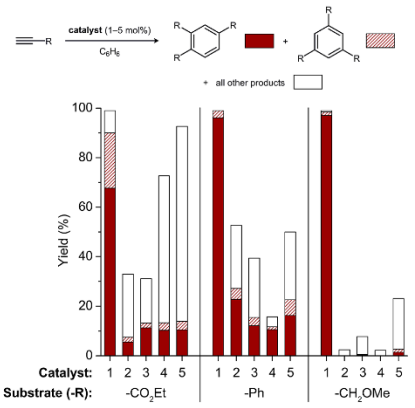

Figure 2. A comparison of catalytic activity for the cyclotrimerization of ethyl propiolate, phenylacetylene, and methyl propargyl ether. Data for catalysts **1**−**4** and $Ni(COD)_2$ (**5**) are shown. Reaction conditions for ethyl propiolate and methyl propargyl ether: 22 °C, 11 min, 1 mol % catalyst. Reaction conditions for phenylacetylene: 60 °C, 40 min, 5 mol % catalyst. Yields and conversions were averaged over two runs and determined by GC-FID analysis. The total heights of the bars are the total conversion of starting material. The product fraction corresponding to the 1,2,4-isomer (solid red), 1,3,5-isomer (dashed red), and all other products (white) are plotted.

mononuclear and dinuclear catalysts (Scheme 1) were active, with **1** affording the highest conversion of substrate under a standardized set of conditions. Consistent with previous reports,[12j] [$^{i\text{-Pr}}$IP]Ni(COD) (**2**), [BPY]Ni(COD) (**3**), [$^{i\text{-Pr}}$DAD]Ni(COD) (**4**), and $Ni(COD)_2$ (**5**) yielded significant amounts of both cyclotrimerized and cyclotetramerized products. Among these four mononickel catalysts, no greater than 14% combined yield of aromatic products was observed, with cyclooctatetraenes being formed in 11−71% yield. By comparison, **1** was selective for cyclotrimerization, affording a 90% combined yield of the 1,2,4- and 1,3,5-regioisomer. No cyclooctatetraene products were detected using **1**.

Similar effects were observed using more electron-rich alkyl- and aryl-substituted terminal alkynes. Phenylacetylene and methyl propargyl ether were poorly reactive using catalysts **2**−**5** and produced a mixture of coupled products. Catalyst **1** effected rapid cyclotrimerization, with nearly exclusive formation of the 1,2,4-regioisomer. Methyl propargyl ether is converted to 1,2,4-tris(methoxymethyl)benzene in 98% GC yield using 1 mol % of **1** in <15 min at room temperature. This rate and selectivity is noteworthy among those observed using the most efficient cyclotrimerization catalysts, including precious metal-based systems.[13]

Substrate Scope for Alkyne Cyclotrimerizations. The high selectivity for cyclotrimerization using **1** is general across a range of terminal alkynes (Figure 3). In all cases, the 1,2,4-

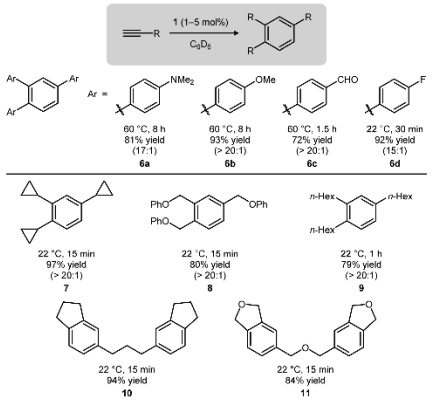

Figure 3. Substrate scope for alkyne cyclotrimerizations catalyzed by **1**. Conditions: 5 mol % catalyst loading for arylacetylenes and 1 mol % for all other substrates. Yields are of isolated products and are averaged over two runs. The ratio of the 1,2,4- to 1,3,5-regioisomer is shown in parentheses.

regioisomer is highly favored, and no competing formation of cyclooctatetraenes is observed.[14] Alkylacetylenes reach full conversion within 1 h at room temperature using 1 mol % of **1** (products **7**−**11**). A higher catalyst loading of 5 mol % was used for arylacetylenes (products **6a**−**d**). To probe electronic effects, a series of para-substituted phenylacetylenes was studied. Substrates bearing electron-withdrawing substituents reacted at a faster rate than substrates bearing electron-donating substituents. Using cyclopropylacetylene, cyclotrimerization occurred without cyclopropane rearrangement through either a radical or organometallic mechanism. Finally, 1,6-heptadiyne and propargyl ether reacted to form the corresponding tethered diarene products (**10** and **11**).

Stoichiometric Alkyne Coupling Reactions. We investigated the origin of the observed dinuclear effect by pursuing the characterization of plausible intermediates. Terminal alkynes bearing bulky silyl substituents, such as $-SiMe_3$ and $-SiMe_2Ph$, react with **1** but do not generate the cyclized product (Scheme 2). The reaction between **1** and dimethylphenylsilylacetylene (2.0 equiv or greater) in C_6D_6 is complete in 3 h at room temperature, producing the head-to-tail coupled product **12**. In the ^1H NMR spectrum, two signals are observed at 6.20 and 4.79 ppm (doublets with ^4J = 4.5 Hz), corresponding to the two nonequivalent C−H groups of the bound butadienyl fragment. No other isomeric complexes arising from head-to-head or tail-to-tail dimerization are detected under these conditions. The solid-state structure (Figure 4a) reveals that the metallacycle incorporates one Ni into a five-membered ring. The second Ni

DOI: 10.1021/jacs.5b04990
J. Am. Chem. Soc. 2015, 137, 8042−8045

Scheme 2. Stoichiometric Reactions of 1 with Trialkylsilylacetylenes

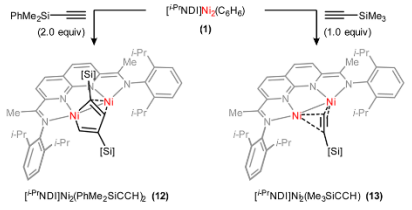

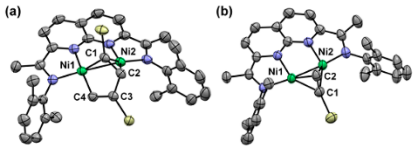

Figure 4. Solid-state structures of (a) **12** and (b) **13** (ellipsoids at 50% probability). *i*-Pr groups on the NDI ligand and substituents on silicon are truncated for clarity. Selected bond distances for **12** (Å): Ni1−Ni2, 2.4814(6); Ni1−C1, 1.942(2); Ni1−C4, 1.868(2); Ni2−C1, 1.875(2); Ni2−C2, 2.042(2); C1−C2, 1.416(4); C2−C3, 1.482(3); C3−C4, 1.350(3). Selected bond distances for **13** (Å): Ni1−Ni2, 2.3140(6); Ni1−C1, 2.023(3); Ni1−C2, 1.911(3); Ni2−C1, 2.015(2); Ni2−C2, 1.904(2); C1−C2, 1.301(4).

provides additional stabilization through an η^2-interaction with a double bond of the diene system. Related π-interactions have been invoked in alkyne cyclotrimerizations[3c,15] and Pauson−Khand reactions[3a,b] mediated by $Co_2(CO)_8$. In support of the catalytic relevance of the structurally characterized complex **12**, a directly analogous metallacycle is observed with phenylacetylene under turnover conditions (^{1}H NMR: 6.70 and 4.52 ppm, ^4J = 4.3 Hz).

The reversibility of the C−C coupling was examined to determine whether the regioisomer **12** is formed under thermodynamic or kinetic control. When **12** is exposed to trimethylsilylacetylene (10 equiv), no exchange of $-SiMe_2Ph$ for $-SiMe_3$ in the metallacycle is observed even after heating at 70 °C for 48 h. The formation of **12** is therefore sufficiently thermodynamically favorable to preclude the reverse reaction from occurring at catalytically relevant temperatures. A plausible explanation for the high head-to-tail selectivity is the steric hindrance imposed by the flanking 2,6-diisopropylphenyl substituents of the catalyst. The solid-state structure of **12** suggests that substituents at C2 or C4 would be highly disfavored by interactions with a catalyst *i*-Pr group or arene respectively (Figure 4a).

The metallacycle **12** does not react with additional equivalents of dimethylphenylsilylacetylene; however, when a less hindered alkyne, methyl propargyl ether, is introduced, cyclotrimerization proceeds to form the heterocoupled product **14** (Scheme 3). This reaction is accompanied by catalytic homocyclotrimerization of methyl propargyl ether. The regioselectivity in this stoichiometric process is consistent with that observed under standard catalytic conditions. Collectively, these experiments support the competence of metallacycles analogous to **12** as intermediates in the formation of 1,2,4-substituted arene products.

Scheme 3. Stoichiometric Conversion of 12 to the Heterocoupled Product 14

The presumed monoalkyne complex (**13**), en route to the metallacycle **12**, was characterized from the reaction of **1** with one equivalent of trimethylsilylacetylene. In the solid state, the alkyne exhibits μ-η^2:η^2 coordination and is perpendicular to the Ni−Ni bond vector (Figure 4b). The C−C distance is significantly elongated from approximately 1.20 Å for free trimethylsilylacetylene[16] to 1.301(4) Å in the complex. The alkyne complex **13** is sufficiently stable to permit structural characterization; however, over the course of 24 h at room temperature in C_6D_6, it disproportionates to form a mixture of the corresponding metallacycle and the benzene complex **1**.

Origin of the Dinuclear Effect. The observed ratio of 1,2,4- to 1,3,5-substituted products in the alkyne cyclotrimerization arises from regioselectivity considerations in two sequential steps: the dimerization to form the metallacyclic intermediate and the subsequent incorporation of the third alkyne to yield the arene product. The stoichiometric reactivity studies described above provide insight into the selectivity of the first C−C coupling; however, less information is readily apparent regarding the product formation step.

DFT calculations (M06/6-31G(d,p) level of theory) were performed on a model catalyst system (*i*-Pr groups on the aryl substituent were truncated to Me groups) to assess potential pathways for the conversion of this intermediate into the final product. Using propyne as a substrate, a concerted transition state was optimized, corresponding to a [4 + 2]-cycloaddition of a Ni-coordinated alkyne to the butadienyl system (Figure 5a).[17]

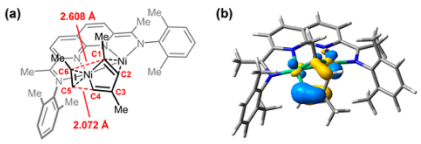

Figure 5. DFT calculations (M06/6-31G(d,p) level of theory) addressing the selectivity of alkyne addition to the bound butadienyl ligand. Propyne was used as a model substrate and *i*-Pr substituents on the catalyst were truncated to Me substituents. (a) The lowest-energy transition structure corresponding to the [4 + 2]-cycloaddition of the bound alkyne and butadienyl ligands. Distances for the two forming C−C bonds are shown in red. (b) The HOMO−1 for the metallacycle intermediate.

Stationary points associated with alternative stepwise pathways could not be located. Consistent with the fast rates observed experimentally for cyclotrimerizations with alkylacetylenes, the activation energy for this step was calculated to be only 9.3 kcal/mol. The competing transition state leading to the minor 1,3,5-substituted product was 2.0 kcal/mol higher in energy.

The calculated cycloaddition transition state (Figure 5a) is highly asynchronous with bond formation between C4 and C5 (2.07 Å) being significantly more advanced than that between C1 and C6 (2.61 Å). This asymmetry arises from stabilization of one of the double bonds through η^2 coordination to the second Ni

DOI: 10.1021/jacs.5b04990
J. Am. Chem. Soc. 2015, 137, 8042−8045

center. The calculated HOMO−1, which primarily corresponds to the delocalized π-orbital of the diene system, shows significantly greater density at the uncoordinated double bond (Figure 5b). This electronic structure is manifested in the solid-state geometry of **6** as an elongated C1−C2 (1.416(4) Å) distance relative to the C3−C4 distance (1.350(3) Å). A hypothesis that emerges from these calculations is that this electronic asymmetry, induced by the presence of the second Ni center in the catalyst, results in a steric preference for the substituent of the approaching alkyne to be positioned at the carbon where the forming C−C distance is longer in the transition state.

In summary, the dinuclear [NDI]Ni_2 platform provides access to an efficient cyclotrimerization pathway that is not available to its mononuclear counterparts. The catalyst nuclearity effect is particularly significant for alkyl-substituted alkynes: reactions are complete within 1 h at room temperature using 1 mol % loading of **1** with nearly exclusive formation of 1,2,4-substituted arene products. Stoichiometric reactivity studies provide structural insight into the metallacyclopentadiene intermediate that is implicated in the catalytic mechanism. Combined with DFT calculations, these experiments suggest several distinct features of the bimetallic system. First, binding across two metals constrains the geometry of the metallacycle, disfavoring the formation of other possible regioisomers. Second, the [4 + 2]-cycloaddition of the butadienyl ligand and the approaching alkyne is facilitated by metal coordination to both partners. Third, the selectivity of the cycloaddition is controlled by an electronic bias in the diene π-system, caused by a secondary η^2 interaction. Exploring the implications of these dinuclear effects for other catalytic cycloadditions is ongoing in our laboratory.

■ ASSOCIATED CONTENT

Supporting Information

Experimental methods, computational methods, characterization data, and spectra. This material is available free of charge via the Internet at http://pubs.acs.org."The Supporting Information is available free of charge on the ACS Publications website at DOI: 10.1021/jacs.5b04990.

■ AUTHOR INFORMATION

Corresponding Author

*cuyeda@purdue.edu

Notes

The authors declare no competing financial interest.

■ ACKNOWLEDGMENTS

This work was generously supported by Purdue University. We thank Dr. Phillip Fanwick and Ian Powers for assistance with X-ray crystallography, Dr. John Harwood for assistance with NMR spectroscopy, and Ravikiran Yerabolu for the collection of mass spectrometry data.

■ REFERENCES

(1) (a) Doyle, M. P. *J. Org. Chem.* **2006**, *71*, 9253−9260. (b) Davies, H. M. L.; Morton, D. *Chem. Soc. Rev.* **2011**, *40*, 1857−1869. (c) Cooper, B. G.; Napoline, J. W.; Thomas, C. M. *Catal. Rev.* **2012**, *54*, 1−40. (d) Kornecki, K. P.; Berry, J. F.; Powers, D. C.; Ritter, T. In *Progress in Inorganic Chemistry*; Karlin, K. D., Ed.; John Wiley & Sons, Inc.: Hoboken, NJ, 2014; Vol. *58*, p 225−302.

(2) (a) Velian, A.; Lin, S.; Miller, A. J. M.; Day, M. W.; Agapie, T. *J. Am. Chem. Soc.* **2010**, *132*, 6296−6297. (b) Krogman, J. P.; Foxman, B. M.; Thomas, C. M. *J. Am. Chem. Soc.* **2011**, *133*, 14582−14585. (c) Powers, T. M.; Fout, A. R.; Zheng, S.-L.; Betley, T. A. *J. Am. Chem. Soc.* **2011**, *133*, 3336−3338.

(3) (a) Magnus, P.; Principe, L. M. *Tetrahedron Lett.* **1985**, *26*, 4851−4854. (b) Yamanaka, M.; Nakamura, E. *J. Am. Chem. Soc.* **2001**, *123*, 1703−1708. (c) Giordano, R.; Sappa, E.; Predieri, G. *Inorg. Chim. Acta* **1995**, *228*, 139−146. (d) Hostetler, M. J.; Bergman, R. G. *J. Am. Chem. Soc.* **1990**, *112*, 8621−8623. (e) Zhou, W.; Marquard, S. L.; Bezpalko, M. W.; Foxman, B. M.; Thomas, C. M. *Organometallics* **2013**, *32*, 1766−1772.

(4) (a) Shibasaki, M.; Sasai, H.; Arai, T. *Angew. Chem., Int. Ed.* **1997**, *36*, 1236−1256. (b) van den Beuken, E. K.; Feringa, B. L. *Tetrahedron* **1998**, *54*, 12985−13011. (c) Li, H.; Marks, T. J. *Proc. Natl. Acad. Sci. U.S.A.* **2006**, *103*, 15295−15302. (d) Park, J.; Hong, S. *Chem. Soc. Rev.* **2012**, *41*, 6931−6943.

(5) (a) Tsutsumi, H.; Sunada, Y.; Shiota, Y.; Yoshizawa, K.; Nagashima, H. *Organometallics* **2009**, *28*, 1988−1991. (b) Walker, W. K.; Kay, B. M.; Michaelis, S. A.; Anderson, D. L.; Smith, S. J.; Ess, D. H.; Michaelis, D. J. *J. Am. Chem. Soc.* **2015**, in press. (c) Powers, D. C.; Ritter, T. *Acc. Chem. Res.* **2011**, *45*, 840−850. (d) Mazzacano, T. J.; Mankad, N. P. *J. Am. Chem. Soc.* **2013**, *135*, 17258−17261.

(6) (a) Zhou, Y.-Y.; Hartline, D. R.; Steiman, T. J.; Fanwick, P. E.; Uyeda, C. *Inorg. Chem.* **2014**, *53*, 11770−11777. (b) Steiman, T. J.; Uyeda, C. *J. Am. Chem. Soc.* **2015**, *137*, 6104−6110.

(7) (a) Broere, D. L. J.; Ruijter, E. *Synthesis* **2012**, *44*, 2639−2672. (b) Kumar, P.; Louie, J. In *Transition-Metal-Mediated Aromatic Ring Construction*; Tanaka, K., Ed.; John Wiley & Sons, Inc.: Hoboken, NJ, 2013; p 37−70. (c) Amatore, M.; Aubert, C. *Eur. J. Org. Chem.* **2015**, *2015*, 265−286.

(8) Reppe, W.; Schlichting, O.; Klager, K.; Toepel, T. *Justus Liebigs Ann. Chem.* **1948**, *560*, 1−92.

(9) Čermák, J.; Blechta, V.; Chvalovský, V. *Collect. Czech. Chem. Commun.* **1988**, *53*, 1274−1286.

(10) Simons, L. H.; Lagowski, J. J. *J. Org. Chem.* **1978**, *43*, 3247−3248.

(11) (a) Alphonse, P.; Moyen, F.; Mazerolles, P. *J. Organomet. Chem.* **1988**, *345*, 209−216. (b) Lawrie, C. J.; Gable, K. P.; Carpenter, B. K. *Organometallics* **1989**, *8*, 2274−2276. (c) Chini, P.; Palladino, N.; Santambrogio, A. *J. Chem. Soc. C* **1967**, 836−840.

(12) (a) Reppe, W.; Schweckendiek, W. J. *Justus Liebigs Ann. Chem.* **1948**, *560*, 104−116. (b) Chini, P.; Santambrogio, A.; Palladino, N. *J. Chem. Soc. C* **1967**, 830−835. (c) Sato, Y.; Nishimata, T.; Mori, M. *J. Org. Chem.* **1994**, *59*, 6133−6135. (d) Mori, N.; Ikeda, S.-i.; Odashima, K. *Chem. Commun.* **2001**, 181−182. (e) Müller, C.; Lachicotte, R. J.; Jones, W. D. *Organometallics* **2002**, *21*, 1975−1981. (f) Teske, J. A.; Deiters, A. *J. Org. Chem.* **2008**, *73*, 342−345. (g) Rodrigo, S. K.; Powell, I. V.; Coleman, M. G.; Krause, J. A.; Guan, H. *Org. Biomol. Chem.* **2013**, *11*, 7653−7657. (h) Diercks, R.; Stamp, L.; Kopf, J.; tom Dieck, H. *Angew. Chem., Int. Ed.* **1984**, *23*, 893−894. (i) Diercks, R.; Stamp, L.; Dieck, H. T. *Chem. Ber.* **1984**, *117*, 1913−1919. (j) Diercks, R.; Dieck tom, H. *Chem. Ber.* **1985**, *118*, 428−435. (k) Xi, C.; Sun, Z.; Liu, Y. *Dalton Trans.* **2013**, *42*, 13327−13330.

(13) (a) Tanaka, K.; Toyoda, K.; Wada, A.; Shirasaka, K.; Hirano, M. *Chem.−Eur. J.* **2005**, *11*, 1145−1156. (b) Perekalin, D. S.; Karslyan, E. E.; Trifonova, E. A.; Konovalov, A. I.; Loskutova, N. L.; Nelyubina, Y. V.; Kudinov, A. R. *Eur. J. Inorg. Chem.* **2013**, *2013*, 481−493.

(14) For examples of cyclotrimerizations selective for the 1,2,4-regioisomer, see ref 7 and: (a) Ozerov, O. V.; Ladipo, F. T.; Patrick, B. O. *J. Am. Chem. Soc.* **1999**, *121*, 7941−7942. (b) Ozerov, O. V.; Patrick, B. O.; Ladipo, F. T. *J. Am. Chem. Soc.* **2000**, *122*, 6423−6431.

(15) (a) Bennett, M. A.; Donaldson, P. B. *Inorg. Chem.* **1978**, *17*, 1995−2000. (b) Baxter, R. J.; Knox, G. R.; Pauson, P. L.; Spicer, M. D. *Organometallics* **1999**, *18*, 197−205.

(16) Bond, A. D.; Davies, J. E. *Acta Crystallogr., Sect. E* **2002**, *58*, o777−o778.

(17) Agenet, N.; Gandon, V.; Vollhardt, K. P. C.; Malacria, M.; Aubert, C. *J. Am. Chem. Soc.* **2007**, *129*, 8860−8871.

DOI: 10.1021/jacs.5b04990
J. Am. Chem. Soc. 2015, 137, 8042−8045

JACS
JOURNAL OF THE AMERICAN CHEMICAL SOCIETY
Communication
pubs.acs.org/JACS

Catalytic Reductive Vinylidene Transfer Reactions

Sudipta Pal,[‡] You-Yun Zhou,[‡] and Christopher Uyeda*

Department of Chemistry, Purdue University, West Lafayette, Indiana 47907, United States

Supporting Information

ABSTRACT: Methylenecyclopropanes are important synthetic intermediates that possess strain energies exceeding those of saturated cyclopropanes by >10 kcal/mol. This report describes a catalytic reductive methylenecyclopropanation reaction of simple olefins, utilizing 1,1-dichloroalkenes as vinylidene precursors. The reaction is promoted by a dinuclear Ni catalyst, which is proposed to access Ni_2(vinylidenoid) intermediates via C—Cl oxidative addition.

Vinylidenes (methylidene carbenes) are reactive intermediates comprising a divalent carbon atom incorporated into a C=C double bond.[1] Like their saturated carbene counterparts, vinylidenes undergo reactions that allow the valence-deficient carbon to increase its coordination number: for example, through cheletropic reactions with π-systems or insertions into C—H bonds.[2] Free vinylidenes are accessible from the decomposition of transiently generated diazoalkenes.[3] Alternatively, (R_2C=C)(M)(X) species (vinylidenoids) serve as R_2C=C: surrogates, eliminating metal halides as stoichiometric byproducts.[1d] A key challenge associated with developing efficient transfer reactions of vinylidenes is their susceptibility to competing Fritsch—Buttenberg—Wiechell (FBW) rearrangements that form alkynes (Figure 1).[4] The rate of the 1,2-shift varies as a function of the migrating group, but when one of the alkene substituents is an H atom, the rearrangement becomes nearly barrierless.[5] This process underlies the well-known Corey—Fuchs and Seyferth—Gilbert alkyne syntheses.[6]

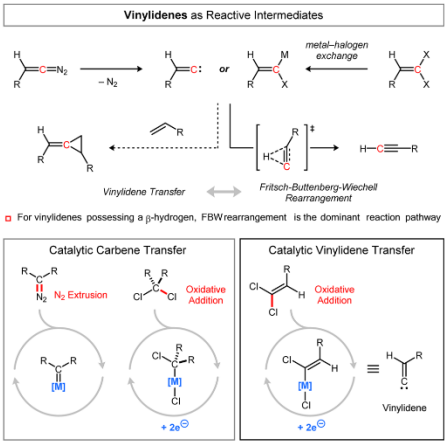

Figure 1. Vinylidenes as reactive intermediates and design principles for a catalytic reductive vinylidene transfer reaction.

Transition metal catalysis may provide an avenue to address the instability of vinylidenes, allowing group transfer reactions to be favored over competing FBW rearrangement. Nevertheless, current carbene transfer catalysts are largely unsuitable for vinylidene transfer due to their reliance on diazoalkane

Table 1. Catalyst Structure—Activity Relationships[a]

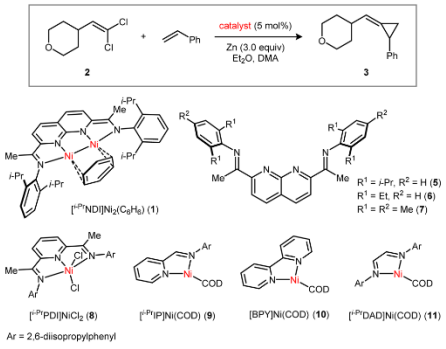

entry	catalyst	yield	E/Z ratio
1	[$^{t\text{-Pr}}$NDI]$Ni_2(C_6H_6)$ (**1**)	94%	1:5
2	[$^{t\text{-Pr}}$NDI]Ni_2Cl_2 (**4**)	87%	1:5
3[b]	$^{i\text{-Pr}}$NDI (**5**) + $Ni(DME)Cl_2$	92%	1:5
4[b]	^{Et}NDI (**6**) + $Ni(DME)Cl_2$	50%	1:1
5[b]	^{Me}NDI (**7**) + $Ni(DME)Cl_2$	<2%	–
6	[$^{t\text{-Pr}}$PDI]$NiCl_2$ (**8**)	<2%	–
7	[$^{t\text{-Pr}}$IP]Ni(COD) (**9**)	<2%	–
8	[BPY]Ni(COD) (**10**)	<2%	–
9	[$^{t\text{-Pr}}$DAD]Ni(COD) (**11**)	<2%	–

[a]Yields and E/Z ratios were determined by ^{1}H NMR integration. Reaction conditions: **2** (0.21 mmol), styrene (0.2 mmol), catalyst (5 mol %), 24 h, 22 °C. [b]Reactions were conducted with 5 mol % of the NDI ligand and 10 mol % of $Ni(DME)Cl_2$.

Received: June 7, 2017
Published: August 14, 2017

DOI: 10.1021/jacs.7b05901
J. Am. Chem. Soc. 2017, 139, 11686–11689

Table 2. Substrate Scope for the Catalytic Methylenecyclopropanation Reaction[a]

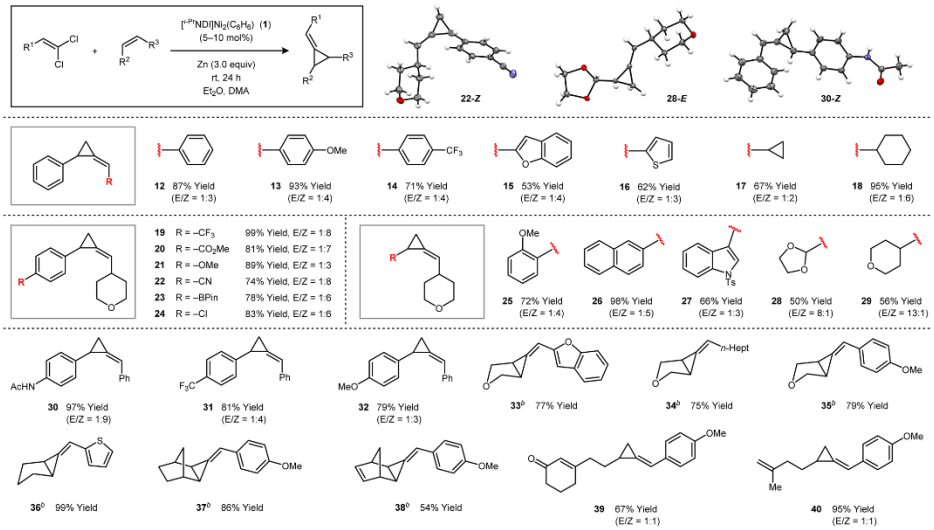

[a]Isolated yields were determined following purification and are averaged over two runs. See Supporting Information for experimental details. [b]The alkene partner was used in excess (4–10 equiv).

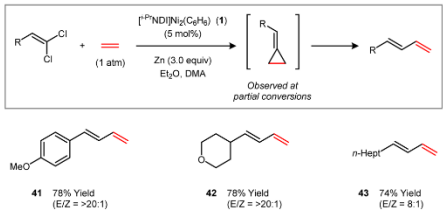

Figure 2. Tandem methylenecyclopropanation–isomerization reactions.

decomposition as an activation strategy.[7] Diazoalkenes, the equivalent vinylidene precursors, are not known to be isolable and undergo N_2 elimination spontaneously at room temperature.[1d,3a] Transition metal-bound vinylidenes are accessible by an alternative route involving a metal-induced isomerization of an alkyne.[8] Buono described a Pd-catalyzed methylenecyclopropanation reaction that operates by this pathway and is effective for a range of norbornene-derived substrates.[9,10] Other classes of alkenes are not currently viable in catalytic vinylidene [2+1]-cycloadditions.

Our group is interested in developing new modes of carbene generation based on the reductive dehalogenation of readily available and indefinitely stable 1,1-dihaloalkanes. In this context, we recently described a dinuclear Ni catalyst that promotes the cyclopropanation of alkenes using CH_2Cl_2 as a carbene source and Zn as a terminal reductant.[11] Here, we report the reductive transfer of vinylidenes from 1,1-dichloroalkenes (Figure 1). This method provides direct access to methylenecyclopropanes, a class of synthetic intermediates valued for their ability to engage in strain-induced ring-opening reactions.[2d,e,12]

In our initial studies, we arrived at an optimal set of conditions for a model methylenecyclopropanation reaction based on our previously reported CH_2 transfer method.[11] The Ni_2 catalyst **1**[13] promotes the addition of **2** to styrene in 94% yield using Zn as a reductant (Table 1, entry 1). Of note, none of the 1,1-dichloroalkene is lost to polymerization, reductive dehalogenation, or FBW rearrangement, allowing the reaction to be conducted with near-equimolar quantities of the two reaction partners. The [$^{i\text{-Pr}}$NDI]Ni_2Cl_2 complex **4** is also a high-yielding catalyst, demonstrating efficient entry into the catalytic cycle from multiple oxidation states of the Ni_2 complex (entry 2). The reaction is amenable to *in situ* catalyst generation using the free $^{i\text{-Pr}}$NDI ligand (**5**, 5 mol %) and Ni(DME)Cl_2 (10 mol %) in the place of preformed **1** (entry 3). Decreasing the steric profile of the imine aryl substituents leads to rapidly diminishing yields (entries 4 and 5). Finally, the importance of the dinuclear catalyst structure was assessed using a series of mononickel complexes bearing structurally related N-donor ligands. In these cases, there is significant consumption of the 1,1-dichloroalkene (**2**) but no productive vinylidene transfer to form **3** (entries 6–9).

The substrate scope of the catalytic methylenecyclopropanation is summarized in Table 2. 1,1-Dichloroalkenes bearing alkyl, aryl, or heteroaryl substituents afford high yields in their reactions with styrene (**12**–**18**). With regard to the alkene partner, monosubstituted terminal alkenes are effective substrates (**19**–**32**), and a variety of common functional groups are tolerated, including esters, ethers, nitriles, boronate esters, aryl chlorides, sulfonyl protecting groups, acetals,

DOI: 10.1021/jacs.7b05901
J. Am. Chem. Soc. 2017, 139, 11686−11689

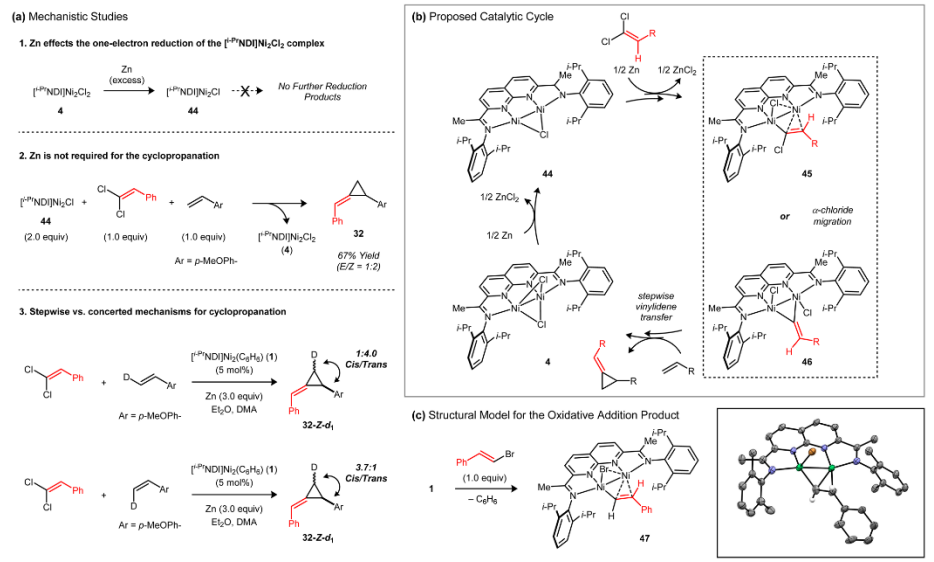

Figure 3. (a) Mechanistic studies probing the relevant catalyst oxidation states, the role of Zn, and the concertedness of the cyclopropanation. (b) Proposed catalytic mechanism. (c) Structurally characterized model (**47**) for the proposed Ni_2 vinylidenoid intermediate (**45**).

primary amides, and ketones. The observed *E*/*Z* ratios vary over a range of values and are dependent on the identity of the alkene substituent: alkyl groups with α-branching favor the *E*-isomer, linear alkyl groups afford low stereoselectivity, and aryl groups favor the *Z*-isomer.

Relatively unhindered internal alkenes, such as cyclopentene, 2,5-dihydrofuran, and norbornene, also react to form cyclopropanated products (**33**–**37**). More hindered alkenes than those shown in Table 2 are a current limitation and generally result in low yields. In accordance with these observations, the selectivity properties of the reaction are highly sensitive to steric effects. For example, norbornene and norbornadiene are selectively cyclopropanated on the exo face (**37**–**38**), and polyalkene substrates are monocyclopropanated at the less substituted alkene (**39**–**40**).

Unexpectedly, attempts to carry out the methylenecyclopropanation of ethylene (1 atm) yielded 1,3-diene products (**41**–**43**), a reaction that constitutes a formal vinylidene insertion into a $C(sp^2)$—H bond (Figure 2). We reasoned that these products may be forming in a catalyst-promoted ring-opening of a transient methylenecyclopropane intermediate.[14] At partial conversions, the reaction to form **42** contains significant amounts of the corresponding methylenecyclopropane, the concentration of which decreases as the reaction approaches completion.

Experiments pertaining to the mechanism of the catalytic methylenecyclopropanation are summarized in Figure 3a. By cyclic voltammetry, the Ni_2Cl_2 complex **4** exhibits two reversible reduction events at −1.15 and −1.72 V relative to the F_c/F_c^+ couple.[11] Zn is capable of accessing only the first of these two reductions, suggesting that the Ni_2Cl complex **44** is the most reduced state of the catalyst that is accessible. Next, we questioned whether the role of Zn is restricted to catalyst reduction[15] or whether it might be more intimately involved in the cyclopropane-forming steps of the mechanism: for example, through the generation of Zn vinylidenoid species.[16] This latter possibility was ruled out by conducting a cyclopropanation in the absence of Zn, where the Ni_2Cl complex **44** was used stoichiometrically as the only source of reducing equivalents. Accordingly, the reaction between β,β-dichlorostyrene (1.0 equiv), *p*-methoxystyrene (1.0 equiv), and **44** (2.0 equiv) provided **32** in 67% yield (1:2 *E*/*Z* ratio).

Finally, there is substantial evidence to support a stepwise mechanism for the cyclopropanation. The *E*- and *Z*-stereoisomers of β-deuterated *p*-methoxystyrene react with incomplete retention of the alkene stereochemistry, yielding product **32**-d_1 as a mixture of cis and trans diastereomers. In principle, this loss of stereochemical fidelity may be due to an off-path, catalyst-promoted *E*/*Z* isomerization of the *p*-methoxystyrene starting material. This possibility was tested by running these reactions to partial conversion and examining the stereochemistry of the recovered alkene. At a reaction time of 20 min, the recovered alkene is diastereomerically pure, suggesting that stereochemical scrambling is intrinsic to the mechanism of cyclopropane formation.

A proposed catalytic cycle based on these data is outlined in Figure 3b. Two-electron oxidative addition of the 1,1-dichloroalkene using the Ni_2Cl complex **44** would require an additional reducing equivalent provided by either a second molecule of **44** or by Zn. The resulting Ni_2(1-chloroalkenyl)Cl intermediate **45** could then engage the alkene partner and form the corresponding methylenecyclopropane product. An alternative possibility is that **45** first isomerizes by α-chloride migration to produce the Ni_2(vinylidene)Cl_2 species **46**.[17]

DOI: 10.1021/jacs.7b05901
J. Am. Chem. Soc. 2017, 139, 11686−11689

According to DFT models (BP86/6-311G(d,p)), this isomerization is moderately endothermic but potentially accessible under the reaction conditions (ΔG = 10.5 kcal/mol, 298 K). In both scenarios, the Ni_2Cl_2 complex **4** is generated following vinylidene transfer, and a one-electron reduction closes the catalytic cycle.

Attempts to obtain characterization data on the postulated vinylidenoid intermediate **45**/**46** proved unsuccessful due to its instability. To access a more stable structural surrogate, the Ni_2(μ-styrenyl)Br complex **47** was prepared from an oxidative addition reaction between **1** and β-bromostyrene. This complex lacks the additional halogen at the β-position and is thus incapable of engaging in vinylidene transfer. A notable feature of the solid-state structure is the η^2-coordination of the alkenyl π-system to the second Ni. This interaction constrains the orientation of the β-hydrogen substituent and may contribute to the absence of FBW rearrangement side products in these reactions.

In summary, the Ni_2 catalyst **1** has proven to be uniquely effective relative to analogous mononickel complexes in promoting reductive methylenecyclopropanation reactions using 1,1-dichloroalkenes. Of particular significance, vinylidene transfer predominates over competing rearrangement to the alkyne despite the presence of a β-hydrogen. Our current efforts are directed at generalizing this catalytic vinylidene transfer strategy to other classes of cycloadditions.

■ ASSOCIATED CONTENT

Supporting Information

The Supporting Information is available free of charge on the ACS Publications website at DOI: 10.1021/jacs.7b05901.

X-ray crystallographic data for $C_{12}H_{18}O_3$ (CIF)
X-ray crystallographic data for $C_{18}H_{17}NO$ (CIF)
X-ray crystallographic data for $C_{16}H_{17}NO$ (CIF)
X-ray crystallographic data for $C_{44}H_{51}BrN_4Ni_2$, 1.264(C_4H_8O), 0.368(C_5H_{12}) (CIF)
Experimental procedures and characterization data (PDF)

■ AUTHOR INFORMATION

Corresponding Author

*cuyeda@purdue.edu

ORCID

Christopher Uyeda: 0000-0001-9396-915X

Author Contributions

‡These authors contributed equally.

Notes

The authors declare no competing financial interest.

■ ACKNOWLEDGMENTS

This work was supported by Purdue University. We thank Dr. Matthias Zeller for assistance with XRD experiments and Ravikiran Yerabolu for assistance with mass spectrometry experiments. C.U. is an Alfred P. Sloan Foundation Research Fellow.

■ REFERENCES

(1) (a) Stang, P. J. *Chem. Rev.* **1978**, *78*, 383−405. (b) Stang, P. J. *Acc. Chem. Res.* **1982**, *15*, 348−354. (c) Kirmse, W. *Angew. Chem., Int. Ed. Engl.* **1997**, *36*, 1164−1170. (d) Knorr, R. *Chem. Rev.* **2004**, *104*, 3795−3850. (e) Grainger, R. S.; Munro, K. R. *Tetrahedron* **2015**, *71*, 7795−7835.

(2) (a) Brandi, A.; Goti, A. *Chem. Rev.* **1998**, *98*, 589−636. (b) Audran, G.; Pellissier, H. *Adv. Synth. Catal.* **2010**, *352*, 575−608. (c) Yamaguchi, J.; Yamaguchi, A. D.; Itami, K. *Angew. Chem., Int. Ed.* **2012**, *51*, 8960−9009. (d) Brandi, A.; Cicchi, S.; Cordero, F. M.; Goti, A. *Chem. Rev.* **2014**, *114*, 7317−7420. (e) Pellissier, H. *Tetrahedron* **2014**, *70*, 4991−5031.

(3) (a) Gilbert, J. C.; Weerasooriya, U. *J. Org. Chem.* **1982**, *47*, 1837−1845. (b) Ohira, S.; Okai, K.; Moritani, T. *J. Chem. Soc., Chem. Commun.* **1992**, 721−722. (c) Gilbert, J. C.; Giamalva, D. H. *J. Org. Chem.* **1992**, *57*, 4185−4188.

(4) (a) Fritsch, P. *Justus Liebigs Ann. Chem.* **1894**, *279*, 319−323. (b) Buttenberg, W. P. *Justus Liebigs Ann. Chem.* **1894**, *279*, 324−337. (c) Wiechell, H. *Justus Liebigs Ann. Chem.* **1894**, *279*, 337−344. (d) Jahnke, E.; Tykwinski, R. R. *Chem. Commun.* **2010**, *46*, 3235−3249.

(5) (a) Ervin, K. M.; Ho, J.; Lineberger, W. C. *J. Chem. Phys.* **1989**, *91*, 5974−5992. (b) Chang, N.-Y.; Shen, M.-Y.; Yu, C.-H. *J. Chem. Phys.* **1997**, *106*, 3237−3242.

(6) (a) Corey, E. J.; Fuchs, P. L. *Tetrahedron Lett.* **1972**, *13*, 3769−3772. (b) Colvin, E. W.; Hamill, B. J. *J. Chem. Soc., Perkin Trans. 1* **1977**, *2*, 869−874. (c) Gilbert, J. C.; Weerasooriya, U. *J. Org. Chem.* **1979**, *44*, 4997−4998. (d) Habrant, D.; Rauhala, V.; Koskinen, A. M. P. *Chem. Soc. Rev.* **2010**, *39*, 2007−2017.

(7) (a) Doyle, M. P.; McKervey, M. A.; Ye, T. *Modern catalytic methods for organic synthesis with diazo compounds*; Wiley: New York, 1998. (b) Davies, H. M. L.; Manning, J. R. *Nature* **2008**, *451*, 417−424. (c) Ford, A.; Miel, H.; Ring, A.; Slattery, C. N.; Maguire, A. R.; McKervey, M. A. *Chem. Rev.* **2015**, *115*, 9981−10080.

(8) (a) Bruce, M. I. *Chem. Rev.* **1991**, *91*, 197−257. (b) Bruneau, C.; Dixneuf, P. H. *Acc. Chem. Res.* **1999**, *32*, 311−323. (c) Varela, J. A.; Saá, C. *Chem. - Eur. J.* **2006**, *12*, 6450−6456. (d) Bruneau, C.; Dixneuf, P. H. *Angew. Chem., Int. Ed.* **2006**, *45*, 2176−2203. (e) *Metal vinylidenes and allenylidenes in catalysis: from reactivity to applications in synthesis*; Bruneau, C.; Dixneuf, P., Eds.; Wiley-VCH: Wenheim, Germany, 2008. (f) Lynam, J. M. *Chem. - Eur. J.* **2010**, *16*, 8238−8247.

(9) (a) Bigeault, J.; Giordano, L.; Buono, G. *Angew. Chem., Int. Ed.* **2005**, *44*, 4753−4757. (b) Clavier, H.; Lepronier, A.; Bengobesse-Mintsa, N.; Gatineau, D.; Pellissier, H.; Giordano, L.; Tenaglia, A.; Buono, G. *Adv. Synth. Catal.* **2013**, *355*, 403−408.

(10) Mao, J.; Bao, W. *Org. Lett.* **2014**, *16*, 2646−2649.

(11) Zhou, Y.-Y.; Uyeda, C. *Angew. Chem., Int. Ed.* **2016**, *55*, 3171−3175.

(12) (a) Trost, B. M. *Angew. Chem., Int. Ed. Engl.* **1986**, *25*, 1−20. (b) Nakamura, I.; Yamamoto, Y. *Adv. Synth. Catal.* **2002**, *344*, 111−129. (c) Yamago, S.; Nakamura, E. *Org. React.* **2002**, *61*, 1−217.

(13) (a) Zhou, Y.-Y.; Hartline, D. R.; Steiman, T. J.; Fanwick, P. E.; Uyeda, C. *Inorg. Chem.* **2014**, *53*, 11770−11777. (b) Steiman, T. J.; Uyeda, C. *J. Am. Chem. Soc.* **2015**, *137*, 6104−6110.

(14) (a) Englert, M.; Jolly, P. W.; Wilke, G. *Angew. Chem., Int. Ed. Engl.* **1971**, *10*, 77−77. (b) Binger, P.; Brinkmann, A.; Wedemann, P. *Chem. Ber.* **1983**, *116*, 2920−2930.

(15) For studies of Ni-catalyzed reductive cross-coupling reactions using Zn or Mn: (a) Everson, D. A.; Shrestha, R.; Weix, D. J. *J. Am. Chem. Soc.* **2010**, *132*, 920−921. (b) Weix, D. J. *Acc. Chem. Res.* **2015**, *48*, 1767−1775.

(16) Rezaei, H.; Yamanoi, S.; Chemla, F.; Normant, J. F. *Org. Lett.* **2000**, *2*, 419−421.

(17) (a) Fontaine, X. L. R.; Higgins, S. J.; Shaw, B. L.; Thornton-Pett, M.; Yichang, W. *J. Chem. Soc., Dalton Trans.* **1987**, 1501−1507. (b) Heise, J. D.; Nash, J. J.; Fanwick, P. E.; Kubiak, C. P. *Organometallics* **1996**, *15*, 1690−1696.

DOI: 10.1021/jacs.7b05901
J. Am. Chem. Soc. 2017, 139, 11686−11689